YUNIBESITI YA BOKONE-BOPHIRIMA
NORTH-WEST UNIVERSITY
NOORDWES-UNIVERSITEIT

EXPERIMENTAL DETERMINATION OF THE FORCED CONVECTIVE BOILING HEAT TRANSFER COEFFICIENTS OF R407C IN FLUTED-TUBES

PHILIP WOUTER DE VOS B. Eng.

Dissertation submitted in partial fulfilment of the requirements

for the degree Master of Engineering

at the

North-West University

Supervisor: Mr. M. van Eldik

May 2006

Potchefstroom Campus

ACKNOWLEDGEMENTS

I firstly bring praise to my Heavenly Father for providing the opportunities and the talents to complete this study. Also for His guidance, love and support during my studies and for always being there for me and my family.

To my father, thank you for all of his guidance, for being a living example of determination and for giving the opportunity and financial support for my studies. I thank my mother for all her love, care and understanding. Thanks to my three sisters for all your love and support. You are all an inspiration to me.

Martin van Eldik, my promoter, I thank for all his excellent guidance and advice in this field of study. Thank you for your enthusiasm and interest shown during the past years of my study. I will never forget it.

Thank you to Robbie Arrow for his assistance in helping me with my experimental test bench and teaching me so much about heat pumps.

Thank you to my fellow postgraduate students for all of your help.

I finally thank the School of Mechanical Engineering for the opportunity to further my studies, for the work environment and the financial support.

ABSTRACT

Titel: Experimental determination of the forced convective boiling heat transfer coefficients of R407C in fluted-tubes
Author: Philip Wouter de Vos
Supervisor: Mr. M van Eldik
School: School of Mechanical Engineering
Degree Master of Engineering

Due to the phase-out of all refrigerants with ozone depletion potential, a large void is left in the refrigeration market. This void was caused due to a lack of new, ozone friendly, pure refrigerants with similar thermodynamic properties to those of the banned refrigerants. As a result mixtures of refrigerants are used to create replacement refrigerants. These new mixtures have to be experimentally evaluated to derive correlations for the prediction of the heat transfer coefficients.

One of these mixtures is R407C. With this new refrigerant and the need for smaller, more compact heat exchangers, a search was initiated for a correlation describing the heat transfer coefficients of R407C in fluted-tube compact heat exchangers. The need for such a correlation is to accurately design compact fluted-tube heat exchangers for use in heat pumps and refrigeration systems. Fluted-tube heat exchangers are in general, much smaller and more compact than standard smooth tube-in-tube heat exchangers.

The purpose of this study was to experimentally determine the forced convective boiling heat transfer coefficients of R407C in fluted-tubes; furthermore, to test these experimental values against existing heat transfer correlations. The product of this study is experimental boiling data for R22 and R407C in fluted-tubes, together with a correlation to predict the boiling heat transfer coefficient of R407C in fluted-tubes.

The test bench used, was a 15 kW heat pump with a split evaporator design. The split evaporator is made up of a bypass evaporator and a test evaporator, with the test evaporator consisting of three separate heat exchangers: the pre-evaporator, test section and the super-heater. Of the three heat exchangers only the test section was a fluted tube-in-tube heat

exchanger with the other two smooth tube-in-tube heat exchangers. The test section was operated in a counter flow configuration with water flowing inside the fluted-tube and the refrigerant flowing in the annulus.

The accuracy of the test bench was validated using R22 in a smooth tube-in-tube heat exchanger, resulting in a maximum deviation between the water and the refrigerant heat transfer of 2.5%. After the validation the smooth tube test section was replaced with the fluted-tube section and tested with R22 and R407C. The refrigerant mass flow rates ranged from 0.01 kg/s – 0.03 kg/s. Along with the mass flow rates the heat fluxes were varied from 0.89 kW/m^2 – 20.34 kW/m^2 and with evaporating pressures set at 4.0, 4.5, 5.0 and 5.5 bar respectively. The maximum deviation between the water heat transfer and the refrigerant heat transfer for all the tests was 2.77% with an overall average deviation of 0.83%.

The experimental results for R22 and R407C were evaluated against seven correlations found in the literature consulted: Gungor and Winterton (1986:351), Gungor and Winterton (1987:148), Liu and Winterton (1991:2759), Pierre (ASHRAE Fundamentals, 1997:4.7), Chen (1963:1), Rousseau *et al.* (2003:232) and Kattan *et al.* (1998c:156). All the correlations were used as found in the literature, with the exception on the Rousseau *et al.* (2003:232) correlation. The enhancement factor used in this correlation was adapted to fit the experimental data better.

Comparing results of all the correlations, it was found that Rousseau *et al.* (2003:232), with the adapted enhancement factor, gave the best results for R22 as well as R407C, with the respective average deviations of 12.67% and 3.83% and respective mean deviations of 35.16% and 22.01%. A new correlation was proposed combining the geometric properties of the Rousseau *et al.* (2003:232) correlation with the boiling heat transfer of the Gungor and Winterton (1987:148) correlation.

UITTREKSEL

Titel: Eksperimentele bepaling van die geforseerde konvektiewe kook hitte-oordrag koëffisiente van R407C in gedraaide buise
Outeur: Philip Wouter de Vos
Studieleier: Mnr. M van Eldik
Skool: Skool vir Meganiese Ingenieurswese
Graad Magister in Ingenieurswese

Die uitfasering van alle verkoelingsmiddels met osoon-afbrekende potensiaal, het 'n groot leemte gelaat in die verkoelingsmark. Hierdie leemte is veroorsaak deur 'n gebrek aan nuwe, osoon-vriendelike, suiwer verkoelingsmiddels met dieselfde termodinamiese eienskappe as dié wat verban is. Gevolglik is mengsels van verkoelingsmiddels gebruik om as plaasvervangers te dien. Hierdie nuwe mengsels moet eksperimenteel geëvalueer word om korrelasies te ontwikkel vir die voorspelling van die hitte-oordrag koëffisiënte.

Een van hierdie mengsels is R407C. Met hierdie nuwe verkoelingsmiddel en die behoefte aan kleiner, meer kompakte hitteruilers, is 'n soektog begin na 'n korrelasie wat die hitte-oordrag koëffisiënte van R407C in gedraaide buis kompakte hitteruilers beskryf. Die behoefte vir so 'n korrelasie is om kompakte gedraaide buis hitteruilers akkuraat te ontwerp, vir gebruik in hittepompe en verkoelingstelsels. Gedraaide buis kompakte hitteruilers is oor die algemeen baie kleiner en meer kompak as standaard gladde pyp-in-pyp hitteruilers.

Die doel van hierdie studie was om eksperimenteel vas te stel wat die geforseerde konvektiewe hitte-oordrag koëffisiënte van R407C in gedraaide buise tydens verdamping is, en verder om hierdie eksperimentele waardes teen bestaande hitte-oordrag korrelasies te toets. Die produk van hierdie studie is eksperimentele verdampingsdata vir R22 en R407C in gedraaide buise, tesame met 'n korrelasie wat die verdampings hitte-oordrag koëffisiënt van R407C in gedraaide buise voorspel.

Die toetsbank wat gebruik is, is 'n 15 kW hittepomp met 'n verdeelde verdamper ontwerp. Die verdeelde verdamper bestaan uit 'n omleidingsverdamper en 'n toets-verdamper, met die toets-

verdamper wat bestaan uit drie aparte hitteruilers: die voor-verdamper, toetsseksie en die super-verhitter. Van die drie hitteruilers, was slegs die toetsseksie 'n gedraaide buis-in-buis hitteruiler, en die ander twee gladde buis-in-buis hitteruilers. Die toetsseksie is bedryf in 'n teen-vloei konfigurasie met water wat binne die gedraaide buis vloei, en die verkoelingsmiddel wat in die annulus vloei.

Die akkuraatheid van die toetsbank is gevalideer deur R22 in 'n gladde buis-in-buis hitteruiler te gebruik, wat 'n maksimum afwyking tussen die water hitte-oordrag en die verkoelingsmiddel hitte-oordrag van 2.5% tot gevolg gehad het. Ná die validasie, is die gladde buis toetsseksie vervang met 'n gedraaide buis seksie en getoets met R22 en R407C. Die verkoelingsmiddel massavloei tempo is gevarieer tussen 0.01 kg/s - 0.03 kg/s. Tesame met die massavloei tempo, is die hittevloed gevarieer tussen 0.89 kW/m^2 - 20.34 kW/m^2 met die verdampingsdruk gestel by onderskeidelik 4.0, 4.5, 5.0 en 5.5 bar. Die maksimum afwyking tussen die water hitte-oordrag en die verkoelingsmiddel hitte-oordrag vir al die toetse was 2.77% met 'n algehele gemiddelde afwyking van 0.83%.

Die eksperimentele resultate vir R22 en R407C is geëvalueer in terme van sewe korrelasies wat in die literatuurstudie gevind is: Gunger en Winterton (1986:351), Gunger en Winterton (1987:148), Liu en Winterton (1991:2759), Pierre (ASHRAE Fundamentals, 1997:4.7), Chen (1963:1), Rousseau *et al.* (2003:232) en Kattan *et al.* (1998c:156). Al die korrelasies is gebruik soos dit in die literatuur gevind is, behalwe die Rousseau *et al.* (2003:232) korrelasie. In die geval is die verbeterings faktor aangepas om die eksperimentele data beter te pas.

Deur die resultate van al die korrelasies te vergelyk, is gevind dat dié van Rousseau *et al.* (2003:232), met die aangepasde verbeterings faktor, die beste resultate vir R22 sowel as R407C gegee het. Die gemiddelde afwykings van onderskeidelik 12.67% en 3.83%, en mediaan-afwykings van onderskeidelik 35.16% en 22.01% is gevind. 'n Nuwe korrelasie is voorgestel wat die geometriese eienskappe van die Rousseau *et al.* (2003:232) korrelasie met die verdampings hitte-oordrag van die Gungor en Winterton (1987:148) korrelasie te kombineer.

TABLE OF CONTENTS

LIST OF FIGURES

LIST OF TABLES

NOMENCLATURE

A	Area	m^2
Bo	Boiling number	
C_p	Specific heat	kJ/kgK
C	Constant value	
D, d	Diameter	m
D_h	Hydraulic diameter	m
ΔT_{sat}	Super heat, $T_{wall} - T_{sat}$	°C
ΔT_{lm}	Log mean temperature difference	°C
Δp_{sat}	Difference in vapour pressure corresponding to ΔT_{sat}	kPa
e	Surface finish	
e_h, E	Enhancement factor	
e	Flute depth	m
e^*	Non-dimensional flute depth	
f	Friction factor	
$f_{helical}$	Helical coil friction factor	
$f_{straight}$	Straight tube friction factor	
F	Forced convective heat transfer enhancement factor	
Fr	Froude number	
g	Acceleration of gravity	m/s^2
G	Mass flux	kg/m^2s
h	Heat transfer coefficient	W/m^2K
$h_{helical}$	Heat transfer coefficient for helical coils	W/m^2K
$h_{straight}$	Heat transfer coefficient for straight coils	W/m^2K
k	Thermal conductivity	W/mK
K_f	Pierre's boiling number	
L	Length	m
$\dot{m}$	Mass flow rate	kg/s

M	Molecular weight	mol
n	Constant value	
N	Number of flute starts	
Nu	Nusselt number	
P	Pressure	kPa
p	Flute pitch	m
Pr	Prandtl number	
P_r	Reduced pressure	kPa
pr	Pressure ratio	
p^*	Non-dimensional flute pitch	
q	Heat flux	W/m^2
Q	Heat transfer rate	J/s or W
r	Radius	m
Re	Reynolds number	
r_h	Heat transfer enhancement ratio according to the Chilton-Colburn analogy	
R_f	Thermal resistance because of fouling	m^2K/W
R_w	Thermal resistance of the wall	m^2K/W
S	Suppression factor	
t	Wall thickness	m
T	Temperature	°C
U	Overall heat transfer coefficient	W/m^2K
V	Velocity	m/s
Vol	Volume	m^3
wt	Weight	
x	Quality	
X , X_{tt}	Martinelli parameter	

Greek symbols

β	Aspect ratio	
θ	Helix angle	°
θ^*	Non-dimensional helix angle	
λ	Latent heat	J/kg
μ	Kinematic viscosity	Ns/m^2
π	Constant (3.141592654)	
ρ	Density	
ϕ_f	Two-phase friction multiplier	

Subscripts

c	Cold
cal	Calculated value
Cu	Copper
e	Equivalent
exp	Experimental value
h	Hot
i	Variable
i	Inside
in	At the inlet
l, *liq*	Liquid
m	Mean value
n	Variable
o	Outside
out	At the outlet
pool	Pool boiling
r	Refrigerant
R22	R22
R407C	R407C
tot	Total value

tp	Two-Phase
v	Vapour
vi	Inside volume
vo	Outside volume
w	Water
wall	Property at the wall

Mathematical Symbols

max	Maximum

CHAPTER 1

1 INTRODUCTION

1.1 BACKGROUND

Refrigerants in the late 1800s and early 1900s consisted of three toxic gases: ammonia, methyl chloride and sulphur dioxide. After a series of fatal accidents in the 1920's when methyl chloride leaked out, the search for less toxic refrigerants started. Chlorofluorocarbons (CFCs) were discovered and were synthesized for the first time in 1928. This was a great breakthrough for the refrigeration as well as the air-conditioning industry. After World War II, CFCs were also used as propellants for bug sprays, paints, hair conditioners and other health care products (Elkins, 1997).

Then in 1974, two chemists of the University of California, Professor F.S. Roland and Dr. M. Molina, showed that CFCs could be the major source of inorganic chlorine in the stratosphere. They also found that the CFC gases can be decomposed by the UV radiation with some of the chlorine becoming active in destroying the ozone in the stratosphere. This discovery led to a global environmental treaty, the Montreal Protocol to Reduce Substances that Deplete the Ozone Layer, which was signed by 27 nations in 1987. This treaty originally made provision to reduce the 1986 production levels of CFCs by 50% before the year 2000, but a reassessment of the treaty in the year 1990 called for a total elimination by 2000 (Elkins, 1997).

The industry developed two classes of halocarbon substitutes; the hydrochlorofluorocarbons (HCFCs) and hydrofluorocarbons (HFCs). The ability of the HCFCs to destroy ozone is about 5% of that of the CFCs. This ability is reduced by the addition of hydrogen which shortens the atmospheric lifetime of the refrigerant. After another reassessment of the treaty in 1995, it was decided that the use of HCFC in South Africa had to be scaled down to 35% of the total amount used in 1989 by the year 2010, 10% of the amount used in 1989 in 2015, a mere 0.5% of the amount used in 1989 by the year 2020 and a total phase-out by the year 2030 (UNEP, 2000).

With the phase-out of CFCs and HCFCs, the only answer is the use of HFCs in the heat pump and refrigeration industries. These replacement refrigerants may be in the form of pure refrigerants or refrigerant mixtures, adhering to certain requirements. According to Atwood (1985:914) typical requirements would be:

- Ozone depletion potential;
- global warming potential;
- toxicity;
- flammability;
- chemical and thermal stability;
- compatibility with lubricating oil; and
- commercial availability.

Pretorius (1999:2) stated that there are no sufficient pure refrigerants to meet all of these requirements, and still cover the total range of operating conditions. This led to the inclusion of some flammable refrigerants to be investigated. Although flammability is not an outright exclusion, very few manufacturers are willing to take the risks involved in using flammable refrigerants. Most manufacturers have come up with the solution of mixing a flammable refrigerant with one or more non-flammable refrigerants resulting in a non-flammable mixture. According to Hwang *et al.* (1997:765) R32 is one of the most promising pure alternative refrigerants to use in heat pumps operating with R22. Unfortunately R32 is a flammable substance and thus not recommended for use as a pure substance. A possible answer is in the form of a mixture of R32 (23% wt), R125 (25% wt) and R134a (52% wt), which is known as R407C.

Another aspect that receives a lot of attention is the development of compact heat exchangers due to the constant need for smaller and more compact refrigeration units and heat pumps. One way of reducing the size of the heat exchanger is to modify the geometry in some way for more effective heat transfer. Another way of doing this is with the help of new refrigerants. With these new compact heat exchangers and new gases, new correlations have to be derived to calculate the size of the heat exchanger for sufficient heat transfer.

Various ways exist to increase the performance of the heat exchanger with geometric modifications to the heat exchanger resulting in a reduction in size. This is an important factor in the design of compact heat exchangers to be used in water heat pumps. The heat exchangers in water heat pumps consist mainly of tube-in-tube and shell-in-tube heat exchangers. Ways of improving the performance is to increase the refrigerant's contact area or by increasing the refrigerant's turbulence. This can be done with the use of micro-fins on the tube (Figure 1.1), fluted-tubes (Figure 1.2) or the use of twisted tape in the tube (Figure 1.3). A very compact heat exchanger can be manufactured by coiling of a fluted-tube.

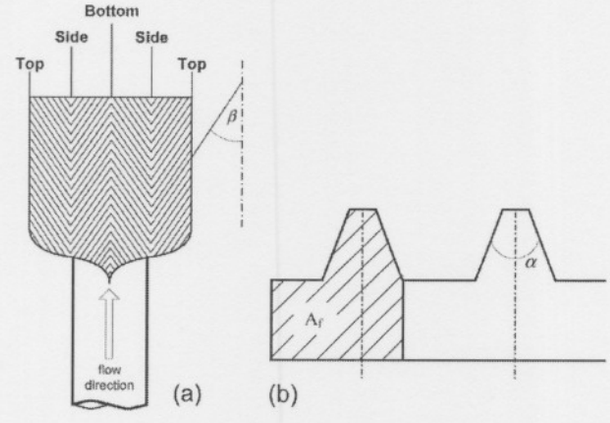

Figure 1.1 Micro-fin tube configuration a) micro-fin pattern; b) fin cross section.

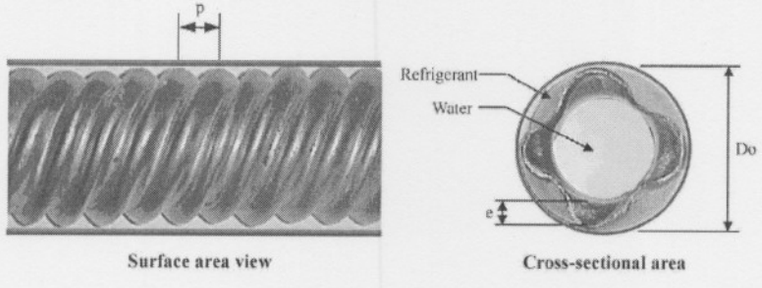

Figure 1.2 Fluted-tube configuration. (Rousseau *et al.* 2003:233)

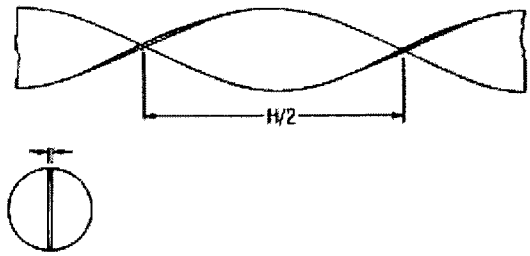

Figure 1.3 Twisted tape configuration.

The micro-fin tube is manufactured with various micro-fin patterns, micro-fin sizes and helical angles which are usually used in a tube-in-tube configuration. As can be deducted from Figure 1.1 the micro-fin tube provides an increase in heat transfer area and refrigerant turbulence. The fluted-tube (Figure 1.2) consists of an inner tube that is fluted to various flute depths and helical angles and an outer smooth tube. With this configuration the best results are found with the refrigerant in the annulus and the other liquid on the inside. In the case of the fluted-tube, the heat transfer area and the refrigerant's turbulence increase. The twisted tape can be used in a tube-in-tube heat exchanger with the tape inserted into the inner smooth tube. This configuration, with the refrigerant in the inner tube, only increases the refrigerant's turbulence and does not add much to the heat transfer area.

1.2 PROBLEM STATEMENT

In the design of energy efficient compact heat exchangers it is necessary to know the properties of the refrigerant used to calculate the heat transfer, pressure drop and efficiency of the heat exchanger. A problem arises in the fact that there are many correlations to predict the properties and heat transfer coefficients of the banned CFC and HCFC gases but very few are available for the calculation of the properties of the new halofluorocarbon (HFC) refrigerants, in pure form and in mixtures of different HFC refrigerants. The same limited number of correlations is found in the calculation of the heat transfer coefficients of refrigerants in fluted-tubes.

Limited literature and data are available on the heat transfer coefficients of R407C and even less data on the heat transfer coefficients of R407C in fluted-tubes. There is a need to experimentally determine the heat transfer coefficients of R407C in fluted-tubes to further the

ongoing research done in the School of Mechanical Engineering at the North-West University, as the only current work done was on R22 in fluted-tubes and R407C in smooth tubes.

1.3 AIM OF THE STUDY

The aim of this research study is to find an accurate correlation for the prediction of the forced convective boiling heat transfer coefficient of R407C in fluted-tubes.

To accomplish this, the following has to be done:

- The equipment developed by Venter (2000:36) need to be tested with R22 in a smooth tube-in-tube heat exchanger test section, to verify that all the measuring equipment is functional and working correctly. This is due to the fact that the test bench was decommissioned in 2002.
- The smooth tube-in-tube test section will then be replaced with a fluted-tube test section, after which the fluted-tube test section will be tested with R22 for a refrigerant mass flow range of 0.01 – 0.03 kg/s, evaporating pressures of 4 – 5.5 bar and various heat fluxes by varying the water inlet temperature between 13-22°C.
- After these tests, the R22 will be replaced with R407C. The fluted-tube will then be tested for the same refrigerant mass flow range, evaporating pressure range and heat flux range, as for R22.
- The data collected will be processed and compared to various existing heat transfer correlations.
- Based on the results of the different correlations a discussion will be entered into, on whether to derive a new correlation or combine various correlations.

1.4 IMPACT OF THE STUDY

The outcome of this study will be:

- Experimental data on the forced convective boiling heat transfer coefficient of R407C in fluted-tubes.
- Verification of various general correlations with the experimental data.

- A new correlation to accurately predict the forced convective boiling heat transfer coefficient of R407C in fluted-tubes.

The new correlation will be helpful in the design of compact heat exchangers for calculating the heat transfer and the efficiency of the heat exchanger. This will result in a more accurate design of compact heat exchangers with the new refrigerants. The correlation will also help to accurately calculate the heat transfer coefficients of the refrigerant in a simulation program.

1.5 SUMMARY

This chapter gives a brief overview of the history of refrigerants as well as ways to improve the heat transfer and efficiency of heat exchangers. The problem was stated that there is a scarcity of correlations to calculate the properties and heat transfer coefficients of new refrigerants and refrigerants in fluted-tubes. After the problem statement, the aim and plan of action was given with the intended impact of the study.

The following chapter lists all relevant information on R407C and fluted-tubes that was found in the detail literature survey. This information includes the heat transfer characteristics of R407C, the definition of refrigerant mixtures, and the correlations found relating to fluted-tubes and the boiling of R407C.

CHAPTER 2

2 LITERATURE STUDY

2.1 INTRODUCTION

In the previous chapter a brief history of refrigerants over the years was provided. Furthermore, a few methods to improve the heat transfer by changing the geometry of the heat exchanger were discussed. In this chapter a review is given of the heat transfer characteristics of pure refrigerants and refrigerant mixtures under forced convective conditions in smooth tubes as well as in enhanced tubes. Forced convection boiling of refrigerants is a complex process that is not yet fully understood. Now with zeotropic mixtures to complicate matters even more, it is necessary to have a clear understanding of zeotropic refrigerant behaviour.

For this reason the fundamentals of zeotropic behaviour are discussed first. This is followed by the theory of flow boiling of refrigerants and a brief discussion on the heat transfer degradation of zeotropic refrigerant mixtures. The chapter then concludes with a summary of work done on R407C for smooth and enhanced tubes.

2.2 BACKGROUND ON THE HEAT TRANSFER CHARACTERISTICS OF REFRIGERANT MIXTURES

2.2.1 MIXTURES OF REFRIGERANTS

With the phase-out of CFC and HCFC refrigerants according to the Montreal Protocol, it is necessary to find replacements that have similar thermodynamic and transport properties. Currently there are not enough pure refrigerants to function as replacements or drop-in replacements. To overcome that problem it was decided to use mixtures of the refrigerants.

Mixtures of two or more refrigerants can be formed to obtain specific thermodynamic properties. These mixtures provide easy ways of obtaining environmentally friendly substances and can be divided into three main groups:

- Azeotropic mixtures that behave as if the mixture is a homogeneous substance.
- Near-azeotropic mixtures that have a temperature glide less than 2.8°C during evaporation and condensation.
- Zeotropic mixtures that have a distinct temperature glide of more than 2.8°C during evaporation and condensation.

Most refrigerant mixtures, including R407C, form zeotropic mixtures when the pure refrigerants are mixed.

Raoult's law describes the vapour pressure curve for a gas mixture consisting of two components. It states that in an ideal solution the following has to be obeyed (Logan, 1997):

$p_i = p_i^* x_i \ (i = 1,2)$

p_i^* is the vapour pressure of pure liquid i at the temperature T of the ideal solution.

x_i is the mole fraction of i in the ideal solution

p_i is the vapour pressure of each component, thus

$P_{tot} = p_1^* x_1 + p_2^* x_2$

The total vapour pressure is therefore linearly related to the molar concentration between the vapour pressure curve of each component. This is illustrated in Figure 2.1, which shows an ideal mixture where the bubble point curve is a straight line. In the case of real mixtures all of the lines have a curve either deviating over or under the ideal case.

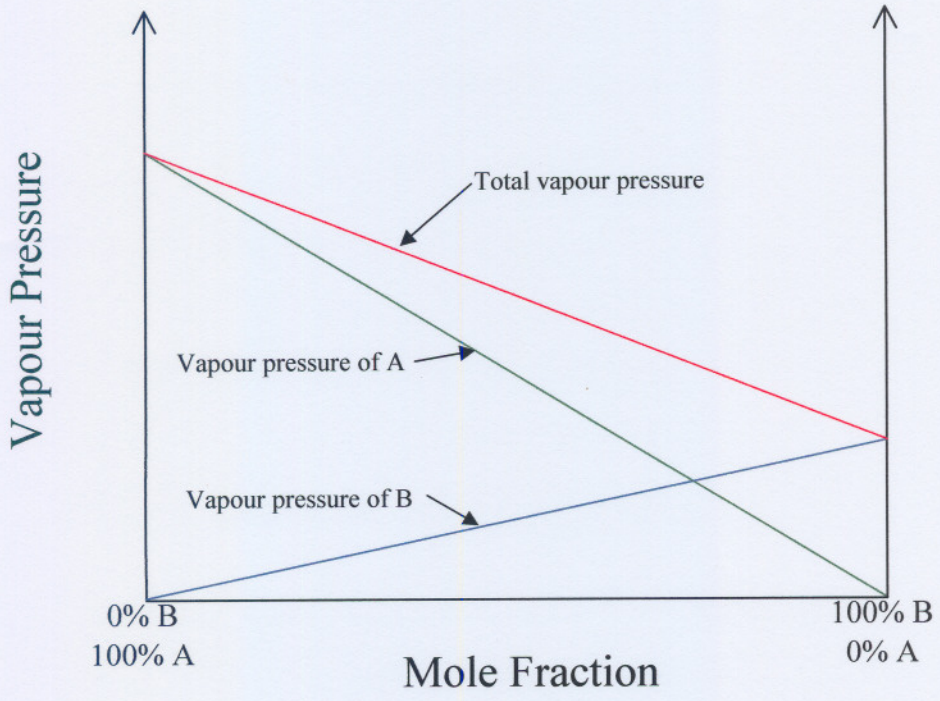

Figure 2.1 Pressure-molar fraction of ideal binary mixture.

For real mixtures at a constant temperature, three different behaviours may occur that are illustrated in Figure 2.2 and is described by Venter (2000:8) as follows:

- Curve 1: At some concentrations the vapour pressure is higher for the mixture than for any one of the pure components. Such a mixture has a positive azeotropic composition at the extreme point (p) in the curve. Examples of such mixtures are R502 and the R410 series of refrigerants.
- Curve 2: At some concentrations the vapour pressure is lower for the mixture than for any one of the pure components. Such a mixture has a negative azeotropic composition at the extreme point (q) in the curve. An example of such a mixture is R507.
- Curve 3: In this mixture, the vapour pressure curve of the mixture lies between the curves of the pure components over the entire range of the concentration. An example of such a mixture is R407C.

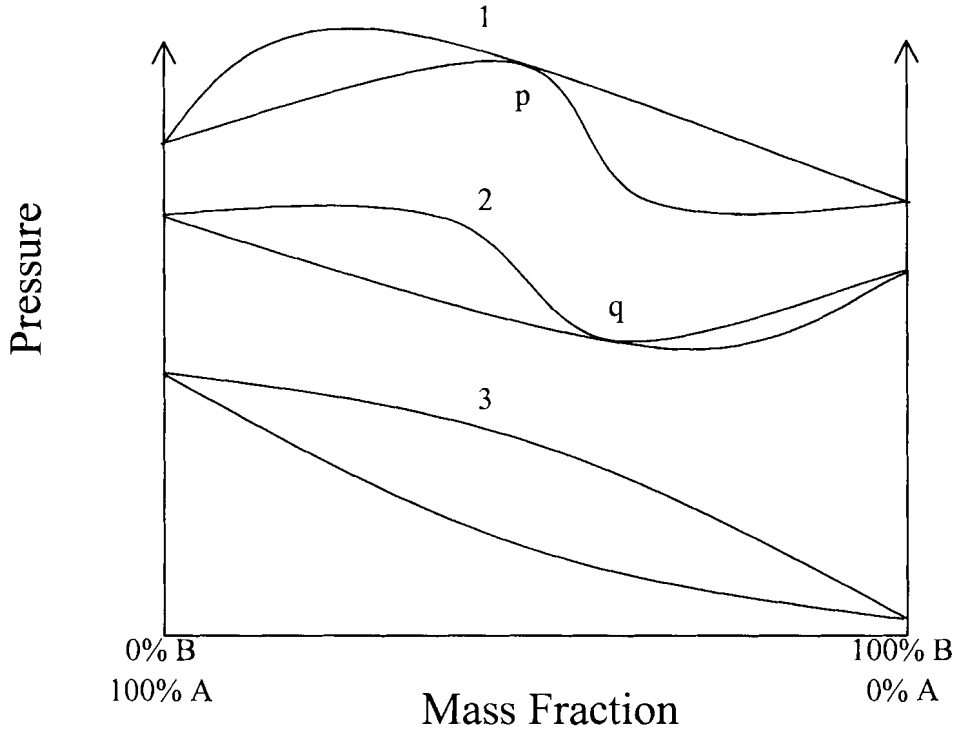

Figure 2.2 Pressure-mass fraction behaviour of real binary mixtures. (Venter, 2000:8).

The points p and q in Figure 2.2 are called extreme points. This is where the bubble and dew point lines are at the same pressure with no change in concentration during phase change. These extreme points define an azeotropic mixture at the given mass fraction composition that behaves as a pure substance during phase change. From curve 3 it is clear that no extreme points exist and is thus defined as a zeotropic mixture.

2.2.2 ZEOTROPIC MIXTURES

Certain benefits can be derived by using refrigerant mixtures compared to pure refrigerants. Some of these benefits include lower operating pressures, increased capacity and higher condensing temperatures. The temperature glide of zeotropic refrigerant mixtures during evaporation and condensation can provide an inherent improvement on the refrigeration system efficiency (Albrecht, 1996).

In the case of a pure refrigerant the temperature will remain constant during evaporation or condensation if the pressure is kept at a constant value during the entire phase changing process. The phase change temperature is related to the pressure by a vapour pressure function

that can be presented as a vapour pressure curve. This can be seen in the saturated vapour pressure curve of R32 as shown in Figure 2.3. This figure was plotted with the property calculations of EES (Engineering Equation Solver).

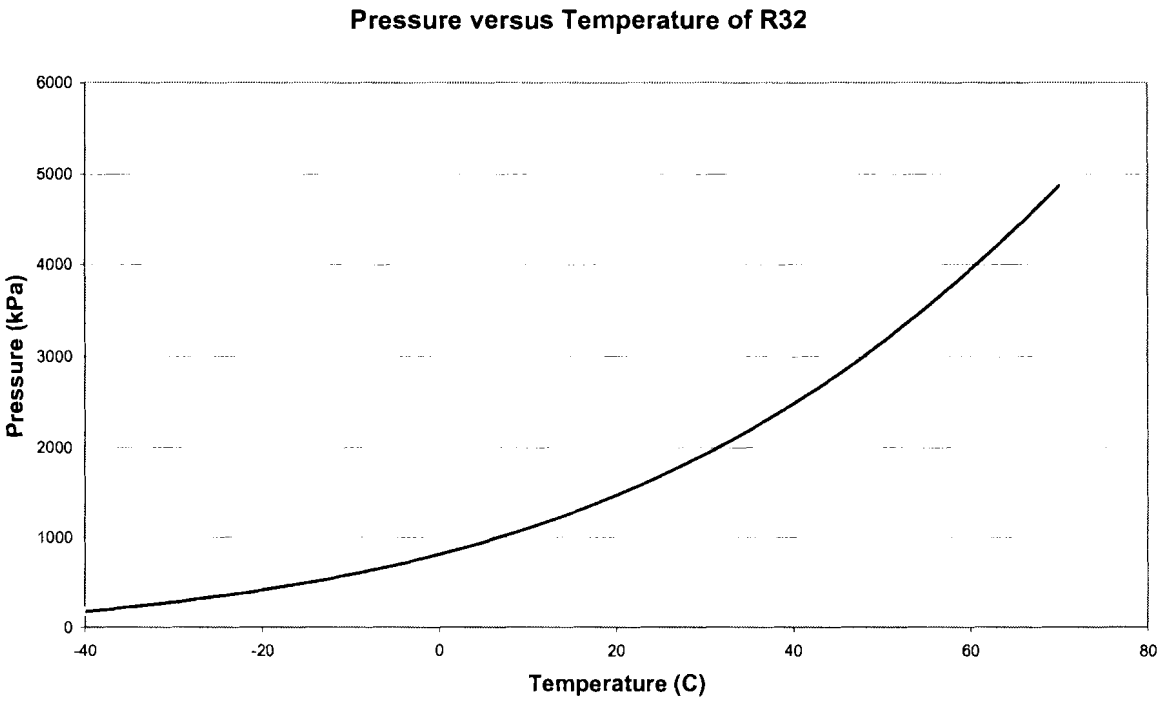

Figure 2.3 Vapour pressure-temperature chart of R32.

When a mixture consisting of two or more refrigerants is formed, the temperature at which phase change will occur will not only be a function of the pressure but also a function of the mixture composition. Figure 2.4 shows the pressure-temperature relation of a binary refrigerant mixture. The respective vapour pressure curves for the two components A and B at a specific temperature can be seen on the front side of the graph, with the lower curve the bubble point curve and the upper curve the dew point curve. The area enclosed by the two curves is where both the liquid and vapour phases will exist.

To fully understand the boiling and condensation processes of a binary mixture it is easier to study the phase change process by varying the temperature and keeping the pressure constant, as shown in Figure 2.5.

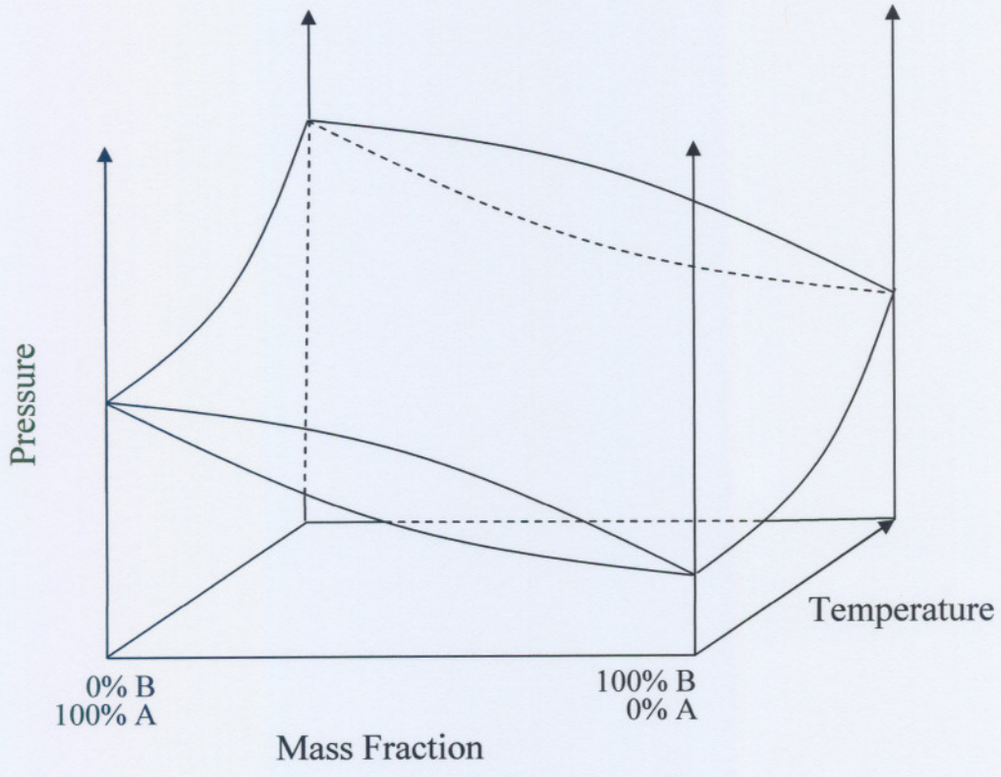

Figure 2.4 Vapour pressure-temperature-mass fraction chart of binary mixture.

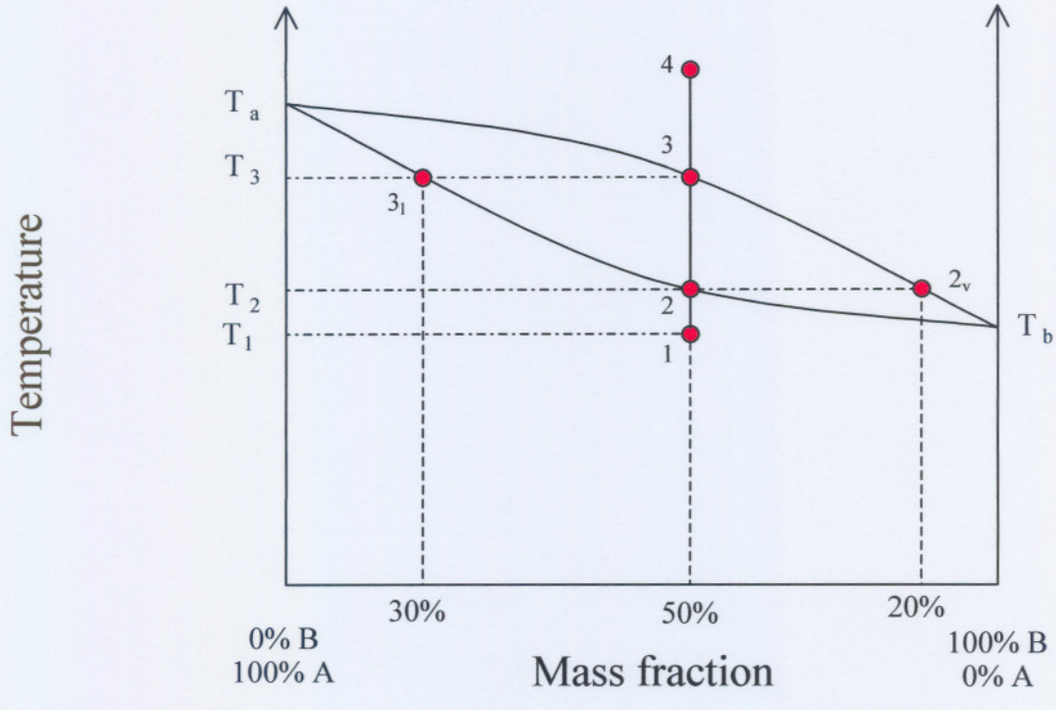

Figure 2.5 Phase change process of a binary mixture.

In Figure 2.5, the phase change process for a binary mixture with 50% A composition and 50% B composition is illustrated. Consider the case where heat is added to the refrigerant at constant pressure. The refrigerant temperature will increase from point 1 where it is a sub-cooled liquid at temperature T_1 to point 2 at temperature T_2. At this point the first bubbles start to form; the first vapour bubble has a composition of 20% A and 80% B with the liquid composition still at 50% A and 50% B.

With more heat added to the refrigerant the temperature will increase with a reduction of liquid and an increase of vapour. The liquid composition will change along the bottom curve from 2 to 3_l, whereas the vapour composition will change along the top curve from point 2_v to 3. When the temperature reaches T_3 the last drop of liquid will have a composition of 70% A and 30% B with the vapour composition the original composition of 50% A and 50% B. More heat will result in a super heated vapour.

The temperature difference between points 2 and 3 is called the temperature glide of the mixture and is dependant on the single phase mixture composition. This temperature glide theoretically could result in improved system efficiencies of heat pumps and refrigeration systems. This is described more clearly in the following paragraph.

2.2.3 STEADY-STATE EFFICIENCY IMPROVEMENT

The efficiency of any thermodynamic cycle can be improved by reducing the enclosed area of the cycle on a temperature-entropy diagram (Venter, 2000:12). One way to reduce the area is by reducing the refrigerant superheat at the outlet of the compressor by selecting an appropriate refrigerant. Another way is to reduce the temperature difference between the refrigerant and the outside source by increasing the heat transfer surface and/or increasing the outside fluids' flow rate.

The enclosed area of the T-s diagram can also be reduced if the temperature profile of the refrigerant in the heat exchanger is matched to the temperature of the outside fluid. This is where the temperature glide of the zeotropic refrigerant mixtures can play an important role in the system efficiency. This process will now be discussed in detail in the following paragraphs and with the help of Figure 2.6.

Diagram 1 in Figure 2.6 shows the most common isothermal vapour compression cycle for pure refrigerants or azeotropic refrigerant mixtures. The enclosed area can be reduced in an ideal process to the temperatures shown in diagram 2. Since ideal processes do not exist and the possibility for pinch point is too great, this situation is avoided. With the use of zeotropic refrigerant mixtures diagram 1 can be swivelled on the points as shown in diagram 3.

This does not result in a reduction of the enclosed area on the T-s diagram but it enables both phase change processes to be shifted towards the temperature gradient of both outside fluids as shown in diagram 4. This in turn reduces the enclosed area in the T-s diagram for the cycle while maintaining the same exit temperatures of the outside fluids. The possibility of pinch points are thus reduced with the use of the temperature glide of the zeotropic refrigerant mixtures during phase change. The temperature glide also allows the heat transfer process to be shifted closer together.

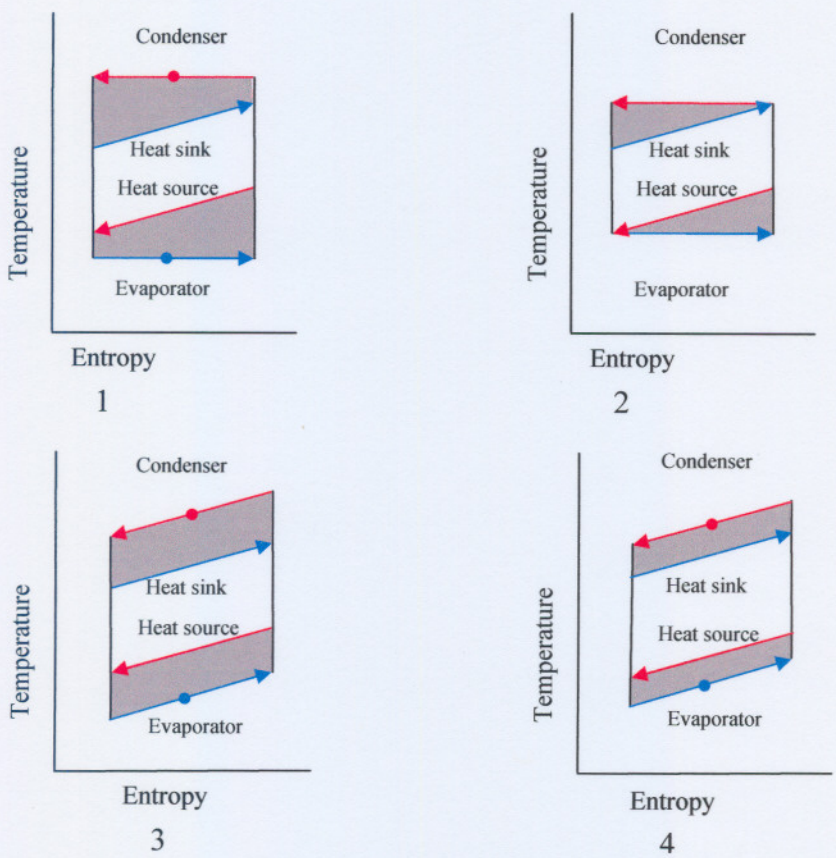

Figure 2.6 Process of heat pump efficiency improvement.

The modification of the isothermal vapour compression cycle to the system shown in diagram 4 in Figure 2.6 is referred to as the Lorenz vapour compression cycle (Johannsen, 1992). Figure 2.7 shows the difference between the isothermal vapour compression cycle of a pure refrigerant and the Lorenz cycle.

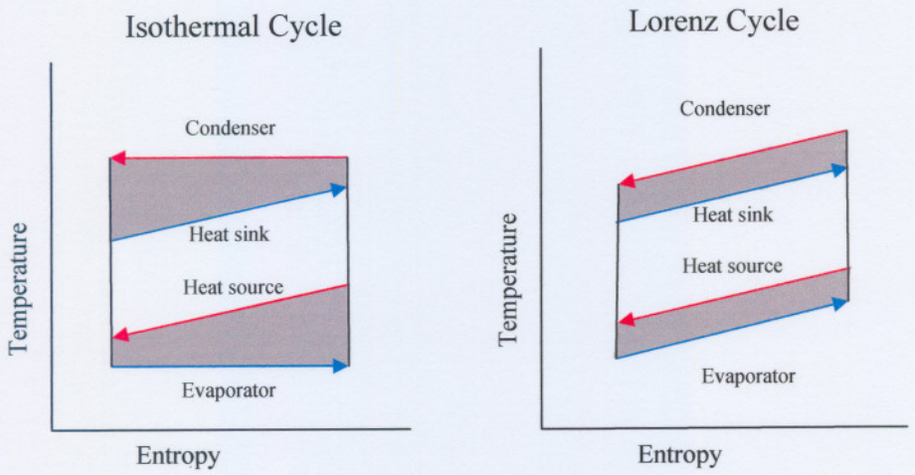

Figure 2.7 Isothermal and Lorenz vapour compression cycle.

2.2.4 HEAT TRANSFER CHARACTERISTICS

2.2.4.1 TWO-PHASE FLOW PATTERNS

Most researchers treat the heat transfer coefficients during the boiling of refrigerants as two different components. The one component is the pool boiling component and the other one is the forced convective boiling component. The reason for this is because of the complex nature of forced convective boiling. With refrigerant mixtures this process is even more complex.

Various distinct flow patterns can be identified during the evaporation process of refrigerants inside tubes. Some of these include bubbly flow, slug flow and annular flow. To predict the flow pattern for a specified system is a difficult task, even more difficult is the prediction of the pressure drop and heat transfer. Figure 2.8 shows the flow pattern characteristics of horizontal flow of a two-phase substance (Mills, 1995:649). The gravity force perpendicular to the flow causes certain differences from that of flow in a vertical tube, especially at low flow rates. The actual flow pattern encountered in the system will depend primarily on the flow velocity and the relative amounts of liquid and vapour.

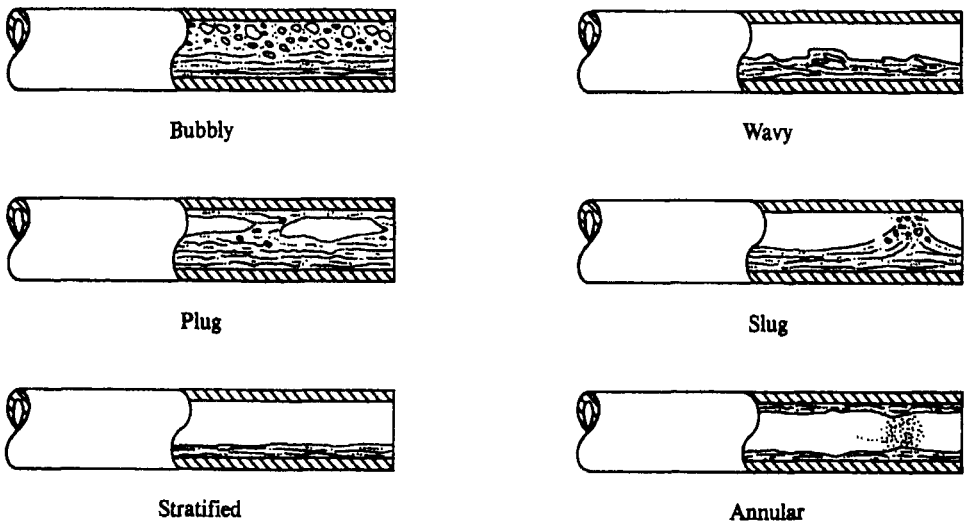

Figure 2.8 Flow patterns of horizontal co-current two-phase flow (Mills, 1995:649).

The flow patterns are defined as follows (Mills, 1995:647):

a. *Bubbly flow.* The vapour is in the form of isolated bubbles in the liquid phase. The bubbles may be small and spherical, or large enough to develop a spherical cap shape.
b. *Plug flow.* Small bubbles come together to form larger bubbles. These bubbles then result in an increase in the fluid's velocity. The bubbles tend to flow in the upper half of the tube.
c. *Slug flow.* Bubbles are approximately of the diameter of the tube, and a film of liquid runs down the tube wall. In between the bubbles are slugs of liquid, which may contain some small bubbles.
d. *Intermitted flow.* (Not shown) Is a combination of slug and plug flow.
e. *Annular flow.* The phases are almost completely separated into a vapour core and a liquid film on the wall. There is, however, some entrainment of droplets from the crests of waves that form on the surface film.
f. *Stratified flow.* At low liquid and vapour flow rates the liquid flows with a relatively smooth surface along the bottom of the tube. In this case the vapour velocity is usually higher than the velocity of the liquid.

g. *Wavy flow*. As in the case with stratified flow, but in this case the flow rates are higher resulting in waves in the liquid part of the fluid. If the flow rate increases more the flow would become slug flow.

2.2.4.2 *INTERNAL FORCED CONVECTIVE BOILING*

The internal forced convective boiling of a fluid in a tube is explained with the help of Figure 2.9. Sub-cooled liquid enters the tube and is heated by forced convection to its saturation temperature in the first section of the tube. With added heat the pool boiling process produce bubbles on the surface of the tube. These bubbles grow in size until they are carried into the mainstream of the liquid. This is the start of the bubbly flow regime. In this regime there is a sharp increase in the convection heat transfer coefficient. As more and more bubbles form, the bubbles continuously grow in size and break down until some of the bubbles are big enough to form liquid slugs.

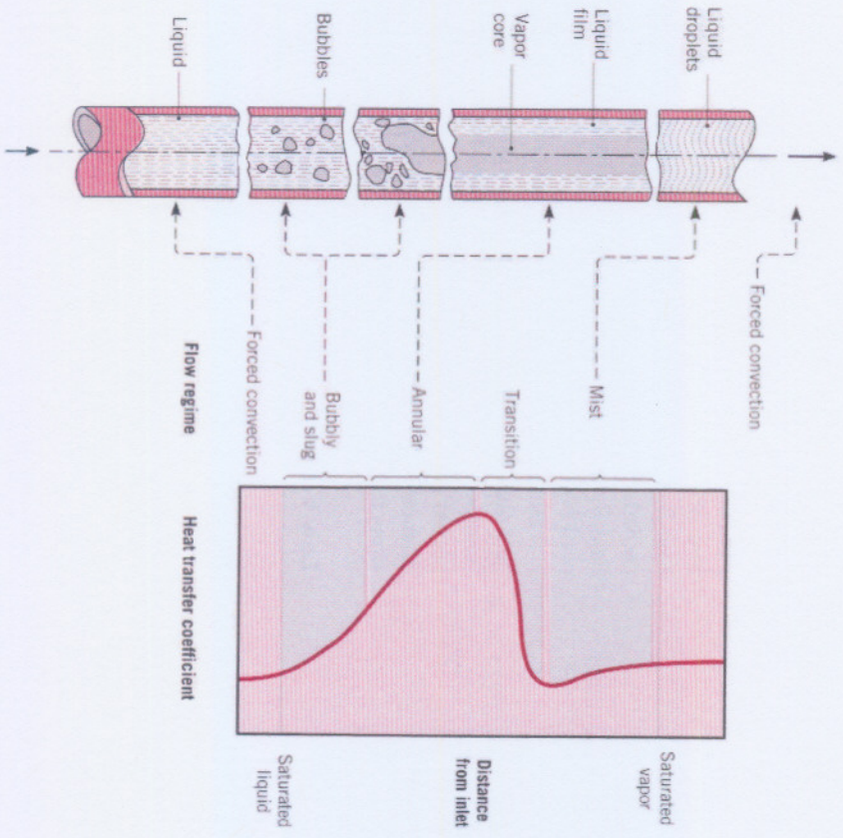

Figure 2.9 Flow regimes inside a horizontal evaporator (Incopera and DeWitt, 2001:612).

Following the slug region is the annular region, a transition region, the mist region and ultimately the superheated gas region. The heat transfer coefficient continues to increase through the bubble region and much of the annular region. However, dry spots start to form in the annular region and results in a reduction of the heat transfer coefficient until the beginning of the mist region. There is then a slight increase in the heat transfer coefficient through the mist region and then the coefficient stabilizes through the superheat region.

Evaporation processes are dominated by two modes of heat transfer. The first mode is pool boiling. This is where the motion of the liquid near the surface is due to free convection with mixing through the movement of bubbles. The second mode of heat transfer is called forced convective boiling. In this mode the fluid motion is due to external means, as well as free convection and the mixing effect of the bubbles forming.

2.2.4.3 HEAT TRANSFER DEGRADATION

The heat transfer degradation of zeotropic refrigerant mixtures is the result of mass transfer resistance and can be explained as follows (Venter, 2000:19). During evaporation, the more volatile component of the mixture boils initially at a higher rate than the less volatile component, leaving the liquid rich in the high boiling-point component (less volatile) at the interface between the liquid and the growing bubble. The result is a locally increased liquid temperature that reduces the temperature difference between the liquid at the interface and the vapour bubble. This diminished temperature difference causes degradation of the heat transfer across the interface and results in a reduction of the heat transfer coefficient based on the bulk equilibrium temperature. The reduction in the heat transfer coefficient gets more pronounced when the equilibrium concentration difference between the liquid and vapour phase increases and also for an increase in the heat flux and pressure.

2.2.5 NORMAL BOILING POINT

The normal boiling point of a substance is defined as the temperature where the substance in liquid form will start to boil at atmospheric pressure. By comparing the boiling points of various substances a method of measurement is provided with which the correct system pressure can be approximated. Substances with a lower normal boiling point will have a

higher system pressure and substances with a higher boiling point will result in a lower system pressure.

Using the normal boiling point as a measurement, a possible replacement for R22 can be selected where the replacement refrigerant has approximately the same value. Table 2-1 shows a selected amount of refrigerants sorted according to their normal boiling points. The table also shows some physical properties.

Refrigerant	Molecular mass	Normal boiling point (°C)	Latent heat of evaporation (kJ/kg)	Critical temperature (°C)	Critical pressure (Bar)	Critical density (kg/m^3)	Ozone depletion potential	Global warming potential	Flammable	Composition
R32	52.0	-51.8	383	78.4	58.1	430	0.0	220	Yes	HFC
R410a	72.5	-51.6	373	70.2	47.7	552	0.0	1890	No	R32/R125
R125	120.0	-48.6	164	66.3	36.3	572	0.0	860	No	HFC
R143a	84.0	-47.4	230	73.1	38.1	434	0.0	1000	Yes	HFC
R407C	**86.2**	**-43.8**	**248**	**86.1**	**46.3**	**513**	**0.0**	**1610**	**No**	**R32/R125/ R134a**
R22	**86.4**	**-40.8**	**234**	**96.2**	**49.9**	**513**	**0.05**	**1700**	**No**	**HCFC**
R134a	102.0	-26.1	217	101.1	40.6	515	0.0	1300	No	HFC
R152a	66.0	-24.7	325	113.2	44.9	369	0.0	120	Yes	HFC

Table 2-1 Physical properties of selected refrigerants sorted according to normal boiling point. (Venter, 2000:21; Allchem, 2002)

From the table it can be seen that the normal boiling point of R407C is the closest to that of R22. R407C is non-flammable and will result in a slightly higher system pressure. The main concern in using R407C as a drop-in substitute for R22 systems is that R407C is not compatible with the mineral oil used by most R22 systems. The mineral oil should therefore be removed, the system thoroughly cleaned and then replaced with a suitable ester oil. In some cases some of the equipment components should also be replaced in case the components are not compatible with ester oil.

The temperature glide of R407C might have an improvement in the coefficient according to the Lorenz cycle (paragraph 2.2.3) provided the system was designed for R407C. Some of the equipment in two systems with identical capacities, one using R22 and the other one using R407C could vary. It is these equipment variations that present the biggest problems in using R407C as a drop-in substitute for R22.

Certain disadvantages arise with the use of zeotropic mixtures. The first comes in the form of leakages. In this case the possibility is very good that the more volatile component of the mixture has been lost, thus resulting in a change in composition of the mixture. For the same reason it is very important to always charge liquid into a system. The second comes from the possibility that the more volatile component is boiled off, resulting in system efficiency drop.

2.3 REVIEW OF PREVIOUS WORK ON PURE REFRIGERANTS AND REFRIGERANT MIXTURES

Numerous studies have been completed on the determination the heat transfer coefficients of various refrigerants. The following section reviews the most relevant of these studies.

Gungor and Winterton (1986:351) formulated a general correlation for forced convection boiling in horizontal and smooth tubes, with the help of a data bank of 4300 data points. These data points are from water, various refrigerants and ethylene glycol, covering a total of seven fluids and 28 authors. The new correlation is simpler to apply and gives an overall closer fit to the data than existing correlations. The mean deviation between the calculated and measured boiling heat transfer coefficient were 21.4% for saturated boiling and 25.0% for sub-cooled boiling.

Gungor and Winterton (1987:148) developed a simplified general correlation for the prediction of the heat transfer coefficients of pure substances. This is an improved correlation to the Gungor and Winterton (1986:351) correlation. The correlation was tested with 4202 data points for saturated boiling and 946 data points for sub-cooled boiling that included data on R11, R12, R22 and R113. Gungor and Winterton (1987:148) found that the correlation predicted the heat transfer coefficients of the mentioned refrigerants with a mean deviation,

defined as $\frac{1}{n}\sum_{1}^{n}\left|\left(h_{cal}-h_{\exp}\right)/h_{\exp}\right|\cdot 100$ of 20.4% and an average deviation, defined as $\frac{1}{n}\sum_{1}^{n}\left(\left(h_{cal}-h_{\exp}\right)/h_{\exp}\right)\cdot 100$, of -7.9%.

Another general correlation for the prediction of the heat transfer coefficients was developed by Liu and Winterton (1991:2759). This correlation was tested against the same data used by Gungor and Winterton (1987:148), with the exception of the sub-cooled data that was increased to 991 data points. It was found that the correlation predicted the heat transfer coefficients of all the data with mean and average deviations of 20.5% and -2.3% respectively.

Zhang *et al.* (1997:2009) experimentally investigated the boiling heat transfer of R407C inside a horizontally smooth tube with an inside diameter of 6.0 mm. The authors also presented a theoretical model predicting the heat transfer coefficients of the mixture. Results showed that the heat transfer coefficients of the mixture were on average 30% lower than those of R134a, this being attributed to the mass transfer resistance near the gas-liquid phase. The correlation predicted the experimental data within ± 30%.

Kattan *et al.* (1998c:156) developed a new heat transfer model for intube boiling in horizontal plain tubes that incorporates the effect of local two-phase flow patterns, flow stratification and partial dryout in annular flow. The local peak in the heat transfer coefficient versus the vapour quality can be determined from the prediction of the location of onset of partial dryout in annular flow. The new model accurately predicts a large, new database of flow boiling data, and is particularly better than exciting methods at high vapour qualities ($x > 0.85$) and for stratified types of flows.

Choi *et al.* (2000:3651) did experimental tests on the evaporative heat transfer of R32, R134a, R32/R134a and R407C inside horizontal smooth tubes. The tests were done for evaporating temperatures of -12 to 17 °C, mass flux of 240-1060 kg/m^{2}s and heat flux of 4.1-28.6 kW/m^2. Evaporative heat transfer characteristics of R407C have been compared to those of R22. A new correlation based on a superposition model for pure refrigerants and refrigerant mixtures was presented. Experimental results were compared to several correlations which predicted

evaporative heat transfer characteristics. Comparison with the experimental data in the open literature showed that their correlation gave a satisfactory result with a mean deviation of 13.2% based on 2971 data points obtained from the experiments for pure refrigerants and refrigerant mixtures.

Venter (2000:1) did experiments on R407C inside a horizontally smooth tube. The experimental data were acquired with variations of heat flux, mass flux and evaporating pressures. The results were then evaluated against five different correlations. These correlations included Pierre (ASHRAE, 1997:4.7), Gungor and Winterton (1987:148), Liu and Winterton (1991:2759), Melin (Venter, 2000:72) and Zang *et al.* (1997:2009). It was found that the correlations were unable to correlate the experimental data for vapour qualities higher than 0.95. For qualities less than 0.95 the correlation of Gungor and Winterton (1987:148) predicted the experimental data the best, with mean and average deviations of 6.1% and 14.0% respectively.

A performance test was done by Kim (2002:167) on R22 and four alternative fluids (R134a, R32/R134a (30/70%), R407C and R410A) at operating conditions typical for residential air conditioners. In the study it was found that at the same capacity R410a had the highest coefficient of performance. R407C and the R32/R134a mixture had the closest characteristics to R22 with R32/R134a having a slightly better coefficient of performance (COP), where the COP is divined as: cooling capacity divided by input power. The important parameters including the evaporating and condensing pressures and the compressor discharge pressure did not deviate significantly from the R22 values.

Lee *et al.* (2002:575) did a drop in test of R407C in a commercial chiller with shell-and-tube heat exchangers originally designed for R22. The test results showed a severe performance reduction when substituting the refrigerant with R407C. The major factor causing the performance reduction was assessed as the degradation of the heat transfer in using R407C. It was found that the heat transfer degradation in the evaporator was double the degradation of the heat transfer in the condenser, with a 10 – 20 % reduction of cooling capacity. This reduced heat transfer in the evaporator resulted in a 20 – 30 % reduction of the system COP.

Experimental tests were done by Jung *et al.* (2003:764) on mixtures containing R32, R125 and R134a inside a 19 mm tube with constant heat flux. The heat flux was decreased from 80 – 10 kW/m^2. From the experiments it was found that zeotropic mixtures of R32/R134a, R125/R134a and R32/R125/R134a showed a reduction in the heat transfer coefficients up to 40% of the ideal values while the near-azeotropic mixture of R32/R125 did not show the reduction. Four well-known correlations were compared against the data for binary mixtures with some of the correlations giving a deviation of less than 10%. A new correlation was developed and with regression analyses, to account for the reduction of the heat transfer coefficients, it yielded a deviation of 7% for all binary and ternary mixtures.

Zhang *et al.* (2004:5749) defined three types of channels: conventional channels (D_h larger as 3 mm), mini-channels (D_h between 200 μm and 3 mm) and micro-channels (D_h between 10 μm and 200 μm). With this they stated that liquid-laminar and gas-turbulent flow is common features in many applications of mini-channels and that traditional heat transfer correlations for saturated flow boiling were developed for liquid-turbulent and gas-turbulent flow conditions, and thus may not be suitable to predict the heat transfer coefficient in mini-channels. The Chen correlation was then modified and used for liquid-laminar, liquid-turbulent, gas-laminar and gas-turbulent. This modified correlation showed a satisfactory agreement with a mean deviation of 18.3% with existing data for mini-channels.

Because of the potential variation of the fluid composition, many designers are concerned by the use of zeotropic refrigerant mixtures in refrigeration and air-conditioning system. Youbi-Idrissi *et al.* (2005) proposed a local simulation model of a water-to-water heat pump by adapting a modular approach. Their numerical results showed that, compared to the nominal composition of R407C, the circulating composition in the machine is low in the less volatile component R134a (-3% variation) and rich in the most volatile component R32 (+3% absolute). In the regions where the condensation begins and the evaporation ends, the local composition is noticeably different from both the circulating and nominal compositions.

2.4 *REVIEW OF PREVIOUS WORK ON ENHANCED TUBES*

Various correlations for the determination and prediction of the heat transfer coefficients of refrigerants were tested and developed in the use of enhanced tubes. All of the relevant correlations are reviewed in this section.

Research was done by Christensen and Garimella (1990:1) on spirally-fluted tubes and enhanced tubes in confined cross flow configurations. The study included heat transfer and friction losses through spirally fluted inner tubes in the laminar, transition and the turbulent flow regimes. Fourteen different fluted-tubes were tested with up to three different outer smooth tubes for each of the fluted-tubes. Correlations to calculate the heat transfer coefficient, friction factor and Nusselt number were developed from the research.

Christensen *et al.* (1993:1) wrote a heat exchanger design manual for fluted-tubes, which includes tube-in-tube and confined cross flow geometries. The manual gives all the necessary equations to be used and explains step-by-step how to use them in the design of compact heat exchangers. This manual is based on the work done by Christensen and Garimella (1990:1).

MacBain *et al.* (1997:65) did heat transfer and pressure drop experiments with R22 and R134a inside a horizontally deep spirally fluted tube. They found that the heat transfer for R12 increased by 50 – 170% but the pressure drop was 6 to 20 times greater in comparison with a smooth tube. The heat transfer of R134a was 40 – 150% higher with the pressure drop of 11 – 19 times greater than for the smooth tube.

Experiments on micro-fin tubes were done by Sami and Desjardins (2000:1047). In their experiments R404a, R407b, R407C and R408a were tested and it was found that with a high Reynolds number ($Re > 26\ 000$), R404a and R408a had the best heat transfer coefficient. The pressure drop was the lowest for R407C for all of the test range ($30\ 000 < Re < 50\ 000$).

An experimental investigation of two-phase flow condensation of alternatives to R22 inside enhanced surface tubing was done by Sami and Maltais (2000:1113). The alternatives consisted of R507, R404a, R407C, R408a and R410a. It was evident from the data that R408a had the highest heat transfer rate compared to the other refrigerants. However, when the thermo-physical properties were factored in, the condensation data showed that R410a had

the highest heat transfer rate at Reynolds numbers higher than 2.35×10^7. The test also showed that R410a had the highest convective pressure drop.

Tests were conducted by Bukasa (2002:44) for the condensation of R22, R134a and R407C inside a smooth and three micro-fin tubes. These micro-fin tubes were identical to each other with only the spiral angles that were varied at respectively 10, 18 and 37 degrees. The experimental results showed an increase in heat transfer with the increase of spiral angle degrees. This increase of heat transfer was explained due to the increase of the heat transfer surface area, combined with the increase in turbulence, and to the redistribution of liquid around the tube perimeter due to surface tension drainage induced by the fin.

Passos *et al.* (2003:705) did experimental work on the nucleate and convective boiling of R407C inside plain and micro-fin tubes with outside diameters (OD) of 7.0 and 12.7 mm. The heat flux was varied from 10 to 20 kW/m^2 and mass flux velocities between 200-300 kg/m^{2}s at a pressure of 770 kPa. The experimental data was discussed in terms of the heat transfer coefficient and the pressure drop as a function of the vapor quality. For a heat flux of 10 kW/m^2 and a mass flux velocity of 200 kg/m^{2}s, the dominant heat transfer mechanisms for the 7 mm tube is the nucleate boiling regime whereas for the 12.7 mm tube it is the convective boiling regime.

A detailed simulation of fluted-tube water heating condensers using R22, was done by Rousseau *et al.* (2003:232). The simulation allows for an extension of the model to simulate heat exchangers for cycles employing zeotropic refrigerant mixtures. As mentioned by them, no correlations were available at that time for the refrigerant side to calculate friction and heat transfer coefficients in the annulus. This simulation was based on the design manual of Christensen *et al.* (1993:1).

An experimental investigation of in-tube evaporation of R134a was carried out for a 4m long herringbone micro-fin tube with an outer diameter of 9.53 mm by Wellstandt *et al.* (2005). The data from the tests were compared to the literature and available helical micro-fin correlations. With the vapour quality less than 50% the correlations predicted the values within ± 30% of the experimental values. In the case where the vapour was more than 50% no correlation was able to reflect the early peak of heat transfer coefficients.

2.5 SUMMARY

This chapter explained that refrigerant mixtures can form three different kinds of mixtures, which include azeotropic, near-azeotropic and zeotropic mixtures. It was explained how the temperature glide of the zeotropic refrigerant can be used to improve the cycle efficiency with the use of the Lorenz cycle. The different flow regimes for horizontal two-phase flows were illustrated and explained. Together with the flow regimes it was explained that the heat transfer coefficient is dependant on the type of flow. It could also be seen that from the beginning of the boiling process to where all the liquid are a superheated vapour the heat transfer coefficient increases and then starts to decrease when dry spots start to form on the tube surface.

In the literature survey it was found that there is little information on boiling of R407C in fluted-tubes. Various correlations were found on boiling of refrigerants in smooth tubes and some of the correlations were for micro-fin tubes. The only correlation for refrigerants and fluted-tubes that was found was the simulation of a fluted tube water heating condenser using R22 by Rousseau *et al.* (2003:232). With this information it is evident that there is a deficiency in the current research of boiling of the zeotropic refrigerant R407C in fluted-tubes.

In the following chapter the layout of the experimental facility to be used in this research and the layout of the support mixing systems are explained. The explanation includes the detail of each component used in the experimental facility. The support systems include various water loops that supply the test bench with the correct temperature and/or mass flow rate. All of the components of the water loops and the control logic are also explained in detail.

CHAPTER 3

3 LAYOUT OF THE EXPERIMENTAL FACILITY

3.1 INTRODUCTION

This chapter describes the layout of the test bench for the measurement of the forced convective boiling. The test bench consists of a vapour-compression system with external water supply loops. First, the layout of the vapour-compression system and water supply loops is discussed, and thereafter the data acquisition system. Other topics that are addressed are the control of the test bench and the validation of the measuring equipment.

3.2 LAYOUT OF THE EXPERIMENTAL TEST BENCH

3.2.1 BASIC LAYOUT OF THE TEST BENCH

The layout of the vapour-compression system is shown in Figure 3.1. The system is almost identical to the one used by Venter (2000:37) for his experimental determination of the forced convective boiling heat transfer coefficient of R407C in smooth tubes.

This system is of a split evaporator design with separate expansion valves for each evaporator. The evaporator and expansion valve described by points 3-6-9 is the main evaporator, whereas the section 3-4-5-7-8-9 includes the sub-cooler and the test evaporator. The test evaporator is divided into three sections namely the pre-evaporator, test section and super-heater and they will be discussed in more detail in Par. 3.2.2.4.

In the main evaporator an automatic expansion valve is used to provide a constant pressure drop that can be adjusted with a setting screw; allowing control of the evaporating pressure in both the test evaporator and main evaporator.

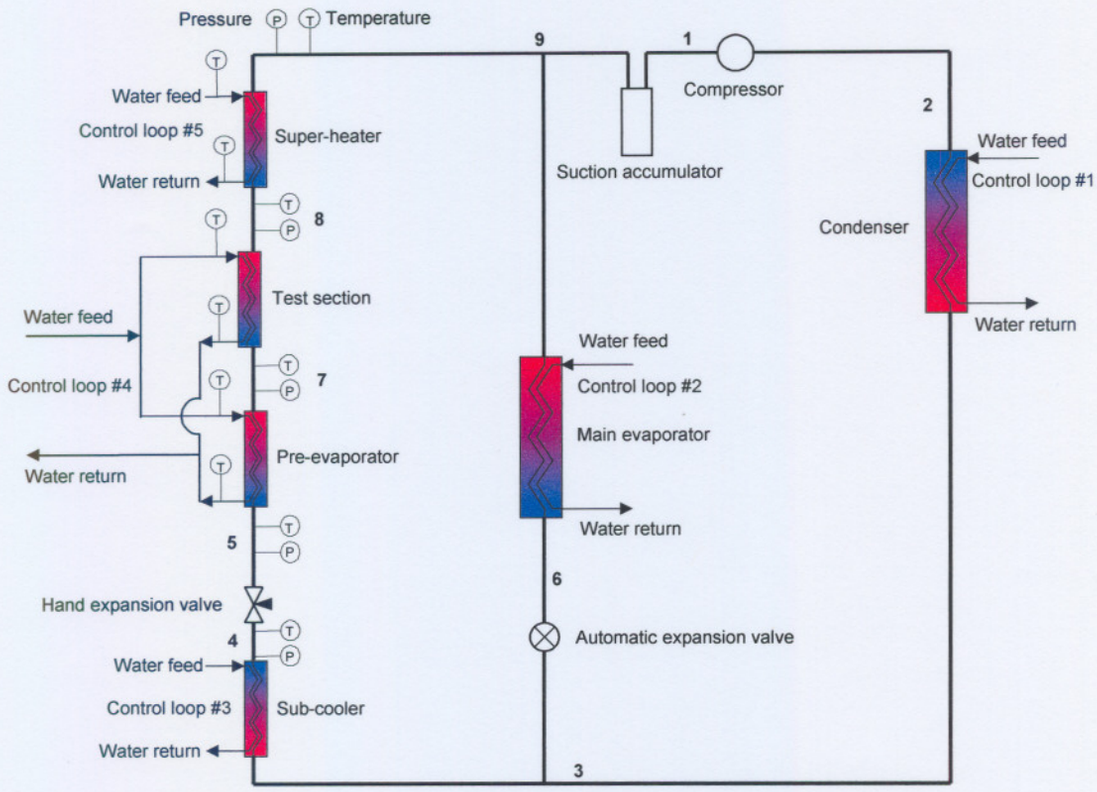

Figure 3.1 Layout of the test bench refrigerant circuit (Venter, 2000:37).

The test evaporator uses a hand expansion valve that provides control of the refrigerant mass flow through the test evaporator. Since the refrigerant heat transfer coefficient is a function of vapour quality, the refrigerant is passed through a sub-cooler, shown between points 3 and 4, in order to vary and control the dryness fraction at point 5 just before the refrigerant enters the test evaporator.

As shown by Figure 3.1, all the heat exchangers are supplied with water through external water loops. Each of these water loops is capable of controlling the water temperature and/or the water mass flow rate at the inlet of the heat exchangers. The layouts of these systems are discussed in more detail in par. 3.2.3.

Figure 3.2 shows the refrigerant cycle of the test bench on a temperature-entropy diagram with the numerical points and measurement sensors corresponding to those in Figure 3.1. In this figure points 5 and 5' show the effect of the sub-cooler on the vapour quality of the refrigerant entering the test evaporator. The qualities of the refrigerant at points 5, 7 and 8 can be calculated from the water-side heat transfer, since the refrigerant enthalpy at point 1 can be measured.

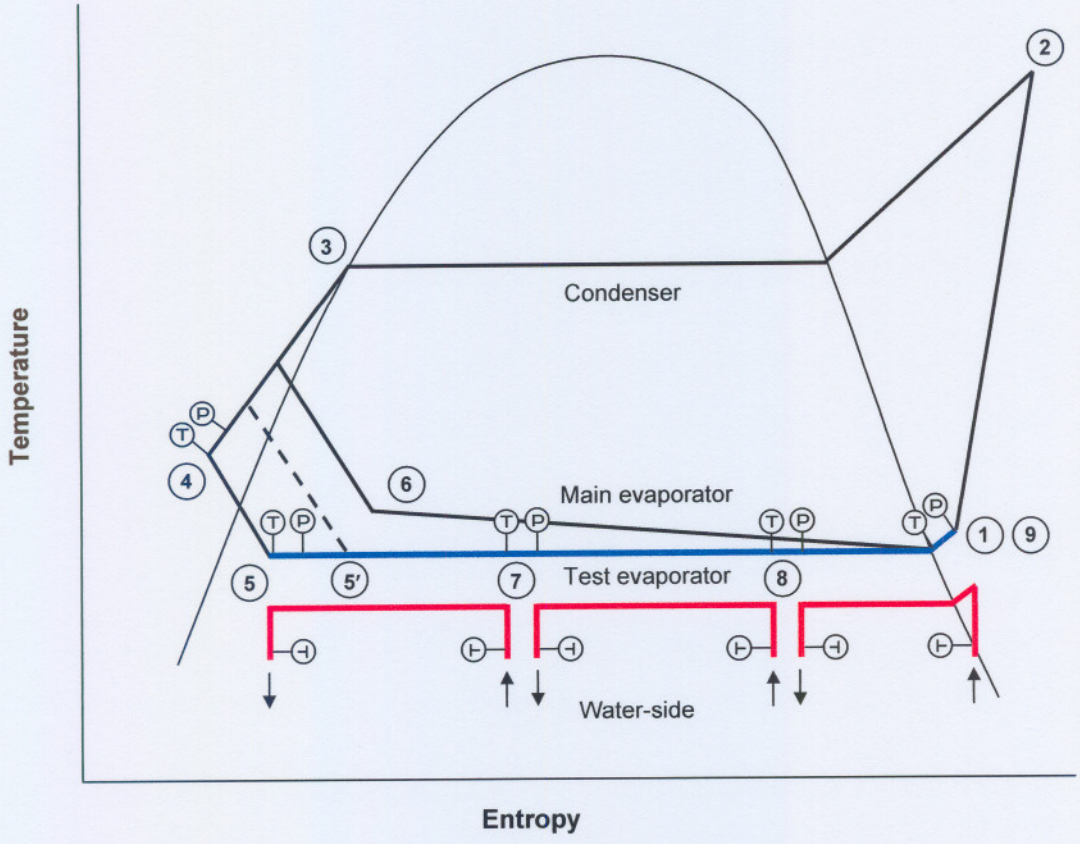

Figure 3.2 Temperature-entropy diagram of the test bench refrigerant cycle.

The temperature and pressure sensors at points 5, 7 and 8 along with the water-side heat transfer will allow the calculation of the overall heat transfer coefficient. Since some indication of the measurement accuracy is required, a heat balance can be carried out between points 4 and 1 to determine the performance of the data acquisition system.

3.2.2 TEST BENCH COMPONENTS

The main components used in the test bench include the compressor, heat exchangers, expansion valves and the test evaporator. All of these components will now be discussed in detail.

3.2.2.1 COMPRESSOR

The compressor used in the test bench is a three-phase Copeland ZR72KCE-TFD-523 scroll compressor. The compressor was charged with synthetic polyol ester refrigerant lubricant (Emkarate RL 32H) suitable for use with R22 and R407C.

3.2.2.2 HEAT EXCHANGERS

All the heat exchangers used, excluding the test sections, were Turbotec fluted-tube heat exchanger coils. The heat exchangers include the condenser, main evaporator and sub-cooler. In all the heat exchangers a counter-flow configuration of the refrigerant and water was applied. The following models were used:

- Condenser Turbotec BTSSC 72 (26 kW heating capacity)
- Main evaporator Turbotec BTSSC 48 (11 kW cooling capacity)
- Sub-cooler Turbotec BTSSC 30 (8 kW cooling capacity)

The heat exchangers used for the test evaporator are discussed in paragraph 3.2.2.4.

3.2.2.3 EXPANSION DEVICES

As mentioned in paragraph 3.2.1 two expansion valves were used in the test bench. The expansion valve used in the main evaporator loop is an Egelhof AEK 4 automatic expansion valve. It is manually used to vary and control the evaporating pressure in the evaporators. In the test loop a Danfoss 6F0009 hand expansion valve is used to provide manual control of the test section refrigerant mass flow rate.

3.2.2.4 *TEST EVAPORATOR*

The test evaporator consists of a total of three water heated, heat exchanger sections. They include the pre-evaporator section, the test section and the superheater section. For the calibration tests, all three sections were smooth tube-in-tube heat exchangers with the water flowing in the annulus and the refrigerant flowing in the inner tube. After the calibration the tube-in-tube test section was replaced with a fluted-tube test section with the refrigerant in the annulus and the water in the inner tube (Figure 3.3).

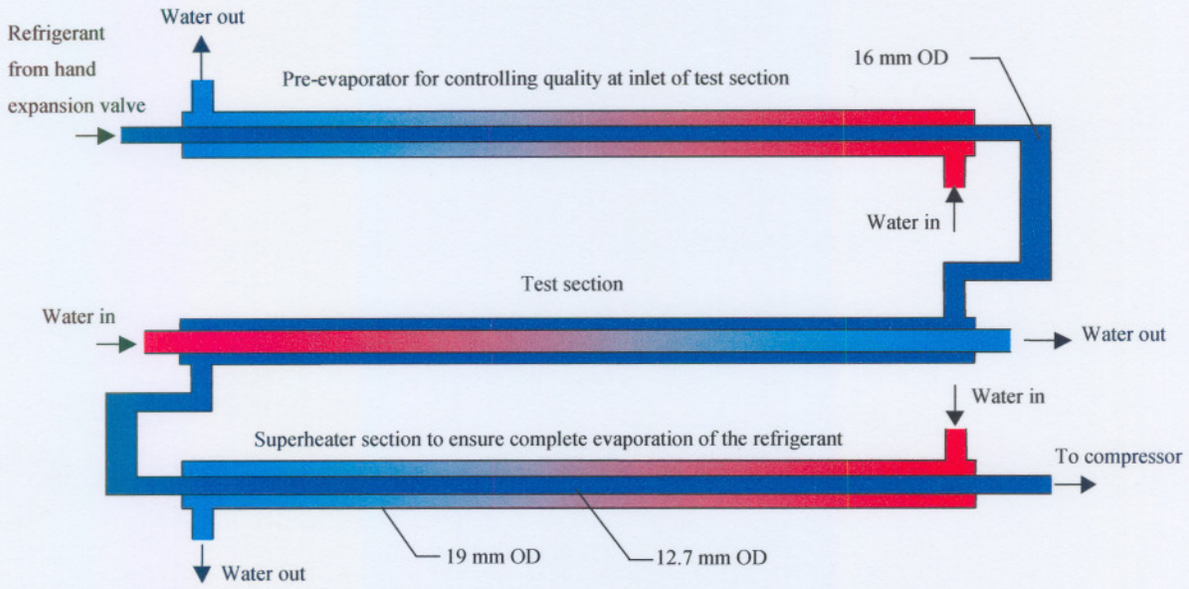

Figure 3.3 Layout of the refrigerant test section.

Since experimental data is required for various qualities, the first section, the pre-evaporator, is used to control the dryness fraction of the refrigerant entering the test section. The test section is then used for the near complete evaporation of the refrigerant. Since some liquid still remains at the exit of this section, the third section is used to ensure that the refrigerant has completely evaporated before entering the compressor.

The inside tube of the smooth tube-in-tube heat exchanger sections is a 12.7 mm OD standard refrigeration pipe and the outside tube is a 19 mm OD standard refrigeration pipe. The fluted tube section was manufactured with a fluted-tube inside a smooth tube, with an outside flute

diameter of 14.95 mm, a flute depth (e) of 2.09 mm and a flute pitch (p) of 7.407 mm. The outer smooth tube is a 3/4" OD refrigerant pipe (Do), as shown in Figure 1.2.

The volume of the inside tube was experimentally measured as 0.0003102 m^3. With this known the inside volume diameter (D_{vi}) was calculated as 11.389 mm and the outside volume diameter (D_{vo}) was calculated as 13.289 mm. The calculation of the volume diameter was done according to the Rousseau *et al.* (2003:234) correlation.

Provision is made for the temperature measuring equipment that is located directly in the refrigeration line by increasing the pipe diameter to 16 mm, and this is done to prevent refrigerant throttling. All three the sections are insulated using 37 mm of polyethylene foam insulation to prevent heat loss. The water supply lines were also partly insulated with polyethylene.

3.2.3 WATER LOOPS

All the water used for the condenser and evaporators were supplied from two 10 000 ℓ water tanks. Water in the one tank is heated to between 45 and 50°C. This tank supplies the test evaporator and the main evaporator with warm water. The water in the other tank is cooled to between 10 and 15°C and supplies the sub-cooler and the condenser with cold water.

The water loops supplying the main evaporator and condenser were designed by Pretorius (1999:91). These can supply water at a specific water temperature and mass flow rate to the two heat exchangers. It is clear from Figure 3.5 and Figure 3.6 that there are two mixing valves and two pumps in each of the layouts. The first pump is used to supply water from the storage tank and the second one is used to pump water through the heat exchanger. The mixing valve that is the closest to the water tank is used to regulate the temperature and the other one is used to regulate the water mass flow rate through the heat exchanger.

A three-way mixing valve, as shown in Figure 3.4, mixes two streams of fluids A and B into one stream C. The mixing valve has an oval seat attached to a stem that can move up and down to control the flow of A and B into C. If the seat is at the bottom position as in the first figure only stream A is sent through to C. With the seat at the top position as in the last figure

only stream B is sent through to C. With the seat between the top and bottom positions as in the middle figure a mixture of A and B is sent through to C. This mixing principle was used to control the water mass flow rate and temperature that is supplied to the heat exchangers. The mixing valve can sometimes be used as a diverting valve. In this case the flow will come from C and divert to A, A and B or B, depending on the position of the seat.

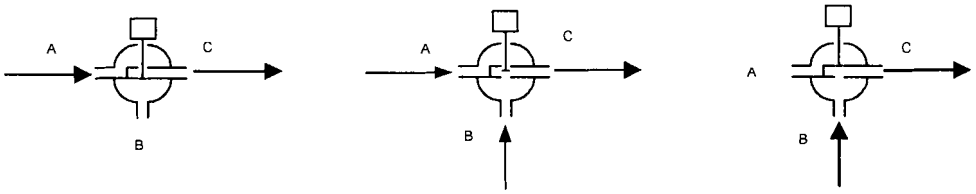

Figure 3.4 Working principle of a 3-way mixing valve.

The principle of operating the system is as follows:

Assume the condenser (Figure 3.5) is in a steady state with the supply water at a mass flow of 0.3 kg/s and a temperature of 20°C together with a constant heat load from the condenser. The temperature is measured at T and the mass flow is measured at point M in Figure 3.5. This will imply that both the mixing valves' seats are at a position between points A and B.

If the water mass flow rate set-point is reduced to 0.2 kg/s a signal is sent via the instrumentation to mixing valve 2, resulting in the valve seat moving in the direction of A. This will result in a decrease in water being pumped through the heat exchanger and the mass flow meter and an increase in water being pumped via path 2. When the set-point is reached the instrumentation sends a signal to stop the movement of the mixing valve. If the mass flow rate set-point is increased, the mixing valves' seat will move in the direction of B until the set-point is reached.

If the water temperature set-point is now reduced to 10°C, a signal is sent via the instrumentation to mixing valve 1. The signal will cause the mixing valves' seat to move to position B. This will result in less cold water being diverted through the bypass path 1 and more cold water being pumped to the second pump. With this the warmer water is pumped back to the tank. If the temperature set-point was increased then the mixing valves' seat will move to position A.

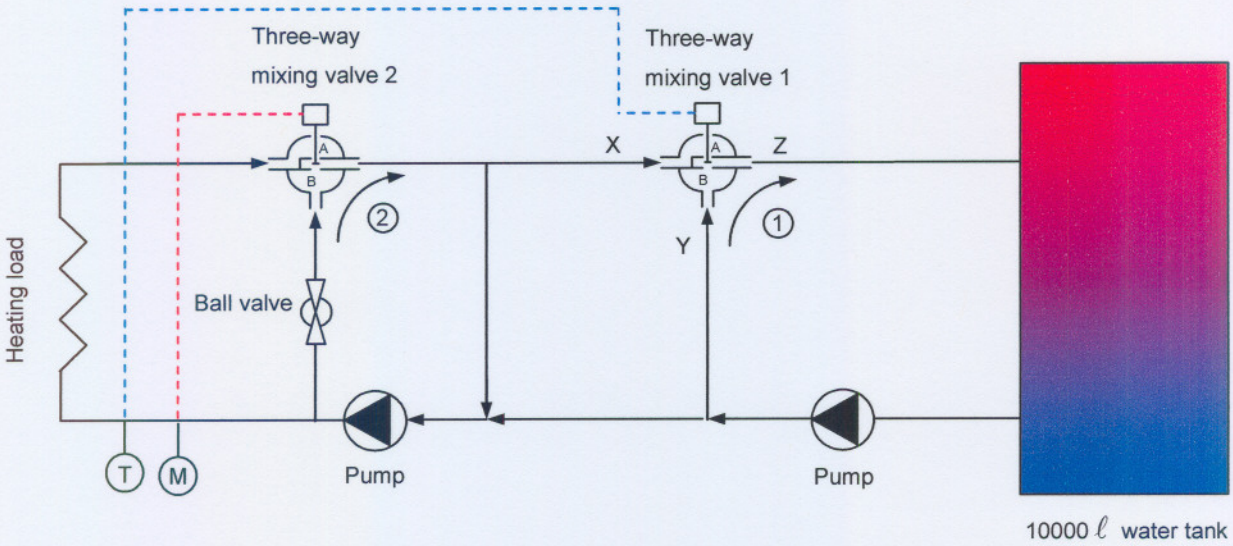

Figure 3.5 Water loop supplying the condenser.

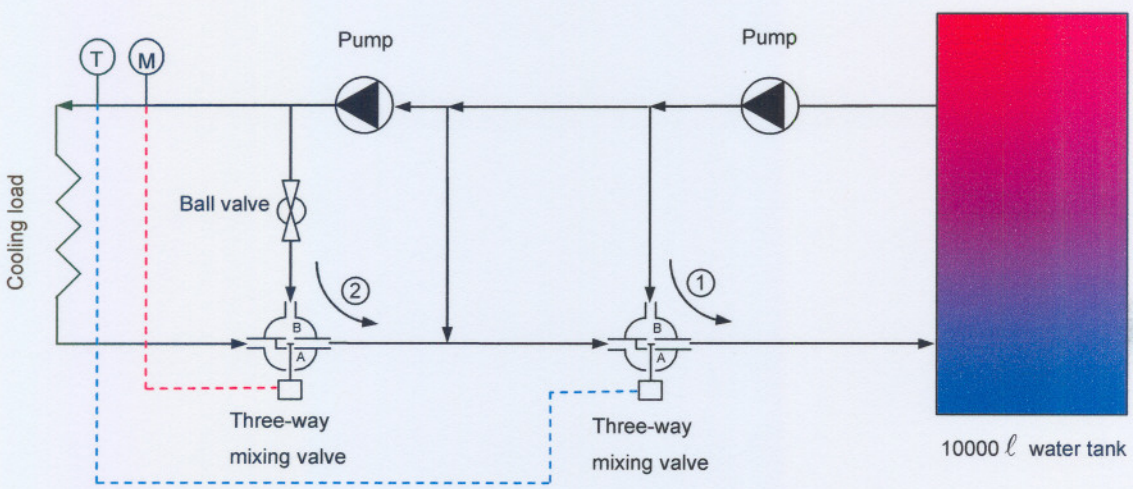

Figure 3.6 Water loop supplying the main evaporator.

The same principal of operation is valid for the main evaporator (Figure 3.6). The only difference is that if the temperature set-point is increased the mixing valves' seat moves to position B and if the set-point is decreased then it will move to position A.

In the actual operation of the system, the heat load and the mass flow vary with time. This resulted in a need for a dynamic Proportional-Integral-Derivative (PID) controlled system to

ensure a minimum difference between the set-point value and the actual value of both the water temperature and mass flow rate.

The systems used to supply the test evaporator and the sub-cooler are similar to the system used to supply the main evaporator and the condenser with only a few minor differences. These systems are shown in Figure 3.7 and Figure 3.8. The first difference is that there is only one mixing valve with the mixing valve being used as a diverting valve. These diverting valves are computer controlled with a PID controller to supply the correct water temperature to the heat exchangers. Other small differences are the needle valve after the heating or cooling load, to manually adjust the water mass flow rate, and the ball valve (1) after the first pump and before the mixing valve to manually stabilize the water temperature oscillations caused by the instability of the control of the mixing valve. Ball valve (1) in Figure 3.7 is installed only in the two systems supplying the test evaporator.

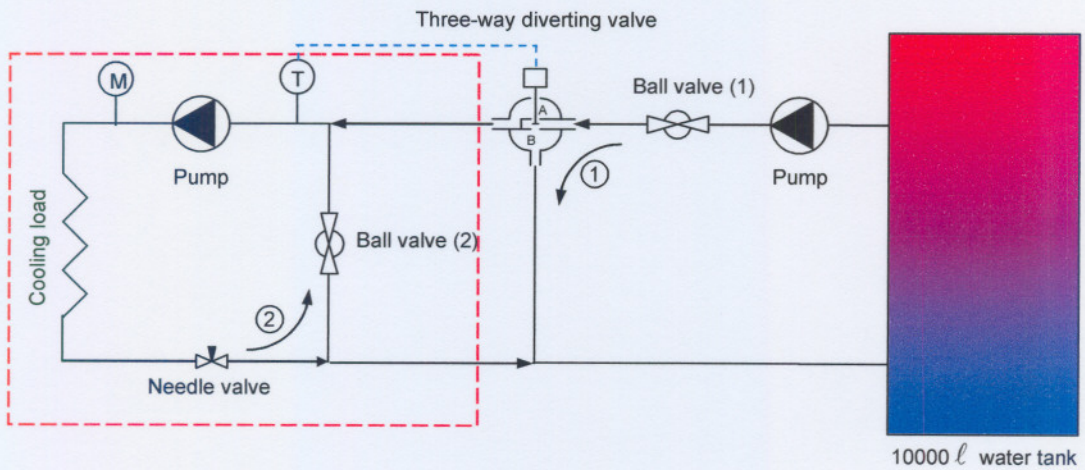

Figure 3.7 Water loop supplying the test sections.

The principle of operation for the two water supply loops supplying the test evaporator is as follows:

Assume the system is stable with the mixing valve seat in a position between A and B. If the temperature in the red control volume now decreases because of an increased cooling load the

mixing valve's seat move more to B letting more hot water into the control volume. This will increase the temperature of the control volume to the set-point temperature. The water mass flow rate has to be adjusted manually with the needle valve. To ensure a stable supply temperature the mixing valve is controlled by a PID controller. One of the water loops supplies the super heater and the other loop supplies the pre-evaporator and the test section.

The reason for the ball valve between the pump and the mixing valve (ball valve (1) in Figure 3.7) is to adjust the water mass flow from the pump to the mixing valve. If the water flow rate from the pump is too high the water temperature supplied to the red control volume will have excessive oscillations resulting in inaccurate readings. In the situation where the water flow rate is too low the water temperature will never reach the set-point value, it will always be too low. With the ball valve set correctly the temperature oscillations of the water supplying the test evaporator is about 0.7 °C.

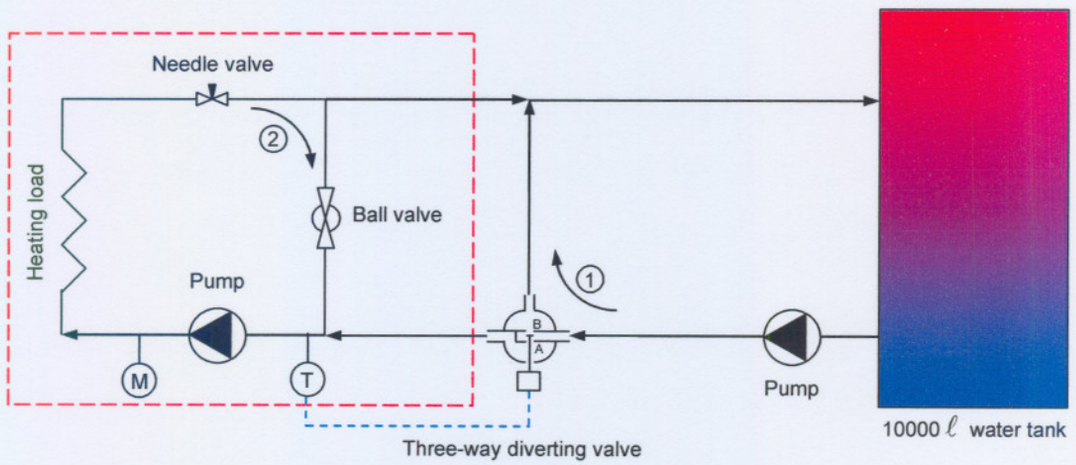

Figure 3.8 Water loop supplying the sub-cooler

The principle of operation for the water loop supplying the sub-cooler is the same as discussed for test evaporator (Figure 3.8). The only difference is that if the temperature is above the set-point, the mixing valve's seat moves to B and if the temperature is below the set-point the seat moves to A.

The sub-cooler supply loop does not have a ball valve between the first pump and the mixing valve. The reason for this is that the water temperature supplying the sub-cooler was close to the temperature of the supplying tank. This causes the system to be stable without the ball valve.

3.2.4 WATER LOOP COMPONENTS

The components used in the water loops include the pipes, mixing valves and flow meters. All the pipes supplying the test bench are either 2"(50.8 mm) or ¾" (19.1 mm) galvanised pipes. The 2" pipes are used for the loops supplying the condenser and the main evaporator, whereas the ¾" pipes are used for the loops in the pre-cooler and test evaporator.

3.2.4.1 MIXING VALVES

Two kinds of mixing valves are used in the water loops. The reason for this is to accommodate the 2" as well as the ¾" pipes.

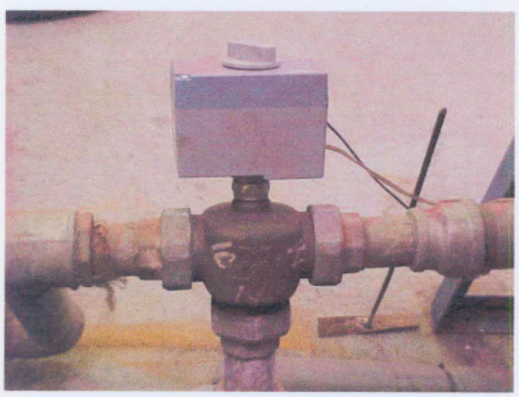

Figure 3.9 Landis & Staefe VXG44.40-25 mixing valve with SQS65 actuator.

The mixing valves in the 2" pipe are Landis & Staefe VXG44.40-25 (Figure 3.9) which are controlled by SQS65 actuators. There are a total of four mixing valves with actuators, two for each line supplying the main evaporator and the condenser.

The mixing valves in the ¾" pipes are Johnson Controls VG7822LT (Figure 3.10) with factory mounted actuators. There are a total of three mixing valves located in the loop supplying the sub-cooler and the two loops supplying the test sections.

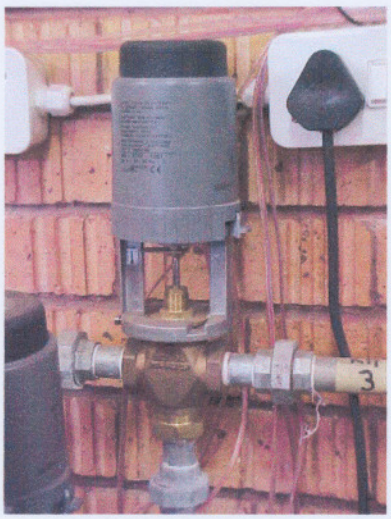

Figure 3.10 Johnson Controls VG7822LT mixing valve.

3.2.4.2 WATER MASS FLOW METERS

Water mass flow rates of the loops supplying the main evaporator and the condenser are measured with Burkert paddle water mass flow meters with an 8035 flow transmitter (Figure 3.11). The accuracy of the meters is less than 0.5% of the total mass flow range. The mass flow rate meters of the loops supplying the three test evaporator sections are Coriolis mass flow meters and are discussed in paragraph 3.3.1.c.

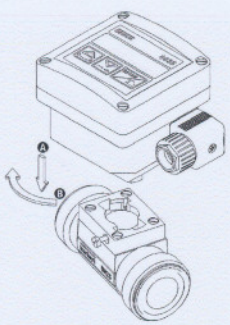

Figure 3.11 Burkert 8035 water mass flow meters (Burkert, 2006).

3.3 DATA ACQUISITION SYSTEM

The system acquiring the temperature, pressure and flow data of the experimental set up consists of two sub-systems, the PREMA sub-system and the VisiDAQ sub-system.

The PREMA sub-system is used for reading and storing the temperatures of the refrigerant and the water supplying the test evaporator, while the VisiDAQ sub-system is used for reading and storing the refrigerant pressures and water mass flow rates through the test evaporator. The VisiDAQ sub-system also measure the temperatures of all five the water loops together with the water mass flow rate of the loops supplying the main evaporator and condenser. The reason the VisiDAQ sub-system is used to measure the supplying water temperature and the water mass flow rates for the main evaporator and condenser, is because the PID controller is incorporated into this system. In the following paragraphs the measurement and acquisition equipment are described.

3.3.1 MEASURING EQUIPMENT

The primary measurements on the water loops consist of temperature and flow measurements whereas for the refrigerant, it includes the temperature, pressure and flow measurements.

a) Temperature measurement

The temperature is measured by two types of configurations.

Type 1

The first type of temperature sensor configuration consists of grade A, four-wire Pt100 sensors (Figure 3.12) connected with shielded four-wire extensions to a PREMA 3040 electronic temperature scanner and logger (Figure 3.13). The Pt100 elements, together with thermal conduction paste, were placed into stainless steel thermowells soldered into the water- and refrigerant lines. The temperature of the refrigerant is measured at five positions and the water is measured at six points as is shown in Figure 4.1.

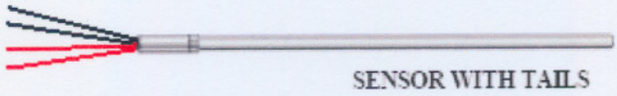

Figure 3.12 4-Wire Pt 100 sensor (Pyrosales, 2006)

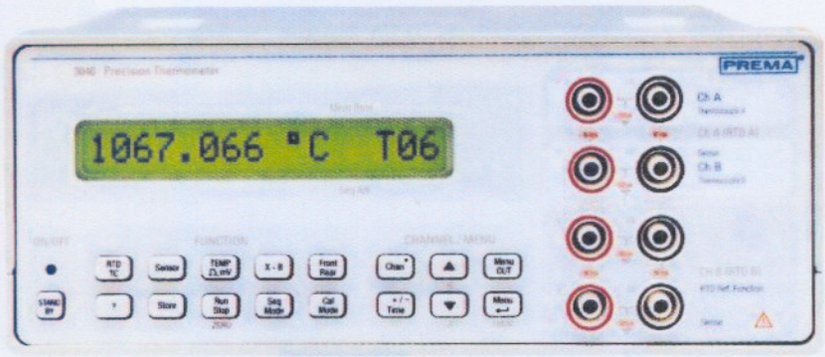

Figure 3.13 PREMA 3040 scanner and logger (3040 Precision Thermometer, 1998).

Type 2

The second type consists of Grade A, three-wire Pt100 elements together with 4-20 mA transmitters, also inside thermowells. The temperature of the water supplying the test sections and sub-cooler from the mixing valves together with the inlet and outlet temperature of the main evaporator and condenser are measured. These temperatures measurements are mainly used for the control of the mixing valves to supply water at the correct temperatures.

Figure 3.14 Pt100 temperature sensor with the transmitter

b) Pressure measurement

Pressure data are acquired from five pressure sensors. The first sensor is located upstream from the hand expansion valve. This sensor is an Endress + Hauser PMC731 with a 0 – 40 bar range. The other four pressure sensors are located at the inlet and outlet of the pre-heater, test and super-heater sections. These sensors are also Endress + Hauser PMC731 sensors but with a range of 0 – 10 bar (Figure 3.15).

Figure 3.15 Endress + Hauser PMC731 pressure sensor (Endress + Hauser, 2006).

The reason why only four sensors are used to measure the pressure of the inlet and outlet of the three sections is because the outlet pressure of the pre-heater is also the inlet of the test section and the outlet of the test section is also the inlet of the super-heater as shown in Figure 4.1.

The principle of operation of the pressure transmitters is the proportionality of the capacitance between two plates to the distance between them. This capacitance reading is then converted to a 4-20 mA signal proportional to the pressure that is actuating two gold-plated disks. The transmitters provide an accuracy of 0.1% of full span according to the equipment manufacturer.

c) Flow measurement

The water flow rates to the pre-evaporator, test and super-heater sections, together with the refrigerant mass flow rate through the test sections are measured. All four mass flow meters are Coriolis type flow meters. The three water flow meters are Endress + Hauser Promass 63F flow meters (Figure 3.16) with a span of 0 – 0.1204 kg/s and an accuracy of 0.1% of the full span according to the manufacturer.

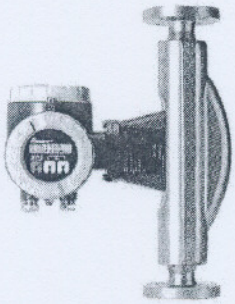

Figure 3.16 Endress + Hauser Promass 63F flow meter (Endress + Hauser, 2005).

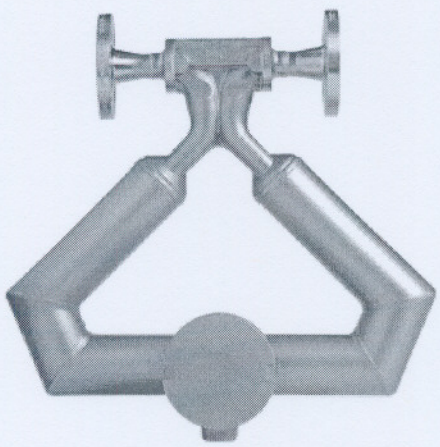

Figure 3.17 Micromotion RTF9739 flow meter (Micromotion, 2004).

The gas flow meter is a Micromotion RTF9739 flow meter (Figure 3.17) with a measuring range of 0-0.5 kg/s with a liquid measuring accuracy of 0.2% and a vapour measuring accuracy of 0.5% of the full span according to the manufacturer. This sensor is located between the sub-cooler and the hand expansion valve. This location was chosen for the measurement of liquid and to eliminate the possibility of two-phase flow through the flow meter resulting in flow errors.

3.3.2 ACQUISITION OF TEMPERATURE DATA

As mentioned previously, two sub-systems are used to acquire the temperature data.

The PREMA sub-system (Figure 3.18) is used to acquire the temperature of the refrigerant and the water entering and leaving the test evaporator. For this the PREMA 3040 temperature scanner and logger is used with the 11 four-wire Pt100 sensors directly connected to the scanner. The PREMA logger-and-scanner is connected via an RS232 connection cable to a personal computer. PREMA control 3040 computer software is used to control the scanner and logger remotely and to download the stored data into an ASCI data file. This file can then be imported into Microsoft Excel for further calculations. The PREMA sub-system do not continuously take readings from the 11 Pt100 sensors. It cycles through the sensors and takes two second readings of each of the sensors, together with a one second delay at the end. Thus each of the temperature sensors is measured for two seconds in a 23 second cycle time.

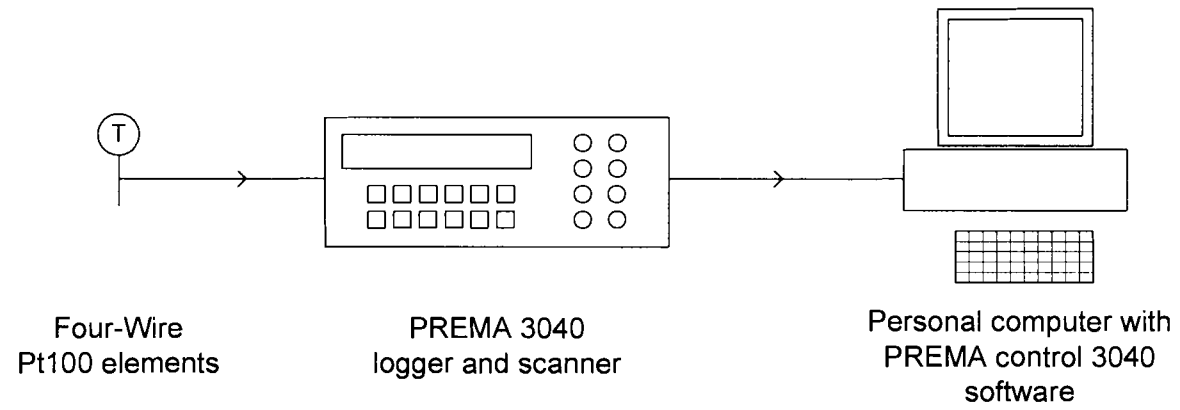

Figure 3.18 Graphic layout of the PREMA temperature acquisition system.

According to the manufacturer the scanner is capable of temperature readings accurate to within 0.004°C. The scanner's temperature readings were compared to that of a –0.01 to +10.01°C mercury thermometer calibrated to an accuracy of 0.04°C by the South African Bureau of Standards by Venter (2000:44), and excellent agreement was found. As mentioned by Venter (2000:44) human error has an effect on the readings, therefore the accuracy is accepted as being at least 0.06°C.

The VisiDAQ sub-system (Figure 3.19) consists of seven Grade A, three-wire Pt100 elements together with 4-20 mA transmitters. These Pt100 temperature sensors were calibrated with the Pt100 elements used with the PREMA 3040 scanner and logger. The same type of three-wire Pt100 elements were used by Venter (2000:43) who found that the elements were unstable over a three month period. Since the water temperature set-point only has to be in a specific region the accuracy was not of critical importance. The accuracy was accepted to be 0.5°C. This system was connected to an Advantech ADAM/VisiDAQ hardware-software interface.

The 4-20mA signal form the Pt100 transmitters is fed into analogue input modules (ADAM 4018 modules) with a resistance circuit to provide a voltage reference. This analogue input is then converted by the modules into a digital signal where it is sent via another module (ADAM 4852 module) via RS232 to a personal computer where it is displayed by the VisiDAQ software. In the software, user-defined equations are used to convert each signal into the appropriate form. In this case the signal is converted from mA to °C. According to the manufacturer, the analogue input hardware provides an accuracy of better than 0.1 %, of the measured value in the signal conversion process.

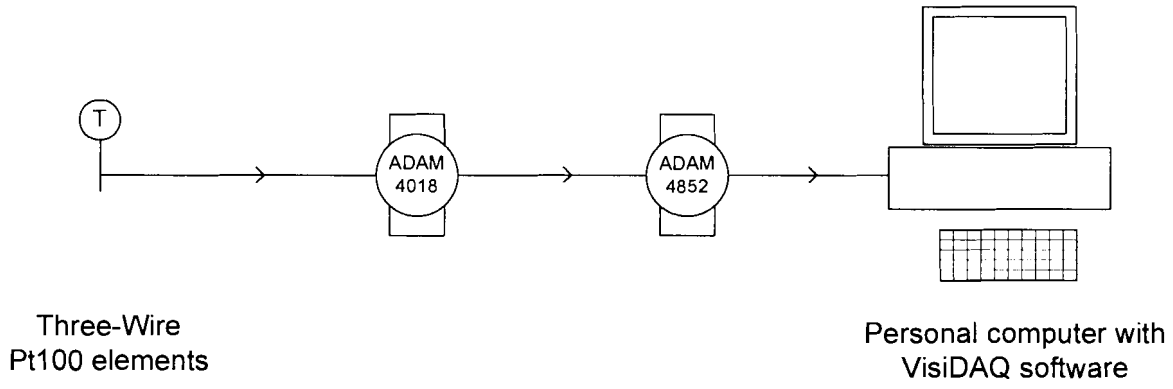

Figure 3.19 Graphic layout of the VisiDAQ temperature data acquisition system.

3.3.3 ACQUISITION OF PRESSURE AND FLOW DATA

The refrigerant pressure sensors and all the flow meters have signal outputs of 4-20 mA. These signals are then connected to the Advantech ADAM/VisiDAQ hardware-software interface, the same system used by the three-wire Pt100 elements. As with the Pt100 elements the analogue signals are converted into digital signals by the modules and sent via an ADAM

4852 module via RS232 to the VisiDAQ software on the personal computer where the signal is either converted into bar or kg/s (Figure 3.20).

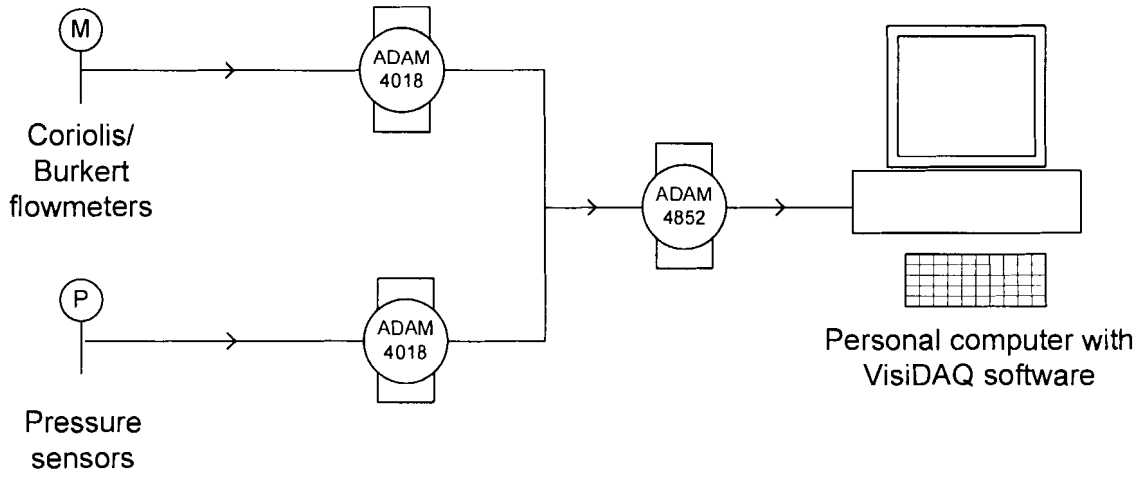

Figure 3.20 Graphic layout of the VisiDAQ flow and pressure data acquisition system.

3.3.4 TEMPERATURE AND FLOW CONTROL

Control of the water temperature supplied by the control loops and the control of the water mass flow rate to the main evaporator and condenser are achieved by the Advantech ADAM/VisiDAQ hardware-software interface used in paragraph 3.3.2 and paragraph 3.3.3.

In the VisiDAQ program PID controllers are used to control the mixing valves. The PID controllers have as inputs a) the current water temperature or water mass flow rate together with b) the set-point value. With these inputs the PID can send a signal via the RS232 via the ADAM 4852 module to the ADAM 4021 module where a 0-10 V control signal is sent to the mixing valve. Each of the mixing valves has its own PID controller and ADAM 4021 module (Figure 3.21).

Control of the water flow rate in the test evaporator and sub-cooler is done by manual adjustment of needle valves in the water loops.

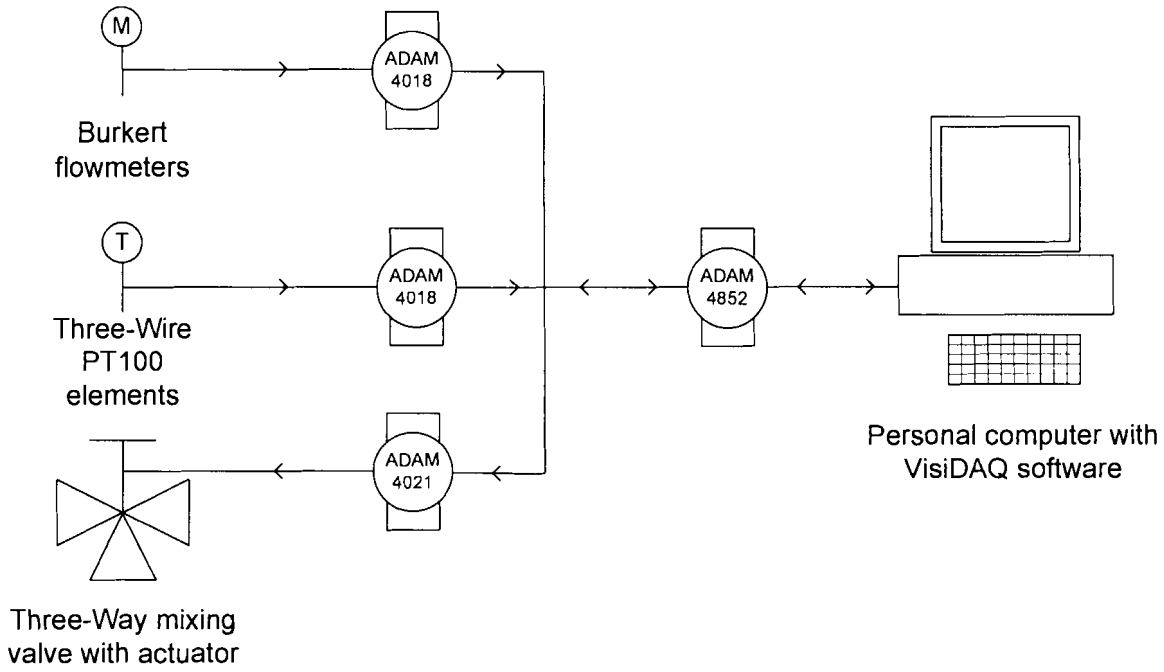

Figure 3.21 Graphic layout of the VisiDAQ temperature and flow control system.

3.4 HEAT BALANCE

To ensure that all the equipment on the test bench worked properly and the performance and accuracy are acceptable, the test bench was operated in the same configuration with R22 and smooth tube-in-tube test sections as tested by Venter (2000:59).

After these tests were completed, with all the equipment working properly, the smooth tube-in-tube test section was removed and replaced with the fluted tube test section. The fluted tube was then tested with R22 and R407C respectively. Both the refrigerants were tested with various refrigerant mass flow rates and evaporating pressures and a variety of heat fluxes. When these tests were completed the refrigerant was removed and water-to-water heat transfer tests were done in the fluted-tube test section.

3.4.1 WATER-TO-REFRIGERANT HEAT BALANCE

Before the water-to-refrigerant tests could be done the test bench had to be re-assembled after being decommissioned in 2002 and all the equipment checked to ensure the working condition of all the equipment. After the test bench was operational, with minor repairs, a

number of tests were done to ensure that all the equipment was working properly and accurately. The duration of each of the test was approximately 10 minutes.

All the data from the VisiDAQ program and PREMA 3040 logger were loaded to a personal computer where it was processed by using Microsoft Excel to calculate the average values. These values were then imported into Engineering Equation Solver (EES), to calculate the heat transfer and deviation. The data are shown in Table 3-1

	Test Evaporator		
Test no.	**Q_{Gass} (W)**	**Q_{Water} (W)**	**% Deviation**
1	4220	4247	0.635
2	5085	5138	1.051
3	5048	5093	0.884
4	4875	4998	2.507
5	5644	5760	2.056

Table 3-1 Heat balance results of water-to-refrigerant calibration tests.

3.5 SUMMARY

In this chapter a detailed description of the test bench layout, the components used and the water loops supplying the test bench are described. In addition to this, the operation of the control system and the data acquisition system were also explained.

Tests on the system were performed with a smooth tube-in-tube heat exchanger with water in the annulus and R22 in the inner tube. The maximum deviation of the heat transfer rate in the test evaporator was 2.507%.

In the following chapter the experimental layout and procedure of the test facility is explained in detail. The procedure includes the start-up of the system, the adjustment of the refrigerant mass flow, adjustment of the evaporating pressure and the adjustment of the water temperature that is supplied to the test evaporator. This is followed by an explanation of all the correlations used to calculate the heat transfer coefficient of the refrigerant and the water.

CHAPTER 4

4 EXPERIMENTAL PROCEDURE AND CORRELATIONS

4.1 INTRODUCTION

This chapter describes the experimental design and the various correlations used for the determination of the heat transfer coefficients. In the experimental design the experimental set-up, controlled variables and the experimental procedure are explained.

Various correlations exist to calculate the heat transfer coefficients for single and two-phase flow in tubes and annuli for condensing or evaporating conditions. However, this is not the case for fluted-tubes where only the correlation by Rousseau *et al.* (2003:232) could be found. This correlation was developed for a fluted-tube condenser using R22. Since the fluted-tube in this study is used as an evaporator, various two-phase correlations were tested against the experimental data. These correlations include the following:

- Gungor and Winterton (1986:351)
- Gungor and Winterton (1987:148)
- Liu and Winterton (1991:2759)
- Pierre (ASHRAE Fundamentals, 1997:4.7)
- Chen (quoted from Zhang *et al.* 2004:5751)
- Rousseau *et al.* (2003:232) and
- Kattan *et al.* (1998c:156)

All of these correlations are described in detail in paragraph 4.4. Together with these correlations a new correlation is derived by combining two of these correlations. This new correlation is referred to as the Modified Rousseau *et al.* correlation.

4.2 EXPERIMENTAL DESIGN

The acquisition of the experimental data requires a structured experimental procedure to ensure the data is correct and applicable for the calculations. This procedure plays an important role in the accuracy of the acquired data. If this procedure is incorrect the system will be unstable resulting in inaccurate data readings and inaccurate deviation between the correlations and the actual values.

4.2.1 EXPERIMENTAL SET-UP

The layout of the test evaporator is illustrated in Figure 4.1. The temperature probes are indicated by a T, the pressure sensors by a P, and the mass flow sensors are indicated by an M. As shown in the figure, there are a total of 11 temperature probes, five pressure sensors and four mass flow meters.

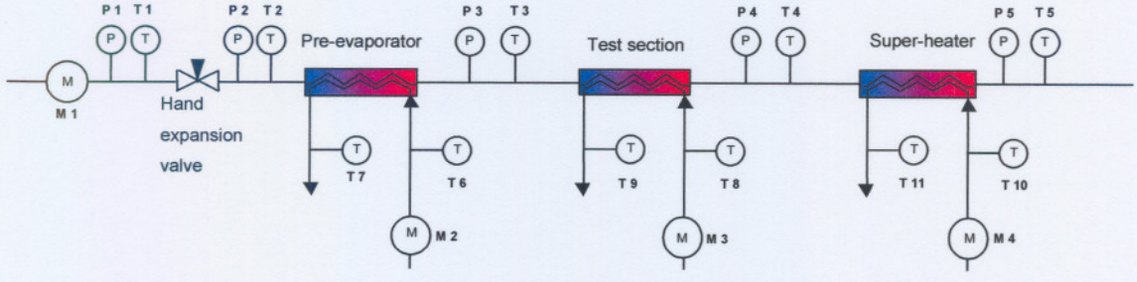

Figure 4.1 Configuration of the equipment on the test evaporator.

Figure 4.1 shows the refrigerant temperatures are measured at points T 1 to T 5, the pressures at points P 1 to P 5 and the mass flow rate at M 1, located before the hand expansion valve. This is done to ensure only liquid is sensed by the mass flow meter. To determine the quality of the refrigerant entering and leaving the test section, water energy balances have to be done. For this the water flow rates as well as the inlet and outlet water temperatures have to be

measured. The inlet temperatures are shown by T 6, T 8 and T 10, the outlet temperatures are shown by T 7, T 9 and T 11 and the water mass flow rates are shown by M 2, M 3 and M 4.

It is clear from Figure 4.2 that the enthalpy at point 2, 3 and 4 could not be determined directly from only the temperature and pressure of the refrigerant since the refrigerant is in a two-phase state. On the other hand, the refrigerant at points 1 and 5 is in a single phase state and its properties can be determined with only the temperature and pressure.

The unknown properties at points 2, 3 and 4 can be determined if the water heat transfer is known. This is the reason the water temperature and mass flow rate need to measured accurately. According to the conservation of energy law, the heat loss of the water must equal the heat gained by the refrigerant if minor losses are ignored and if the heat exchanger is well isolated. Knowing this, equation 4-1 can be used to determine the unknown enthalpy and thus the properties at the unknown points.

$$Q = \dot{m}_w C_{p,w} \left(T_{w,in} - T_{w,out} \right) = \dot{m}_r \left(h_{r,out} - h_{r,in} \right) \tag{4-1}$$

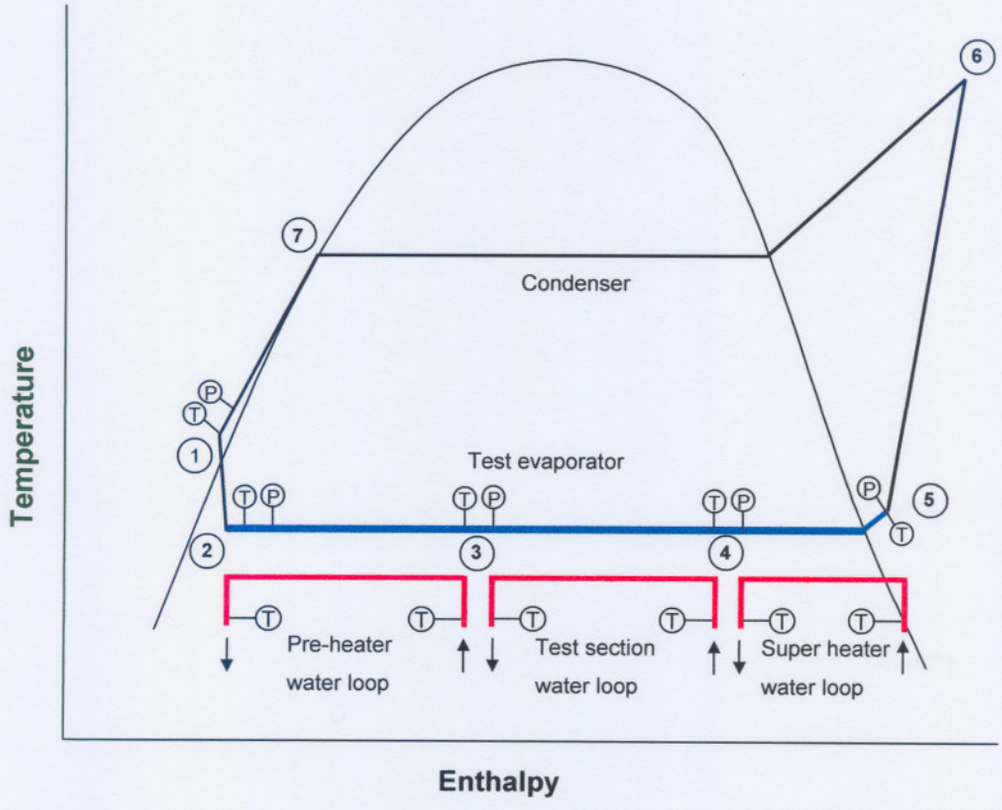

Figure 4.2 Temperature-enthalpy diagram of the test evaporator part of the refrigeration cycle.

Knowing that the heat loss of the water in the super-heater is equal to the heat gained by the refrigerant, the refrigerant properties at point 5 can be used to calculate the refrigerant enthalpy at point 4. With the enthalpy at point 4 known, together with the heat loss of the water in the test section water loop the refrigerant enthalpy at point 3 can be calculated. Using the same procedure, but using the heat loss of the water in the pre-heater water loop, the refrigerant enthalpy for point 2 can be calculated. The enthalpy at point 2 and point 1 should match with a high percentage accuracy to ensure that the system is operating within the desirable experimental range.

Another means of ensuring that the system is operating accurately is to compare the total heat transfer of the refrigerant between points 1 and 5 in Figure 4.1, to the sum of the heat transferred by the three water loops. These two values should also be within a high percentage accuracy to ensure accuracy of the measured values and to satisfy the conservation of energy law.

4.2.2 CONTROLLED VARIABLES

To ensure that the experimental data from the test is an accurate representation of the heat transfer coefficients of the refrigerant the tests should be varied over a range of different evaporating conditions. For this reason certain variables should be adjusted to vary the state of the refrigerant entering the test section with respect to quality, temperature and pressure. From the fundamentals of heat transfer it is clear that the heat transfer coefficient of the refrigerant is proportional to the rate of heat transferred to the refrigerant. The variables that were adjusted are as follow:

- Evaporator pressure
- Refrigerant mass flux
- Refrigerant heat flux

To vary the evaporating pressure the automatic expansion valve is adjusted, but this also results in the variation of the refrigerant mass flow through the test evaporator. Since the experimental data require a constant refrigerant mass flow at different evaporating pressures, the hand expansion valve has to be adjusted until the refrigerant mass flow is corrected. This adjustment will then affect the evaporating pressure and the whole procedure has to be

repeated. The procedure usually has to be repeated two or three times to find the desired test pressure and mass flow conditions.

In the case where the refrigerant mass flux is varied, the hand expansion valve is adjusted. This adjustment will result in a change in the evaporating pressure. To keep the pressure at a specific value the automatic expansion valve is adjusted. This procedure usually has to be repeated two or three times to find the desired conditions.

The variation of the refrigerant heat flux can be adjusted by either increasing the water mass flow through the test sections, varying the inlet water temperature or a combination of both. The water flow rate through each of the test sections are controlled by adjusting the needle valves in the water loops (see Figure 3.7). Temperature adjustment is done with the help of the PID in the control program, VisiDAQ, and three-way mixing valves in the loops supplying the test sections. It was possible to keep the temperature constant with a temperature offset of approximately 0.5°C off the set-point value while the temperature oscillations were less than 0.6°C.

4.2.3 EXPERIMENTAL PROCEDURE

To obtain the required experimental data for the calculation of the heat transfer coefficients with the various correlations, two procedures have to be followed. The first is the start-up procedure and the second is where test conditions need to be changed to a new desired setting.

It is important to note that before any of the procedures can be followed, the two water tanks should be at the correct water temperature. This is to ensure that the water tanks have the capacity to supply the test bench with the appropriate water temperatures. With a little help from the heat pump continuous tests of up to eight hours could be done.

The start-up procedure is as follows:

(1.1) Ensure the VisiDAQ program is running correctly with the required set-point values.

(1.2) Switch on all the water pumps in the water loops. This is to ensure water flow through the heat exchangers and to start the water circulation from the water tanks for the water loops to supply the correct water temperature.

(1.3) After ensuring all the water pumps are running, switch on the compressor.

(1.4) After 20-40 minutes when all the systems have stabilised, the expansion valves can be adjusted for the desired evaporating pressure and refrigerant mass flow rate.

(1.5) With the pressure, temperature and refrigerant mass flow rate stable, the data can be logged.

The reason for the waiting period of 20-40 minutes, is to ensure that the system stabilises and the water temperature oscillations minimise. With an adjustment of one expansion valve the system has to be allowed five minutes to stabilize before the other expansion valve is adjusted. In some cases it was found that the refrigerant mass flow meter gave incorrect readings, and this was a result of two-phase flow flowing through the meter. To correct this, one must reset the meter by switching it off for a few minutes and then switch it back on.

With the first reading completed, three properties could be varied independently of each other, i.e. the water temperature, the refrigerant mass flow and the evaporating pressure. After various test runs it was found that the most efficient way is to vary the water inlet temperature and thus the heat flux while keeping the refrigerant mass flow rate and evaporating pressure constant. After this the same heat flux range is completed at a different refrigerant mass flow rate at the same evaporating pressure. When all the refrigerant flow rates were tested, each for the whole heat flux range, the evaporating pressure is adjusted.

For example, if five different heat fluxes (G1 – G5) for five different refrigerant mass flow rates ($\dot{m}$ 1 – $\dot{m}$ 5) and for five different evaporating pressures (P1 – P5) must be tested, the process could be described as follows:

Keeping the flow rate and the evaporating pressure constant at $\dot{m}$ 1 and P1 respectively the heat fluxes is tested for G1 – G5. With this completed the mass flow rate is set to $\dot{m}$ 2 keeping the pressure constant at P1 and then varying the heat fluxes for G1 – G5. After all the mass fluxes are tested for all the mass flow rates the evaporating pressure is set to P2, then the whole process starts again for all the heat fluxes and all the mass flow rates. The result will be a total of 125 data sets with each data point that is the average value of a 20 minute logging time interval.

For variation of the water temperature the following was done:

(2.1) Change the water inlet temperature set-point in the VisiDAQ program.

(2.2) Allow 5 minutes for the water temperature to stabilise via the PID control and the mixing valve.

(2.3) Check the water mass flow and adjust if necessary.

(2.4) Ensure the evaporating pressure is correct, if not, correct it.

(2.5) Ensure the refrigerant mass flow is correct, if not, correct it.

(2.6) Repeat 2.4 and 2.5 until the correct values are established, since they are dependent on each other as mentioned in paragraph 4.2.2.

(2.7) Ensure the refrigerant temperature at the super-heater outlet is between 20 and 30°C to ensure superheated gas. If the temperature is incorrect the water temperature supplying the super-heater should be adjusted by adjusting the set-point value in the VisiDAQ program. The reason for the superheat is to avoid liquid slugs that in turn can cause false temperature readings and then incorrect calculations. In the case where liquid slugs are formed the liquid is trapped by the suction accumulator to prevent damage to the compressor.

(2.8) After the readings are stabilised, log the data for 20 minutes.

The logging interval of 20 minutes was chosen to ensure a sufficient average for the data and to make sure the system is not transient. Another reason for the 20 minute logging interval is to make sure the temperature data is sufficient since every temperature sensor is only sampled every 23 seconds, as explained in paragraph 3.3.2.

To vary the refrigerant mass flow the following was done:

(3.1) Make sure the system is stable with the correct water temperature and water mass flow.

(3.2) Adjust the hand expansion valve carefully until the correct refrigerant mass flow rate is obtained.

(3.3) Now the automatic expansion valve has to be adjusted carefully, following a waiting period of five minutes after the hand expansion valve was adjusted, until the evaporating pressure is returned to the value before the hand expansion valve was adjusted.

(3.4) Repeat 3.2 and 3.3 until both the values are at the desired set-points.

(3.5) Allow the system to stabilise.

(3.6) Follow procedure 2.3 to 2.8.

To change the evaporating pressure, the same procedure is followed as the procedure used to change the refrigerant mass flow but with procedure point 3.3 followed by point 3.2.

Precaution should be taken in the choice of water inlet temperature and mass flow rate as well as the refrigerant mass flow rate. If the water temperature is too low insufficient evaporation will occur and cause liquid slugs at the end of the super-heater. If the water inlet temperature is too high the heat flux could be too high and cause excessive liquid slugs in the test-section. These liquid slugs can cause temperature reading errors resulting in incorrect experimental calculations. The water flow rate should be kept high enough to avoid laminar flow, since most of the correlations are for turbulent conditions, but not too high since this will result in the heat flux being too high. With so many test properties that can vary (water mass flow rate, water inlet temperature, evaporating pressure and refrigerant mass flow rate) the only way to make sure the heat flux is not too high is to look at the experimental temperature data. The temperature should not vary more than 0.5°C. If there are many spikes in the data then the chances are good that the heat flux might be too high resulting in invalid data.

4.3 SINGLE-PHASE HEAT TRANSFER COEFFICIENTS

To determine the experimental heat transfer coefficient of the refrigerant the first step is to determine the heat transfer coefficients of the water. To obtain the experimental heat transfer coefficients, the Wilson plot method, the modified Wilson plot (Briggs and Young, 1969:35), the modified Wilson plot (Shah, 1990:51) and the water correlation of Christensen *et al.* (1993) as discussed by Rousseau *et al.* (2003:234) are explained. The reason why at least two correlations are used to determine the experimental heat transfer coefficient is to ensure the experimental heat transfer coefficients are calculated accurately.

4.3.1 WILSON PLOT (VENTER 2000)

Consider the flow configuration shown in Figure 4.3 where the evaporating refrigerant (blue) in the annulus side, the copper pipe separating the two streams (grey) and the warm water (red) on the inside are illustrated. With this configuration the heat transfer coefficient of the

water has to be determined with the heat transfer coefficient of the refrigerant known or unknown.

To determine the heat transfer coefficient, the refrigerant mass flow rate and the log-mean average temperature have to be kept constant resulting in the thermal resistance being approximately constant. With the resistance constant the water flow rate is then varied systematically. The fluid flow rate of both the fluids and the inlet and outlet temperatures of the two fluids are recorded. With this configuration and the assumption that the fouling resistance on both sides of the copper tube is kept constant, the heat transfer is given by equation 4-2.

$$\frac{1}{U_h} = \frac{1}{h_h} + A_h R_{f,h} + A_h R_w + A_h R_{f,c} + \frac{A_h}{h_c A_c} \tag{4-2}$$

Since h_c is maintained constant, the last four terms on the right-side of the equation are constant, say equal to C_1.

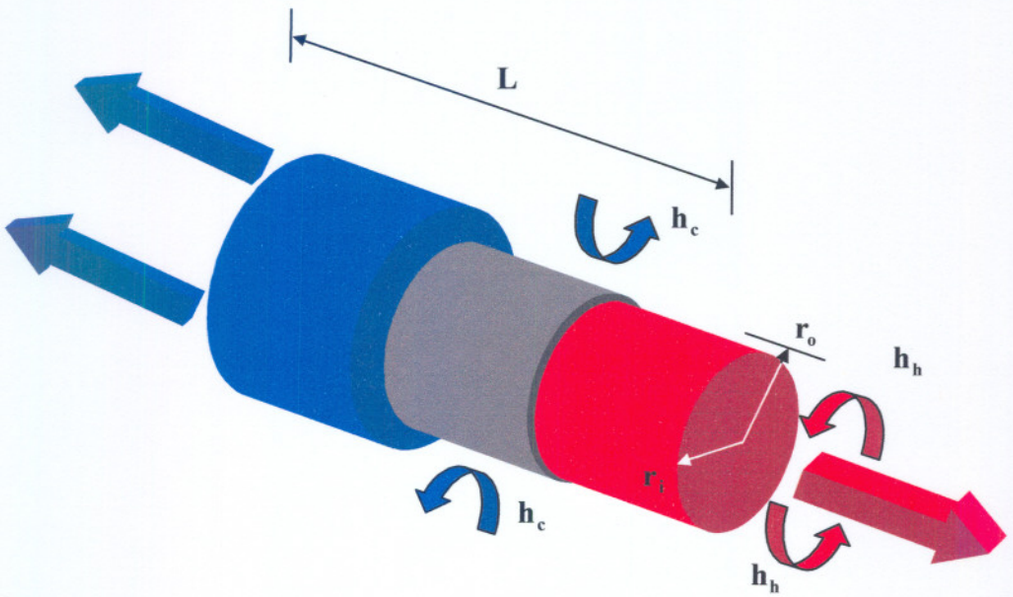

Figure 4.3 Inside and outside fluids in a smooth tube-in-tube heat exchanger.

For fully developed turbulent flow through a constant cross sectional duct and with the fluid transferring heat to the cooler fluid, the Nusselt number is given by

$$Nu = C_0 \, \mathrm{Re}^{0.8} \, \mathrm{Pr}^{0.3} \tag{4-3}$$

with C_0 a constant. Substitution of the definitions of the Nusselt, Reynolds and Prandtl numbers into equation 4-3 yields

$$h_h = \left(\frac{C_0 k^{0.6} \rho^{0.8} C_p^{\ 0.4}}{\mu^{0.4} D_H^{0.2}} \right) V^{0.8} = C_2 \cdot V^{0.8} \tag{4-4}$$

In equation 4-4, V represents the mean fluid velocity through the minimum flow area and C_2 a constant independent of V. Substituting equation 4-4 into equation 4-2 result in

$$\frac{1}{U_h} = \frac{1}{C_2 \cdot V^{0.8}} + C_1 \tag{4-5}$$

A plot of $\frac{1}{U_h}$ versus $\frac{1}{V^{0.8}}$ on a linear scale, with the variation of the test fluid velocity, will result in a straight line provided equation 4-3 applies. The interception of the plot with the y-axis is represented by the constant C_1 and the slope is $\frac{1}{C_2}$. The heat transfer coefficient of the hot fluid can then be calculated.

4.3.2 Modified Wilson plot (Briggs and Young 1969)

There are three distinct disadvantages of the traditional Wilson plot techniques according to Briggs and Young (1969:35). First, the data are troublesome to obtain because of the constant flow rate and the constant average bulk fluid temperature requirements. Second, a considerable number of data points are required for accurate shell and tube heat transfer correlations. Third, the variations in fluid properties are also not taken into account.

Briggs and Young (1969:35) proposed working directly with the Nusselt expression as follows

$$Nu_h = C_3 \, \mathrm{Re}_h^{0.8} \, \mathrm{Pr}_h^{0.4} \left(\frac{\mu_{wall}}{\mu_m} \right)^n \tag{4-6}$$

In equation 4-6, C_3 is a constant to be determined. The value of n is given in Table 4-1.

Heating	Cooling
n = -0.11 for $0.025 < \frac{\mu_{wall}}{\mu_m} < 1$	n = -0.25 for $1 < \frac{\mu_{wall}}{\mu_m} < 12.5$
$2 < Pr < 140$ and $5000 < Re < 123000$	

Table 4-1 Table showing values and constraints for n in equation 4-6. (Venter 2000:57)

By substituting the definitions of Nusselt, Reynolds and Prandtl numbers into equation 4-6, then evaluating h_h and then substituting the result into equation 4-2, one obtains

$$\frac{1}{U_h} = \frac{1}{C_3} \left\{ \frac{1}{\left(\frac{k}{D_h} \right)_h \cdot \mathrm{Re}_h^{0.8} \cdot \mathrm{Pr}_h^{0.4} \cdot \left(\frac{\mu_{wall}}{\mu_m} \right)^n} \right\} + \left[\left(\frac{1}{(h \cdot A)_c} + R_{f,c} + R_w + R_{f,h} \right) \cdot A_h \right] \tag{4-7}$$

Which is also in the form of $y = m \cdot x + C_4$. In the equation $y = \frac{1}{U_h}$, $m = \frac{1}{C_3}$, x equals the values in the { } brackets and C_4 equals the values in the [ ] brackets. A plot of y versus x will result in a straight line from which the gradient and the y-intercept can be obtained, as in the case of the Wilson plot. Once C_3 is known the heat transfer coefficients can be calculated using equation 4-6.

The correction factor $\left(\frac{\mu_{wall}}{\mu_m} \right)^n$ will be close to unity since the fluid used is water and the viscosity variation between the bulk (μ_m) and the wall (μ_{wall}) is small and can be treated as such for the first calculation of h_h. With h_h known the wall temperature can be calculated for each point, from here the correct temperature can be used to determine the two viscosities for

the correction factor. This technique is restricted by equation 4-2; same as in the case of the Wilson Plot technique.

4.3.3 MODIFIED WILSON PLOT (SHAH 1990)

With the Modified Wilson Plot (Shah 1990:51) applied to a fluted-tube the *Nu*–number of the flow in the inner tube is calculated as follows:

$$Nu_h = C_h \, \mathrm{Re}_h^a \, \mathrm{Pr}_h^{0.4} \left(\frac{\mu_{wall}}{\mu_m} \right)_h^{-0.14} \tag{4-8}$$

and the *Nu*–number of the flow in the annulus side is calculated as:

$$Nu_c = C_c \, \mathrm{Re}_c^b \, \mathrm{Pr}_c^{0.4} \left(\frac{\mu_{wall}}{\mu_m} \right)_c^{-0.14} \tag{4-9}$$

According to Shah (1990:52) the general Wilson Plot Technique is expressed as:

$$\frac{1}{U_h A_h} = \frac{1}{C_h \cdot \mathrm{Re}_h^a \cdot \mathrm{Pr}_h^{0.4} \cdot \left(\frac{A_h \cdot k}{D_h} \right)_h \left(\frac{\mu_{wall}}{\mu_m} \right)_h^{-0.14}} + R_w + \frac{1}{C_c \cdot \mathrm{Re}_c^b \cdot \mathrm{Pr}_c^{0.4} \cdot \left(\frac{A_c \cdot k}{D_h} \right)_c \left(\frac{\mu_{wall}}{\mu_m} \right)_c^{-0.14}} \tag{4-10}$$

This equation has five unknowns; C_h , a , C_c , b and R_w. In the Modified Wilson Plot Technique of Briggs and Young, 1969 a was assumed to be equal to 0.8 and R_w was assumed to be known.

In the case of fluted-tubes, Shah (1990:54) recommends that all five unknowns have to be calculated by an iterative scheme devised by Khartabil *et al.* (1988). The equations needed for the iterative scheme are as follows:

Equation 1

$$\left[\frac{1}{U_h A_h}-R_w\right]\cdot\left[\mathrm{Re}_c^b\cdot\mathrm{Pr}_c^{0.4}\cdot\left(\frac{A_c\cdot k}{D_h}\right)_c\left(\frac{\mu_{wall}}{\mu_m}\right)_c^{-0.14}\right]=\frac{1}{C_h}\left\{\frac{\mathrm{Re}_c^b\cdot\mathrm{Pr}_c^{0.4}\cdot\left(\frac{A_c\cdot k}{D_h}\right)_c\left(\frac{\mu_{wall}}{\mu_m}\right)_c^{-0.14}}{\mathrm{Re}_h^a\cdot\mathrm{Pr}_h^{0.4}\cdot\left(\frac{A_h\cdot k}{D_h}\right)_h\left(\frac{\mu_{wall}}{\mu_m}\right)_h^{-0.14}}\right\}+\frac{1}{C_c} \quad (4\text{-}11)$$

This equation is written in the form $y=m\cdot x+c$, with the values on the left hand side of the equation equal to y, m is equal to $\frac{1}{C_h}$, x equal to the values in the {} brackets and c equals to $\frac{1}{C_c}$. This equation is used to calculate C_t and C_s with an internal iterative scheme as explained by Shah (1990:53). The values of x and y are plotted on a graph and a linear regression line plotted through the plotted date. From this regression line m and c are determined.

Equation 2

$$\ln\left(\frac{1}{y_c}\right)=b\cdot\ln\left(\mathrm{Re}_c\right)+\ln\left(C_c\right) \quad (4\text{-}12)$$

With

$$y_c=\left[\frac{1}{U_c A_c}-R_w-\frac{1}{C_h\cdot\mathrm{Re}_h^a\cdot\mathrm{Pr}_h^{0.4}\cdot\frac{A_h k}{D_h}\left(\frac{\mu_w}{\mu_m}\right)_h^{-0.14}}\right]\cdot\mathrm{Pr}_c^{0.4}\cdot\frac{A_c k}{D_h}\left(\frac{\mu_w}{\mu_m}\right)_c^{-0.14} \quad (4\text{-}13)$$

Equation 4-12 is also in the form $y=m\cdot x+c$, with y equals $\ln\left(\frac{1}{y_c}\right)$, m equals to b, x equals to $\ln\left(\mathrm{Re}_c\right)$ and c equals to $\ln\left(C_c\right)$.

Equation 3

$$\ln\left(\frac{1}{y_h}\right) = a \cdot \ln(\mathrm{Re}_h) + \ln(C_h) \tag{4-14}$$

With

$$y_h = \left[\frac{1}{U_c A_c} - R_w - \frac{1}{C_c \cdot \mathrm{Re}_c^a \cdot \mathrm{Pr}_c^{0.4} \cdot \frac{A_c k}{D_h}\left(\frac{\mu_w}{\mu_m}\right)_c^{-0.14}}\right] \cdot \mathrm{Pr}_h^{0.4} \cdot \frac{A_h k}{D_h}\left(\frac{\mu_w}{\mu_m}\right)_h^{-0.14} \tag{4-15}$$

Equation 4-14 is also in the form $y = m \cdot x + c$, with y equals $\ln\left(\frac{1}{y_h}\right)$, m equals to a, x equals to $\ln(\mathrm{Re}_h)$ and c equals to $\ln(C_h)$

Equation 4

$$\frac{1}{U_c A_c} = \left[\frac{1}{(n_o \cdot h \cdot A)_h} + \frac{1}{(n_o \cdot h \cdot A)_c}\right] + R_w \tag{4-16}$$

Equation 4-16, the last equation, is also in the form $y = m \cdot x + c$, with y equals to $\frac{1}{U_c A_c}$, m equals to 1, x equals to $\left[\frac{1}{(n_o \cdot h \cdot A)_h} + \frac{1}{(n_o \cdot h \cdot A)_c}\right]$ and c equals to R_w.

Three test data sets are needed for the analysis:

Set 1 – Dominant shell side resistance data.

Set 2 – Dominant tube side resistance data.

Set 3 – Dominant wall resistance data.

The Khartibil *et al.* (1988) procedure is explained with Figure 4.4. With this procedure all four of the main equations are plotted on their own graph. With this graph plotted a linear regression line can be plotted through the points and the unknown variables determined.

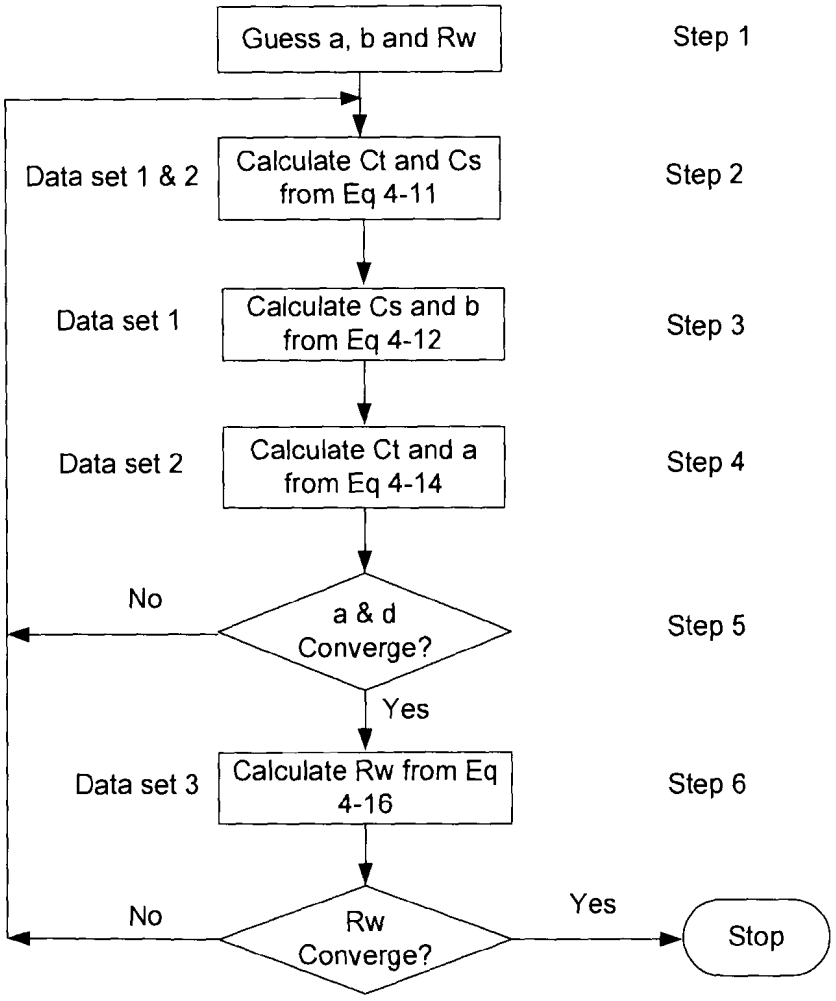

Figure 4.4 Iterative scheme of Khartabil *et al.* (1998)

Step 1:

Guess the values of the exponents a and b and the value of the wall resistance R_w.

Step 2:

This step has to be repeated approximately three to four times until the values converge. The process starts as follows:

1. Guess the values of C_h and C_c or take the values from the previous iteration.
2. Calculate C_h and C_c using Equation 4-11.

The reason for this iterative procedure is because you need C_h and C_c in Equations 4-8 and 4-9 to calculate the Nu numbers. With these Nu values the wall temperature can be calculated

and then used to determine the wall viscosity of the fluid being used and then used in Equation 4-11.

Step 3:

By using Equation 4-12 C_c and b can be calculated.

Step 4:

By using Equation 4-14 C_h and a can be calculated.

Step 5:

Now the calculated values of a and b from Steps 3 and 4 are compared to the guessed values of Step 1. If these values are not the same the process have to be repeated from Step 2 using the calculated values of a and b.

Step 6:

Calculate the value of R_w by using Equation 4-16.

Step 7:

Now the calculated value of R_w are compared to the guessed value or the value from the previous iteration. If the value does not converge the process starts all over from Step 2.

After the iterative scheme the values of a, b, C_h, C_c *and* R_w are determined and can be used in the calculation of the heat transfer coefficient in either the annulus or the tube side.

4.3.4 CORRELATION OF ROUSSEAU ET AL. (2003)

The correlation of Christensen *et al.* (1993) as used by Rousseau *et al.* (2003:235) was the only correlation found to predict the heat transfer coefficient of a fluid inside a fluted-tube. This correlation is based on extensive empirical work done by Christensen *et al.* (1993). The Nusselt number for the inner fluted-tube is dependant on the Reynolds number of the water in the inner tube as follows:

$$Nu_h = 0.014 \cdot \mathrm{Re}_h^{0.842} \left(e^*\right)^{-0.067} \left(p^*\right)^{-0.293} \left(\theta^*\right)^{-0.705} \mathrm{Pr}_h^{0.3} \qquad 500 < \mathrm{Re}_h \leq 5000$$

$$Nu_h = 0.064 \cdot \mathrm{Re}_h^{0.773} \left(e^*\right)^{-0.242} \left(p^*\right)^{-0.108} \left(\theta^*\right)^{-0.599} \mathrm{Pr}_h^{0.3} \qquad 5000 < \mathrm{Re}_h \leq 80\ 000 \tag{4-17}$$

The Prandtl number is determined by $\mathrm{Pr} = \frac{C_p \cdot \mu}{k}$ and the heat transfer coefficient by $h_h = \frac{Nu \cdot k}{D_{vi}}$. The values of e^*, p^*, θ^* and D_{vi} are explained in paragraph 4.4.6.

4.4 TWO-PHASE HEAT TRANSFER CORRELATIONS

Various heat transfer correlations for boiling exist, and most of them were derived for pure refrigerants in smooth tubes. Only a small number of these correlations are for either zeotropic refrigerants or fluted-tubes. No correlations were found for boiling of zeotropic refrigerants in fluted-tubes. The correlations used are described in detail in the following paragraphs.

4.4.1 CORRELATION OF GUNGOR AND WINTERTON (1986)

Gungor and Winterton (1986:351) divided the heat transfer for saturated boiling into two parts; nucleate boiling $\left(E \cdot h_l\right)$ and forced convection $\left(S \cdot h_{pool}\right)$. The basic form of the correlation is:

$$h_{tp} = E \cdot h_l + S \cdot h_{pool} \tag{4-18}$$

h_l is calculated using the Dittus-Boelter equation for boiling but only the liquid part of the refrigerant is taken into account.

$$h_l = 0.023 \cdot \mathrm{Re}_l^{0.8} \mathrm{Pr}_l^{0.4} \frac{k_l}{D_h} \tag{4-19}$$

Using a large amount of data available for saturated boiling the expressions for E and S were found to be:

$$E = 1 + 24\ 000 \cdot Bo^{1.16} + 1.37 \cdot \left(\frac{1}{X_{tt}}\right)^{0.86} \tag{4-20}$$

and

$$S = \frac{1}{1 + 1.15 \times 10^{-6} \cdot E^2 \, \mathrm{Re}_l^{1.17}} \tag{4-21}$$

With the Martinelli parameter (X_{tt}) defined as:

$$X_{tt} = \left(\frac{1-x}{x}\right)^{0.9} \cdot \left(\frac{\rho_v}{\rho_l}\right)^{0.5} \cdot \left(\frac{\mu_l}{\mu_v}\right)^{0.1} \tag{4-22}$$

the generation of vapour in the boiling process results in a significant disturbance of the layer and this improves the heat transfer. The dimensionless measurement of how important this effect may be is given by the boiling number:

$$Bo = \frac{q}{\lambda \cdot G} \tag{4-23}$$

Bo is the ratio of the heat flux perpendicular to the wall, due to boiling, to the total mass flux.

The pool boiling heat transfer coefficient h_{pool} is calculated as follows:

$$h_{pool} = 55 \cdot P_r^{0.12} \left(-\log_{10}[P_r]\right)^{-0.55} \cdot M^{-0.5} \cdot q^{0.67} \tag{4-24}$$

and the Froude number is calculated by

$$Fr = \frac{G^2}{\rho_l^2 \cdot g \cdot D_h} \tag{4-25}$$

If the tube is horizontal and the Froude number is less than 0.05, then E should be multiplied by:

$$E_2 = Fr^{(0.1-2Fr)} \tag{4-26}$$

and S should be multiplied by:

$$S_2 = \sqrt{Fr} \tag{4-27}$$

In case the boiling is inside an annuli, an equivalent diameter d_e must be used instead of the hydraulic diameter in all the calculations. The value of d_e depends on the width of the annular gap:

$$d_e = \frac{4 \times \textit{flow area}}{\textit{wetted perimeter}} \qquad d_e > 4 \text{ mm} \tag{4-28}$$

$$d_e = \frac{4 \times \textit{flow area}}{\textit{heated perimeter}} \qquad d_e < 4 \text{ mm} \tag{4-29}$$

Equation 4-29 is only valid in the case where one of the annulus walls is heated.

This correlation was developed using a data bank of more than 4300 points for flow boiling in horizontal and vertical smooth tubes and annuli of water, ethylene glycol and refrigerants including R11, R12, R22, R112, R113 and R114.

4.4.2 CORRELATION OF GUNGOR AND WINTERTON (1987)

Venter (2000:68) did experimental tests with R407C in smooth tubes, as mentioned in paragraph 2.3. He found that the correlation of Gungor and Winterton (1987:148) gave the best results while evaluating five different correlations.

The heat transfer correlation is given in the basic form by:

$$\frac{h_{tp}}{h_l} = 1 + 3000 \cdot Bo^{0.86} + 1.12 \cdot \left\{\frac{x}{1-x}\right\}^{0.75} \cdot \left\{\frac{\rho_l}{\rho_v}\right\}^{0.41} \tag{4-30}$$

h_l is calculated using the Dittus-Boelter equation for boiling for only the liquid part of the refrigerant (Equation 4-19). The boiling number (Bo) is calculated in the same manner as the correlation of Gungor and Winterton (1986) (Equation 4-23). In the calculation of the Reynolds and Nusselt numbers an equivalent diameter (Equation 4-29) is used instead of the standard hydraulic diameter for all sizes of d_e.

This correlation was developed using the same data bank used by Gungor and Winterton (1986) with some added data. This added data includes flow boiling in horizontal and vertical smooth tubes and annuli of n-butanol and ethanol.

4.4.3 *CORRELATION OF LIU AND WINTERTON (1991)*

The correlation of Liu and Winterton (1991:2759) is divided into two mechanisms, the forced convection mechanism $\left(F \cdot h_l\right)$ and the nucleate boiling mechanism $\left(S \cdot h_{pool}\right)$. F is the forced convection heat transfer enhancement factor and S is the suppression factor. The correlation is given by:

$$h_{tp}^2 = \left(F \cdot h_l\right)^2 + \left(S \cdot h_{pool}\right)^2 \tag{4-31}$$

h_l is calculated with the Dittus-Boelter equation with the entire mass flow rate flowing as a liquid in the same channel (Equation 4-19) and h_{pool} is calculated from Cooper's pool boiling correlation that is the same as the pool boiling calculated using equation 4-24, with the expressions of F and S as

$$F = \left[1 + x \cdot \mathrm{Pr}_l \cdot \left(\frac{\rho_l}{\rho_v} - 1\right)\right]^{0.35} \tag{4-32}$$

$$S = \left(1 + 0.055 \cdot F^{0.1} \cdot \mathrm{Re}_l^{0.16}\right)^{-1} \tag{4-33}$$

This correlation was developed out of the same data used by Gungor and Winterton (1987:148).

4.4.4 *CORRELATION OF PIERRE*

The correlation of Pierre (ASHRAE Fundamentals, 1997:4.7) was developed for calculating average heat transfer coefficients and is given by

$$Nu_{tp} = C \cdot \left(\mathrm{Re}_l^2 \cdot K_f\right)^n \tag{4-34}$$

where Re_l is the liquid Reynolds number assuming all the flow to be liquid, and K_f is Pierre's boiling number defined as:

$$K_f = \frac{\Delta h}{g \cdot L} = \frac{\Delta x \cdot h_{fg}}{g \cdot L} \tag{4-35}$$

The values of C and n in equation 4-34 are 0.0009 and 0.5 respectively. These values are suggested by the American Society for Heating, Refrigeration and Air-conditioning Engineers (ASHRAE Fundamentals, 1997:4.7).

This correlation was developed for the boiling heat transfer coefficients of R12 and R22 in copper tubes of 12.0 and 18.0 mm ID with lengths from 4.1 to 9.5 m. The evaporation temperatures were varied from -20 to 0 °C.

4.4.5 CORRELATION OF CHEN (1963)

According to Zhang *et al.* (2004:5751) the modified Chen (1963:1) correlation showed the best predictive behaviour amongst a total of six other existing correlations. The other correlations included the Liu-Winterton, the Kandlikar, the Shah, the Gungor-Winterton and the Steiner-Taborek correlations.

The basic modified Chen (1963:1) equation is defined as

$$h_{tp} = S \cdot h_{nb} + F \cdot h_{sp} \tag{4-36}$$

where S, the suppression factor, is calculated as

$$S = \frac{1}{1 + 2.53 \times 10^{-6} \cdot \mathrm{Re}_l^{1.17}} \tag{4-37}$$

and h_{nb} calculated with

$$h_{nb} = 0.00122 \cdot \left(\frac{k_l^{0.79} \cdot C_{p\,l}^{0.45} \cdot \nu_v^{0.24}}{\sigma^{0.5} \cdot \mu_l^{0.29} \cdot h_{fg}^{0.24} \cdot \nu_l^{0.49}} \right) \cdot \Delta T_{sat}^{0.24} \cdot \Delta p_{sat}^{0.75} \tag{4-38}$$

F, the Reynolds number factor, is calculated by

$$F = \max(F', 1) \tag{4-39}$$

where F' is calculated with

$$F' = 0.64 \cdot \phi_f \tag{4-40}$$

and ϕ_f is calculated with

$$\phi_f^2 = 1 + \frac{C}{X} + \frac{1}{X^2} \tag{4-41}$$

The constant C is dependent on the Reynolds number of both the liquid and vapour parts of the refrigerant, and is defined as

$$\begin{aligned} &For\ \mathrm{Re}_l < 1000\ and\ \mathrm{Re}_v < 1000,\ C = 5 \\ &For\ \mathrm{Re}_l > 2000\ and\ \mathrm{Re}_v < 1000,\ C = 10 \\ &For\ \mathrm{Re}_l < 1000\ and\ \mathrm{Re}_v > 2000,\ C = 12 \\ &For\ \mathrm{Re}_l > 2000\ and\ \mathrm{Re}_v > 2000,\ C = 20 \end{aligned} \tag{4-42}$$

For other regions of Re_l and Re_v the value of C has to be interpolated. The Martinelli parameter (X) is calculated with the friction factor as

$$X = \left(\frac{f_l}{f_v}\right) \cdot \left(\frac{1-x}{x}\right) \cdot \left(\frac{\rho_v}{\rho_l}\right) \tag{4-43}$$

where the friction factor(f) for both the liquid and gas is calculated as follows:

$f_k = 0.046 \cdot \mathrm{Re}_k^{-0.2}\ For\ \mathrm{Re}_k > 2000$	(4-44)
$f_k = \frac{24}{\mathrm{Re}_k}\left(1 - 3.55 \cdot \beta + 1.947 \cdot \beta^2 - 1.701 \cdot \beta^3 + 0.956 \cdot \beta^4 - 0.254 \cdot \beta^5\right)\ For\ \mathrm{Re}_k < 1000$	

In the case of $1000 < \mathrm{Re}_k < 2000$, the values in equation 4-44 have to be interpolated to calculate the value of f_k. The constant β represents the aspect ratio, defined as the ratio of the height to the width of the channel cross-section. h_{sp} is calculated with

$$h_{sp} = \frac{k_l}{D_h} \max\left(Nu_{sp,v}^{'}, Nu_{sp,t}\right) \; If \; \mathrm{Re}_l \le 2300$$
$$h_{sp} = \frac{k_l}{D_h} \cdot Nu_{sp,t} \; If \; \mathrm{Re}_l \ge 2300 \tag{4-45}$$

$Nu_{sp,t}$ is calculated with

$$Nu_{sp,t} = 0.023 \cdot \mathrm{Re}_l^{0.8} \cdot \mathrm{Pr}_l^{0.4} \tag{4-46}$$

and $Nu_{sp,v}^{'}$ is calculated with

$$Nu_{sp,t}^{'} = 8.235 \cdot \left(1 - 2.042 \cdot \beta + 3.085 \cdot \beta^2 - \cdot 2.4765\beta^3 + 1.058 \cdot \beta^4 - 0.186 \cdot \beta^5\right) \tag{4-47}$$

The modified Chen (1963:1) correlations together with the other correlations were tested with a various number of databases. These databases include circular and rectangular geometries with vertical and horizontal orientations, with the tube hydraulic diameters (D_h) varying from 0.780-6.00 mm. The fluids used in the databases include water, R11, R12 and R113.

4.4.6 *CORRELATION OF ROUSSEAU ET AL. (2003)*

The correlation of Rousseau *et al.* (2003:232) is based on the work done by Christensen *et al.* (1993). They proposed that due to the complex flower-like shape of the inner fluted-tube (Figure 1.2), the concept of "volume based diameters" is used instead of the conventional diameters associated with a circular cross-section. The volume based inside diameter of the fluted tube (D_{vi}) is calculated as

$$D_{vi} = \sqrt{\frac{4 \cdot Vol}{\pi \cdot L}} \tag{4-48}$$

with Vol the volume enclosed inside the fluted tube and L the length of the fluted-tube. The volume based outside diameter of the fluted-tube (D_{vo}) is calculated as

$$D_{vo} = D_{vi} + 2 \cdot t \tag{4-49}$$

with t the wall thickness of the tube. With the volume based diameters known as well as the inside diameter (D_o) of the outer tube as in Figure 1.2, the cross-section flow area can be

determined. The other important geometric parameters are the flute depth (e), flute pitch (p) and the helix angle (θ). The helix angle is calculated as follows:

$$\theta = \arctan\left(\frac{\pi \cdot D_{vo}}{N \cdot p}\right) \tag{4-50}$$

with N the number of flute starts at any cross-section. These parameters are non-dimensionalised by dividing the flute depth and pitch with D_{vi} to obtain e^* and p^* and the helix angle is divided by 90° to obtain θ^*.

The correlation of Rousseau *et al.* (2003:232) is given by

$$h_{helical} = e_h \cdot r_h \cdot h_{straight} \tag{4-51}$$

with r_h a heat transfer enhancement ratio according to the Chilton-Colburn analogy (see for instance Incropera and DeWitt, 2001:364). This ratio should be approximately equal the friction enhancement ratio (r_f) for simple geometries (Equation 4-53). e_h is an additional enhancement factor to cater for differences in the helical coil and fluted-tube annulus as well as other deviations from the assumptions originally made in the friction-heat transfer analogy (Rousseau *et al.*,2003:232) and is equal to 0.867. $h_{straight}$ is calculated with the Dittus-Boelter correlation if the flow is in a single phase or with a technique used by Shah (1979:547) if the flow is two-phase.

The technique by Shah (1979:547) determines the liquid heat transfer coefficient (h_{liq}) with the aid of the Dittus-Boelter correlation and then adjusting it for the average quality of the refrigerant in the tube section, being analysed as follows:

$$h_{tp} = h_{liq}\left[(1-x)^{0.8} + \frac{3.8 \cdot x^{0.76} \cdot (1-x)^{0.04}}{pr^{0.38}}\right] \tag{4-52}$$

with pr, the reduced pressure, equal to the ratio of local static pressure to the critical pressure of the refrigerant.

The heat transfer enhancement ratio is calculated as

$$r_f = \frac{f_{helical}}{f_{straight}} \tag{4-53}$$

with $f_{straight}$ based on the standard single-phase correlation of Swamee and Jain (quoted from Shames, 1992:365) given as

$$f_{straight} = \frac{0.25}{\left\{\log\left[\left(\frac{e}{3.7 \cdot D_h}\right) + \left(\frac{5.74}{\mathrm{Re}^{0.9}}\right)\right]\right\}^2} \tag{4-54}$$

$f_{helical}$ on the other hand is calculated from the single-phase correlation put forward by Das (1993:971) for helical coils and is given by

$$f_{helical} = 4 \cdot \left[\begin{array}{l} 0.079 \cdot \mathrm{Re}_v^{-0.25} + 0.0075 \cdot \left(\frac{D_{ho}}{d_{coil}}\right)^{0.5} + \\ 17.5782 \cdot \mathrm{Re}_v^{-0.3137} \cdot \left(\frac{D_{ho}}{d_{coil}}\right)^{0.3621} \cdot \left(\frac{e}{D_{ho}}\right)^{0.6885} \end{array} \right]. \tag{4-55}$$

D_{ho} in equation 4-55 is given by the difference between the inside diameter of the outer tube and the outside volumetric diameter (D_{vo}). d_{coil} is given by $D_{ho}/sin\theta$. This single-phase enhancement ratio is assumed to apply for two-phase flow as well.

The correlation of Rousseau *et al.* (2003:232) was developed by means of a simulation with available R22 data inside a commercial fluted-tube condenser. From the simulations it was found that the average difference between the measured and calculated log mean temperature difference was 4.41%. This correlation allows for the extension of the model to simulate heat exchangers for cycles employing zeotropic refrigerant mixtures.

4.4.7 CORRELATION OF KATTAN ET AL. (1998)

The correlation of Kattan *et al.* (1998c:164) is based on calculating the heat transfer coefficient based on the type of two-phase flow pattern in the tube. The basic form of the equation is:

$$h_{tp} = \frac{\theta_{dry} h_v + (2\pi - \theta_{dry}) h_{wet}}{2\pi} \tag{4-56}$$

Since the flow is in the annulus, it is assumed that the flow is always annular. In this case the dry angle (θ_{dry}) is equal to zero resulting in

$$h_{tp} = h_{wet} \tag{4-57}$$

According to Kattan *et al.* (1998c:159) h_{wet} is calculated as follows:

$$h_{wet} = \left(h_{nb}^3 + h_{cb}^3\right)^{1/3} \tag{4-58}$$

h_{nb} is the nucleate pool boiling heat transfer coefficient calculated as follows:

$$h_{nb} = F_c \cdot 55 \cdot P_r^{0.12} \left(-\log_{10}[P_r]\right)^{-0.55} \cdot M^{-0.5} \cdot q^{0.67} \tag{4-59}$$

F_c is a mixture boiling coefficient when working with zeotropic mixtures. It is calculated as follows:

$$F_c = \left[1 + \frac{h_{id}}{q} \Delta T_{bp} \left[1 - \exp\left(\frac{-B_o \cdot q}{\rho_l \cdot \Delta h_v \beta_L}\right)\right]\right]^{-1} \tag{4-60}$$

h_{id} is the ideal heat transfer coefficient, determined with equation 4-59 with ΔT_{bp}, the boiling range, set to 0.0. The mass transfer coefficient (β_L) is set to a fixed value of 0.0003 m/s. In the case the correlation is used with a non-zeotropic refrigerant F_c is also set to 1 since ΔT_{bp} will equal 0.0. B_o, the scaling factor, is set to a fixed value of 1.0.

The convective liquid heat transfer coefficient h_{cb} is determined by the following equation:

$$h_{cb} = C \cdot \mathrm{Re}_L^m \cdot \mathrm{Pr}_L^{0.4} \frac{k_L}{\delta} \tag{4-61}$$

From experiments it was found by Kattan *et al.* (1998c:160) that the values of C and m were found to be 0.0133 and 0.69 respectively. δ, the liquid film thickness, is calculated as follows:

$$\delta = \frac{\pi D_h (1-\alpha)}{2(2\pi - \theta_{dry})} \tag{4-62}$$

α, the void fraction, is calculated by

$$\alpha = \frac{x}{\rho_v}\left[\left(1+0.12(1-x)\left(\frac{x}{\rho_v}+\frac{1-x}{\rho_L}\right)\right)+\frac{1.18(1-x)\left[g\cdot\sigma_L(\rho_L-\rho_v)\right]^{0.25}}{G\cdot\rho_L^{0.5}}\right]^{-1} \tag{4-63}$$

The correlation of Kattan *et al.* (1998c:156) was compared to a new heat transfer database of 1141 points consisting out of five different refrigerants in horizontal tubes. These refrigerants included R134a, R502, R123 R402A and R404A. This correlation predicted all the data points with a mean deviation of 13.3% and an average deviation of 2.0%. Other correlations that were tested included Gungor and Winterton (1986) and Gungor and Winterton (1987), but they did not give satisfactory results.

4.4.8 MODIFIED CORRELATION OF ROUSSEAU ET. AL.

It was decided to use the Rousseau *et al.* (2003:232) correlation to develop a modified Rousseau et al correlation. The first reason for this is because this correlation was developed by the North-West University and there is a continuous process to improve the correlation. Another reason is that this was the only correlation found for fluted-tubes.

As mentioned in paragraph 4.4.6, the correlation of Rousseau *et al.* (2003:232) uses the general correlation of Shah (1979:547), for calculating the heat transfer during film condensation inside tubes. It is proposed that this correlation is replaced by the Gungor and Winterton (1987:148) correlation for saturated flow boiling. This was done because the Gungor and Winterton (1987:148) correlation gave the best results, as a standard correlation, as will be seen in paragraph 5.2.

The modified correlation is determined with

$$h_{helical} = e_h \cdot r_h \cdot h_{straight} \tag{4-64}$$

where $h_{straight}$ is still calculated with the Dittus-Boelter correlation if the flow is single phase but if the fluid is two-phase it is calculated with the Gungor and Winterton (1987:148) correlation as described by equation 4-30. The enhancement factor (e_h) is to include additional differences in the helical coil and annulus.

4.5 REFRIGERANT HEAT TRANSFER COEFFICIENTS

The experimental heat transfer coefficients of the refrigerant side can easily be calculated once the water side coefficients have been determined as described in paragraph 4.3. Consider the flow configuration in Figure 4.3 where the heat transfer coefficient of the outside fluid has to be determined. The total heat transfer rate (Q) is calculated from

$$Q = \dot{m}_w \cdot C_{pw} \cdot \left(T_{h,in} - T_{h,out}\right) \tag{4-65}$$

where $\dot{m}_w$ is the water-side mass flow rate and C_{pw} is the mean specific heat capacity of the water. The heat transfer rate can also be calculated from

$$Q = U_c \cdot A_c \cdot \Delta T_{lm} \tag{4-66}$$

with U_c the overall heat transfer coefficient based on the heat transfer area A_c with ΔT_{lm} the log mean temperature difference calculated as (Inropera and DeWitt, 2001:651)

$$\Delta T_{lm} = \left(\frac{\left(T_{h,in} - T_{c,out}\right) - \left(T_{h,out} - T_{c,in}\right)}{\ln\left(\frac{T_{h,in} - T_{c,out}}{T_{h,out} - T_{c,in}}\right)} \right) \tag{4-67}$$

The overall heat transfer coefficient can also be written in terms of the thermal resistance as (Inropera and DeWitt, 2001:105)

$$U_c = \frac{1}{\frac{1}{h_c} + \frac{r_o}{k_{Cu}} \cdot \ln\left(\frac{r_o}{r_i}\right) + \frac{1}{h_h} \cdot \left(\frac{r_o}{r_i}\right)} \tag{4-68}$$

As shown in Figure 4.3, h_c and h_h are the heat transfer coefficients of the cold fluid (refrigerant) and the hot fluid (water), with r_i and r_o the inside and outside radii of the inside of the inner tube and the outside of the inner tube and k_{Cu} the thermal conductivity of the copper tube. Equation 4-68 can be solved in terms of the heat transfer coefficient of the refrigerant (h_c) for easy determination of the coefficient:

$$h_c = \frac{1}{\frac{1}{U_c} - \left(\frac{r_o}{k_{Cu}} \cdot \ln\left(\frac{r_o}{r_i}\right) + \frac{1}{h_h} \cdot \frac{r_o}{r_i}\right)} \tag{4-69}$$

Using h_c to calculate Nu_c the experimental values can be compared for the various correlations described in paragraph 4.4 using a mean and average deviation. The mean deviation is calculated as follows

$$Mean\ deviation = \left|\frac{Nu_{cal} - Nu_{\exp}}{Nu_{\exp}}\right| \cdot 100\% \tag{4-70}$$

with the average deviation calculated as

$$Average\ deviation = \left(\frac{Nu_{cal} - Nu_{\exp}}{Nu_{\exp}}\right) \cdot 100\% \tag{4-71}$$

4.6 SUMMARY

In the preceding paragraphs various correlations were explained in detail for the determination of the heat transfer coefficients of single-phase and two-phase fluids. The single-phase correlations are used in the determination of the water heat transfer coefficient to calculate the experimental heat transfer coefficient of the refrigerant. This value is then compared to the various two-phase correlations to ultimately find a correlation to accurately predict the heat transfer coefficient of R407C in fluted-tubes.

None of the correlations explained have test results for the evaporation flow boiling of R407C in fluted-tubes. Only the correlation of Rousseau *et al.* (2003:232) was developed by conducting condensation tests on fluted-tubes. All the other correlations were derived using smooth tubes and R22 together with selected other refrigerants and fluids.

A Modified Rousseau *et al.* correlation is proposed incorporating the boiling heat transfer correlation of Gungor and Winterton (1987:148) into the fluted-tube geometry of the Rousseau *et al.* (2003:232) correlation.

In the next chapter all the experimental and correlation results are shown and explained. The experimental results include the calculation of the heat transfer coefficients of R22 and R407C in fluted-tubes. The correlation results also include the predicted heat transfer coefficients of R22 and R407C in the fluted-tubes using the refrigerant properties from the experiments conducted.

CHAPTER 5

5 EXPERIMENTAL RESULTS

5.1 INTRODUCTION

The first part of this chapter explains how the coefficients of the Modified Wilson plot are calculated using water-to-water tests. With the coefficient known, the water heat transfer coefficient of the refrigerant-to-water tests with R22 and R407C can be calculated. The experimental refrigerant heat transfer coefficient is then determined using the Log Mean Temperature Difference (LMTD) method and the water heat transfer coefficient. The experimental refrigerant heat transfer coefficients, calculated with the Modified Wilson Plot (Shah, 1990:55) and using the LMTD, are compared to the refrigerant heat transfer coefficients calculated with the single-phase correlation of Rousseau *et al.* (2003:232), together with the LMTD, to validate the correlation. The experimental refrigerant heat transfer coefficients are then compared to those determined from the various correlations found in the literature study.

5.1.1 MODIFIED WILSON PLOT (SHAH 1990)

Water-to-water test were done on the fluted-tube test section of the test evaporator to experimentally determine the five constants a, b, C_c, C_h and R_w as explained in paragraph 4.3.3. It was decided to calculate the wall resistance R_w with the following equation (Incropera and DeWitt:2001,106):

$$R_w = \frac{\ln\left(\frac{r_o}{r_i}\right)}{2\pi Lk} \tag{5-1}$$

The reason for this is because only the thermal conductivity of the copper tube will change the wall resistance since all the other variables in equation 5-1 are constant for all the experimental tests. The conductivity on the other hand, is only dependant on the tube temperature. This temperature only varies between 7 – 20 °C resulting in a 0.5 % variation in the wall resistance. The wall resistance was taken as 0.00002 m.K/W. With this known only steps 1 through 5 of the iterative scheme of Khartabil *et al.* (1998) have to be done.

The mass flow rate in the annulus side was kept constant at four values of 0.01, 0.02, 0.03 and 0.06 kg/s respectively. With each of these four values the inner tube mass flow rate was varied from 0.01 kg/s to 0.10 kg/s with increments of 0.01 kg/s. All of these tests were done while keeping both inlet temperatures constant for the full duration of the tests. Temperature and mass flow data were stored for an interval of three minutes for each increment. The values were then transferred to Microsoft Excel to calculate the average values, from where the values were transferred to EES to calculate the respective x and y values of Steps 2, 3 and 4 of the iterative scheme as in equations 4-11 through to 4-15 to be plotted against each other to determine a, b, C_c and C_h, as described in paragraph 4.3.3.

Table 5-1 shows all the values as used in the first iteration of the scheme as recommended by Khartabil *et al.* (1988). Table 5-2 shows all the initial values of the last five iterations and finally, Table 5-3 shows all the values of the last iteration. From this table it can be seen that there are only minor changes of the values.

	Initial values	Step 2				Step 3	Step 4
		Iteration 1	Iteration 2	Iteration 4	Iteration 4		
a	0.8						0.69717
b	0.8					0.81581	
C_c	0.023	0.04953	0.03248	0.03292	0.03291	0.02701	
C_h	0.023	0.03244	0.04884	0.04813	0.04815		0.13331

Table 5-1 Results of the first iteration of the Khartabil *et al.* (1988) scheme

	a	b	C_c	C_h
Iteration 15	0.565	0.985	0.0110	0.3555
Iteration 16	0.565	0.999	0.0093	0.3718
Iteration 17	0.5614	1.012	0.0087	0.3788
Iteration 18	0.5611	1.023	0.0081	0.3826
Iteration 19	0.55897	1.03200	0.00764	0.38854

Table 5-2 Initial values of the last five iteration of the scheme

	Initial values	Step 2				Step 3	Step 4
		Iteration 1	Iteration 2	Iteration 4	Iteration 4		
a	0.55897						0.55732
b	1.03200					1.04103	
C_c	0.00764	0.00771	0.00770	0.00770	0.00770	0.00722	
C_h	0.38854	0.38614	0.38618	0.38618	0.38618		0.39315

Table 5-3 Results of the final iteration of the Khartabil *et al.* (1988) scheme

Thus the equation used to calculate the experimental *Nu*-numbers in the inner fluted-tube is:

$$Nu_h = 0.39315 \cdot \mathrm{Re}_h^{0.55732}\, \mathrm{Pr}_h^{0.4} \left(\frac{\mu_{wall}}{\mu_m} \right)_h^{-0.14} \tag{5-2}$$

The final results of the iteration process are graphically represented in Figure 5.1, Figure 5.2 and Figure 5.3. Figure 5.1 shows the data of Iteration 4 of Step 2. As can be seen the regression is 0.99812, resulting in an acceptable accuracy. Figure 5.2 shows the data of Step 3 with a regression of 0.99224. The last step of the iterative scheme used, Step 3, is represented in Figure 5.3 showing also a regression of 0.99256.

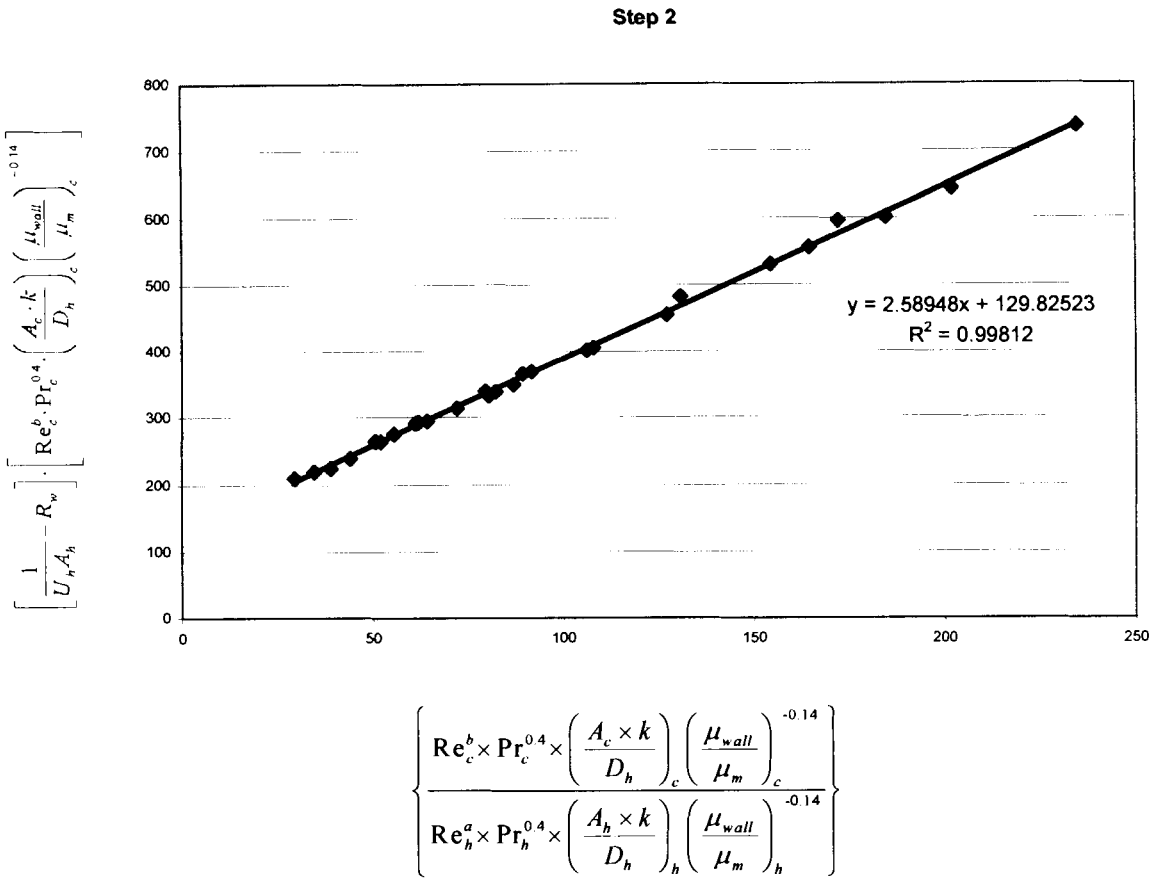

$$\left[\frac{1}{U_h A_h} - R_w\right] \cdot \left[\frac{\mathrm{Re}_c^b \cdot \mathrm{Pr}_c^{0.4} \cdot \left(\frac{A_c \cdot k}{D_h}\right)_c \left(\frac{\mu_{wall}}{\mu_m}\right)_c^{-0.14}}{\mathrm{Re}_h^a \times \mathrm{Pr}_h^{0.4} \times \left(\frac{A_h \times k}{D_h}\right)_h \left(\frac{\mu_{wall}}{\mu_m}\right)_h^{-0.14}}\right]$$

Figure 5.1 Experimental final results of Step 2 of the Modified Wilson Plot (Shah, 1990:53)

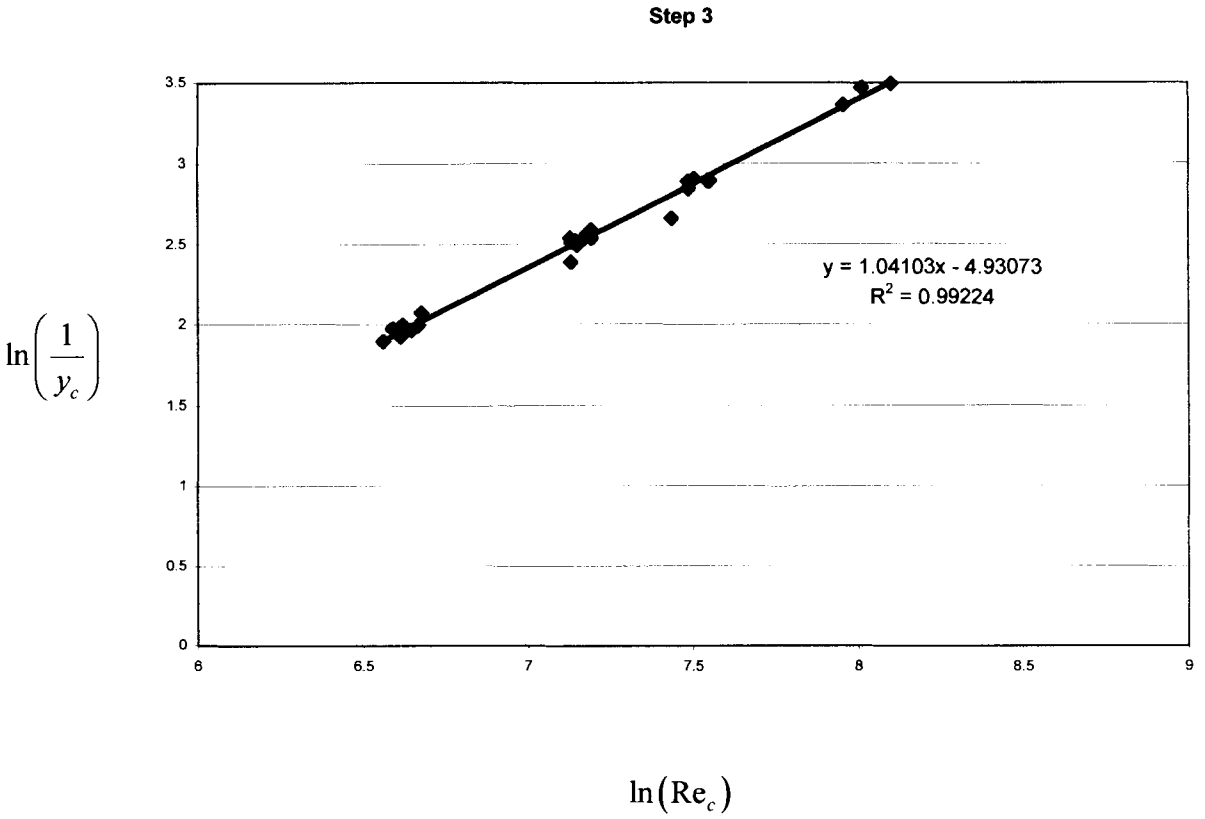

Figure 5.2 Experimental final result of Step 3 of the Modified Wilson Plot (Shah, 1990:53)

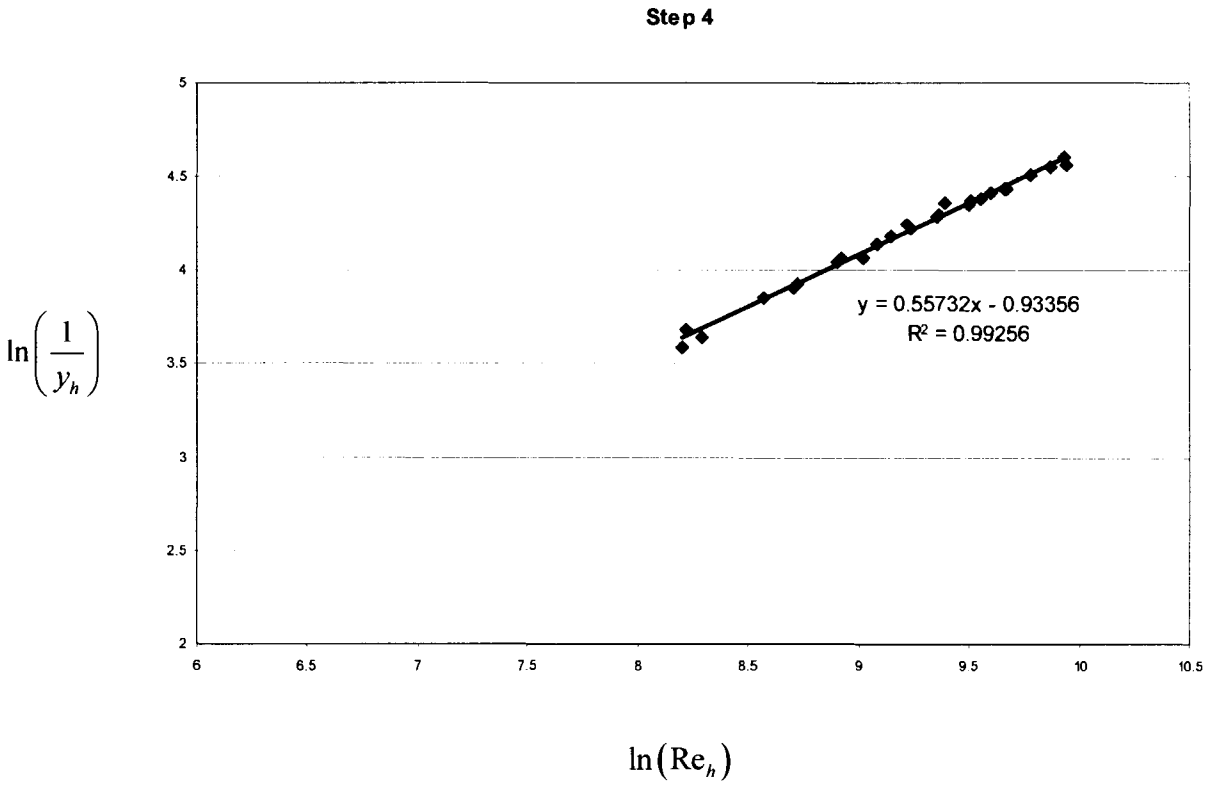

Figure 5.3 Experimental final result of Step 4 of the Modified Wilson Plot (Shah, 1990:54)

5.1.2 CORRELATION OF ROUSSEAU ET AL. (2003)

It can be clearly seen from Figure 5.4 and Figure 5.5 that a good comparison was found between the two calculated refrigerant Nusselt numbers with the R22, as well as the R407C data. The maximum deviation was found to be 1.80 % (Table 5-4). This is a clear indication that the Modified Wilson plot (Shah, 1990:55) is accurate in the calculation of the refrigerant heat transfer coefficient.

The mean and average deviations for all the data were found to be:

	Average deviation (%)	Mean deviation (%)
R22	-1.76	1.80
R407C	-1.62	1.63

Table 5-4 Deviation of the measured water Nusselt number to the calculated water Nusselt number for the R22 and R407C data according to Rousseau *et al.* (2003:232).

The refrigerant heat transfer coefficient was calculated by firstly calculating the water *Nu*-numbers, from the R22 and R407C experiments, with Equation 5-2 and 4-17 and then using the LMTD-method to calculate the refrigerant heat transfer coefficients.

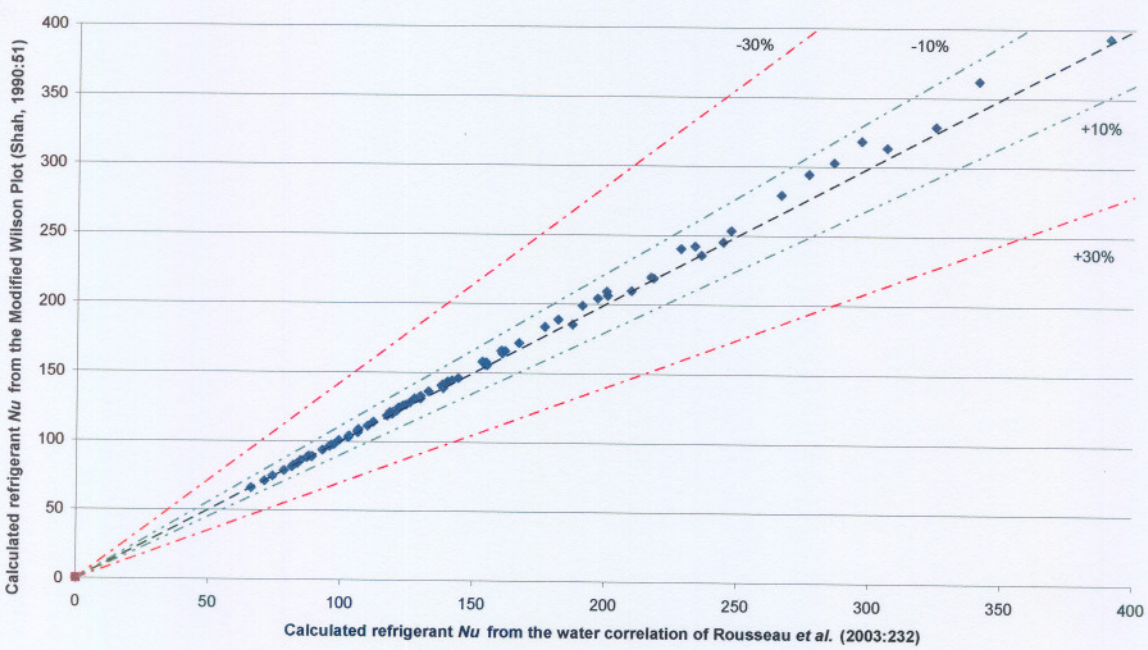

Figure 5.4 Calculated refrigerant Nusselt numbers for the R22 data.

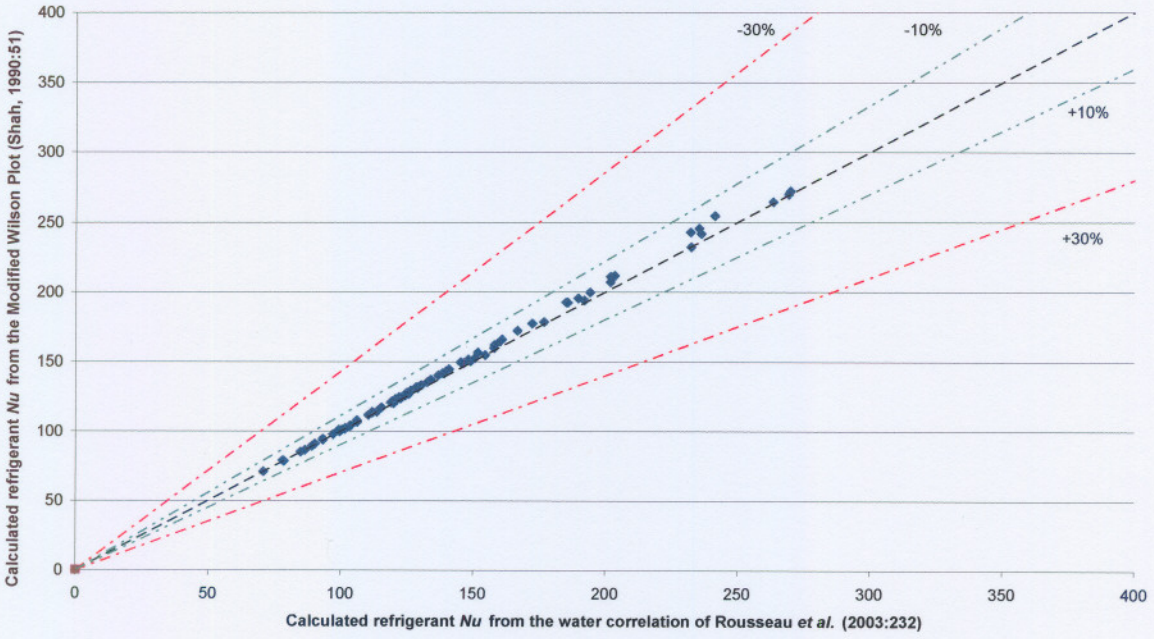

Figure 5.5 Calculated refrigerant Nusselt numbers with the R407C data.

Knowing that the calculation of the refrigerant heat transfer coefficient is correct, the calculated coefficients can be used to test the various refrigerant two-phase correlations.

5.2 TWO-PHASE HEAT TRANSFER CORRELATIONS

All the refrigerant correlations as discussed in paragraph 4.4 are tested in the original form as they are found in the literature, except for the refrigerant Rousseau *et al.* (2003:232) correlation. In this case the enhancement factor was changed since the correlation was developed for condensation in fluted-tubes.

In general it will be ideal if one of the correlations could predict the heat transfer coefficients within 10% of the experimental values. A total of five lines are drawn in all the graphs of experimental versus calculated results. The two outer lines are the –30% and the +30%, the two inner lines are the –10% and the +10%, with the last line the 0% deviation. In conclusion, for a good correlation the data points will be between the –10% and the +10% lines.

5.2.1 *Correlation of Gungor and Winterton (1986)*

From Table 5-5 it can be seen that the correlation over-predicts the values by more than 90% for both the R22 and R407C.

	Average deviation (%)	Mean deviation (%)
R22	92.0	97.32
R407C	96.2	97.56

Table 5-5 Deviation of the measured Nusselt numbers to the calculated Nusselt numbers for R22 and R407C according to Gungor and Winterton (1986:351).

It is clear from Figure 5.6 and Figure 5.7 that the correlation over predicts most of the R22 as well as the R407C data. A possible reason for this is due to the following:

- the correlation does not incorporate the geometry of the fluted-tube, or
- the correlation does not bring the temperature glide of R407C into account.

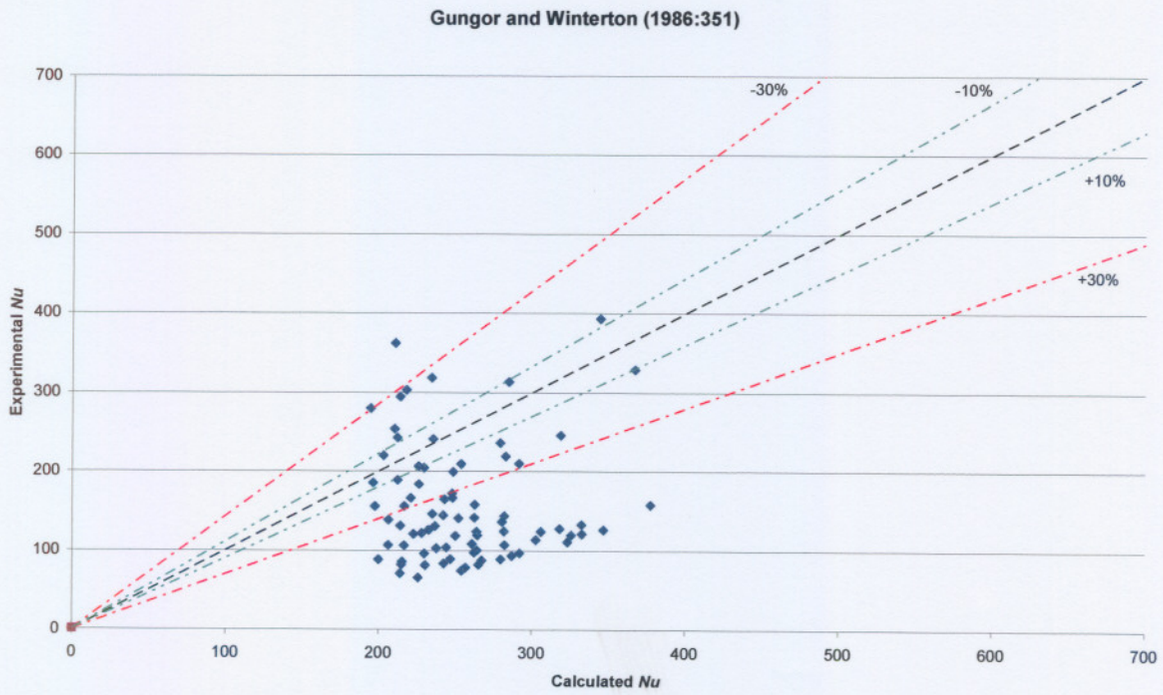

Figure 5.6 Experimental versus calculated Nusselt numbers for R22 with the correlation of Gungor and Winterton (1986:351).

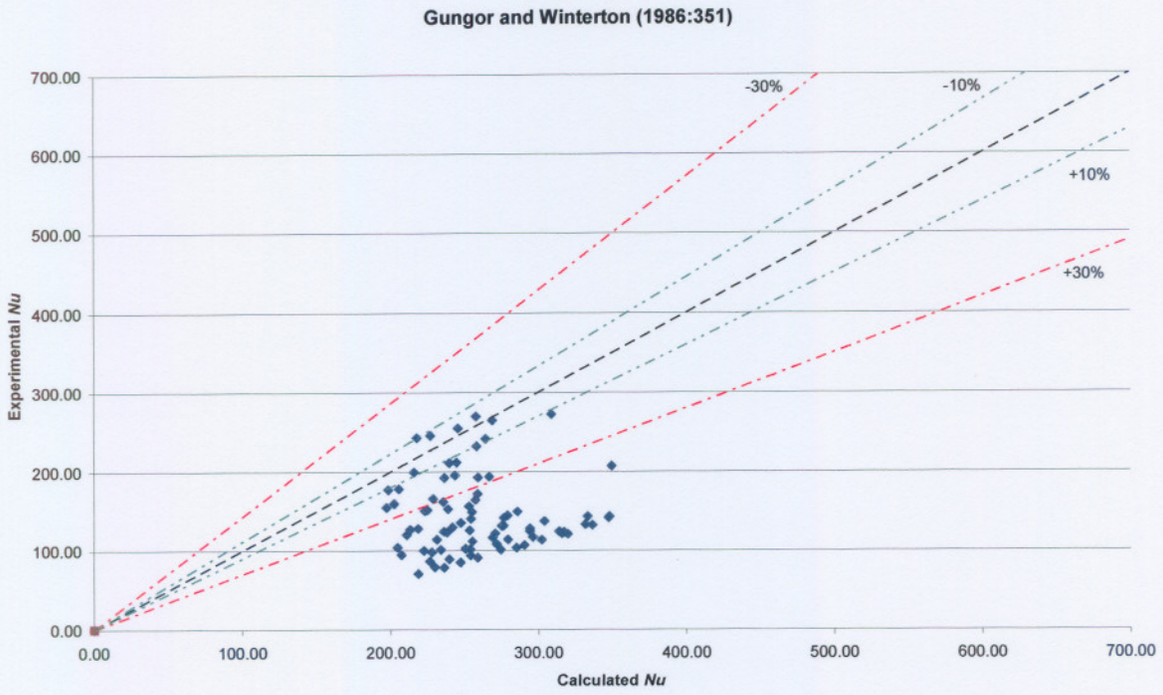

Figure 5.7 Experimental versus calculated Nusselt numbers for R407C with the correlation of Gungor and Winterton (1986:351).

Some of the data points that are under-predicted are a result of an excessive heat flux that may result in large liquid slugs and can result in false experimental readings as explained in paragraph 4.2.3.

5.2.2 Correlation of Gungor and Winterton (1987)

Table 5-6 shows a maximum average deviation of less than 20% and mean deviation of less than 50% for both R22 and R407C. From the results it is clear that the Gundor and Winterton (1987) correlation is a better correlation than the Gundor and Winterton (1986) correlation. It is also clear from Figure 5.8 and Figure 5.9 that the R407C data are more packed together thus giving better results.

	Average deviation (%)	Mean deviation (%)
R22	13.86	43.08
R407C standard	-0.03	31.50

Table 5-6 Deviation of the measured Nusselt numbers to the calculated Nusselt numbers for R22 and R407C according to Gungor and Winterton (1987:148).

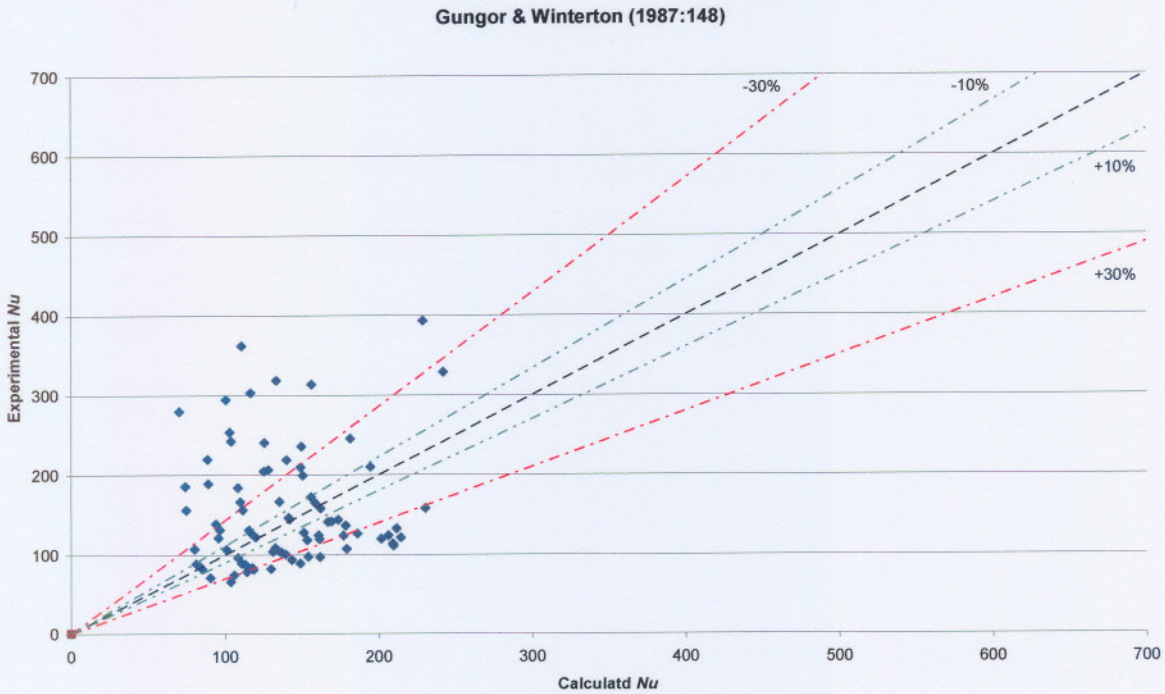

Figure 5.8 Experimental versus calculated Nusselt numbers for R22 with the correlation of Gungor and Winterton (1987:148).

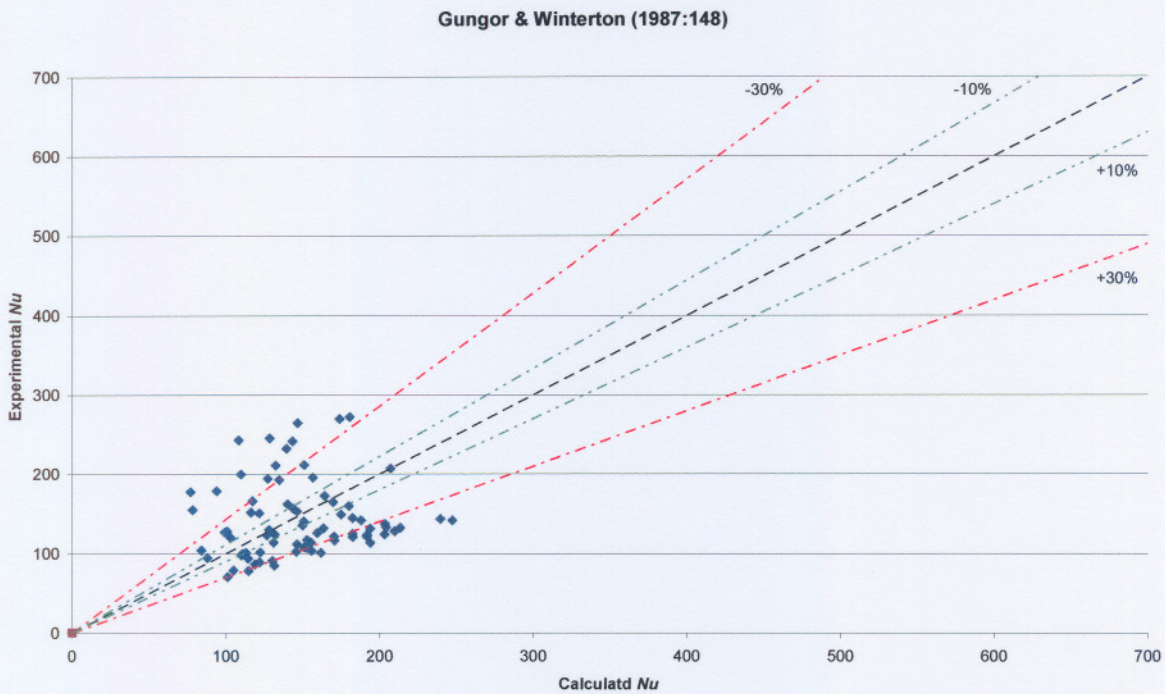

Figure 5.9 Experimental versus calculated Nusselt numbers for R407C with the correlation of Gungor and Winterton (1987:148).

From the literature survey is was found that the Gungor and Winterton (1987) is an improved correlation on the Gungor and Winterton (1986) correlation. The experimental data proves this with the Gungor and Winterton (1987) getting better results than the Gungor and Winterton (1986). The fact that there are still some scattered points could be a result of the following:

- the correlation does not incorporate the geometry of the fluted-tube, or
- the correlation does not bring the temperature glide of R407C into account.

5.2.3 Correlation of Liu and Winterton (1991)

Table 5-7 shows deviations of less than 100% for both R22 and R407C.

	Average deviation (%)	Mean deviation (%)
R22	84.66	91.05
R407C	91.53	94.35

Table 5-7 Deviation of the measured Nusselt numbers to the calculated Nusselt numbers for R22 and R407C according to Liu and Winterton (1991:2759).

From Figure 5.10 and Figure 5.11 it can be clearly seen that the correlation over predicts most of the data. The reason for this is due to the one of the following:

- the correlation does not incorporate the geometry of the fluted-tube, or
- the correlation does not bring the temperature glide of R407C into account.

The R22 and R407C data that are under-predicted is where the heat flux is too high due to the high water inlet temperature. This high heat flux resulted in liquid slugs and caused experimental data errors.

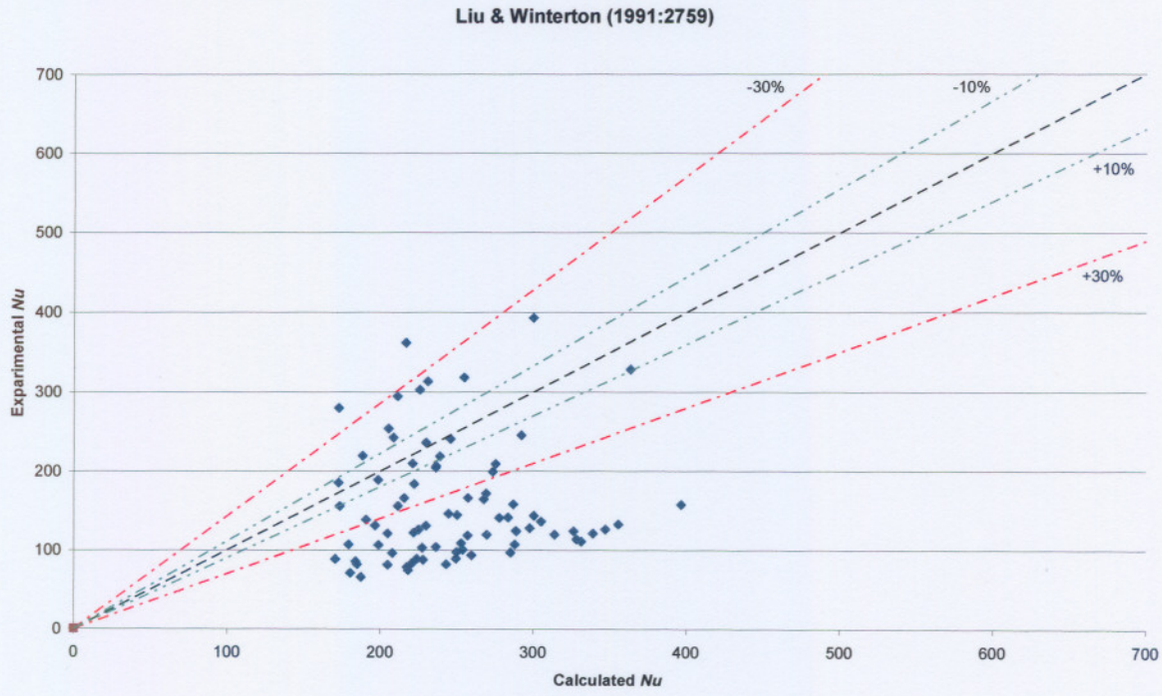

Figure 5.10 Experimental versus calculated Nusselt numbers for R22 according to the correlation of Liu and Winterton (1991:2759).

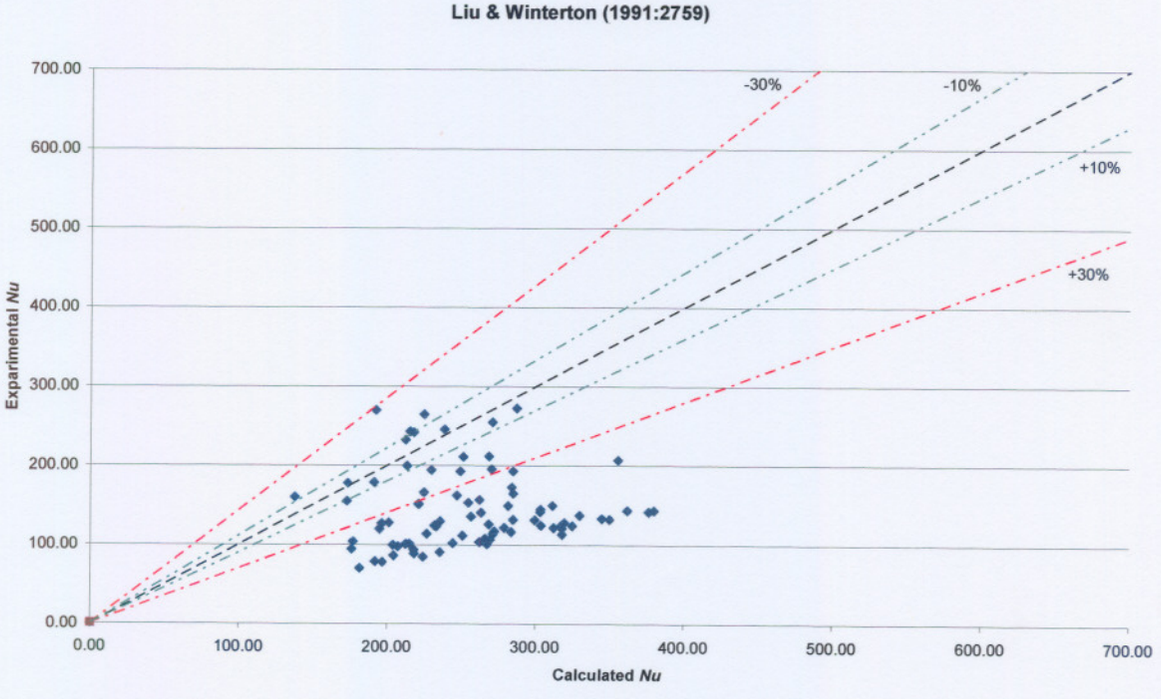

Figure 5.11 Experimental versus calculated Nusselt numbers for R407C according to the correlation of Liu and Winterton (1991.2759).

5.2.4 *CORRELATION OF PIERRE*

It is clear from Figure 5.12 and Figure 5.13 that most of the data are over-predicted by the correlation. Venter (2000:78) found that a better correlation could be found if the original coefficient of 0.0009 in the correlation of Pierre (Equation 4-24) was replaced with the value of 0.0004. This was found in the case of evaporating test data with R407C in a smooth tube. It was furthermore found by Venter (2000:78) that the correlation was insufficient for qualities higher than 95%. Venter (2000:78) stated that the biggest deviation for the current data is in the case where the heat flux is too high.

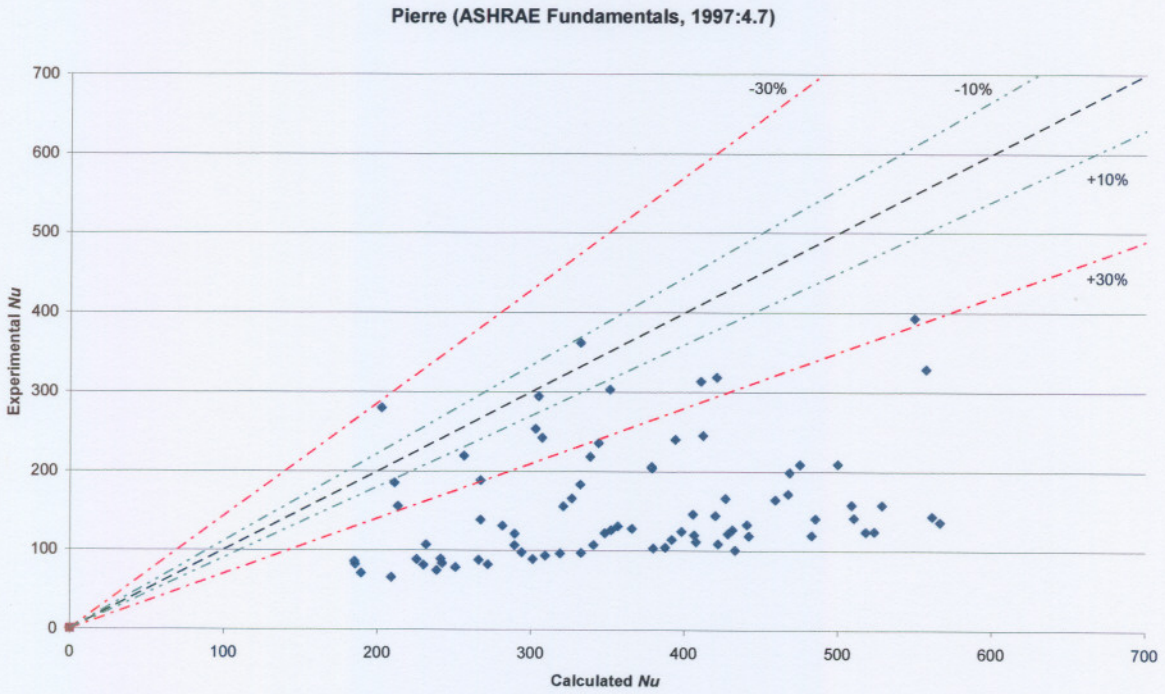

Figure 5.12 Experimental versus calculated Nusselt numbers for R22 with the correlation of Pierre (ASHRAE Fundamentals, 1997:4.7).

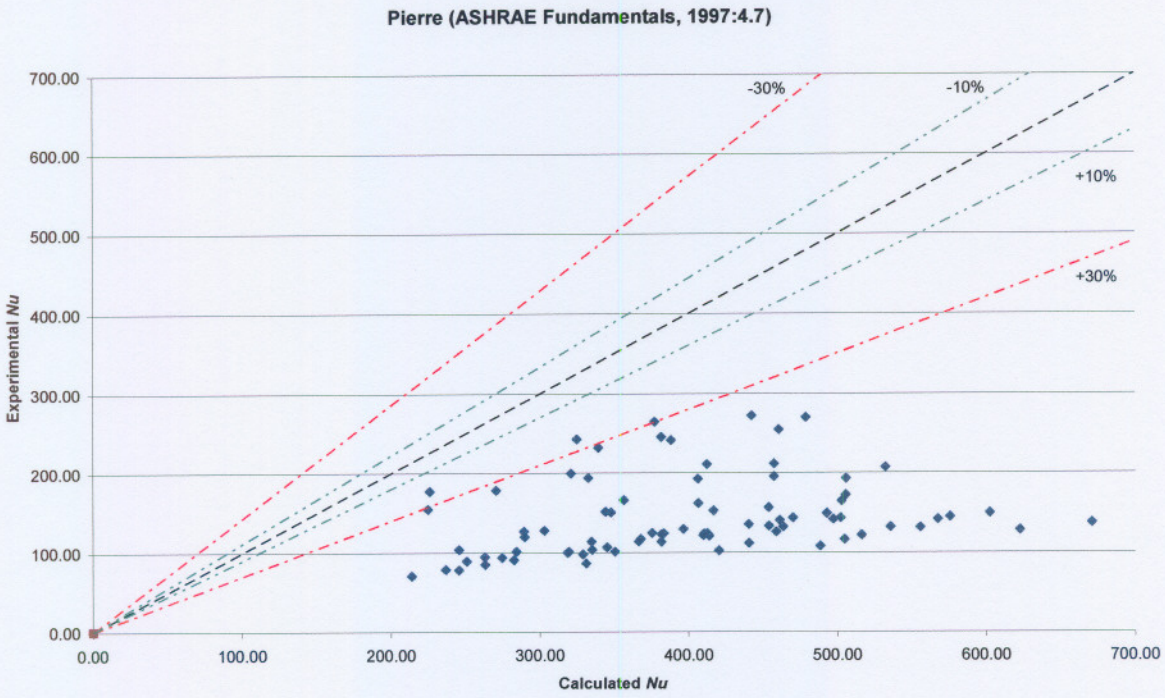

Figure 5.13 Experimental versus calculated Nusselt numbers for R407C with the correlation of Pierre (ASHRAE Fundamentals, 1997:4.7).

The deviations with the correlation of Pierre (ASHRAE Fundamentals, 1997:4.7) are in excess of 150 % as shown in Table 5-8.

	Average deviation (%)	Mean deviation (%)
R22	161.67	162.55
R407C	196.37	196.59

Table 5-8 Deviation of the measured Nusselt numbers to the calculated Nusselt numbers for R22 and R407C according to Pierre (ASHRAE Fundamentals, 1997:4.7).

5.2.5 CORRELATION OF CHEN

It can be clearly seen from Figure 5.14 and Figure 5.15 that data points with the R22 and R407C are very scattered.

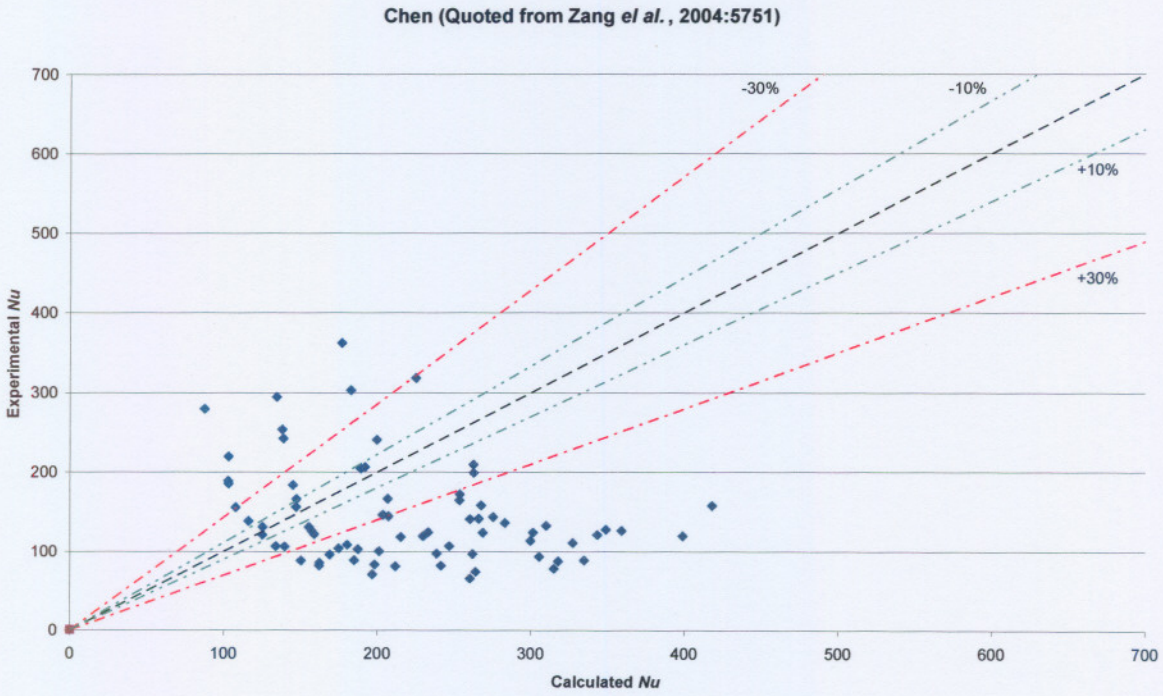

Figure 5.14 Experimental versus calculated Nusselt numbers for R22 according to the correlation of Chen (1963:1).

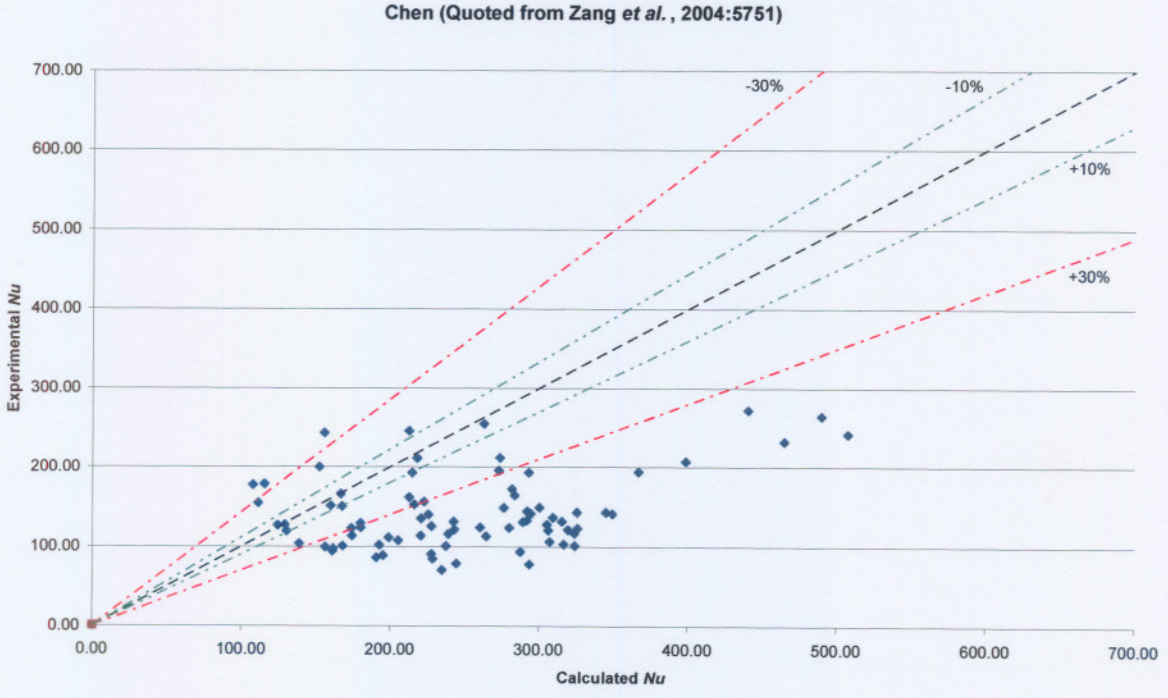

Figure 5.15 Experimental versus calculated Nusselt numbers for R407C according to the correlation of Chen (1963:1).

The correlation of Chen (quoted from Zhang *et al.*, 2004:5751) gave smaller average and mean deviation compared to most of the other correlations (Table 5-9). But looking at Figure 5.14 and Figure 5.15 it is clear that the correlation is inadequate for the prediction of the boiling heat transfer coefficient of R407C in fluted-tubes.

	Average deviation (%)	Mean deviation (%)
R22	61.86	94.00
R407C	81.29	81.29

Table 5-9 Deviation of the measured Nusselt numbers to the calculated Nusselt numbers for R22 and R407C according to Chen (1963:1).

5.2.6 *CORRELATION OF ROUSSEAU ET AL. (2003)*

Deviations of the standard correlation of Rousseau *et al.* (2003:232) were found to be in excess of 250% (Table 5-10). This could be expected since the correlation was developed for condensation of R22 in fluted-tubes. If the enhancement factor (e_h) is changed to the following:

$e_{h\,R22} = 0.2658$

and

$e_{h\,R407C} = 0.2391.$

much better results are found.

	Average deviation (%)	Mean deviation (%)
R22 standard	267.43	267.43
R22 with the changed enhancement factor	12.67	35.16
R407C standard	276.36	276.36
R407C with the changed enhancement factor	3.83	22.01

Table 5-10 Deviation of the measured Nusselt numbers to the calculated Nusselt numbers for R22 and R407C according to Rousseau *et al.* (2003:232).

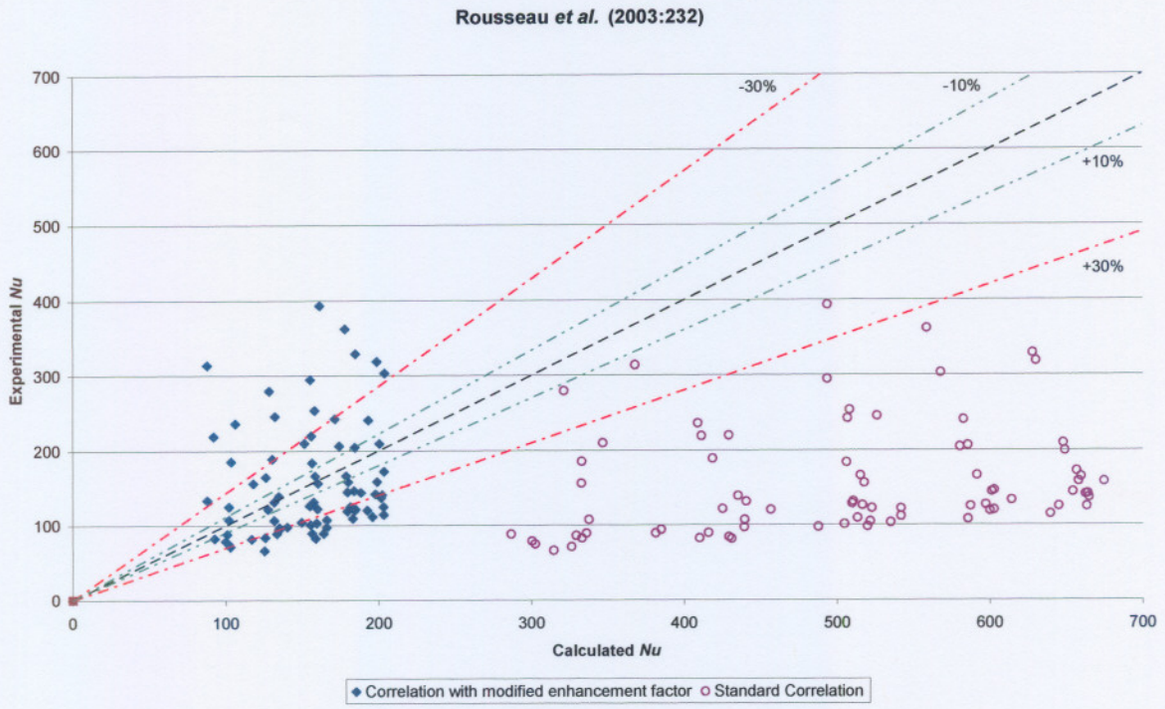

Figure 5.16 Experimental versus calculated Nusselt numbers for R22 according to the correlation of Rousseau *et al.* (2003:232).

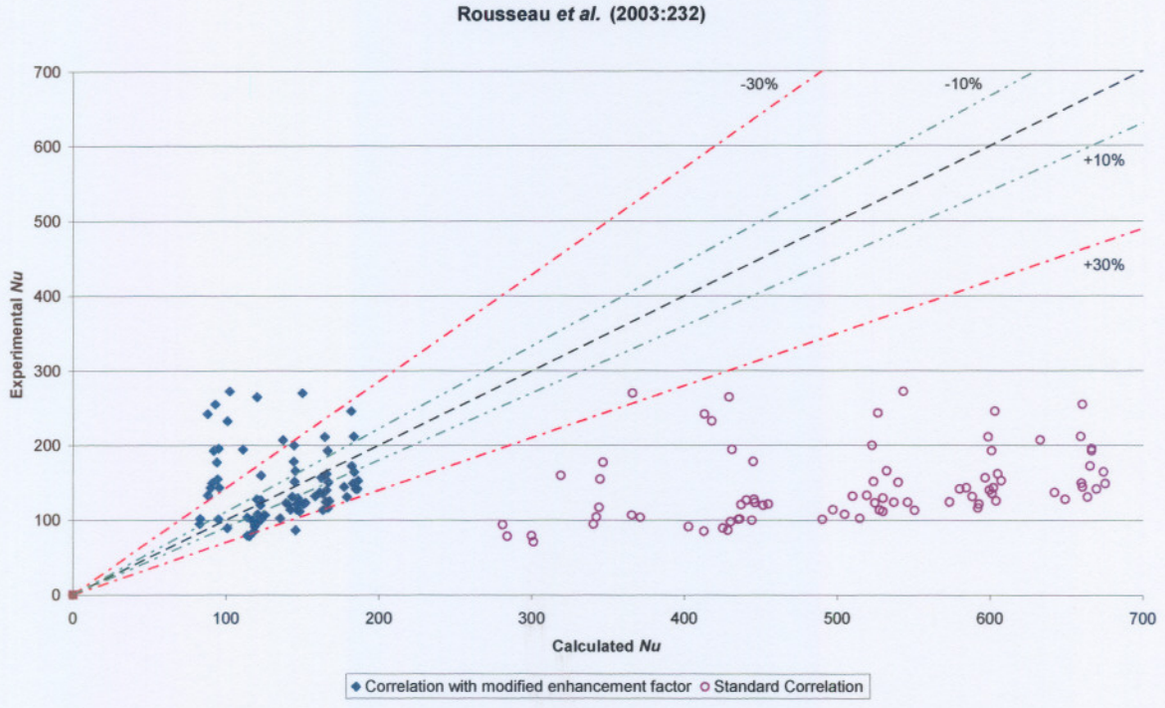

Figure 5.17 Experimental versus calculated Nusselt numbers for R407C according to the correlation of Rousseau *et al.* (2003:232).

From Figure 5.16 and Figure 5.17 it can be seen that all the data of the standard correlation is over-predicted. With the different enhancement factor, more than 70% of the data is in the ±30% error bandwidth. Some of the data points that were under-predicted were when the heat flux was too high (as explained in paragraph 4.2.3).

5.2.7 *CORRELATION OF KATTAN ET AL. (1998)*

From Table 5-11 it can be seen that the deviations are for both the refrigerants higher than 70%

	Average deviation (%)	Mean deviation (%)
R22	100.80	105.35
R407C	73.78	77.80

Table 5-11 Deviation of the measured Nusselt numbers to the calculated Nusselt numbers for R22 and R407C according to the Kattan *et al.* (1998c:156) correlation.

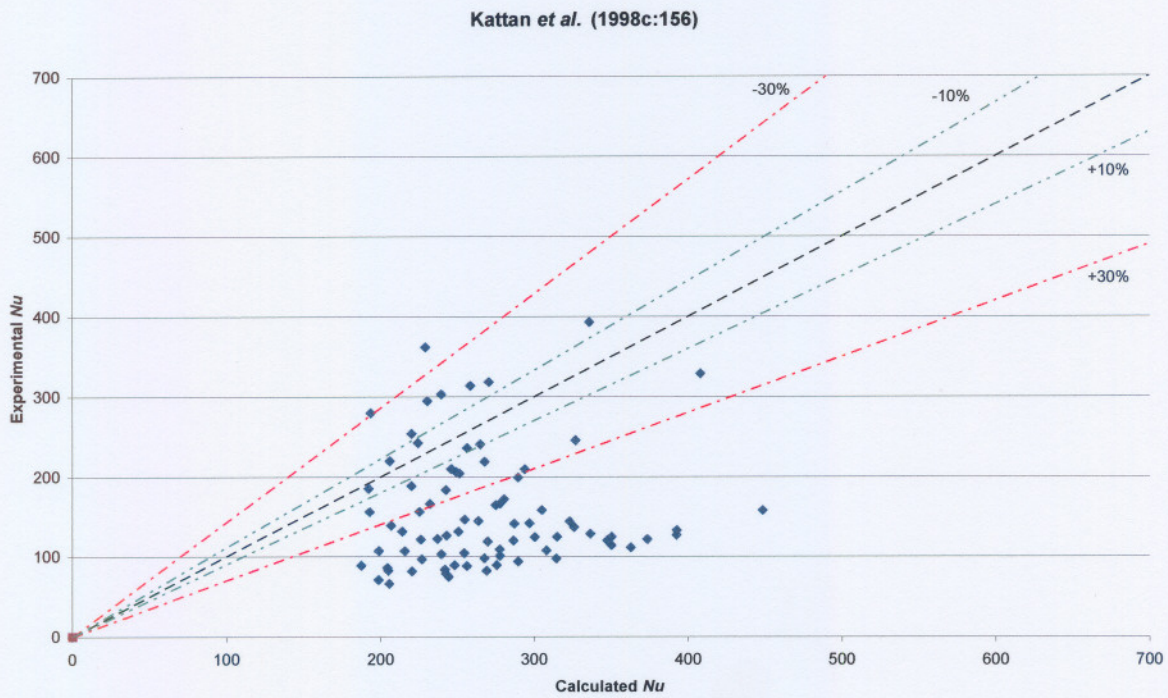

Figure 5.18 Experimental versus calculated Nusselt numbers for R22 according to the Kattan *et al.* (1998c:156) correlation.

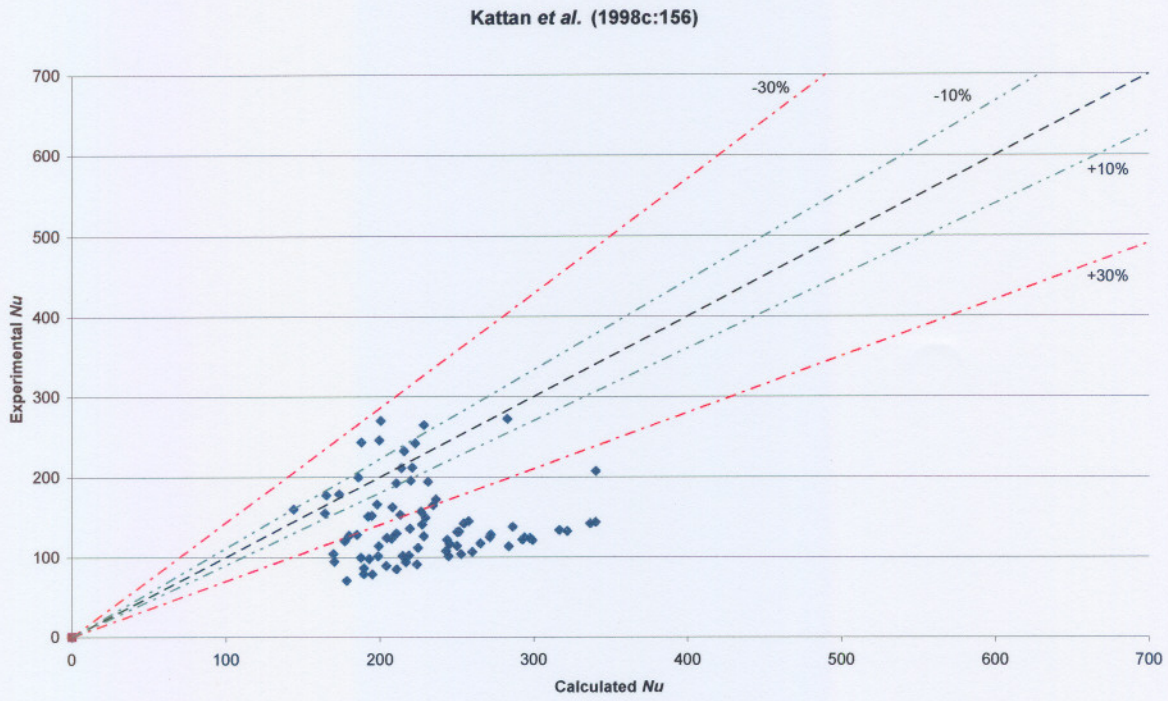

Figure 5.19 Experimental versus calculated Nusselt numbers for R407C according to the Kattan *et al.* (1998c:156) correlation.

Figure 5.18 and Figure 5.19 show the experimental versus calculated Nusselt numbers for the Kattan *et al.* (1998c:156) correlation. It can be seen that the data for R407C is less scattered than the R22 data. A possible reason for the over-prediction of the data is that the assumption that the dry angle (θ_{dry}) is equal to zero, with the annular flow, was wrong. Another reason is that the correlation was developed by using flow regimes in smooth tubes, thus not taking the geometry of the fluted-tube into account.

5.2.8 MODIFIED CORRELATION OF ROUSSEAU ET AL.

As explained in paragraph 4.4.8, the condensing two-phase heat transfer coefficient calculated with the technique used by Shah (1979:547) that is used in the correlation of Rousseau *et al.* (2003:232) is replaced with the evaporation correlation of Gungor and Winterton (1987:148). This resulted in the Modified Rousseau *et al.* correlation. From the experimental data it was found that the additional heat transfer coefficients are as follows:

$e_{h\ R22} = 0.0671$ (for R22)

and

$e_{h\ R407C} = 0.0567$ (for R407C).

Table 5-12 shows the average and mean deviation for the R22 and R407C data. It is clear that the correlation predicts the heat transfer coefficient of R407C better than that of R22.

	Average deviation (%)	Mean deviation (%)
R22 standard	13.86	43.08
R407C standard	-0.03	31.49

Table 5-12 Deviation of the measured Nusselt numbers to the calculated Nusselt numbers for R22 and R407C according to the Modified Rousseau *et al.* correlation.

Figure 5.20 and Figure 5.21 show the experimental versus calculated Nusselt numbers for the Modified Rousseau *et al.* correlation. It can be seen that the data for R407C is less scattered as in the case of the R22 data. From the experimental data it was found that all the data points that were under-predicted had a high heat flux resulting in experimental error as explained in paragraph 4.2.3.

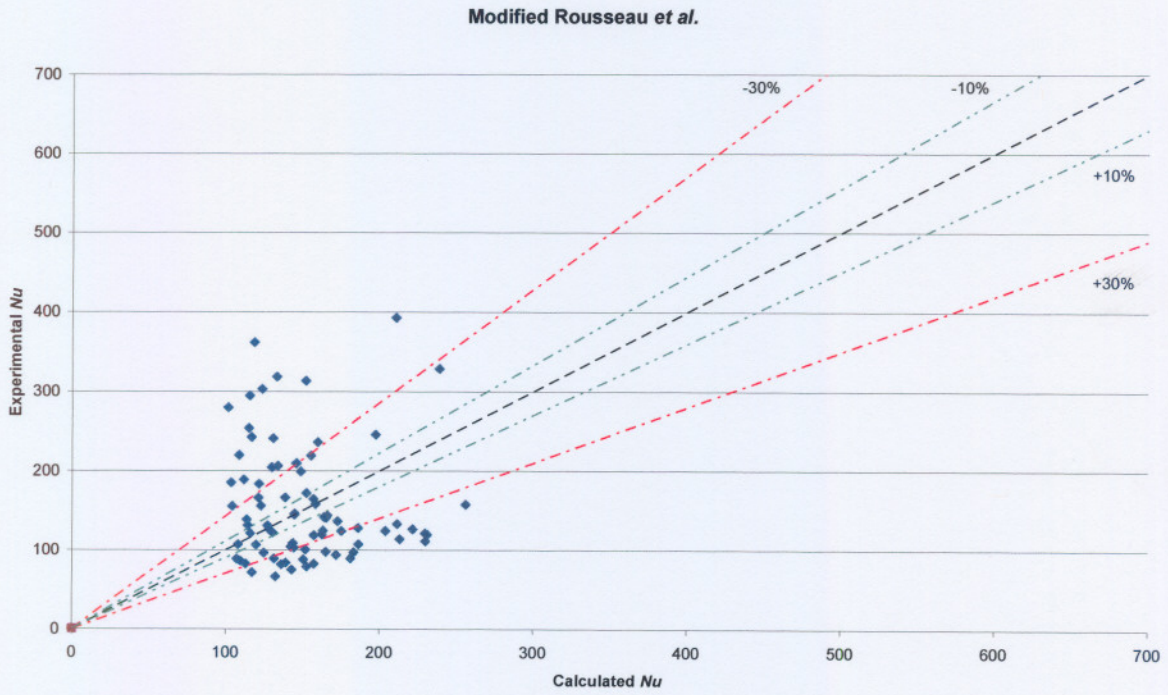

Figure 5.20 Experimental versus calculated Nusselt numbers for R22 according to the Modified Rousseau *et al.* correlation.

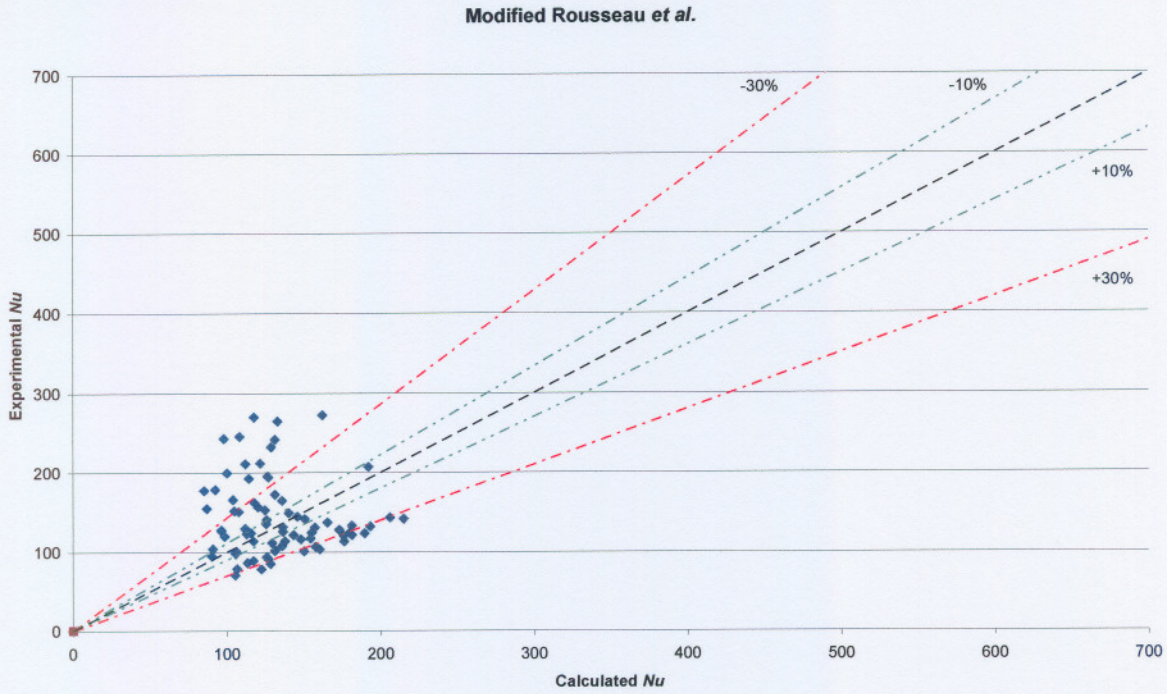

Figure 5.21 Experimental versus calculated Nusselt numbers for R407C with the Modified Rousseau *et al.* correlation.

5.3 EXPERIMENTAL UNCERTAINTIES

The experimental uncertainties were calculated with the help on a build in function of EES. EES determines the uncertainty propagation as described in NIST Technical Note 1297 (Taylor and Kuyatt, 1994). Results from two data sets of each of R22 and R407C are shown in Table 5-13 and Table 5-14. These are typical results as found through all the experimental calculations. The maximum uncertainty deviation of the calculated *Nu*-numbers was 1.78% with an average uncertainty of 0.53%. The complete results of the four data sets are shown in Appendix D.

Correlation used to calculate the Refrigerant *Nu*-number	R22			
	Data set 1		Data set 2	
	Calculated value	Uncertainty ±	Calculated value	Uncertainty ±
Chen (1963)	327.230	5.114	267.621	0.934
Gungor and Winterton (1986)	323.016	0.880	262.602	0.460

Gungor and Winterton (1987)	209.635	1.377	162.164	0.497
Modified Rousseau *et al.*	229.769	0.995	158.253	0.338
Kattan *et al.* (1998)	362.600	1.056	304.675	0.643
Lui and Winterton (1991)	331.318	0.856	286.828	0.596
Modified Wilson Plot (Shah, 1990)	111.149	1.100	158.248	0.425
Pierre	407.525	1.954	508.938	1.782
Rousseau *et al.* (2003) (Inner fluted-tube)	110.093	1.070	153.312	0.403
Rousseau *et al.* (2003) (Fluted-tube annulus)	541.752	0.444	657.737	0.981

Table 5-13 Uncertainty results of two data sets of R22

Correlation used to calculate the Refrigerant *Nu*-number	R407C			
	Data set 1		Data set 2	
	Calculated value	Uncertainty ±	Calculated value	Uncertainty ±
Chen (1963)	325.922	5.788	344.936	2.158
Gungor and Winterton (1986)	317.166	0.777	348.090	0.692
Gungor and Winterton (1987)	191.824	1.333	239.543	1.385
Modified Rousseau *et al.*	189.599	0.922	206.268	0.731
Kattan *et al.* (1998)	297.400	0.703	340.200	0.979
Lui and Winterton (1991)	316.833	0.834	379.916	1.371
Modified Wilson Plot (Shah, 1990)	123.509	1.345	143.224	1.913
Pierre	410.474	2.579	502.307	2.236
Rousseau *et al.* (2003) (Inner fluted-tube)	122.554	1.314	140.165	1.807
Rousseau *et al.* (2003) (Fluted-tube annulus)	123.066	0.366	161.170	0.210

Table 5-14 Uncertainty results of two data sets of R407C

5.4 SUMMARY

In this chapter, seven correlations were evaluated against the R22 and R407C experimental data: Gungor and Winterton (1986:351), Gungor and Winterton (1987:148), Liu and Winterton (1991:2759), Pierre (ASHRAE Fundamentals, 1997:4.7), Chen (quoted by Zhang *et al.*, 2004:5751), Rousseau *et al.* (2003:232), and Kattan *et al.* (1998c:156). Of these seven standard correlations only the one by Gungor and Winterton (1987:148) gave acceptable results, with the rest of the correlations over predicting the values.

The enhancement factor of the correlation of Rousseau *et al.* (2003:232) was then changed resulting in better mean and average deviation with both the R22 and the R407C data. From the data plots it could also be seen that the data were more grouped together. This correlation gave the best results of all the correlations tested in this experiment. This conclusion was made by taking into account the average and mean deviations as well as the data point positions on the graphs.

A Modified Rousseau *et al.* correlation was developed by combining the fluted geometry of the correlation of Rousseau *et al.* (2003:232) with the boiling two-phase heat transfer of the correlation of Gungor and Winterton (1987:148). This provided better results than the correlation of Rousseau *et al.* (2003:232) and Gungor and Winterton (1987:148) with average deviations for R22 and R407C of less than 13%.

The next chapter will conclude with a summary of all the previous chapters, a highlight of all the important factors and some recommendations for further work.

CHAPTER 6

6 CONCLUSION AND RECOMMENDATIONS FOR FURTHER WORK

6.1 INTRODUCTION

This chapter will provide a summary of the most important results that were found in the research study. Conclusions from these results will be made, leading to recommendations for further research.

6.2 SUMMARY OF THE WORK

Chapter 1 commences with a short history of refrigerants and shows that there were already two turning points in the refrigerant history. The first was a global tendency to move from toxic to non-toxic refrigerants and the second with the Montreal Protocol and the movement towards ozone-friendly refrigerants. As mentioned by Pretorius (1999:2) the current pure ozone-friendly refrigerants are not sufficient for the various refrigerant applications, thus the forming of refrigerant mixtures. The chapter furthermore shows some methods on tube enhancements and concludes with the problem statement, the aim of the study and the envisaged impact of the study.

An extensive literature survey was done in Chapter 2 on the boiling of R407C and R22, and on enhanced tube surfaces. Various correlations were found for the boiling of R22 in smooth

tubes but only one fluted-tube correlation was found. This correlation was however only developed for the condensation of R22 in fluted-tubes. During this literature survey no literature was found on the boiling of R407C in fluted-tubes. Three kinds of refrigerant mixtures were defined and it was explained how the temperature glide of the zeotropic mixtures can be used to improve the efficiency of the system. Various flow regimes were shown and explained. It was also explained how the heat transfer coefficient is dependent on the type of flow regime.

Chapter 3 shows the layout of the test bench and describes all the components of the test facility in detail. The working of a three-way mixing valve is explained and that was followed by the explanation of the working principle of all the water loops supplying water at a constant water temperature and/or water mass flow rate to the test facility. The data acquisition system was then explained in detail. The data acquisition system includes the temperature probes, the pressure sensors and all the mass flow meters. Tests with the system as it was used by Venter (2000:49) showed a maximum deviation of 2.5%. This demonstrated that all the equipment was still accurate and working correctly.

The experimental procedure and the correlations were explained in Chapter 4. The experimental procedure included the start-up procedure of the test facility together with the procedures to vary the three controlled variables, i.e. the evaporating pressure, the refrigerant mass flux and the refrigerant heat flux. The correlations that were explained in detail were divided into two groups: the single-phase and two-phase correlations. The single-phase correlations included the Wilson plot (Venter, 2000:55), the Modified Wilson plot (Briggs and Young, 1969:35), the Modified Wilson plot (Shah, 1990:51) and the single-phase part of the Rousseau *et al.* (2003:235) correlation.

These single-phase correlations were used to calculate the water heat transfer coefficients. With the LMTD method, the experimental refrigerant heat transfer coefficients were determined. The two-phase correlations included the Gungor and Winterton (1986:351), the Gungor and Winterton (1987:148), the Liu and Winterton (1991:2759), Pierre (ASHRAE Fundementals, 1997:4.7), Chen (1963:1), the Rousseau *et al.* (2003:232) and Kattan et al. (1998c:156) correlations. With the fundamentals of these correlations known, two correlations were combined to form another correlation: the Modified Rousseau *et al.* correlation. This

correlation combines the flute geometry of the Rousseau *et al.* (2003:234) correlation with the boiling heat transfer correlation of Gungor and Winterton (1987:148).

Chapter 5 shows all the experimental results of the water-to-water and the refrigerant-to-water tests. The single-phase correlations of Rousseau *et al.* (2003:235) and the Modified Wilson plot (Shah, 1990:51) showed a satisfactory agreement with all the data. Of the seven two-phase correlations evaluated, the Gungor and Winterton (1987:148) correlation showed the best results, in original form. With the use of a different enhancement factor in the Rousseau *et al.* (2003:232) correction much better results were found. The maximum uncertainty was also found to be 1.78% and the average uncertainty as 0.53%.

6.3 CONCLUSION

Most of the objectives stated in paragraph 1.3 were realised. The equipment developed by Venter (2000:36) was tested and it was found that the system is accurate and working properly with only minor repairs.

After the test run the smooth-tube test section was replaced with a fluted-tube test section. This test section was then tested with R22 with refrigerant mass flows ranging from 0.01 – 0.03 kg/s and evaporating pressures varying from 4 – 5.5 bar at various heat fluxes. With the R22 tests completed the R22 was removed and replaced with R407C. The same range of tests that were completed on R22 was then carried out on the R407C.

The data was processed and compared to the various existing heat transfer correlations. With this completed, the enhancement factor of Rousseau *et al.* (2003:232) was changed. It was also established that a new correlation could be derived by combining two of the existing correlations, i.e. the Rousseau *et al.* (2003:232) and the Gungor and Winterton (1987:148) correlations. This resulted in the Modified Rousseau *et al.* correlation.

From the experimental data it was found that an acceptable comparison was found between the Modified Wilson plot (Shah, 1990:51) and the single-phase Rousseau *et al.* (2003:232) in the prediction of the experimental heat transfer coefficients of the water with an average deviation of -1.7 % and a mean deviation of 1.7%.

The best existing correlation from this experiment was found to be the Rousseau *et al.* (2003:232) correlation with the enhancement factor changed to:

$e_{h\,R22} = 0.2658$

and

$e_{h\,R407C} = 0.2391.$

much better results are found.

With the correction factor the deviations are

	Average deviation (%)	Mean deviation (%)
R22 with coefficient	12.67	35.16
R407C with coefficient	3.83	22.01

Table 6-1 Deviation of the measured Nusselt numbers to the calculated Nusselt numbers for R22 and R407C according to Rousseau *et al.* (2003:232).

Theses deviations are not all the minimum but by taking into account the data points in Figure 5.16 and Figure 5.17 it can be clearly seen that the data points are more grouped together in the acceptable error bandwidth.

6.4 RECOMMENDATIONS FOR FURTHER RESEARCH

During the course of this study the following shortcomings were identified, which could be the subject of further research studies:

1. More experiments must be done to test if the changed enhancement factor for both the R22 and R407C is valid at different test conditions.

2. Tests done were for inlet qualities to the fluted-test, varying from 0.27 – 0.69 for R22 and 0.36 – 0.7 for R407C. The test spectrum needs to be extended to include the whole quality range from 0.0 – 1.0 to thoroughly test the correlations.

3. Only one fluted-tube test section was tested with the inner tube having an outside diameter of 14.95 mm, a flute depth of 2.09 mm and a pitch of 7.407 mm. The outside tube had an inside diameter of 17.43 mm. The influence of the inner tube diameter, the flute depth and the pitch on the heat transfer correlation should be investigated by varying one characteristic and keeping the other two constant.

4. The fluted-tube as it was, was tested with leakage flows over the flutes since the fluted-tube outside diameter was smaller than the inner diameter of the outside tube. The fluted-tube should again be tested but with the outer pipe shrink fitted onto the inner fluted-tube.

5. The current study only focused on the average heat transfer of the refrigerant in the fluted-tube heat exchanger. These tests can be extended to investigate the heat transfer coefficient in different flow regimes, with varied pressures and heat fluxes. The test can also be extended to include local heat transfer coefficients.

6. Numerous studies, including this one, looked at the boiling of R407C whether in smooth-tubes or fluted-tubes, with little tests on the condensation of R407C. Knowing this the test facility may be modified to investigate the condensing heat transfer coefficient of R407C in fluted-tubes.

REFERENCES

3040 Precision Thermometer, 1998. 3040 Precision Thermometer datasheet. [Web:] http://www.google.co.za/search?hl=en&q=PREMA+3040+&meta= [Date of use: 22 May 2006]

ALBRECHT, R. 1996. Investigation of a refrigerant metamorphosis on refrigerator performance. Johannesburg: WITS. (Dissertation - M.Sc. Eng.)

ALLCHEM. 2002. Alternative one-component refrigerants. [Web:] http://www.allchemi.com/eng/refregerants/alternative.html [Date of use: 22 May 2006]

ASHRAE HANDBOOK: FUNDAMENTALS. 1997. American Society for Heating, Refrigeration and Air-conditioning Engineers, Atlanta.

ATWOOD, T. 1985. The ABCs of NARBs (Nonazeotropic Refrigerant Blends). ASHRAE Transactions. Vol. 91, No. 2b, pp. 909 – 917.

BRIGGS, D.E. & YOUNG, E.H. 1969. Wilson plot techniques for obtaining heat transfer correlations for shell and tube heat exchangers. Chemical Engineering Process Symposium Series, No. 92, Vol. 65, pp. 35 – 45.

BUKASA, J.P. 2002. Heat transfer performance during condensation inside spiralled micro-fin tubes. Johannesburg: RAU. (Thesis - D. Eng.)

BURKERT, 2006. Burkert technical datasheets. [Web:] http://www.burkert.com/COM/buerkert_datasheets.php?type=8035 [Date of use: 22 May 2006]

DAS, S.K. 1993. Water flow through helical coils in turbulent condition. The Canadian Journal of Chemical Engineering Vol.71, pp. 971 – 973.

CHEN, J.C. 1963. A correlation for flow boiling heat transfer to saturated fluid in convective flow. ASME Paper, 63-HT-34, pp. 1 – 11.

CHOI, T.Y., KIM, Y.J., KIM, M.S. & RO, S.T. 2000. Evaporation heat transfer of R-32, R-134a , R-32/134a and R-32/125/134a inside a horizontal smooth tube. International Journal of Heat and Mass Transfer, Vol. 43, pp. 3651 – 3660.

CHRISTENSEN, R.N., ARNOLD, J.A. & GARIMELLA, S. 1993. Fluted tube heat exchanger design manual.

CHRISTENSEN, R.N. & GARIMELLA, S. 1990. Spirally-fluted and enhanced tubes in confined crossflow. Ohio State University, engineering experiment station.

DE SOUZA, A.L. & PIMENTA, M. 1995. Prediction of pressure drop during horizontal two-phase flow of pure and mixed refrigerants, Cavitation and multiphase flow, Vol. 210, American Society of Mechanical Engineers, pp. 161 – 171.

ELKINS, J.M. 1997. Chlorofluorocarbons CFCs. [Web:] http://www.cmdl.noaa.gov/noah/publictn/elkins/cfcs.html [Date of use: 25 May 2005].

ENDRESS + HAUSER, 2006. Pressure transmitter cerebar S PMC731, PMP731 user manual. [Web:] http://www.za.endress.com/ [Date of use: 22 May 2006]

ENDRESS + HAUSER, 2005. Coriolis sass slow seasurement system promass 63 Pressure transmitter cerebar S PMC731, PMP731 user manual. [Web:] http://www.za.endress.com/ [Date of use: 15 June 2005]

GUNGOR, K.E. & WINTERTON, R.H.S. 1986. A general correlation for flow boiling in tubes and annuli, International Journal of Heat and Mass Transfer, Vol. 29, No. 3, pp. 351 – 358.

GUNGOR, K.E. & WINTERTON, R.H.S. 1987. Simplified general correlation for saturated flow boiling and comparisons of correlations with data, Chemical Engineering Research, Vol. 65, pp. 148 – 156.

HWANG, Y., JUDGE, J. & RADERMACHER, R. 1997. Experience with refrigerant mixtures, ASHRAE Transactions. 1031 pp. 765 – 776.

INCROPERA, F.P. & DE WITT, D.P. 2001. Fundamentals of Heat and mass transfer, 4th edition Canada: John Wiley & Sons; 981 p.

JOHANNSEN, A. 1992. Potential of non-azeotropic refrigerant mixtures for water heating heat pumps in South Africa, National Energy Council. Prepared for the National Energy Council by the Division of Production Technology, CSIR.

JUNG, D., SONG, K., AHN, K. & KIM, J. 2003. Nucleate boiling heat transfer coefficients of mixtures containing HFC32, HFC125 and HFC134a, International Journal of Refrigeration, Vol. 26, pp. 764 – 771.

KATTAN, N., THOME, J.R., FAFRAT, D. 1998a. Flow boiling in horizontal tubes: Part 1 – Development of a diabatic two-phase flow pattern map, Journal of Heat Transfer, Vol 120, February, pp. 140-147.

KATTAN, N., THOME, J.R., FAFRAT, D. 1998b. Flow boiling in horizontal tubes: Part 2 – New heat transfer data for five refrigerants, Journal of Heat Transfer, Vol 120, February, pp. 148-155.

KATTAN, N., THOME, J.R., FAFRAT, D. 1998c. Flow boiling in horizontal tubes: Part 3 – Development of a new heat transfer model based on flow pattern, Journal of Heat Transfer, Vol 120, February, pp. 156-165.

KHARTABIL, H.F., CHRISTENSEN, R.N., RIDCHARDS, D.E. 1988. A modified Wilson plot technique for determining heat transfer correlations, Proc Second UK Natl. Conf. on heat transfer, Vol II, pp. 1331-1357, Inst. of Mech. Engr., UK.

KIM, M-H. 2002. Performance evaluation of R22 alternative mixtures in a breadboard heat pump with pure cross-flow condenser and counter-flow evaporator, Energy Vol. 27 pp. 167 – 181.

LEE, D.-Y., AHN, Y., KIM, Y., KIM, Y., CHANG, Y.-S. & NAM, L. 2002. Experimental investigation on the drop-in performance of R407C as a substitute for R33 in a screw chiller with shell-and-tube heat exchangers, International Journal of Refrigeration, Vol. 25, pp. 575 – 585.

LIU, Z. & WINTERTON, R.H.S. 1991. A general correlation for saturated and sub-cooled flow boiling in tubes and annuli, based on a nucleate pool boiling equation, International Journal of Heat and Mass Transfer, Vol. 34, No. 11, pp. 2759 – 2766.

MACBAIN, S.M., BERGLES, A.E. & RAINA, S. 1997. Heat Transfer and Pressure Drop Characteristics of Flow in a Horizontal Deep Spirally Fluted Tube, HVAC&R Research, Vol. 3 Part I, pp.65 – 80.

MICROMOTION, 2004. Micro Motion® ELITE® Mass Flow and Density Meters. Product Data sheet. [Web:] www.micromotion.com

MILLS, A.F. 1995. Heat and Mass Transfer, Chicago: Irwin. 1240 p.

PASSOS, J.C., KUSER, V.F., HABERRSCHILL, P. & LALLEMAND, M. 2003. Convective boiling of R407C inside horizontal micro-fin and plain tubes, Experimental Thermal and Fluid Science, Vol. 27, pp. 705 – 713.

PRETORIUS, C.A. 1999. Simulation of non-azeotropic heat pump performance, Potchefstroom. Dissertation M. Eng. - Potchefstroom University for Christian Higher Education.

PYROSALES, 2006. RTD datasheet [Web:] www.pyrosales.com.au/pdfs/ Data%20Sheets%20-%20General%20Purpose%20Sensors.pdf – [Date of use: 22 May 2006]

ROUSSEAU, P.G., VAN ELDIK, M. & GREYVENSTEIN, G.P. 2003. Detailed simulation of fluted tube water heating condensers, International Journal of Heat and Mass Transfer, Vol. 26, pp. 232 – 239.

ROHSENOW, W.M., HARTNETT, J.P. & GANIC, E.N. 1985. Handbook of Heat Transfer Fundamentals. 2nd edition. New-York: McGraw-Hill.

SAMI, S.M. & DESJARDINS, D.E. 2000. Boiling Characteristics of Ternary Mixtures Inside Enhanced Surface Tubing, Int. Comm. Heat Mass Transfer, Vol. 27 8, pp. 1047 – 1056.

SAMI, S.M. & MALTAIS, H. 2000. Experimental investigation of two phase flow condensation of alternatives to HCFC-22 inside enhanced surface tubing, Applied Thermal Engineering, Vol. 20, pp. 1113 – 1126.

SHAH, M.M. 1979. A general correlation for heat transfer during film condensation inside pipes. International Journal of Heat and Mass Transfer, Vol. 22, pp. 547–56.

SHAH, R.K. 1990. Assesment of Modified Wilson plot techniques for obtaining heat exchanger design data, 9th International Heat Transfer Conference, Jerusalem, Israel, August paper 14 HX-9, pp. 51-56.

SHAMES, I.H. 1992. Mechanics of Fluids. 3nd edition. New-York: McGraw-Hill. 855p.

SOUZA, A.L., CHATO, J.C., WATTELET, J.P. & CHRISTOFFERSEN, B.R. 1993. Pressure drop during two-phase flow of pure refrigerants and refrigerant/oil mixtures in horizontal smooth tubes, Heat transfer with alternative refrigerants, Vol. 243, American Society of Mechanical Engineers, pp.35 – 41.

TAYLOR, B.N., KUYATT, C.E. 1994. Guidelines for Evaluating and Expressing the Uncertainty of NIST Measurement Results, National Institute of Standards and Technology Technical Note 1297.

UNEP. 2000. Montreal Protocol on substances that deplete the ozone layer. Beijing: United Nations Environment Programme.

VENTER, J.M. 2000. Experimental Determination of the heat transfer coefficients of R407C. Potchefstroom: PU for CHE. (Dissertation - M. Eng.)

WELLSTANDT, S. & VAMLING, L. 2005. Evaporation of R134a in a horizontal herringbone micro-fin tube: heat transfer and pressure drop., International Journal of Refrigeration, Vol. 28 .

YOUBI-IDRISSI, M., BONJOUR, J. & MEUNIER, F. 2005. Local shifts of the fluid composition in the simulated heat pump using R407C. Applied thermal engineering.

ZHANG, L., HIHARA, E. & SAITO, T. 1997. Boiling heat transfer of a ternary refrigerant mixture inside a horizontal smooth tube. International Journal of Heat and Mass Transfer, Vol. 40 IX, pp. 2009 – 2017.

ZHANG, W., HIBIKI, T. & MISHIMA, K. 2004. Correlation for the flow boiling heat transfer in mini-channels. International Journal of Heat and Mass Transfer, Vol. 47, pp. 5749 – 5763.

APPENDIX A

EES program

Procedure KTF ($Q_{w,2}$, m_{R22}, Fr_{R22}, MassFlux, HeatFlux, x_3, x_4, h_3, h_4, D_h, $\mu_{R22,Lave}$, $\mu_{R22,Vave}$, $Pr_{P22,Lave}$, $k_{R22,Lave}$, T_4, T_3, P_4, P_3, $\rho_{R22,Vave}$, $\rho_{R22,Lave}$, $Lengte_1$, $Area_g$, D_{vo} : $h_{R22,KTF}$)

If [$x_3 = 100$] Then

x3 := 1

Else

x3 := x_3

EndIf

If [$x_4 = 100$] Then

x4 := 1

Else

x4 := x_4

EndIf

$$x_{ave} := \frac{x3 + x4}{2}$$

$$Y_{ave} := \frac{Q_{w,2}}{[x4 - x3] \cdot m_{R22}}$$

$$Re_{lo,ave} := MassFlux \cdot [1 - x_{ave}] \cdot \frac{D_h}{\mu_{P22,Lave}}$$

$$Re_{vap,ave} := MassFlux \cdot x_{ave} \cdot \frac{D_h}{\mu_{R22,Vave}}$$

$$P_{crit} := P_{Crit}['R22']$$

M := MolarMass ['R22']

$$p_r := \frac{P_3 + P_4}{2 \cdot P_{crit}}$$

$$\sigma := SurfaceTension\left['R22', T = \frac{T_4 + T_3}{2}\right]$$

$$A := 1 + 0.12 \cdot [1 - x_{ave}] \cdot \left[\frac{x_{ave}}{\rho_{R22,Vave}} + \frac{1 - x_{ave}}{\rho_{R22,Lave}}\right]$$

$$B := \frac{1.18 \cdot [1 - x_{ave}] \cdot [9.81 \cdot \sigma \cdot (\rho_{R22,Lave} - \rho_{R22,Vave})]^{0.25}}{MassFlux^{0.5} \cdot \rho_{P22,Lave}}$$

$$\alpha := \frac{x_{ave}}{\rho_{R22,Vave}} \cdot [A + B]^{-1}$$

$$\delta := D_h \cdot \left[\frac{1 - \alpha}{4}\right]$$

$$h_{cb} := 0.0133 \cdot Re_{lo,ave}^{0.69} \cdot Pr_{R22,Lave}^{0.4} \cdot \frac{k_{R22,Lave}}{\delta}$$

$$C := -\log[p_r]$$

$$h_{id} := 55 \cdot p_r^{0.12} \cdot C^{-0.55} \cdot M^{-0.5} \cdot HeatFlux[2/3]$$

$$P_{ave} := \frac{P_3 + P_4}{2}$$

$$DelT := |T['R22', x = 1, P = P_{ave}] - T['R22', x = 0, P = P_{ave}]|$$

$DelH := h['R22', x = 1, P = P_{ave}] - h['R22', x = 0, P = P_{ave}]$

$F_c := \left[1 + \frac{h_{id}}{HeatFlux} \cdot DelT \cdot \left(1 - \exp\left[\frac{-1 \cdot HeatFlux}{\rho_{R22,Lave} \cdot DelH \cdot 0.0003}\right]\right)\right]^{-1}$

$h_{nb} := F_c \cdot 55 \cdot p_r^{0.12} \cdot C^{-0.55} \cdot M^{-0.5} \cdot HeatFlux^{[2/3]}$

$h_{R22,KTF} := [h_{cb}^3 + h_{nb}^3]^{[1/3]}$

End KTF

Procedure GunWinPhil(x_3, x_4: MassFlux, $D_h, \mu_{R22,Lave}, \mu_{R22,Vave}, \mu_{R22,Lin}, \mu_{R22,Lout}, \mu_{R22,Vin}, \mu_{R22,Vout}, T_3, T_4, P_3, P_4, k_{R22,Lave}, Pr_{R22,Lave}, d_{coil}, Q_{w,2}, m_{R22}$, HeatFlux, $Area_s, D_{vo}, Fr_{R22}$: $h_{R22,GunWinPhil}$)

If $[x_3 = 100]$ Then

x3 := 1

Else

x3 := x_3

EndIf

If $[x_4 = 100]$ Then

x4 := 1

Else

x4 := x_4

EndIf

$x_{ave} := \frac{x3 + x4}{2}$

$\rho_{R22,Lin} := \rho['R22', T = T_3, x = 0]$

$\rho_{R22,Lout} := \rho['R22', T = T_4, x = 0]$

$\rho_{R22,Lave} := \frac{\rho_{R22,Lin} + \rho_{R22,Lout}}{2}$

$\rho_{R22,Vin} := \rho['R22', T = T_3, x = 1]$

$\rho_{R22,Vout} := \rho['R22', T = T_4, x = 1]$

$\rho_{R22,Vave} := \frac{\rho_{R22,Vin} + \rho_{R22,Vout}}{2}$

$e_{h2} := 0.06713$

e := 0.0015

$k_{R22,Vin} := k['R22', T = T_3, x = 1]$

$k_{R22,Vout} := k['R22', T = T_4, x = 1]$

$k_{R22,Vave} := \frac{k_{R22,Vout} + k_{R22,Vin}}{2}$

$Re_{Vin} := MassFlux \cdot x3 \cdot \frac{D_h}{\mu_{R22,Vin}}$

$Re_{Vout} := MassFlux \cdot x4 \cdot \frac{D_h}{\mu_{R22,Vout}}$

$$Re_{Vave2} := \frac{Re_{Vurf} + Re_{Vin}}{2}$$

$$Re_{Vave1} := MassFlux \cdot x3 \cdot \frac{D_h}{\mu_{R22,Vave}}$$

If $[x_{ave} <= 0]$ Then

$$Re1 := MassFlux \cdot \frac{D_h}{\mu_{R22,Lave}}$$

$$h_{liq,ave} := \frac{k_{R22,Lave}}{D_h} \cdot 0.023 \cdot Re1^{0.8} \cdot Pr_{R22,Lave}^{0.4}$$

If $[x3 >= 1]$ Then

$$Re1 := MassFlux \cdot \frac{D_h}{\mu_{R22,Vave}}$$

$$h_{liq,ave} := \frac{k_{R22,Vave}}{D_h} \cdot 0.023 \cdot Re1^{0.8} \cdot Pr_{R22,Vave}^{0.4}$$

If $[(x3 < 1) \text{ and } (x3 > 0)]$ Then

$$Re1 := MassFlux \cdot [1 - x3] \cdot \frac{D_h}{\mu_{R22,Lave}}$$

$$h_{liq,ave} := \frac{k_{R22,Lave}}{D_h} \cdot 0.023 \cdot Re1^{0.8} \cdot Pr_{R22,Lave}^{0.4}$$

$$f_{sh} := \frac{0.25}{\log^2\left[\frac{e}{3.7 \cdot D_h} + \frac{5.74}{Re1^{0.9}}\right]}$$

$$f_{heli} := 4 \cdot \left[0.079 \cdot Re_{Vave2}^{-0.25} + 0.0075 \cdot \left(\frac{D_h}{d_{coil}}\right)^{0.5} + 17.5782 \cdot Re_{Vave2}^{-0.3137} \cdot \left(\frac{D_h}{d_{coil}}\right)^{0.3621} \cdot \left(\frac{e}{D_h}\right)^{0.8985}\right]$$

$$r_f := \frac{f_{heli}}{f_{sh}}$$

$$\gamma_{ave} := \frac{Q_{w,2}}{[x4 - x3] \cdot m_{R22}}$$

$$Bo := \frac{HeatFlux}{\gamma_{ave} \cdot MassFlux}$$

$$Re_{lo,ave} := MassFlux \cdot [1 - x_{ave}] \cdot \frac{D_h}{\mu_{R22,Lave}}$$

$$d_e := 4 \cdot \frac{Area_a}{D_{vn}}$$

$$e := 1 + 3000 \cdot Bo^{0.86} + 1.12 \cdot \left[\frac{x_{ave}}{1 - x_{ave}}\right]^{0.75} \cdot \left[\frac{\rho_{R22,Lave}}{\rho_{R22,Vave}}\right]^{0.41}$$

If $[Fr_{R22} < 0.05]$ Then

$$E_2 := e \cdot Fr_{R22}^{[0.1 - 2 \cdot Fr_{R22}]}$$

Else

$$E_2 := e$$

EndIf

$$h_{R22,GunWinPhil} := e_{h2} \cdot r_f \cdot h_{liq,ave} \cdot E_2$$

End GunWinPhil

Procedure **Philip** (Re_{wTest}, Pr_{wTest}, D_{vi}, U_c, r_o, r_i, k_{Cu}, k_{wTest}, μ_b, μ_w : $h_{R22,Philip}$, $Nus_{wPhilip}$, $h_{wPhilip}$)

$a := 0.55732$

$C_t := \exp[-0.93356]$

$$Nus_{wPhilip} := C_t \cdot Re_{wTest}^{\ a} \cdot Pr_{wTest}^{\ 0.4} \cdot \left[\frac{\mu_w}{\mu_b}\right]^{-0.14}$$

$$h_{wPhilip} := Nus_{wPhilip} \cdot \frac{k_{wTest}}{D_{vi}}$$

$$h_{R22,Philip} := \frac{1}{\frac{1}{U_c} - \frac{r_o}{k_{Cu}} \cdot \ln\left[\frac{r_o}{r_i}\right] - \frac{r_o}{r_i \cdot h_{wPhilip}}}$$

End **Philip**

Procedure **Philip$_{oud}$** (Re_{wTest}, Pr_{wTest}, D_{vi}, U_c, r_o, r_i, k_{Cu}, k_{wTest}, μ_b, μ_w : $h_{R22,Philip,oud}$, $Nus_{wPhilip,oud}$, $h_{wPhilip,oud}$)

$$Nus_{wPhilip,oud} := \frac{1}{17.276} \cdot Re_{wTest}^{\ 0.8} \cdot Pr_{wTest}^{\ [1/3]} \cdot \left[\frac{\mu_w}{\mu_b}\right]^{-0.14}$$

$$h_{wPhilip,oud} := Nus_{wPhilip,oud} \cdot \frac{k_{wTest}}{D_{vi}}$$

$$h_{R22,Philip,oud} := \frac{1}{\frac{1}{U_c} - \frac{r_o}{k_{Cu}} \cdot \ln\left[\frac{r_o}{r_i}\right] - \frac{r_o}{r_i \cdot h_{wPhilip,oud}}}$$

End **Philip$_{oud}$**

Procedure **Rousseau** (Re_{wTest}, e_{star}, p_{star}, θ_{star}, Pr_{wTest}, k_{wTest}, D_{vi}, U_c, r_o, r_i, k_{Cu} : $h_{R22,Rous}$, Nus_{wRous}, h_{wRous})

If $[Re_{wTest} <= 5000]$ Then

$$Nus_{wRous} := 0.014 \cdot Re_{wTest}^{\ 0.642} \cdot e_{star}^{\ -0.067} \cdot p_{star}^{\ -0.293} \cdot \theta_{star}^{\ -0.705} \cdot Pr_{wTest}^{\ 0.3}$$

Else

$$Nus_{wRous} := 0.064 \cdot Re_{wTest}^{\ 0.773} \cdot e_{star}^{\ -0.242} \cdot p_{star}^{\ -0.106} \cdot \theta_{star}^{\ 0.509} \cdot Pr_{wTest}^{\ 0.3}$$

EndIf

$$h_{wRous} := Nus_{wRous} \cdot \frac{k_{wTest}}{D_{vi}}$$

$$h_{R22,Rous} := \frac{1}{\frac{1}{U_c} - \frac{r_o}{k_{Cu}} \cdot \ln\left[\frac{r_o}{r_i}\right] - \frac{r_o}{r_i \cdot h_{wRous}}}$$

End **Rousseau**

Procedure **Bukasa** (Re_{wTest}, Pr_{wTest}, D_{vi}, U_c, r_o, r_i, k_{Cu}, k_{wTest} : $h_{R22,Bukasa}$, $Nus_{wBukasa}$, $h_{wBukasa}$)

$$Nus_{wBukasa} := 0.019 \cdot Re_{wTest}^{\ 0.8} \cdot Pr_{wTest}^{\ [1/3]}$$

$$h_{wBukasa} := Nus_{wBukasa} \cdot \frac{k_{wTest}}{D_{vi}}$$

$$h_{R22,Bukasa} := \frac{1}{\frac{1}{U_c} - \frac{r_o}{k_{Cu}} \cdot \ln\left[\frac{r_o}{r_i}\right] - \frac{r_o}{r_i \cdot h_{wBukasa}}}$$

End **Bukasa**

Procedure Venter (Re_{wTest}, Pr_{wTest}, k_{wTest}, D_{vi}, U_c, r_o, r_i, k_{Cu} : $h_{R22,Venter}$, $Nus_{wVenter}$, $h_{wVenter}$)

$$Nus_{wVenter} := \frac{1}{64.076} \cdot Re_{wTest}^{0.8} \cdot Pr_{wTest}^{0.3}$$

$$h_{wVenter} := Nus_{wVenter} \cdot \frac{k_{wTest}}{D_{vi}}$$

$$h_{R22,Venter} := \frac{1}{\frac{1}{U_c} - \frac{r_o}{k_{Cu}} \cdot \ln\left[\frac{r_o}{r_i}\right] - \frac{r_o}{r_i \cdot h_{wVenter}}}$$

End Venter

Procedure Pierre (x_4, ρ_{liq}, $V_{R22,gas}$, D_h, $\mu_{R22,L}$, h_3, h_4, $lengte_t$: $Nus_{R22,Pierre}$)

$$Re_L := \rho_{liq} \cdot V_{R22,gas} \cdot \frac{D_h}{\mu_{R22,L}}$$

$$K_f := \frac{h_4 - h_3}{9.80665 \cdot lengte_t}$$

Konst := 1

If $[x_4 < 0.9]$ Then

$$Nus_{R22,Pierre} := Konst \cdot 0.0009 \cdot [Re_L^{\,2} \cdot K_f]^{0.5}$$

Else

$$Nus_{R22,Pierre} := Konst \cdot 0.0082 \cdot [Re_L^{\,2} \cdot K_f]^{0.4}$$

EndIf

End Pierre

Procedure GungorWinter86 ($Q_{w,2}$, m_{R22}, Fr_{R22}, MassFlux, HeatFlux, x_3, x_4, h_3, h_4, D_h, $\mu_{R22,Lave}$, $\mu_{R22,Vave}$, $Pr_{R22,Lave}$, $k_{R22,Lave}$, T_4, T_3, P_4, P_3, $\rho_{R22,Vave}$, $\rho_{R22,Lave}$, $lengte_t$, $Area_g$, D_{vo} : $h_{R22,GurWin86}$)

If $[x_3 = 100]$ Then

x3 := 1

Else

$x3 := x_3$

EndIf

If $[x_4 = 100]$ Then

x4 := 1

Else

$x4 := x_4$

EndIf

$$x_{ave} := \frac{x3 + x4}{2}$$

$$X_{tt} := \left[\frac{1 - x_{ave}}{x_{ave}}\right]^{0.9} \cdot \left[\frac{\rho_{R22,Vave}}{\rho_{R22,Lave}}\right]^{0.5} \cdot \left[\frac{\mu_{R22,Lave}}{\mu_{R22,Vave}}\right]^{0.1}$$

$$\gamma_{ave} := \frac{Q_{w,2}}{[x4 - x3] \cdot m_{R22}}$$

$$Bo := \frac{HeatFlux}{\gamma_{ave} \cdot MassFlux}$$

$$Re_{lo,ave} := MassFlux \cdot [1 - x_{ave}] \cdot \frac{D_h}{\mu_{R22,Lave}}$$

$$d_e := 4 \cdot \frac{Area_g}{\pi \cdot D_{vo}}$$

$$h_l := 0.023 \cdot Re_{lo,ave}^{0.8} \cdot Pr_{R22,Lave}^{0.4} \cdot \frac{k_{R22,Lave}}{d_e}$$

$P_{crit} := P_{Crit}$ ['R22']

$M := \mathbf{MolarMass}$ ['R22']

$$p_r := \frac{P_3 + P_4}{2 \cdot P_{crit}}$$

$$h_{pool} := 55 \cdot p_r^{0.12} \cdot -\log[p_r]^{-0.55} \cdot M^{-0.5} \cdot HeatFlux^{0.67}$$

If $[Fr_{R22} < 0.05]$ Then

$$E := Fr_{R22}^{[0.1 - 2 \cdot Fr_{R22}]} \cdot \left[1 + 24000 \cdot Bo^{1.16} + 1.37 \cdot \left(\frac{1}{X_n}\right)^{0.86}\right]$$

$$S := \sqrt{Fr_{R22}} \cdot \left[\frac{1}{1 + 1.15 \cdot 10^{-6} \cdot E^2 \cdot Re_{lo,ave}^{1.17}}\right]$$

Else

$$E := 1 + 24000 \cdot Bo^{1.16} + 1.37 \cdot \left[\frac{1}{X_n}\right]^{0.86}$$

$$S := \frac{1}{1 + 1.15 \cdot 10^{-6} \cdot E^2 \cdot Re_{lo,ave}^{1.17}}$$

Endif

$Konst := 1$

$$h_{R22,GunWin86} := Konst \cdot [E \cdot h_l + S \cdot h_{pool}]$$

End **GungorWinter86**

Procedure **GungorWinter87** ($Q_{w,2}$, m_{R22}, Fr_{R22}, MassFlux, HeatFlux, x_3, x_4, h_g, h_l, D_h, $\mu_{R22,Lave}$, $\mu_{R22,Vave}$, $Pr_{R22,Lave}$, $k_{R22,Lave}$, T_4, T_3, P_4, P_3, $\rho_{R22,Vave}$, $\rho_{R22,Lave}$, $Lengte_1$, $Area_g$, D_{vo}, D_{heat} : $h_{R22,GunWin87}$)

If $[x_3 = 100]$ Then

$x3 := 1$

Else

$x3 := x_3$

Endif

If $[x_4 = 100]$ Then

$x4 := 1$

Else

$x4 := x_4$

EndIf

$$x_{ave} := \frac{x3 + x4}{2}$$

$$\gamma_{ave} := \frac{Q_{w,2}}{[x4 - x3] \cdot m_{R22}}$$

$$Bo := \frac{HeatFlux}{\gamma_{ave} \cdot MassFlux}$$

$$Re_{lo,ave} := MassFlux \cdot [1 - x_{ave}] \cdot \frac{D_h}{\mu_{R22,Lave}}$$

$$d_e := 4 \cdot \frac{Area_g}{\pi \cdot D_{vo}}$$

$$h_l := 0.023 \cdot Re_{lo,ave}^{0.8} \cdot Pr_{R22,Lave}^{0.4} \cdot \frac{k_{R22,Lave}}{D_{heat}}$$

$$E := 1 + 3000 \cdot Bo^{0.86} + 1.12 \cdot \left[\frac{x_{ave}}{1 - x_{ave}}\right]^{0.75} \cdot \left[\frac{\rho_{R22,Lave}}{\rho_{R22,Vave}}\right]^{0.41}$$

If $[Fr_{R22} < 0.05]$ Then

$$E_2 := E \cdot Fr_{R22}^{[0.1 - 2 \cdot Fr_{R22}]}$$

Else

$$E_2 := E$$

EndIf

$$h_{R22,GunWin87} := h_l \cdot E_2$$

End GungorWinter87

Procedure LiuWinterton ($Q_{w,2}$, m_{R22}, Fr_{R22}, MassFlux, HeatFlux, x_3, x_4, h_3, h_4, D_h, $\mu_{R22,Lave}$, $\mu_{R22,Vave}$, $Pr_{R22,Lave}$, $K_{R22,Lave}$, T_4, T_3, P_4, P_3, $\rho_{R22,Vave}$, $\rho_{R22,Lave}$, $Lengte_1$, $Area_g$, D_{vo} : $h_{R22,LuWin}$)

If $[x_3 = 100]$ Then

$$x3 := 1$$

Else

$$x3 := x_3$$

EndIf

If $[x_4 = 100]$ Then

$$x4 := 1$$

Else

$$x4 := x_4$$

EndIf

$$x_{ave} := \frac{x3 + x4}{2}$$

$$\gamma_{ave} := \frac{Q_{w,2}}{[x4 - x3] \cdot m_{R22}}$$

$$Re_{lo,ave} := MassFlux \cdot [1 - x_{ave}] \cdot \frac{D_h}{\mu_{R22,Lave}}$$

$$Re_{vap,ave} := MassFlux \cdot x_{ave} \cdot \frac{D_h}{\mu_{R22,Vave}}$$

$$h_l := 0.023 \cdot Re_{lo,ave}^{0.8} \cdot Pr_{R22,Lave}^{0.4} \cdot \frac{k_{R22,Lave}}{D_h}$$

$$P_{crit} := P_{Crit}['R22']$$

$$M := MolarMass['R22']$$

$$p_r := \frac{P_3 + P_4}{2 \cdot P_{crit}}$$

$$h_{pool} := 55 \cdot p_r^{0.12} \cdot -\log[p_r]^{-0.55} \cdot M^{-0.5} \cdot HeatFlux[2/3]$$

$$F := \left[1 + x_{ave} \cdot Pr_{R22,Lave} \cdot \left(\frac{\rho_{R22,Lave}}{\rho_{R22,Vave}} - 1\right)\right]^{0.35}$$

$$S := [1 + 0.055 \cdot F^{0.1} \cdot Re_{lo,ave}^{0.16}]^{-1}$$

$$Konst := 1$$

$$h_{R22,LiuWin} := Konst \cdot \left[\sqrt{(F \cdot h_l)^2 + (S \cdot h_{pool})^2}\right]$$

End **LiuWinterton**

Procedure **Chen** (x_3, x_4, MassFlux, D_h, $\mu_{R22,Lave}$, $\mu_{R22,Vave}$, $T_{wallBulk}$, $Q_{w,2}$, m_{R22}, T_3, T_4, $k_{R22,Lave}$, $\rho_{R22,Lave}$, $\rho_{R22,Vave}$, $\mu_{R22,Vave}$, D_o, D_{vo}, D_{vi}, $Pr_{R22,Lave}$: $h_{R22,Chen}$)

If $[x_3 = 100]$ Then

$x3 := 1$

Else

$x3 := x_3$

EndIf

If $[x_4 = 100]$ Then

$x4 := 1$

Else

$x4 := x_4$

EndIf

$$x_{ave} := \frac{x3 + x4}{2}$$

$$Re_{R22,Lave} := MassFlux \cdot [1 - x_{ave}] \cdot \frac{D_h}{\mu_{R22,Lave}}$$

$$Re_{R22,Vave} := MassFlux \cdot x_{ave} \cdot \frac{D_h}{\mu_{R22,Vave}}$$

$$Re_{R22,k} := \frac{Re_{R22,Vave} + Re_{R22,Lave}}{2}$$

$$Pr_{R22,Wall} := Pr['R22', T = T_{wallBulk}, x = 1]$$

$$Y_{ave} := \frac{Q_{w,2}}{[x4 - x3] \cdot m_{R22}}$$

$$\sigma_{R22} := \text{SurfaceTension}\left['R22', T = \frac{T_3 + T_4}{2}\right]$$

$$\Delta T_{sat} := \left|T_{wallBulk} - \left[\frac{T_3 + T_4}{2}\right]\right|$$

$$\Delta P_{sat} := \left|P\left['R22', T = T_{wallBulk}, x = 1\right] - P\left['R22', T = \frac{T_3 + T_4}{2}, x = 1\right]\right|$$

$$S := \frac{1}{1 + 2.53 \cdot 10^{-6} \cdot Re_{R22,Lave}^{1.17}}$$

$$Cp_{R22,Lave} := Cp\left['R22', T = \frac{T_3 + T_4}{2}, x = 0\right]$$

$$h_{nb} := 0.00122 \cdot \frac{k_{R22,Lave}^{0.79} \cdot Cp_{R22,Lave}^{0.45} \cdot \rho_{R22,Lave}^{0.49}}{\sigma_{R22}^{0.5} \cdot \mu_{R22,Vave}^{0.29} \cdot \gamma_{ave}^{0.24} \cdot \rho_{R22,Vave}^{0.24}} \cdot \Delta T_{sat}^{0.24} \cdot \Delta P_{sat}^{0.75}$$

If $[(Re_{R22,Vave} < 1000)$ and $(Re_{R22,Lave} < 1000)]$ Then

$C := 5$

If $[(Re_{R22,Vave} < 1000)$ and $(Re_{R22,Lave} > 2000)]$ Then

$C := 10$

If $[(Re_{R22,Vave} > 2000)$ and $(Re_{R22,Lave} < 1000)]$ Then

$C := 12$

If $[(Re_{R22,Vave} > 2000)$ and $(Re_{R22,Lave} > 2000)]$ Then

$C := 20$

If $[([Re_{R22,Vave} < 1000]$ and $[1000 <= Re_{R22,Lave}])$ and $(Re_{R22,Lave} <= 2000)]$ Then

$$C := 5 + \left[\frac{Re_{R22,Lave} - 1000}{1000}\right] \cdot 5$$

If $[([Re_{R22,Vave} > 2000]$ and $[1000 <= Re_{R22,Lave}])$ and $(Re_{R22,Lave} <= 2000)]$ Then

$$C := 12 + \left[\frac{Re_{R22,Lave} - 1000}{1000}\right] \cdot 8$$

If $[([1000 <= Re_{R22,Vave}]$ and $[Re_{R22,Vave} <= 2000])$ and $(Re_{R22,Lave} < 1000)]$ Then

$$C := 5 + \left[\frac{Re_{R22,Vave} - 1000}{1000}\right] \cdot 7$$

If $[([1000 <= Re_{R22,Vave}]$ and $[Re_{R22,Vave} <= 2000])$ and $(Re_{R22,Lave} > 2000)]$ Then

$$C := 10 + \left[\frac{Re_{R22,Vave} - 1000}{1000}\right] \cdot 10$$

If $[([(1000 <= Re_{R22,Vave})$ and $(Re_{R22,Vave} <= 2000)]$ and $[1000 <= Re_{R22,Lave}])$ and $(Re_{R22,Lave} <= 2000)]$ Then

$$C := 5 + \left[\frac{Re_{R22,Vave} - 1000}{1000}\right] \cdot 7 + \left[\frac{Re_{R22,Lave} - 1000}{1000}\right] \cdot 8$$

$$L := \pi \cdot \left[\frac{D_o + D_{vo}}{2}\right]$$

$$H := \frac{D_{vo} - D_{vi}}{2}$$

$$\beta := \frac{H}{L}$$

If $[Re_{R22,Lave} < 1000]$ Then

$$f_{R22,Lave} := \frac{24}{Re_{R22,Lave}} \cdot \left[1 - 3.55 \cdot \beta + 1.947 \cdot \beta^2 - 1.701 \cdot \beta^3 + 0.956 \cdot \beta^4 - 0.254 \cdot \beta^5\right]$$

If $\left[Re_{R22,Lave} > 2000\right]$ Then

$$f_{R22,Lave} := 0.046 \cdot Re_{R22,Lave}^{-0.2}$$

If $\left[\left(Re_{R22,Lave} >= 1000\right) \text{and} \left(Re_{R22,Lave} <= 2000\right)\right]$ Then

$$f_{R22,Lave} := 0.046 \cdot 2000^{-0.2} \cdot \left[\frac{Re_{R22,Lave} - 1000}{1000}\right] + \frac{24}{1000} \cdot \left[1 - 3.55 \cdot \beta + 1.947 \cdot \beta^2 - 1.701 \cdot \beta^3 + 0.956 \cdot \beta^4 - 0.254 \cdot \beta^5\right] \cdot \left[1 - \left\{\frac{Re_{R22,Lave} - 1000}{1000}\right\}\right]$$

If $\left[Re_{R22,Vave} < 1000\right]$ Then

$$f_{R22,Vave} := \frac{24}{Re_{R22,Vave}} \cdot \left[1 - 3.55 \cdot \beta + 1.947 \cdot \beta^2 - 1.701 \cdot \beta^3 + 0.956 \cdot \beta^4 - 0.254 \cdot \beta^5\right]$$

If $\left[Re_{R22,Vave} > 2000\right]$ Then

$$f_{R22,Vave} := 0.046 \cdot Re_{R22,Vave}^{-0.2}$$

If $\left[\left(Re_{R22,Vave} >= 1000\right) \text{and} \left(Re_{R22,Vave} <= 2000\right)\right]$ Then

$$f_{R22,Vave} := 0.046 \cdot 2000^{-0.2} \cdot \left[\frac{Re_{R22,Vave} - 1000}{1000}\right] + \frac{24}{1000} \cdot \left[1 - 3.55 \cdot \beta + 1.947 \cdot \beta^2 - 1.701 \cdot \beta^3 + 0.956 \cdot \beta^4 - 0.254 \cdot \beta^5\right] \cdot \left[1 - \left\{\frac{Re_{R22,Vave} - 1000}{1000}\right\}\right]$$

$$X_{tt} := \left[\frac{1 - x_{ave}}{x_{ave}}\right] \cdot \left[\frac{\rho_{R22,Vave}}{\rho_{R22,Lave}}\right]^{0.5} \cdot \left[\frac{f_{R22,Lave}}{f_{R22,Vave}}\right]^{0.5}$$

$$\Phi_{R22,L} := \sqrt{1 + \frac{C}{X_{tt}} + \frac{1}{X_{tt}^2}}$$

$$F_{eka} := 0.64 \cdot \Phi_{R22,L}$$

$$F := \text{Max}\left[F_{eka}, 1\right]$$

$$Nus_{sp,l} := 0.023 \cdot Re_{R22,Lave}^{0.8} \cdot Pr_{R22,Lave}^{0.4}$$

$$Nus_{sp,v} := 8.235 \cdot \left[1 - 2.042 \cdot \beta + 3.085 \cdot \beta^2 - 2.4765 \cdot \beta^3 + 1.058 \cdot \beta^4 - 0.186 \cdot \beta^5\right]$$

If $\left[Re_{R22,Lave} < 2300\right]$ Then

$$h_{sp} := \frac{k_{R22,Lave}}{D_h} \cdot \text{Max}\left[Nus_{sp,v}, Nus_{sp,l}\right]$$

Else

$$h_{sp} := \frac{k_{R22,Lave}}{D_h} \cdot Nus_{sp,l}$$

Endif

$$Konst := 1$$

$$h_{R22,Chen} := Konst \cdot \left[S \cdot h_{nb} + F \cdot h_{sp}\right]$$

End Chen

Procedure RousAnn ($Pr_{R22,Lin}$, $Pr_{R22,Lut}$, $k_{R22,Lin}$, $k_{R22,Lut}$, D_h, x_3, x_4, MassFlux, $\mu_{R22,Lin}$, $\mu_{R22,Lut}$, $\mu_{R22,Vin}$, $\mu_{R22,Vut}$, P_3, P_4, T_3, T_4, $k_{R22,Lin}$, $k_{R22,Lut}$, d_{coil} : $h_{R22,RousAnn}$)

If $\left[x_3 = 100\right]$ Then

$$x3 := 1$$

Else

$x3 := x_3$

EndIf

If $[x_4 = 100]$ Then

$x4 := 1$

Else

$x4 := x_4$

EndIf

$e_h := 0.867$

$e := 0.0015$

$k_{R22,Vin} := k['R22', T = T_3, x = 1]$

$k_{R22,Vult} := k['R22', T = T_4, x = 1]$

$Re_{Vin} := MassFlux \cdot x3 \cdot \frac{D_h}{\mu_{R22,Vin}}$

$Re_{Vult} := MassFlux \cdot x4 \cdot \frac{D_h}{\mu_{R22,Vult}}$

If $[x3 <= 0]$ Then

$Re1 := MassFlux \cdot \frac{D_h}{\mu_{R22,Lin}}$

$h_{R22,in} := \frac{k_{R22,Lin}}{D_h} \cdot 0.023 \cdot Re1^{0.8} \cdot Pr_{R22,Lin}^{0.4}$

If $[x3 >= 1]$ Then

$Re1 := MassFlux \cdot \frac{D_h}{\mu_{R22,Vin}}$

$h_{R22,in} := \frac{k_{R22,Vin}}{D_h} \cdot 0.023 \cdot Re1^{0.8} \cdot Pr_{R22,Lin}^{0.4}$

If $[(x3 < 1) \text{ and } (x3 > 0)]$ Then

$Re1 := MassFlux \cdot [1 - x3] \cdot \frac{D_h}{\mu_{R22,Lin}}$

$pr_{in} := \frac{P_3}{P_{Crit}['R22']}$

$h_{liq,in} := \frac{k_{R22,Lin}}{D_h} \cdot 0.023 \cdot Re1^{0.8} \cdot Pr_{R22,Lin}^{0.4}$

$h_{R22,in} := h_{liq,in} \cdot \left[(1 - x3)^{0.8} + \frac{3.8 \cdot x3^{0.76} \cdot (1 - x3)^{0.04}}{pr_{in}^{0.38}} \right]$

If $[x4 <= 0]$ Then

$Re2 := MassFlux \cdot \frac{D_h}{\mu_{R22,Lult}}$

$h_{R22,ult} := \frac{k_{R22,Lult}}{D_h} \cdot 0.023 \cdot Re2^{0.8} \cdot Pr_{R22,Lult}^{0.4}$

If [x4 >= 1] Then

$$Re2 := MassFlux \cdot \frac{D_h}{\mu_{R22,Vuit}}$$

$$h_{R22,uit} := \frac{k_{R22,Vuit}}{D_h} \cdot 0.023 \cdot Re2^{0.8} \cdot Pr_{R22,Luit}^{0.4}$$

If [(x4 < 1) and (x4 > 0)] Then

$$Re2 := MassFlux \cdot [1 - x4] \cdot \frac{D_h}{\mu_{R22,Luit}}$$

$$pr_{uit} := \frac{P_4}{P_{Crit}['R22']}$$

$$h_{liq,uit} := \frac{k_{R22,Luit}}{D_h} \cdot 0.023 \cdot Re2^{0.8} \cdot Pr_{R22,Luit}^{0.4}$$

$$h_{R22,uit} := h_{liq,uit} \cdot \left[(1 - x4)^{0.8} + \frac{3.8 \cdot x4^{0.76} \cdot (1 - x4)^{0.04}}{pr_{uit}^{0.38}}\right]$$

$$f_{str1} := \frac{0.25}{\log^2\left[\frac{e}{3.7 \cdot D_h} + \frac{5.74}{Re1^{0.9}}\right]}$$

$$f_{hell1} := 4 \cdot \left[0.079 \cdot Re_{Vin}^{-0.25} + 0.0075 \cdot \left(\frac{D_h}{d_{coil}}\right)^{0.5} + 17.5782 \cdot Re_{Vin}^{-0.9137} \cdot \left(\frac{D_h}{d_{coil}}\right)^{0.3621} \cdot \left(\frac{e}{D_h}\right)^{0.6885}\right]$$

$$r_{f1} := \frac{f_{hell1}}{f_{str1}}$$

$$f_{str2} := \frac{0.25}{\log^2\left[\frac{e}{3.7 \cdot D_h} + \frac{5.74}{Re2^{0.9}}\right]}$$

$$f_{hell2} := 4 \cdot \left[0.079 \cdot Re_{Vuit}^{-0.25} + 0.0075 \cdot \left(\frac{D_h}{d_{coil}}\right)^{0.5} + 17.5782 \cdot Re_{Vuit}^{-0.9137} \cdot \left(\frac{D_h}{d_{coil}}\right)^{0.3621} \cdot \left(\frac{e}{D_h}\right)^{0.6885}\right]$$

$$r_{f2} := \frac{f_{hell2}}{f_{str2}}$$

$$h_{R22,Hellin} := e_h \cdot r_{f1} \cdot h_{R22,in}$$

$$h_{R22,Heluit} := e_h \cdot r_{f2} \cdot h_{R22,uit}$$

$$h_{R22,RousAnn} := \frac{h_{R22,Hellin} + h_{R22,Heluit}}{2}$$

End **RousAnn**

Function **GasKonduct** (x_1, x_2, k_{liq}, k_{ges})

If [x_2 = 100] Then

$$GasKonduct := \left[1 - \left(\frac{x_1 + 1}{2}\right)\right] \cdot k_{liq} + \left[\frac{x_1 + 1}{2}\right] \cdot k_{ges}$$

Else

$$GasKonduct := \left[1 - \left(\frac{x_1 + x_2}{2}\right)\right] \cdot k_{liq} + \left[\frac{x_1 + x_2}{2}\right] \cdot k_{ges}$$

EndIf

End **GasKonduct**

Function **GasDigtheid** (x_1, x_2, ρ_{liq}, ρ_{gas})

If [x_2 = 100] Then

$$GasDigtheid := \left[1 - \left(\frac{x_1 + 1}{2}\right)\right] \cdot \rho_{liq} + \left[\frac{x_1 + 1}{2}\right] \cdot \rho_{gas}$$

Else

$$GasDigtheid := \left[1 - \left(\frac{x_1 + x_2}{2}\right)\right] \cdot \rho_{liq} + \left[\frac{x_1 + x_2}{2}\right] \cdot \rho_{gas}$$

EndIf

End **GasDigtheid**

$D_{vi} = 0.011389$

$r_i = \frac{D_{vi}}{2}$

$D_{vo} = 0.013289$

$r_o = \frac{D_{vo}}{2}$

$D_o = 0.01743$

$Lengte_1 = 3.045$

$A_h = \pi \cdot D_{vi} \cdot Lengte_1$

$A_c = \pi \cdot D_{vo} \cdot Lengte_1$

$Area_w = \pi \cdot \left[\frac{D_{vi}}{2}\right]^2$

$Area_g = \pi \cdot \left[\frac{D_o}{2}\right]^2 - \pi \cdot \left[\frac{D_{vi}}{2}\right]^2$

$D_h = D_o - D_{vo}$

$$D_{heat} = \frac{4 \cdot \left[\pi \cdot \left(\frac{D_o}{2}\right)^2 - \pi \cdot r_o^2\right]}{2 \cdot \pi \cdot r_o}$$

$e = 0.00209$

$p = 0.007407$

$N = 4$

$e_{star} = \frac{e}{D_{vi}}$

$p_{star} = \frac{p}{D_{vi}}$

$\theta = \arctan\left[\pi \cdot \frac{D_{vo}}{N \cdot p}\right]$

$\theta_{star} = \frac{\theta}{90}$

$d_{coil} = \frac{D_h}{\sin[\theta]}$

$T_{i,1} = Lookup['Lookup 1', i, 'T_1']$ for i = 1 to 1

$T_{i,2} = \text{Lookup}['\text{Lookup 1}', i, 'T_2'] \quad \text{for } i = 1 \text{ to } 1$

$T_{i,3} = \text{Lookup}['\text{Lookup 1}', i, 'T_3'] \quad \text{for } i = 1 \text{ to } 1$

$T_{i,4} = \text{Lookup}['\text{Lookup 1}', i, 'T_4'] \quad \text{for } i = 1 \text{ to } 1$

$T_{i,5} = \text{Lookup}['\text{Lookup 1}', i, 'T_5'] \quad \text{for } i = 1 \text{ to } 1$

$P_{i,1} = \text{Lookup}['\text{Lookup 1}', i, 'P_1'] \cdot 100 + 85 \quad \text{for } i = 1 \text{ to } 1$

$P_{i,2} = \text{Lookup}['\text{Lookup 1}', i, 'P_3'] \cdot 100 + 85 \quad \text{for } i = 1 \text{ to } 1$

$P_{i,3} = \text{Lookup}['\text{Lookup 1}', i, 'P_4'] \cdot 100 + 85 \quad \text{for } i = 1 \text{ to } 1$

$P_{i,4} = \text{Lookup}['\text{Lookup 1}', i, 'P_2'] \cdot 100 + 85 \quad \text{for } i = 1 \text{ to } 1$

$P_{i,5} = \text{Lookup}['\text{Lookup 1}', i, 'P_5'] \cdot 100 + 85 \quad \text{for } i = 1 \text{ to } 1$

$m_{R22,i} = \text{Lookup}['\text{Lookup 1}', i, 'm_{dot,Freon}'] \quad \text{for } i = 1 \text{ to } 1$

$T_{w,i,1} = \text{Lookup}['\text{Lookup 1}', i, 'T_{w,1}'] \quad \text{for } i = 1 \text{ to } 1$

$T_{w,i,2} = \text{Lookup}['\text{Lookup 1}', i, 'T_{w,2}'] \quad \text{for } i = 1 \text{ to } 1$

$T_{w,i,3} = \text{Lookup}['\text{Lookup 1}', i, 'T_{w,3}'] \quad \text{for } i = 1 \text{ to } 1$

$T_{w,i,4} = \text{Lookup}['\text{Lookup 1}', i, 'T_{w,4}'] \quad \text{for } i = 1 \text{ to } 1$

$T_{w,i,5} = \text{Lookup}['\text{Lookup 1}', i, 'T_{w,5}'] \quad \text{for } i = 1 \text{ to } 1$

$T_{w,i,6} = \text{Lookup}['\text{Lookup 1}', i, 'T_{w,6}'] \quad \text{for } i = 1 \text{ to } 1$

$\dot{m}_{W,i,1} = \text{Lookup}['\text{Lookup 1}', i, 'm_{dot,wPre}'] \quad \text{for } i = 1 \text{ to } 1$

$\dot{m}_{W,i,2} = \text{Lookup}['\text{Lookup 1}', i, 'm_{dot,wTest}'] \quad \text{for } i = 1 \text{ to } 1$

$\dot{m}_{W,i,3} = \text{Lookup}['\text{Lookup 1}', i, 'm_{dot,wSuper}'] \quad \text{for } i = 1 \text{ to } 1$

$CP_{wPre,i} = Cp\left['\text{Water}', T = \frac{T_{w,i,1} + T_{w,i,2}}{2}, P = 85\right] \quad \text{for } i = 1 \text{ to } 1$

$CP_{wTest,i} = Cp\left['\text{Water}', T = \frac{T_{w,i,3} + T_{w,i,4}}{2}, P = 85\right] \quad \text{for } i = 1 \text{ to } 1$

$CP_{wSuper,i} = Cp\left['\text{Water}', T = \frac{T_{w,i,5} + T_{w,i,6}}{2}, P = 85\right] \quad \text{for } i = 1 \text{ to } 1$

$Q_{w,i,1} = \dot{m}_{W,i,1} \cdot CP_{wPre,i} \cdot [T_{w,i,1} - T_{w,i,2}] \quad \text{for } i = 1 \text{ to } 1$

$Q_{w,i,2} = \dot{m}_{W,i,2} \cdot CP_{wTest,i} \cdot [T_{w,i,3} - T_{w,i,4}] \quad \text{for } i = 1 \text{ to } 1$

$Q_{w,i,3} = \dot{m}_{W,i,3} \cdot CP_{wSuper,i} \cdot [T_{w,i,5} - T_{w,i,6}] \quad \text{for } i = 1 \text{ to } 1$

$h_{i,1} = h['R22', T = T_{i,1}, P = P_{i,1}] \quad \text{for } i = 1 \text{ to } 1$

$h_{i,5} = h['R22', T = T_{i,5}, P = P_{i,5}] \quad \text{for } i = 1 \text{ to } 1$

$h_{i,4} = h_{i,5} - \frac{Q_{w,i,3}}{m_{R22,i}} \quad \text{for } i = 1 \text{ to } 1$

$h_{i,3} = h_{i,4} - \frac{Q_{w,i,2}}{m_{R22,i}} \quad \text{for } i = 1 \text{ to } 1$

$h_{i,2} = h_{i,3} - \frac{Q_{w,i,1}}{m_{R22,i}} \quad \text{for } i = 1 \text{ to } 1$

$Q_{rTot,i} = m_{R22,i} \cdot [h_{i,5} - h_{i,1}] \quad \text{for } i = 1 \text{ to } 1$

$$Q_{wTot,i} = Q_{w,i,1} + Q_{w,i,2} + Q_{w,i,3} \quad \text{for } i = 1 \text{ to } 1$$

$$Q_{f,i} = Q_{rTot,i} - Q_{wTot,i} \quad \text{for } i = 1 \text{ to } 1$$

$$Dev_i = \left[\frac{|Q_{rTot,i} - Q_{wTot,i}|}{\text{Max}(Q_{rTot,i}, Q_{wTot,i})} \right] \cdot 100 \quad \text{for } i = 1 \text{ to } 1$$

$$x_{i,1} = x['R22', h = h_{i,1}, P = P_{i,1}] \quad \text{for } i = 1 \text{ to } 1$$

$$x_{i,2} = x['R22', h = h_{i,2}, P = P_{i,2}] \quad \text{for } i = 1 \text{ to } 1$$

$$x_{i,3} = x['R22', h = h_{i,3}, P = P_{i,3}] \quad \text{for } i = 1 \text{ to } 1$$

$$x_{i,4} = x['R22', h = h_{i,4}, P = P_{i,4}] \quad \text{for } i = 1 \text{ to } 1$$

$$x_{i,5} = x['R22', h = h_{i,5}, P = P_{i,5}] \quad \text{for } i = 1 \text{ to } 1$$

$$\overline{T}_{wTest,i} = \frac{T_{w,i,1} + T_{w,i,2}}{2} \quad \text{for } i = 1 \text{ to } 1$$

$$\rho_{wTest,i} = \rho['Water', T = \overline{T}_{wTest,i}, P = 85] \quad \text{for } i = 1 \text{ to } 1$$

$$k_{wTest,i} = k['Water', T = \overline{T}_{wTest,i}, P = 85] \quad \text{for } i = 1 \text{ to } 1$$

$$\Delta T_{1Test,i} = T_{w,i,3} - T_{i,4} \quad \text{for } i = 1 \text{ to } 1$$

$$\Delta T_{2Test,i} = T_{w,i,4} - T_{i,3} \quad \text{for } i = 1 \text{ to } 1$$

$$\Delta T_{lnTest,i} = \frac{\Delta T_{1Test,i} - \Delta T_{2Test,i}}{\ln\left[\frac{\Delta T_{1Test,i}}{\Delta T_{2Test,i}}\right]} \quad \text{for } i = 1 \text{ to } 1$$

$$Q_{w,i,2} = U_{c,i} \cdot A_c \cdot \Delta T_{lnTest,i} \quad \text{for } i = 1 \text{ to } 1$$

$$\dot{m}_{w,i,2} = \rho_{wTest,i} \cdot V_{wTest,i} \cdot Area_w \quad \text{for } i = 1 \text{ to } 1$$

$$\rho_{R22liq,i} = \rho\left['R22', P = \frac{P_{i,3} + P_{i,4}}{2}, x = 0\right] \quad \text{for } i = 1 \text{ to } 1$$

$$\rho_{R22gas,i} = \rho\left['R22', P = \frac{P_{i,3} + P_{i,4}}{2}, x = 1\right] \quad \text{for } i = 1 \text{ to } 1$$

$$\rho_{R22ave,i} = \text{GasDigtheid}[x_{i,3}, x_{i,4}, \rho_{R22liq,i}, \rho_{R22gas,i}] \quad \text{for } i = 1 \text{ to } 1$$

$$m_{R22,i} = \rho_{R22ave,i} \cdot V_{R22gas,i} \cdot Area_g \quad \text{for } i = 1 \text{ to } 1$$

$$\mu_{b,i} = \text{Visc}['Water', T = \overline{T}_{wTest,i}, P = 200] \quad \text{for } i = 1 \text{ to } 1$$

$$\mu_{w,i} = \text{Visc}['Water', T = T_{wallBinne,i}, P = 200] \quad \text{for } i = 1 \text{ to } 1$$

$$Re_{wTest,i} = \frac{\rho_{wTest,i} \cdot V_{wTest,i} \cdot D_{vi}}{\mu_{b,i}} \quad \text{for } i = 1 \text{ to } 1$$

$$Pr_{wTest,i} = Pr['Water', T = \overline{T}_{wTest,i}, P = 200] \quad \text{for } i = 1 \text{ to } 1$$

$$k_{R22,liq,i} = k\left['R22', P = \frac{P_{i,3} + P_{i,4}}{2}, x = 0\right] \quad \text{for } i = 1 \text{ to } 1$$

$$k_{R22,gas,i} = k\left['R22', P = \frac{P_{i,3} + P_{i,4}}{2}, x = 1\right] \quad \text{for } i = 1 \text{ to } 1$$

$$k_{R22,ave,i} = \text{GasKonduct}[x_{i,3}, x_{i,4}, k_{R22liq,i}, k_{R22gas,i}] \quad \text{for } i = 1 \text{ to } 1$$

$$k_{Cu,i} = k['Copper', T_{wallBinne,i}] \quad \text{for } i = 1 \text{ to } 1$$

$$HeatFlux_i = \frac{Q_{w,i,2}}{A_c} \quad \text{for } i = 1 \text{ to } 1$$

$$MassFlux_i = \frac{m_{R22,i}}{Area_g} \quad \text{for } i = 1 \text{ to } 1$$

$$Fr_{R22,i} = \frac{MassFlux_i^{\,2}}{\rho_{R22,Ave,i}^{\,2} \cdot 9.80665 \cdot D_h} \quad \text{for } i = 1 \text{ to } 1$$

$$\rho_{R22,Lin,i} = \rho\,['R22', P = P_{i,3}, x = 0] \quad \text{for } i = 1 \text{ to } 1$$

$$\rho_{R22,Luit,i} = \rho\,['R22', P = P_{i,4}, x = 0] \quad \text{for } i = 1 \text{ to } 1$$

$$\rho_{R22,Ave,i} = \frac{\rho_{R22,Lin,i} + \rho_{R22,Luit,i}}{2} \quad \text{for } i = 1 \text{ to } 1$$

$$\rho_{R22,Vin,i} = \rho\,['R22', P = P_{i,3}, x = 1] \quad \text{for } i = 1 \text{ to } 1$$

$$\rho_{R22,Vuit,i} = \rho\,['R22', P = P_{i,4}, x = 1] \quad \text{for } i = 1 \text{ to } 1$$

$$\rho_{R22,Vave,i} = \frac{\rho_{R22,Vin,i} + \rho_{R22,Vuit,i}}{2} \quad \text{for } i = 1 \text{ to } 1$$

$$\mu_{R22,Lin,i} = Visc\,['R22', T = T_{i,3}, x = 0] \quad \text{for } i = 1 \text{ to } 1$$

$$\mu_{R22,Luit,i} = Visc\,['R22', T = T_{i,4}, x = 0] \quad \text{for } i = 1 \text{ to } 1$$

$$\mu_{R22,Ave,i} = \frac{\mu_{R22,Lin,i} + \mu_{R22,Luit,i}}{2} \quad \text{for } i = 1 \text{ to } 1$$

$$\mu_{R22,Vin,i} = Visc\,['R22', T = T_{i,3}, x = 1] \quad \text{for } i = 1 \text{ to } 1$$

$$\mu_{R22,Vuit,i} = Visc\,['R22', T = T_{i,4}, x = 1] \quad \text{for } i = 1 \text{ to } 1$$

$$\mu_{R22,Vave,i} = \frac{\mu_{R22,Vin,i} + \mu_{R22,Vuit,i}}{2} \quad \text{for } i = 1 \text{ to } 1$$

$$k_{R22,Lin,i} = k\,['R22', T = T_{i,3}, x = 0] \quad \text{for } i = 1 \text{ to } 1$$

$$k_{R22,Luit,i} = k\,['R22', T = T_{i,4}, x = 0] \quad \text{for } i = 1 \text{ to } 1$$

$$k_{R22,Ave,i} = \frac{k_{R22,Lin,i} + k_{R22,Luit,i}}{2} \quad \text{for } i = 1 \text{ to } 1$$

$$Pr_{R22,Lin,i} = Pr\,['R22', T = T_{i,3}, x = 0] \quad \text{for } i = 1 \text{ to } 1$$

$$Pr_{R22,Luit,i} = Pr\,['R22', T = T_{i,4}, x = 0] \quad \text{for } i = 1 \text{ to } 1$$

$$Pr_{R22,Ave,i} = \frac{Pr_{R22,Lin,i} + Pr_{R22,Luit,i}}{2} \quad \text{for } i = 1 \text{ to } 1$$

$$Q_{w,i,2} = \frac{\frac{T_{w,i,3} + T_{w,i,4}}{2} - T_{wallBinne,i}}{\frac{1}{h_{wPhilip,i} \cdot 2 \cdot \pi \cdot r_i \cdot Lengte_1}} \quad \text{for } i = 1 \text{ to } 1$$

$$Q_{w,i,2} = \frac{\frac{T_{w,i,3} + T_{w,i,4}}{2} - T_{wallBuite,i}}{\frac{1}{h_{wPhilip,i} \cdot 2 \cdot \pi \cdot r_i \cdot Lengte_1} + \frac{\ln\left[\frac{r_o}{r_i}\right]}{2 \cdot \pi \cdot k_{Cu,i} \cdot Lengte_1}} \quad \text{for } i = 1 \text{ to } 1$$

$$Call\ Philip\,[Re_{wTest,i}, Pr_{wTest,i}, D_{vi}, U_{c,i}, r_o, r_i, k_{Cu,i}, k_{wTest,i}, \mu_{b,i}, \mu_{w,i} : h_{R22,Philip,i}, Nus_{wPhilip,i}, h_{wPhilip,i}] \quad \text{for } i = 1 \text{ to } 1$$

$$Nus_{R22,Philip,i} = h_{R22,Philip,i} \cdot \frac{D_h}{k_{R22,ave,i}} \quad \text{for } i = 1 \text{ to } 1$$

$$Call\ Philip_{oud}\,[Re_{wTest,i}, Pr_{wTest,i}, D_{vi}, U_{c,i}, r_o, r_i, k_{Cu,i}, k_{wTest,i}, \mu_{b,i}, \mu_{w,i} : h_{R22,Philip,oud,i}, Nus_{wPhilip,oud,i}, h_{wPhilip,oud,i}]$$
for $i = 1$ to 1

$$Nus_{R22,Philip,oud,i} = h_{R22,Philip,oud,i} \cdot \frac{D_h}{k_{R22,ave,i}} \quad \text{for } i = 1 \text{ to } 1$$

Call **Bukasa** [$Re_{wTest,i}$, $Pr_{wTest,i}$, D_{vi} , $U_{c,i}$, r_o , r_i , $k_{Cu,i}$, $k_{wTest,i}$: $h_{R22,Bukasa,1}$, $Nus_{wBukasa,1}$, $h_{wBukasa,i}$] for i = 1 to 1

$$Nus_{R22,Bukasa,i} = h_{R22,Bukasa,i} \cdot \frac{D_h}{k_{R22,ave,i}} \quad \text{for } i = 1 \text{ to } 1$$

Call **Venter** [$Re_{wTest,i}$, $Pr_{wTest,i}$, $k_{wTest,i}$, D_{vi} , $U_{c,i}$, r_o , r_i , $k_{Cu,i}$: $h_{R22,Venter,1}$, $Nus_{wVenter,1}$, $h_{wVenter,i}$] for i = 1 to 1

$$Nus_{R22,Venter,i} = h_{R22,Venter,i} \cdot \frac{D_h}{k_{R22,ave,i}} \quad \text{for } i = 1 \text{ to } 1$$

Call **Rousseau** [$Re_{wTest,i}$, e_{star} , p_{star} , θ_{star} , $Pr_{wTest,i}$, $k_{wTest,i}$, D_{vi} , $U_{c,i}$, r_o , r_i , $k_{Cu,i}$: $h_{R22,Rous,1}$, $Nus_{wRous,1}$, $h_{wRous,i}$] for i = 1 to 1

$$Nus_{R22,Rous,i} = h_{R22,Rous,i} \cdot \frac{D_h}{k_{R22,ave,i}} \quad \text{for } i = 1 \text{ to } 1$$

Call **Pierre** [$x_{i,4}$, $\rho_{R22liq,i}$, $V_{R22gas,i}$, D_h , $\mu_{R22,Lave,i}$, $h_{i,3}$, $h_{i,4}$, $Lengte_1$: $Nus_{R22,Pierre,i}$] for i = 1 to 1

$$h_{R22,Pierre,i} = Nus_{R22,Pierre,i} \cdot \frac{k_{R22,ave,i}}{D_h} \quad \text{for } i = 1 \text{ to } 1$$

Call **GungorWinter86** [$Q_{w,i,2}$, $m_{R22,i}$, $Fr_{R22,i}$, $MassFlux_i$, $HeatFlux_i$, $x_{i,3}$, $x_{i,4}$, $h_{i,3}$, $h_{i,4}$, D_h , $\mu_{R22,Lave,i}$, $\mu_{R22,Vave,i}$, $Pr_{R22,Lave,i}$, $k_{R22,Lave,i}$, $T_{i,4}$, $T_{i,3}$, $P_{i,4}$, $P_{i,2}$, $\rho_{R22,Vave,i}$, $\rho_{R22,Lave,i}$, $Lengte_1$, $Area_g$, D_{vo} : $h_{R22,GunWin86,i}$] for i = 1 to 1

$$Nus_{R22,GunWin86,i} = h_{R22,GunWin86,i} \cdot \frac{D_h}{k_{R22,ave,i}} \quad \text{for } i = 1 \text{ to } 1$$

Call **GungorWinter87** [$Q_{w,i,2}$, $m_{R22,i}$, $Fr_{R22,i}$, $MassFlux_i$, $HeatFlux_i$, $x_{i,3}$, $x_{i,4}$, $h_{i,3}$, $h_{i,4}$, D_h , $\mu_{R22,Lave,i}$, $\mu_{R22,Vave,i}$, $Pr_{R22,Lave,i}$, $k_{R22,Lave,i}$, $T_{i,4}$, $T_{i,3}$, $P_{i,4}$, $P_{i,3}$, $\rho_{R22,Vave,i}$, $\rho_{R22,Lave,i}$, $Lengte_1$, $Area_g$, D_{vo} , D_{heat} : $h_{R22,GunWin87,i}$] for i = 1 to 1

$$Nus_{R22,GunWin87,i} = h_{R22,GunWin87,i} \cdot \frac{D_h}{k_{R22,ave,i}} \quad \text{for } i = 1 \text{ to } 1$$

Call **LiuWinterton** [$Q_{w,i,2}$, $m_{R22,i}$, $Fr_{R22,i}$, $MassFlux_i$, $HeatFlux_i$, $x_{i,3}$, $x_{i,4}$, $h_{i,3}$, $h_{i,4}$, D_h , $\mu_{R22,Lave,i}$, $\mu_{R22,Vave,i}$, $Pr_{R22,Lave,i}$, $k_{R22,Lave,i}$, $T_{i,4}$, $T_{i,3}$, $P_{i,4}$, $P_{i,3}$, $\rho_{R22,Vave,i}$, $\rho_{R22,Lave,i}$, $Lengte_1$, $Area_g$, D_{vo} : $h_{R22,LiuWin,i}$] for i = 1 to 1

$$Nus_{R22,LuWin,i} = h_{R22,LiuWin,i} \cdot \frac{D_h}{k_{R22,ave,i}} \quad \text{for } i = 1 \text{ to } 1$$

Call **RousAnn** [$Pr_{R22,Lin,i}$, $Pr_{R22,Luti,i}$, $k_{R22,Lin,i}$, $k_{R22,Luti,i}$, D_h , $x_{i,3}$, $x_{i,4}$, $MassFlux_i$, $\mu_{R22,Lin,i}$, $\mu_{R22,Luti,i}$, $\mu_{R22,Vin,i}$, $\mu_{R22,Vuti,i}$, $P_{i,3}$, $P_{i,4}$, $T_{i,3}$, $T_{i,4}$, $k_{R22,Un,i}$, $k_{R22,Luti,i}$, d_{coil} : $h_{R22,RousAnn,i}$] for i = 1 to 1

$$Nus_{R22,RousAnn,i} = h_{R22,RousAnn,i} \cdot \frac{D_h}{k_{R22,ave,i}} \quad \text{for } i = 1 \text{ to } 1$$

Call **GunWinPhil** [$x_{i,3}$, $x_{i,4}$, $MassFlux_i$, D_h , $\mu_{R22,Lave,i}$, $\mu_{R22,Vave,i}$, $\mu_{R22,Lin,i}$, $\mu_{R22,Luti,i}$, $\mu_{R22,Vin,i}$, $\mu_{R22,Vuti,i}$, $T_{i,3}$, $T_{i,4}$, $P_{i,3}$, $P_{i,4}$, $k_{R22,Lave,i}$, $Pr_{R22,Lave,i}$, d_{coil} , $Q_{w,i,2}$, $m_{R22,i}$, $HeatFlux_i$, $Area_g$, D_{vo} , $Fr_{R22,i}$: $h_{R22,GunWinPhil,i}$] for i = 1 to 1

$$Nus_{R22,GunWinPhil,i} = h_{R22,GunWinPhil,i} \cdot \frac{D_h}{k_{R22,ave,i}} \quad \text{for } i = 1 \text{ to } 1$$

Call **Chen** [$x_{i,3}$, $x_{i,4}$, $MassFlux_i$, D_h , $\mu_{R22,Lave,i}$, $\mu_{R22,Vave,i}$, $T_{wallBulk,i}$, $Q_{w,i,2}$, $m_{R22,i}$, $T_{i,3}$, $T_{i,4}$, $k_{R22,Lave,i}$, $\rho_{R22,Lave,i}$, $\rho_{R22,Vave,i}$, $\mu_{R22,Vave,i}$, D_o , D_{vo} , D_{vi} , $Pr_{R22,Lave,i}$: $h_{R22,Chen,i}$] for i = 1 to 1

$$Nus_{R22,Chen,i} = h_{R22,Chen,i} \cdot \frac{D_h}{k_{R22,ave,i}} \quad \text{for } i = 1 \text{ to } 1$$

Call **KTF** [$Q_{w,i,2}$, $m_{R22,i}$, $Fr_{R22,i}$, $MassFlux_i$, $HeatFlux_i$, $x_{i,3}$, $x_{i,4}$, $h_{i,3}$, $h_{i,4}$, D_h , $\mu_{R22,Lave,i}$, $\mu_{R22,Vave,i}$, $Pr_{R22,Lave,i}$, $k_{R22,Lave,i}$, $T_{i,4}$, $T_{i,3}$, $P_{i,4}$, $P_{i,3}$, $\rho_{R22,Vave,i}$, $\rho_{R22,Lave,i}$, $Lengte_1$, $Area_g$, D_{vo} : $h_{R22,KTF,i}$] for i = 1 to 1

$$Nus_{R22,KTF,i} = h_{R22,KTF,i} \cdot \frac{D_h}{k_{R22,ave,i}} \quad \text{for } i = 1 \text{ to } 1$$

APPENDIX B

R22 experimental data

The following keys will provide the physical position of each of the measuring devices being represented by numbers in the following tables.

Physical position of temperature probe	Temperature number
Inlet to hand expansion valve (refrigerant)	T1
Pre-heater inlet (refrigerant)	T2
Pre-heater outlet / Test section inlet (refrigerant)	T3
Test section outlet / Super-heat inlet (refrigerant)	T4
Super-heat outlet (refrigerant)	T5
Pre-heater inlet (Water)	T6
Pre-heater outlet (Water)	T7
Test section inlet (Water)	T8
Test section outlet (Water)	T9
Super-heater inlet (Water)	T10
Super-heater outlet (Water)	T11

Physical position of Pressure probe	Pressure number
Inlet to hand expansion valve	P1
Pre-heater inlet	P2
Pre-heater outlet / Test section inlet	P3
Test section outlet / Super-heat inlet	P4
Super-heat outlet	P5

Physical position of mass flow meter	Mass flow number
Refrigerant	M1
Pre-heater	M2
Test section	M3
Super-heater	M4

Pressure = 4 Bar											
Test no	T1 (°C)	T2 (°C)	T3 (°C)	T4 (°C)	T5 (°C)	T6 (°C)	T7 (°C)	T8 (°C)	T9 (°C)	T10 (°C)	T11 (°C)
1	16.889	-0.123	-0.007	-0.971	41.298	13.201	8.954	13.364	9.951	45.147	43.852
2	18.734	-0.587	-0.470	-1.177	41.211	14.465	9.347	14.193	11.464	44.977	43.834
3	18.996	-0.615	-0.508	17.488	42.468	18.309	11.337	18.055	16.018	44.738	44.080
4	18.996	-0.792	-0.548	21.134	42.607	21.317	12.786	21.257	20.060	44.651	43.937
5	19.083	-0.677	-0.692	20.552	42.345	20.808	12.110	20.783	18.463	44.950	43.852
6	19.304	-0.822	-0.815	15.364	41.145	18.052	10.915	18.013	14.736	43.998	43.067
7	19.358	-0.823	-0.761	-2.972	38.250	14.221	9.053	14.142	10.469	44.093	41.740
8	19.358	-0.692	-0.650	-1.763	40.351	16.160	10.139	16.186	12.523	45.027	43.141
9	19.028	-0.930	-0.962	-4.974	36.165	13.984	8.602	14.034	9.217	45.079	41.526
10	19.028	-0.673	-0.734	-4.994	37.813	15.922	9.587	15.962	11.219	44.888	41.743
11	19.422	-0.659	-0.785	-1.614	39.120	17.776	10.312	17.812	13.364	44.337	42.254
12	19.757	-0.655	-0.825	17.923	40.681	20.705	11.485	20.690	16.522	43.783	42.482
13	16.889	-0.385	-0.474	-6.019	30.029	14.002	8.605	13.814	7.680	45.439	39.627
14	17.070	-0.658	-0.782	-6.718	33.042	15.987	9.479	15.802	9.903	45.054	40.210
15	17.180	-0.609	-0.790	-7.426	36.167	18.760	10.702	18.617	12.683	44.785	40.677
16	17.326	-0.626	-0.858	-7.862	37.807	20.556	11.365	20.353	14.736	44.616	41.321
17	17.317	-0.781	-1.115	-11.621	32.865	21.061	11.384	20.672	14.172	44.021	38.460
18	17.333	-0.793	-1.038	-10.281	27.600	18.109	10.180	17.684	10.857	43.248	37.774
19	17.298	-0.880	-1.092	-9.878	24.067	16.231	9.238	15.749	8.883	42.443	37.177
20	17.422	-0.829	-1.005	-9.274	21.445	14.259	8.356	13.870	6.959	42.618	37.721

Pressure = 4 Bar									
Test no	M1 (kg/s)	M2 (kg/s)	M3 (kg/s)	M4 (kg/s)	P1 (Bar)	P2 (Bar)	P3 (Bar)	P4 (Bar)	P5 (Bar)
1	0.01036	0.05416	0.05030	0.09160	10.31974	4.09171	4.07268	3.92680	3.89383
2	0.01035	0.04932	0.06112	0.08521	10.35089	4.01890	3.99553	3.84440	3.81246
3	0.01034	0.04924	0.06029	0.07967	10.39346	4.01724	3.98635	3.82368	3.79087
4	0.01022	0.04813	0.05935	0.06280	10.39242	3.99746	3.95502	3.79380	3.75831
5	0.01494	0.06208	0.06517	0.05790	10.22923	4.01926	3.95351	3.58539	3.51204
6	0.01491	0.06326	0.06745	0.08077	10.26036	3.99823	3.93987	3.57994	3.50574
7	0.01486	0.06049	0.06659	0.07517	10.27060	3.99937	3.95490	3.64367	3.56837
8	0.01473	0.06240	0.06357	0.06556	10.22436	4.02063	3.97141	3.64052	3.56702
9	0.02020	0.07016	0.07016	0.07960	9.99241	3.98419	3.92178	3.35808	3.22850
10	0.02023	0.06888	0.06917	0.07708	10.06077	4.02589	3.95803	3.35287	3.22225
11	0.02022	0.07168	0.07178	0.07702	10.11040	4.02573	3.94940	3.27964	3.15187
12	0.02018	0.06816	0.07136	0.06735	10.16934	4.02585	3.94126	3.24231	3.11024
13	0.02545	0.06585	0.08061	0.07029	10.32035	4.04341	3.99150	3.20526	3.01822
14	0.02495	0.06452	0.07853	0.07478	10.20323	4.00402	3.93976	3.11153	2.91720
15	0.02495	0.06387	0.07476	0.07308	10.13519	4.02085	3.93776	3.02049	2.81474
16	0.02482	0.06380	0.07901	0.07039	10.07011	4.02087	3.92422	2.93477	2.72258
17	0.02990	0.05998	0.08888	0.06213	9.58364	3.99649	3.88074	2.49973	2.17714
18	0.03027	0.05866	0.08729	0.07908	9.72104	3.99533	3.89886	2.66434	2.35627
19	0.03046	0.05821	0.08988	0.08746	9.77770	3.98158	3.89398	2.71595	2.41297
20	0.03042	0.06229	0.08935	0.09837	9.79163	3.99063	3.91032	2.79180	2.49991

Pressure = 4.5 Bar											
Test no	T1 (°C)	T2 (°C)	T3 (°C)	T4 (°C)	T5 (°C)	T6 (°C)	T7 (°C)	T8 (°C)	T9 (°C)	T10 (°C)	T11 (°C)
1	18.605	2.125	2.244	20.181	42.891	21.354	13.944	21.013	18.795	45.188	44.173
2	18.835	2.182	2.308	5.170	41.374	18.535	12.528	18.210	15.357	45.044	43.369
3	18.861	2.445	2.579	1.782	40.953	16.537	11.577	16.213	13.034	44.989	42.451
4	18.963	2.404	2.547	1.735	41.028	14.698	10.565	14.374	10.666	45.288	42.099
5	17.298	2.584	2.682	1.060	39.426	14.352	10.324	14.143	9.035	45.507	41.963
6	17.435	2.531	2.615	0.877	38.822	16.243	11.267	16.012	11.156	45.123	41.349
7	17.891	2.413	2.484	0.558	39.247	19.228	12.734	18.992	14.503	45.100	41.652
8	18.021	2.542	2.604	0.727	39.759	21.122	13.583	20.785	16.327	44.904	42.133
9	17.881	2.268	2.327	-0.448	35.381	14.211	10.140	14.113	8.706	45.147	40.319
10	18.122	2.247	2.285	-0.694	35.439	16.198	11.136	16.031	10.897	44.552	39.615
11	18.563	2.318	2.335	-0.867	35.761	18.172	12.119	17.957	13.154	43.897	39.376
12	18.969	2.415	2.403	-1.142	37.441	21.979	13.819	21.679	16.857	43.234	39.851
13	17.452	2.317	2.103	-3.994	37.059	20.523	12.519	20.465	15.909	43.208	40.286
14	17.481	2.229	2.111	-3.302	33.158	17.782	11.403	17.708	12.816	43.348	38.329
15	17.397	2.183	2.117	-2.722	30.915	15.980	10.660	15.857	10.433	44.262	38.933
16	17.295	2.200	2.201	-2.069	29.630	14.117	9.814	13.858	7.798	45.179	38.104
17	16.168	2.539	2.439	-3.591	15.501	13.721	9.541	13.610	7.268	46.820	41.057
18	16.866	2.458	2.311	-4.204	25.591	15.706	10.446	15.586	9.784	44.819	39.279
19	16.989	2.531	2.333	-4.793	28.783	17.670	11.323	17.518	12.011	44.718	39.506
20	17.134	2.558	2.260	-6.074	34.215	20.534	12.481	20.406	15.201	44.072	39.800

Pressure = 4.5 Bar									
Test no	M1 (kg/s)	M2 (kg/s)	M3 (kg/s)	M4 (kg/s)	P1 (Bar)	P2 (Bar)	P3 (Bar)	P4 (Bar)	P5 (Bar)
1	0.01038	0.04637	0.06027	0.04645	11.30179	4.47430	4.44324	4.30072	4.26241
2	0.01034	0.04590	0.05857	0.04344	11.31460	4.48573	4.45834	4.32789	4.28861
3	0.01034	0.04541	0.05738	0.04195	11.36074	4.53299	4.50931	4.38885	4.34989
4	0.01034	0.04452	0.05591	0.03850	11.37781	4.52766	4.50641	4.39212	4.35294
5	0.01521	0.05265	0.06303	0.06641	11.04738	4.54384	4.52137	4.26837	4.20915
6	0.01528	0.05104	0.06187	0.05664	11.21295	4.53679	4.50865	4.23999	4.17925
7	0.01531	0.05015	0.06088	0.04989	11.30553	4.51979	4.48515	4.18381	4.12036
8	0.01531	0.04705	0.06119	0.05190	11.34814	4.54380	4.50500	4.19544	4.12936
9	0.02001	0.06514	0.07273	0.06913	10.89056	4.51098	4.46760	4.04422	3.92916
10	0.02007	0.06235	0.07324	0.06142	10.95273	4.50852	4.46172	4.00454	3.88887
11	0.02011	0.06110	0.07475	0.05910	11.04786	4.52094	4.46966	3.97601	3.86006
12	0.02017	0.05642	0.07326	0.05625	11.14200	4.53949	4.47981	3.92165	3.80495
13	0.02542	0.08165	0.08857	0.07687	10.62042	4.51356	4.40888	3.47265	3.28246
14	0.02543	0.07910	0.08688	0.06698	10.72799	4.50128	4.41536	3.60432	3.42215
15	0.02545	0.07482	0.08611	0.07334	10.74259	4.49291	4.42213	3.69322	3.51394
16	0.02550	0.06694	0.08562	0.06311	10.78105	4.49776	4.44139	3.79404	3.61605
17	0.03086	0.08341	0.09632	0.09346	10.49859	4.53762	4.47098	3.55574	3.31739
18	0.03004	0.08284	0.09621	0.08529	10.47467	4.52522	4.44492	3.46450	3.23101
19	0.03019	0.08088	0.09734	0.08454	10.43031	4.54145	4.44491	3.38538	3.13751
20	0.03004	0.08217	0.09645	0.08131	10.30164	4.54946	4.43059	3.20794	2.94102

Pressure = 5 Bar											
Test no	T1 (°C)	T2 (°C)	T3 (°C)	T4 (°C)	T5 (°C)	T6 (°C)	T7 (°C)	T8 (°C)	T9 (°C)	T10 (°C)	T11 (°C)
1	17.196	5.300	5.451	4.764	41.177	14.571	11.690	14.374	9.457	45.295	41.828
2	17.946	5.110	5.254	4.523	41.297	16.447	12.668	16.011	12.484	45.260	42.520
3	18.488	5.230	5.374	4.653	41.414	18.542	13.740	17.990	14.808	45.234	42.861
4	18.666	5.192	5.326	6.331	41.801	21.435	15.168	20.866	18.125	45.423	43.761
5	18.235	5.066	5.223	4.510	41.198	14.669	11.655	14.179	10.159	45.096	42.394
6	18.682	5.258	5.319	4.060	39.681	20.662	14.739	20.733	17.380	43.898	42.174
7	18.868	4.961	5.052	3.429	38.314	18.081	13.474	18.083	14.373	43.861	40.701
8	19.258	5.063	5.162	3.664	37.484	16.169	12.523	16.189	11.798	43.220	39.120
9	19.467	5.218	5.348	4.011	37.284	14.201	11.490	14.143	9.255	43.014	38.175
10	19.427	5.045	5.138	2.973	32.841	14.050	11.173	14.100	8.869	41.160	36.241
11	19.649	5.216	5.284	2.923	32.476	15.906	12.210	15.725	11.393	40.568	36.619
12	20.407	5.229	5.280	2.797	33.892	17.880	13.209	17.630	13.615	41.521	37.293
13	20.748	5.098	5.110	2.313	35.548	20.905	14.502	20.606	16.862	41.721	38.726
14	20.047	5.047	5.138	2.927	32.178	14.110	11.187	13.917	9.252	40.429	35.586
15	16.514	5.280	5.335	2.541	31.415	13.844	10.936	13.742	8.230	44.882	38.512
16	16.769	5.206	5.220	1.783	32.027	15.504	11.696	15.416	10.720	45.092	39.849
17	17.397	2.183	2.117	-2.722	30.915	15.980	10.660	15.857	10.433	44.262	38.933
18	17.295	2.200	2.201	-2.069	29.630	14.117	9.814	13.858	7.798	45.179	38.104
19	17.046	5.074	5.113	1.976	30.006	13.921	10.846	13.777	8.730	44.774	39.665
20	17.726	5.144	4.960	-1.679	31.481	21.575	14.091	21.364	15.957	44.866	38.699
21	17.817	5.145	5.024	-0.915	28.710	19.697	13.368	19.462	13.933	44.837	39.575
22	17.855	4.920	4.844	-0.687	25.294	17.838	12.512	17.584	11.596	44.966	39.403
23	18.150	5.236	5.169	-0.038	17.745	15.608	11.600	15.540	9.926	44.731	39.255

Pressure = 5 Bar									
Test no	M1 (kg/s)	M2 (kg/s)	M3 (kg/s)	M4 (kg/s)	P1 (Bar)	P2 (Bar)	P3 (Bar)	P4 (Bar)	P5 (Bar)
1	0.01065	0.04633	0.05383	0.03982	11.68779	5.03578	5.02492	4.91522	4.88825
2	0.01067	0.04714	0.06546	0.04540	11.76566	4.99456	4.98867	4.86980	4.84214
3	0.01060	0.04392	0.06527	0.04739	11.85694	5.02309	5.01190	4.89192	4.86309
4	0.01060	0.04358	0.06612	0.04669	11.90777	5.01803	5.00279	4.87329	4.84280
5	0.01060	0.04551	0.06458	0.04987	11.79056	4.99078	4.98483	4.87250	4.84435
6	0.01542	0.07110	0.06816	0.07057	11.87198	5.03328	4.99994	4.70436	4.64028
7	0.01542	0.06779	0.06966	0.06028	11.84372	4.97928	4.95460	4.69617	4.62807
8	0.01542	0.06613	0.06750	0.05374	11.98207	4.99851	4.97921	4.73753	4.67267
9	0.01531	0.06278	0.06836	0.05058	11.95485	5.02973	5.01468	4.80093	4.73672
10	0.02012	0.07619	0.07671	0.07195	11.72032	4.99907	4.97515	4.62375	4.51651
11	0.02016	0.07307	0.08936	0.08085	11.84211	5.03171	5.00330	4.61558	4.50889
12	0.01992	0.06872	0.08936	0.06732	11.80067	5.03421	5.00273	4.59213	4.48911
13	0.01986	0.06510	0.08773	0.07392	11.80204	5.00968	4.96992	4.50586	4.40308
14	0.02023	0.07163	0.08901	0.07231	11.89640	5.00117	4.97848	4.61632	4.50872
15	0.02475	0.07925	0.08944	0.07858	11.37090	5.03362	5.00048	4.53384	4.39600
16	0.02489	0.08815	0.09965	0.08144	11.30811	5.02290	4.97538	4.40499	4.26464
17	0.02545	0.07482	0.08611	0.07334	10.74259	4.49291	4.42213	3.69322	3.51394
18	0.02550	0.06694	0.08562	0.06311	10.78105	4.49776	4.44139	3.79404	3.61605

19	0.02506	0.08346	0.09939	0.09259	11.39943	5.00123	4.95967	4.44121	4.29940
20	0.03099	0.07764	0.09922	0.06772	11.17376	5.01875	4.92006	3.86194	3.62208
21	0.03064	0.07737	0.10109	0.08607	11.30441	5.02066	4.93762	3.98220	3.75447
22	0.03073	0.07533	0.09950	0.08874	11.32483	4.97975	4.90890	4.02084	3.79332
23	0.03099	0.09352	0.10365	0.09681	11.51367	5.04009	4.97199	4.12672	3.90073

Pressure = 5.5 Bar											
Test no	**T1 (°C)**	**T2 (°C)**	**T3 (°C)**	**T4 (°C)**	**T5 (°C)**	**T6 (°C)**	**T7 (°C)**	**T8 (°C)**	**T9 (°C)**	**T10 (°C)**	**T11 (°C)**
1	19.728	7.921	8.104	24.345	43.038	24.881	18.294	24.402	23.563	44.855	44.270
2	19.128	7.813	7.952	11.431	42.303	21.905	16.857	21.411	19.879	45.286	44.350
3	19.852	7.818	7.969	7.357	42.111	19.090	15.425	18.553	16.665	45.490	43.960
4	20.467	7.812	7.968	7.365	41.744	17.242	14.417	16.695	14.414	45.124	43.443
5	20.879	7.780	7.947	7.372	41.912	14.215	12.637	13.621	10.871	45.377	43.372
6	17.333	7.976	8.112	6.949	40.911	17.015	14.163	16.611	13.152	45.645	42.710
7	17.948	7.768	7.897	6.660	40.580	19.030	15.153	18.595	15.627	45.182	42.679
8	18.478	7.935	8.045	6.712	40.322	21.946	16.628	21.512	18.987	44.903	42.913
9	18.941	8.038	8.121	14.498	41.352	24.763	17.851	24.334	22.010	44.446	43.389
10	18.828	7.589	7.721	6.224	37.253	13.719	11.923	13.543	9.498	45.207	39.405
11	19.083	7.840	7.949	6.156	37.145	16.069	13.355	15.763	11.482	45.065	40.327
12	19.435	7.676	7.764	5.742	37.311	17.895	14.219	17.576	13.565	45.116	40.730
13	19.578	7.724	7.799	5.651	37.930	19.932	15.213	19.600	15.983	45.299	41.370
14	19.968	7.859	7.904	5.463	38.356	22.213	16.235	21.864	18.616	45.076	41.683
15	20.398	7.523	7.535	8.595	41.065	25.789	17.511	25.419	22.173	45.499	43.437
16	20.718	7.647	7.793	6.696	35.759	12.091	10.959	11.742	8.622	44.849	38.354
17	17.843	7.699	7.570	8.335	40.753	25.326	17.132	25.190	21.752	45.261	43.686
18	17.924	7.629	7.579	3.628	37.078	22.590	15.963	22.404	18.544	45.346	42.191
19	18.175	7.670	7.669	4.228	33.809	19.708	14.743	19.517	15.070	45.056	40.637
20	18.506	7.809	7.841	4.725	32.543	17.769	13.910	17.610	12.761	44.993	39.802
21	16.914	7.931	7.907	3.950	26.168	17.527	13.822	17.550	11.658	47.840	41.601
22	17.095	7.789	7.718	3.105	30.249	19.343	14.600	19.340	13.893	47.459	41.989
23	17.322	7.736	7.592	2.244	34.825	22.248	15.800	22.273	17.248	47.288	43.377
24	17.475	7.698	7.500	1.495	38.428	25.073	16.856	24.998	20.447	45.683	42.716

Pressure = 5.5 Bar									
Test no	**M1 (kg/s)**	**M2 (kg/s)**	**M3 (kg/s)**	**M4 (kg/s)**	**P1 (Bar)**	**P2 (Bar)**	**P3 (Bar)**	**P4 (Bar)**	**P5 (Bar)**
1	0.01047	0.06029	0.09845	0.07280	13.09849	5.54550	5.51372	5.39531	5.36918
2	0.01047	0.06014	0.09954	0.07109	13.08915	5.52777	5.50137	5.38954	5.35861
3	0.01047	0.05959	0.10051	0.07204	13.12944	5.53015	5.50849	5.40805	5.37498
4	0.01047	0.05938	0.09842	0.07109	13.17573	5.52862	5.50946	5.41343	5.38153
5	0.01047	0.05899	0.10143	0.06946	13.25472	5.52322	5.50727	5.41890	5.38728
6	0.01514	0.06524	0.09964	0.07937	12.21905	5.54560	5.52639	5.32087	5.27705
7	0.01497	0.06417	0.10025	0.08130	11.89722	5.50902	5.48474	5.26682	5.22329
8	0.01494	0.06325	0.09960	0.08065	11.96224	5.54415	5.51213	5.27231	5.22887
9	0.01502	0.06324	0.10031	0.07759	11.89965	5.56805	5.52744	5.26197	5.21882

10	0.02012	0.08209	0.10029	0.07596	12.05798	5.48641	5.45931	5.21162	5.11537
11	0.02012	0.07256	0.10040	0.07741	12.12450	5.53609	5.50585	5.19728	5.10170
12	0.02013	0.07141	0.10020	0.07446	12.17335	5.50206	5.46769	5.11838	5.02169
13	0.01989	0.07034	0.09984	0.07386	12.07167	5.51167	5.47268	5.09951	5.00556
14	0.02036	0.07043	0.10345	0.07307	11.96226	5.53986	5.49271	5.06362	4.96673
15	0.02008	0.06644	0.09906	0.06221	11.16755	5.47394	5.41583	4.92502	4.83451
16	0.01995	0.07160	0.10069	0.08768	12.28874	5.49964	5.47977	5.30191	5.21417
17	0.02502	0.09005	0.10853	0.10089	11.51515	5.50113	5.40989	4.64121	4.49813
18	0.02553	0.08367	0.10592	0.09913	11.76083	5.49084	5.41805	4.73354	4.58338
19	0.02570	0.08288	0.10394	0.08982	11.88350	5.49821	5.43973	4.84471	4.69441
20	0.02588	0.08447	0.10255	0.08568	12.01566	5.52643	5.47739	4.93580	4.78431
21	0.03036	0.09923	0.09679	0.08901	11.64246	5.54080	5.48538	4.78880	4.59698
22	0.03039	0.09897	0.09944	0.08956	11.65212	5.51433	5.44371	4.64322	4.44542
23	0.03015	0.09757	0.09398	0.10411	11.56442	5.50601	5.41259	4.49164	4.29171
24	0.02988	0.09166	0.10105	0.10170	11.28395	5.50016	5.39349	4.35908	4.15112

APPENDIX C

R407C experimental data

The same keys that were used in Appendix C for the R22 experimental data are used in the R407C experimental data.

Pressure = 4 Bar											
Test no	T1 (°C)	T2 (°C)	T3 (°C)	T4 (°C)	T5 (°C)	T6 (°C)	T7 (°C)	T8 (°C)	T9 (°C)	T10 (°C)	T11 (°C)
1	16.435	-3.146	0.214	1.277	41.470	14.398	9.165	14.468	11.120	45.234	44.008
2	17.024	-3.162	0.500	4.059	41.833	15.343	9.804	15.133	12.493	45.221	44.259
3	17.580	-3.225	1.227	17.449	42.664	18.247	11.618	18.043	15.943	44.927	44.290
4	17.945	-3.279	1.967	21.047	43.076	21.276	13.456	21.075	19.880	45.045	44.468
5	17.975	-3.390	0.621	19.069	42.589	21.052	12.424	20.838	17.221	45.126	44.265
6	18.008	-3.384	-0.029	3.375	41.340	18.313	10.875	18.020	14.031	45.398	44.034
7	18.130	-3.402	-0.413	-0.452	40.491	16.528	9.826	16.240	12.172	44.993	43.143
8	18.188	-3.480	-0.726	-0.673	40.032	14.435	8.773	14.228	10.316	45.232	43.119
9	18.117	-3.247	-1.105	-2.245	37.200	14.306	8.298	14.040	8.753	45.136	41.752
10	18.294	-3.495	-1.049	-2.557	38.400	16.287	9.301	15.982	10.899	44.816	41.887
11	18.280	-3.387	-0.656	-2.368	39.796	18.142	10.371	17.829	12.837	45.161	42.674
12	18.220	-3.382	-0.328	2.586	40.744	21.242	11.770	20.847	15.467	45.312	43.515
13	18.214	-3.287	-0.892	-4.884	38.710	21.440	11.334	20.870	14.621	44.935	41.885
14	18.373	-3.384	-1.379	-5.115	36.393	18.492	9.745	17.849	11.632	44.760	40.857
15	18.369	-3.437	-1.655	-5.150	34.721	16.596	8.726	15.945	9.544	45.248	40.880
16	16.108	-3.019	-1.426	-4.149	32.269	14.218	7.863	13.757	7.338	45.917	41.214
17	17.020	-3.140	-1.497	-7.466	29.353	13.857	7.769	13.689	7.636	45.654	40.334
18	17.065	-3.472	-1.519	-8.497	33.111	15.695	8.562	15.526	9.656	45.367	40.661
19	16.990	-3.196	-1.063	-8.550	35.244	17.721	9.604	17.535	11.507	45.133	40.841
20	16.845	-3.262	-0.572	-1.563	39.124	22.012	11.539	21.806	15.442	45.283	42.590

Pressure = 4 Bar									
Test no	M1 (kg/s)	M2 (kg/s)	M3 (kg/s)	M4 (kg/s)	P1 (Bar)	P2 (Bar)	P3 (Bar)	P4 (Bar)	P5 (Bar)
1	0.01049	0.05055	0.05008	0.09706	11.97932	4.03595	4.01645	3.85584	3.79382
2	0.01011	0.05015	0.06002	0.09712	12.21662	4.02858	4.00693	3.85545	3.79520
3	0.00986	0.05006	0.05961	0.09711	12.12651	4.01264	3.98764	3.83386	3.77408
4	0.00977	0.04990	0.05937	0.09708	11.97857	3.99975	3.97019	3.81206	3.75374
5	0.01465	0.05310	0.06435	0.09694	11.77758	3.98337	3.93545	3.56457	3.47284
6	0.01487	0.05147	0.06568	0.09722	11.91008	3.98668	3.94138	3.58776	3.49476
7	0.01495	0.05060	0.06381	0.09721	12.00666	3.98676	3.94363	3.60707	3.50801
8	0.01474	0.05394	0.06454	0.09709	12.16201	3.97298	3.93208	3.62059	3.52121
9	0.01983	0.05479	0.06897	0.09715	11.90988	4.01526	3.96114	3.43860	3.28770
10	0.01973	0.05433	0.07034	0.09709	11.72064	3.97184	3.91073	3.34530	3.19386
11	0.01967	0.05480	0.07165	0.09737	11.52253	3.99266	3.92768	3.32969	3.17718
12	0.01961	0.05058	0.06998	0.09716	11.33313	3.99389	3.92372	3.28945	3.14234
13	0.02465	0.04928	0.07961	0.09690	11.27202	4.01131	3.92173	2.96485	2.72402
14	0.02521	0.04861	0.08033	0.09698	11.41956	3.99257	3.91097	2.99596	2.75338
15	0.02549	0.04819	0.07877	0.09701	11.85043	3.98357	3.90657	3.02428	2.78328
16	0.02575	0.05350	0.08035	0.10010	11.75204	4.05992	4.00334	3.20221	2.99673
17	0.03031	0.07491	0.09120	0.09996	11.21752	4.03030	3.93462	2.73279	2.42595

18	0.02983	0.07487	0.09118	0.09992	10.76946	3.97525	3.86646	2.55482	2.23694
19	0.02990	0.07260	0.09016	0.09986	10.70327	4.02329	3.90530	2.52042	2.18787
20	0.02973	0.07086	0.08981	0.09986	10.11157	4.01784	3.87578	2.28274	1.90819

Pressure = 4.5 Bar											
Test no	**T1 (°C)**	**T2 (°C)**	**T3 (°C)**	**T4 (°C)**	**T5 (°C)**	**T6 (°C)**	**T7 (°C)**	**T8 (°C)**	**T9 (°C)**	**T10 (°C)**	**T11 (°C)**
1	18.498	-0.341	4.249	20.654	43.007	21.151	14.398	21.077	18.959	45.134	44.505
2	18.572	-0.442	3.407	10.460	42.429	18.206	12.624	18.153	15.408	45.355	44.514
3	18.951	-0.561	2.894	4.219	41.590	16.262	11.407	16.261	13.454	44.973	43.882
4	19.009	-0.324	2.480	3.770	41.478	14.413	10.179	14.446	10.948	45.304	43.761
5	17.615	-0.369	1.884	2.529	39.897	14.222	9.654	14.093	9.657	45.412	42.786
6	17.776	-0.312	2.268	2.722	40.141	16.165	10.872	16.039	11.790	45.280	42.949
7	17.914	-0.337	2.605	2.893	40.598	18.089	11.994	17.979	13.833	45.262	43.287
8	18.124	-0.188	3.299	6.691	41.569	21.063	13.685	20.985	16.658	45.402	44.104
9	16.704	-0.644	2.687	2.348	40.777	20.744	12.888	20.704	16.057	45.277	43.314
10	16.768	-0.425	2.221	0.962	38.841	17.900	11.555	17.819	13.109	45.281	42.270
11	16.433	-0.258	2.109	1.257	37.842	15.847	10.425	15.790	11.098	45.236	41.801
12	17.137	-0.326	1.667	1.106	37.017	13.894	9.343	13.822	8.919	45.393	41.537
13	16.656	-0.483	1.349	-0.711	32.802	13.896	9.098	13.685	9.010	45.042	40.372
14	16.868	-0.318	1.828	-0.541	34.751	15.821	10.207	15.619	11.169	44.802	40.591
15	17.142	-0.649	1.842	-1.287	37.047	17.707	11.032	17.503	13.157	44.886	41.215
16	16.959	-0.413	2.514	-1.098	39.500	20.547	12.524	20.348	15.897	45.197	42.370
17	16.881	-0.524	2.735	5.592	40.616	22.501	13.411	22.308	17.675	45.051	43.042
18	16.704	-0.486	2.327	-3.947	38.906	21.729	12.843	21.623	16.210	45.204	42.058
19	16.609	-0.507	1.587	-3.770	33.191	17.722	10.805	17.570	12.125	45.062	40.248
20	16.495	-0.378	1.398	-3.130	29.557	15.766	9.854	15.609	9.925	45.138	39.771
21	16.592	-0.578	0.948	-2.890	26.567	13.777	8.756	13.601	7.808	44.805	39.105

Pressure = 4.5 Bar									
Test no	**M1 (kg/s)**	**M2 (kg/s)**	**M3 (kg/s)**	**M4 (kg/s)**	**P1 (Bar)**	**P2 (Bar)**	**P3 (Bar)**	**P4 (Bar)**	**P5 (Bar)**
1	0.01061	0.05440	0.05878	0.09756	13.28244	4.51315	4.48335	4.32362	4.28311
2	0.01042	0.05391	0.05757	0.09743	13.29286	4.49603	4.46990	4.32563	4.28479
3	0.01008	0.05310	0.05499	0.09699	13.14919	4.47267	4.44916	4.32245	4.28218
4	0.01087	0.05255	0.05344	0.09672	13.17673	4.51672	4.49429	4.35578	4.31085
5	0.01543	0.05647	0.06425	0.09788	13.14854	4.51843	4.49171	4.21431	4.13697
6	0.01532	0.05601	0.06349	0.09788	13.17991	4.52709	4.49754	4.20785	4.13182
7	0.01513	0.05534	0.06190	0.09776	13.00292	4.52147	4.48843	4.18616	4.11260
8	0.01506	0.05456	0.05924	0.09747	13.05998	4.54667	4.50748	4.18513	4.11647
9	0.02069	0.07020	0.07402	0.09962	11.89492	4.48661	4.41901	3.78956	3.62960
10	0.02080	0.06815	0.07520	0.09953	12.00592	4.52907	4.47440	3.92418	3.76146
11	0.02057	0.07011	0.07536	0.09807	12.51073	4.54944	4.50580	4.00158	3.87458
12	0.02068	0.06940	0.07621	0.09787	12.74857	4.53117	4.49208	4.01815	3.89044
13	0.02531	0.07704	0.09783	0.09962	11.87174	4.51259	4.45270	3.74801	3.53730
14	0.02495	0.07683	0.09721	0.09966	11.91888	4.54075	4.47508	3.73585	3.52744
15	0.02506	0.07677	0.09716	0.09968	11.80181	4.47841	4.40099	3.56470	3.34587

16	0.02507	0.07608	0.09604	0.09957	11.70470	4.52431	4.43475	3.51399	3.29069
17	0.02490	0.07497	0.09417	0.09964	11.54184	4.50532	4.40803	3.44393	3.21993
18	0.02977	0.08364	0.09540	0.09982	10.92380	4.50928	4.38368	3.03113	2.69959
19	0.03058	0.08143	0.09785	0.09964	11.24782	4.50513	4.40191	3.22079	2.89681
20	0.03077	0.08040	0.09723	0.09965	11.38347	4.53136	4.44222	3.36386	3.06456
21	0.03045	0.07862	0.09695	0.09962	11.49785	4.49442	4.41641	3.43688	3.15039

Pressure = 5 Bar											
Test no	**T1 (°C)**	**T2 (°C)**	**T3 (°C)**	**T4 (°C)**	**T5 (°C)**	**T6 (°C)**	**T7 (°C)**	**T8 (°C)**	**T9 (°C)**	**T10 (°C)**	**T11 (°C)**
1	16.644	2.431	4.602	6.737	41.464	14.147	11.173	13.991	10.308	45.117	43.527
2	17.793	2.352	4.964	6.743	41.616	16.194	12.475	15.998	12.782	45.207	43.758
3	16.644	2.384	5.397	6.939	41.752	17.976	13.652	17.770	14.910	45.202	43.917
4	18.421	2.254	6.046	12.205	42.526	21.053	15.498	20.799	18.309	45.364	44.539
5	18.695	2.364	6.648	21.274	42.946	22.956	16.636	22.722	20.459	44.995	44.384
6	18.634	2.237	5.541	5.954	41.221	20.744	14.789	20.670	17.162	45.172	43.465
7	18.777	2.058	4.826	5.493	40.682	18.148	13.286	18.035	14.473	45.336	43.177
8	18.981	2.295	4.570	5.562	40.246	16.101	12.104	15.999	11.980	45.141	42.608
9	19.054	2.382	4.275	5.488	40.113	14.241	10.925	14.131	9.762	45.249	42.386
10	19.241	2.106	3.770	4.060	36.981	13.967	10.442	13.701	9.428	44.941	40.914
11	19.361	2.232	4.183	4.265	37.836	15.916	11.644	15.637	11.562	45.059	41.386
12	19.469	2.250	4.566	4.296	38.449	17.874	12.759	17.598	13.828	45.057	41.751
13	19.653	2.398	5.262	4.513	39.657	21.118	14.514	20.843	17.196	44.817	42.223
14	19.819	2.526	5.867	6.440	41.174	23.424	15.748	23.158	19.530	45.253	43.471
15	19.721	2.228	5.386	2.851	40.195	23.135	15.069	22.950	18.892	45.075	42.653
16	20.017	2.317	5.072	2.563	38.654	21.293	14.128	21.075	17.084	44.797	41.536
17	19.968	2.147	4.339	2.531	36.149	17.906	12.332	17.677	13.537	45.081	40.869
18	15.972	2.181	3.957	2.846	33.991	15.624	10.947	15.386	10.733	45.234	40.173
19	16.666	2.292	3.930	2.906	33.144	13.617	9.903	13.523	8.957	45.462	40.028
20	17.329	2.275	3.944	1.411	29.527	15.595	10.790	15.467	10.270	44.994	39.105
21	17.576	2.321	4.260	1.111	31.635	17.648	11.871	17.514	12.377	45.111	39.705
22	17.743	2.258	4.546	0.702	34.411	19.884	13.011	19.750	14.805	45.009	40.249
23	17.754	2.266	4.849	0.406	37.053	21.860	14.006	21.728	16.790	45.151	40.999
24	17.888	2.136	5.065	0.017	38.861	23.939	14.972	23.813	18.765	44.896	41.720

Pressure = 5 Bar									
Test no	**M1 (kg/s)**	**M2 (kg/s)**	**M3 (kg/s)**	**M4 (kg/s)**	**P1 (Bar)**	**P2 (Bar)**	**P3 (Bar)**	**P4 (Bar)**	**P5 (Bar)**
1	0.01061	0.05508	0.06373	0.09610	13.57658	5.06120	5.05341	4.94098	4.87604
2	0.01062	0.05413	0.06462	0.09591	13.98434	5.03453	5.02353	4.90293	4.84002
3	0.01048	0.05403	0.06479	0.09614	14.05370	5.03612	5.02163	4.89857	4.83819
4	0.01036	0.05308	0.06629	0.09616	14.10427	5.00750	4.98953	4.85862	4.80115
5	0.01036	0.05293	0.06499	0.09602	14.19775	5.02614	5.00473	4.86854	4.81151
6	0.01515	0.06371	0.06899	0.09576	13.50258	5.00600	4.97397	4.68816	4.59722
7	0.01490	0.06317	0.07112	0.09570	13.52353	4.97001	4.94257	4.68902	4.59883
8	0.01503	0.06226	0.06950	0.09566	13.59331	5.01705	4.99255	4.75386	4.66784
9	0.01533	0.06201	0.06962	0.09563	13.64697	5.03526	5.01256	4.78544	4.69585

10	0.02013	0.06884	0.09001	0.09711	13.43353	4.97891	4.94655	4.57292	4.44192
11	0.01997	0.06796	0.08995	0.09699	13.49176	5.00297	4.96485	4.57287	4.46022
12	0.02007	0.06897	0.09260	0.09700	13.46290	5.00712	4.96343	4.53189	4.41622
13	0.02031	0.06860	0.09217	0.09733	13.52631	5.03562	4.98202	4.48680	4.36910
14	0.02006	0.06865	0.09182	0.09724	13.51534	5.06012	4.99861	4.47397	4.36250
15	0.02494	0.08003	0.10019	0.09688	13.06459	5.00238	4.91330	4.08094	3.90291
16	0.02528	0.07907	0.10239	0.09687	13.20134	5.01874	4.93688	4.14957	3.96807
17	0.02514	0.07859	0.10192	0.09677	13.28985	4.98680	4.91939	4.23653	4.06206
18	0.02570	0.07653	0.10233	0.09628	12.94947	5.01798	4.97158	4.35559	4.18532
19	0.02587	0.08883	0.10145	0.09662	13.27284	5.03304	4.98648	4.39859	4.22935
20	0.03009	0.08602	0.10183	0.09621	13.15674	5.02257	4.95341	4.11912	3.89395
21	0.03028	0.08492	0.10125	0.09636	13.10948	5.03073	4.94992	4.02363	3.78953
22	0.03014	0.08484	0.10096	0.09631	13.02451	5.01710	4.92274	3.90106	3.66019
23	0.03012	0.08458	0.10048	0.09631	12.87654	5.01771	4.91142	3.80056	3.54776
24	0.03001	0.08452	0.09981	0.09633	12.74970	4.99100	4.87101	3.65584	3.38955

Pressure = 5.5 Bar											
Test no	**T1 (°C)**	**T2 (°C)**	**T3 (°C)**	**T4 (°C)**	**T5 (°C)**	**T6 (°C)**	**T7 (°C)**	**T8 (°C)**	**T9 (°C)**	**T10 (°C)**	**T11 (°C)**
1	16.354	4.685	7.007	9.084	41.116	14.543	12.545	14.422	12.215	44.541	43.033
2	17.543	4.838	8.030	9.377	41.370	17.586	14.678	17.470	15.814	44.759	43.449
3	18.021	4.795	8.648	9.772	41.727	19.524	15.963	19.395	18.027	44.915	43.905
4	18.335	4.817	9.711	21.713	42.550	22.317	17.733	22.184	21.210	44.599	44.014
5	18.637	4.793	14.840	25.144	43.029	25.338	19.807	25.196	24.938	44.826	44.312
6	16.480	4.797	7.371	8.339	41.178	17.573	14.237	17.471	14.815	45.701	43.297
7	17.165	4.813	7.896	8.488	41.028	19.599	15.510	19.503	17.145	45.325	43.294
8	17.531	4.713	8.674	11.719	42.001	22.356	17.114	22.256	20.101	45.431	44.286
9	18.015	4.802	9.648	24.804	43.057	25.316	18.751	25.200	23.719	45.088	44.372
10	17.335	4.603	9.070	25.315	42.832	26.701	18.383	26.600	24.016	45.139	44.270
11	17.369	4.630	8.624	17.524	41.892	24.846	17.476	24.748	21.695	45.034	43.873
12	17.430	4.607	7.862	7.196	40.360	21.948	15.930	21.827	18.790	45.185	42.885
13	17.495	4.583	7.204	6.978	38.956	19.077	14.304	18.953	15.709	45.135	42.062
14	17.524	4.566	6.770	6.884	38.465	17.077	13.124	16.958	13.421	45.267	41.779
15	17.578	4.663	6.446	6.937	37.767	15.082	11.947	14.957	11.193	45.323	41.422
16	17.621	4.640	6.079	6.790	36.268	13.336	10.880	13.218	9.463	45.333	40.884
17	17.649	4.571	5.675	6.435	35.483	11.490	9.704	11.391	7.976	45.315	39.938
18	17.667	4.796	5.556	5.940	22.013	9.337	8.375	9.278	6.964	46.621	39.682
19	16.356	4.976	6.885	6.243	35.251	17.558	13.268	17.459	12.999	45.243	40.611
20	17.163	4.770	7.074	6.003	36.578	19.455	14.275	19.361	15.239	45.171	41.167
21	17.140	4.603	7.357	5.709	38.175	21.735	15.429	21.646	17.687	45.250	41.847
22	17.156	4.594	7.948	5.885	40.660	24.622	16.902	24.538	20.626	45.407	43.081
23	17.236	4.724	8.467	15.725	41.824	26.617	17.922	26.515	22.590	45.473	43.959
24	17.905	4.511	7.512	3.700	39.210	24.834	16.623	24.758	20.070	45.200	42.055
25	18.022	4.605	7.062	3.797	35.070	22.118	15.248	22.056	17.117	44.777	40.481
26	18.306	4.709	6.662	4.197	30.762	19.132	13.712	19.055	13.895	44.207	39.103
27	18.320	4.765	6.399	4.488	29.100	17.212	12.682	17.123	11.753	44.755	39.096

Pressure = 5.5 Bar									
Test no	M1 (kg/s)	M2 (kg/s)	M3 (kg/s)	M4 (kg/s)	P1 (Bar)	P2 (Bar)	P3 (Bar)	P4 (Bar)	P5 (Bar)
1	0.01066	0.08681	0.10251	0.10044	14.54951	5.53147	5.52004	5.41848	5.37800
2	0.01076	0.08691	0.10246	0.10009	15.06794	5.54908	5.53194	5.41877	5.38070
3	0.01075	0.08665	0.10341	0.10021	15.21791	5.53360	5.51198	5.39069	5.35512
4	0.01075	0.08620	0.10387	0.10027	15.33492	5.53370	5.50650	5.37555	5.34118
5	0.01075	0.08625	0.10458	0.10033	15.46000	5.52543	5.49286	5.35304	5.32005
6	0.01540	0.08749	0.10090	0.10058	14.36361	5.55171	5.52711	5.29759	5.23464
7	0.01543	0.08739	0.10046	0.10075	14.60629	5.54625	5.51560	5.26537	5.20434
8	0.01517	0.08713	0.10023	0.10078	14.44166	5.52320	5.48416	5.21106	5.15701
9	0.01517	0.08668	0.10221	0.10044	14.58366	5.53443	5.48674	5.19393	5.13848
10	0.02047	0.08780	0.10049	0.10376	13.88589	5.49982	5.42771	4.88003	4.77759
11	0.02045	0.08771	0.09967	0.10388	13.93836	5.50749	5.44217	4.91972	4.81854
12	0.02049	0.08623	0.10060	0.10359	13.99248	5.50414	5.44990	4.97597	4.86742
13	0.02049	0.08607	0.10044	0.10366	14.00602	5.49909	5.45491	5.03937	4.93026
14	0.02055	0.08583	0.09948	0.10377	14.05466	5.49641	5.45832	5.07633	4.96441
15	0.02057	0.08553	0.10075	0.10363	14.08278	5.51843	5.48583	5.14189	5.02996
16	0.02064	0.08518	0.10021	0.10317	14.13057	5.51391	5.48542	5.18866	5.07755
17	0.02065	0.08514	0.09969	0.10315	14.15014	5.50130	5.47762	5.23844	5.12820
18	0.02084	0.08919	0.10081	0.10289	14.25973	5.54725	5.52730	5.34978	5.24645
19	0.02570	0.08903	0.10231	0.10377	13.56677	5.59014	5.54509	4.99150	4.83587
20	0.02519	0.08870	0.10144	0.10356	13.78364	5.53565	5.48077	4.88165	4.72949
21	0.02529	0.08873	0.10036	0.10355	13.66530	5.50165	5.43513	4.75478	4.59865
22	0.02509	0.08864	0.09961	0.10359	13.57246	5.50092	5.41998	4.66313	4.50065
23	0.02505	0.08812	0.10099	0.10360	13.58102	5.52626	5.43717	4.65222	4.49882
24	0.02979	0.09126	0.10120	0.10362	13.57149	5.47366	5.36515	4.30737	4.07520
25	0.03054	0.09060	0.09923	0.10371	13.75765	5.49407	5.39885	4.43121	4.20239
26	0.03075	0.09004	0.10060	0.10357	14.02842	5.51464	5.43676	4.58558	4.36470
27	0.03081	0.08861	0.10007	0.10366	14.15804	5.52694	5.46011	4.69424	4.47482

APPENDIX D

Uncertainty results

The following keys will provide the link between the correlation used and the correlation as named in the EES program

R22 data	
Correlation	**Correlation as named in the EES program**
Chen (1963)	$Nus_{R22,Chen}$
Gungor and Winterton (1986)	$Nus_{R22,GunWin86}$
Gungor and Winterton (1987)	$Nus_{R22,GunWin87}$
Modified Rousseau *et al.*	$Nus_{R22,GunWinPhil}$
Kattan *et al.* (1998)	$Nus_{R22,KTF}$
Lui and Winterton (1991)	$Nus_{R22,LuiWin}$
Modified Wilson Plot (Shah, 1990)	$Nus_{R22,Philip}$
Pierre	$Nus_{R22,Pierre}$
Rousseau *et al.* (2003) (Inner fluted-tube)	$Nus_{R22,Rous}$
Rousseau *et al.* (2003) (Fluted-tube annulus)	$Nus_{R22,RousAnn}$

R407C data	
Correlation	**Correlation as named in the EES program**
Chen (1963)	$Nus_{R407C,Chen}$
Gungor and Winterton (1986)	$Nus_{R407C,GunWin86}$
Gungor and Winterton (1987)	$Nus_{R407C,GunWin87}$
Modified Rousseau *et al.*	$Nus_{R407C,GunWinPhil}$
Kattan *et al.* (1998)	$Nus_{R407C,KTF}$
Lui and Winterton (1991)	$Nus_{R407C,LuiWin}$
Modified Wilson Plot (Shah, 1990)	$Nus_{R407C,Philip}$
Pierre	$Nus_{R407C,Pierre}$
Rousseau *et al.* (2003) (Inner fluted-tube)	$Nus_{R407C,Rous}$
Rousseau *et al.* (2003) (Fluted-tube annulus)	$Nus_{R407C,RousAnn}$

The % of uncertainty as indicated on the last column of the uncertainty data is the percentage contribution of the single measurement to the total uncertainty.

R22 DATA SET 1

Unit Settings: [J]/[C]/[kPa]/[kg]/[degrees]

Variable±Uncertainty	Partial derivative	% of uncertainty
$Nus_{R22,Chen,16}$ = 327.225±5.114		
$\dot{m}_{w,16,1}$ = 0.06380±0.00006	$\partial Nus_{R22,Chen,16}/\partial \dot{m}_{w,16,1}$ = 0.00000	0.00 %
$\dot{m}_{w,16,2}$ = 0.07901±0.00008	$\partial Nus_{R22,Chen,16}/\partial \dot{m}_{w,16,2}$ = -4135.47442	0.41 %
$\dot{m}_{w,16,3}$ = 0.07039±0.00007039	$\partial Nus_{R22,Chen,16}/\partial \dot{m}_{w,16,3}$ = -4760	0.43 %
$m_{R22,16}$ = 0.02482±0.00004964	$\partial Nus_{R22,Chen,16}/\partial m_{R22,16}$ = 30276	8.64 %
$P_{16,1}$ = 1092±1.092	$\partial Nus_{R22,Chen,16}/\partial P_{16,1}$ = 7.808E-12	0.00 %
$P_{16,2}$ = 487.1±0.4871	$\partial Nus_{R22,Chen,16}/\partial P_{16,2}$ = 1.751E-11	0.00 %
$P_{16,3}$ = 477.4±0.4774	$\partial Nus_{R22,Chen,16}/\partial P_{16,3}$ = -0.3203	0.09 %
$P_{16,4}$ = 378.5±0.3785	$\partial Nus_{R22,Chen,16}/\partial P_{16,4}$ = -0.2688	0.04 %
$P_{16,5}$ = 357.3±0.3573	$\partial Nus_{R22,Chen,16}/\partial P_{16,5}$ = -0.1176	0.01 %
$T_{16,1}$ = 17.326±0.060	$\partial Nus_{R22,Chen,16}/\partial T_{16,1}$ = 0.000	0.00 %
$T_{16,2}$ = -0.626±0.060	$\partial Nus_{R22,Chen,16}/\partial T_{16,2}$ = -0.000	0.00 %
$T_{16,3}$ = -0.858±0.060	$\partial Nus_{R22,Chen,16}/\partial T_{16,3}$ = -0.570	0.00 %
$T_{16,4}$ = -7.862±0.060	$\partial Nus_{R22,Chen,16}/\partial T_{16,4}$ = -0.513	0.00 %
$T_{16,5}$ = 37.807±0.060	$\partial Nus_{R22,Chen,16}/\partial T_{16,5}$ = 6.036	0.50 %
$T_{w,16,1}$ = 20.556±0.060	$\partial Nus_{R22,Chen,16}/\partial T_{w,16,1}$ = 0.011	0.00 %
$T_{w,16,2}$ = 11.365±0.060	$\partial Nus_{R22,Chen,16}/\partial T_{w,16,2}$ = 0.011	0.00 %
$T_{w,16,3}$ = 20.353±0.060	$\partial Nus_{R22,Chen,16}/\partial T_{w,16,3}$ = -56.885	44.55 %
$T_{w,16,4}$ = 14.736±0.060	$\partial Nus_{R22,Chen,16}/\partial T_{w,16,4}$ = 57.385	45.33 %
$Nus_{R22,GunWin86,16}$ = 323.016±0.880		
$\dot{m}_{w,16,1}$ = 0.06380±0.00006	$\partial Nus_{R22,GunWin86,16}/\partial \dot{m}_{w,16,1}$ = 0.00000	0.00 %
$\dot{m}_{w,16,2}$ = 0.07901±0.00008	$\partial Nus_{R22,GunWin86,16}/\partial \dot{m}_{w,16,2}$ = -484.65135	0.19 %
$\dot{m}_{w,16,3}$ = 0.07039±0.00007039	$\partial Nus_{R22,GunWin86,16}/\partial \dot{m}_{w,16,3}$ = -2146	2.94 %
$m_{R22,16}$ = 0.02482±0.00004964	$\partial Nus_{R22,GunWin86,16}/\partial m_{R22,16}$ = 12798	52.07 %
$P_{16,1}$ = 1092±1.092	$\partial Nus_{R22,GunWin86,16}/\partial P_{16,1}$ = 0	0.00 %
$P_{16,2}$ = 487.1±0.4871	$\partial Nus_{R22,GunWin86,16}/\partial P_{16,2}$ = 0	0.00 %
$P_{16,3}$ = 477.4±0.4774	$\partial Nus_{R22,GunWin86,16}/\partial P_{16,3}$ = 0.005941	0.00 %
$P_{16,4}$ = 378.5±0.3785	$\partial Nus_{R22,GunWin86,16}/\partial P_{16,4}$ = 0.0369	0.03 %
$P_{16,5}$ = 357.3±0.3573	$\partial Nus_{R22,GunWin86,16}/\partial P_{16,5}$ = -0.05301	0.05 %
$T_{16,1}$ = 17.326±0.060	$\partial Nus_{R22,GunWin86,16}/\partial T_{16,1}$ = 0.000	0.00 %
$T_{16,2}$ = -0.626±0.060	$\partial Nus_{R22,GunWin86,16}/\partial T_{16,2}$ = 0.000	0.00 %
$T_{16,3}$ = -0.858±0.060	$\partial Nus_{R22,GunWin86,16}/\partial T_{16,3}$ = -0.397	0.07 %
$T_{16,4}$ = -7.862±0.060	$\partial Nus_{R22,GunWin86,16}/\partial T_{16,4}$ = -0.412	0.08 %
$T_{16,5}$ = 37.807±0.060	$\partial Nus_{R22,GunWin86,16}/\partial T_{16,5}$ = 2.721	3.44 %
$T_{w,16,1}$ = 20.556±0.060	$\partial Nus_{R22,GunWin86,16}/\partial T_{w,16,1}$ = 0.000	0.00 %
$T_{w,16,2}$ = 11.365±0.060	$\partial Nus_{R22,GunWin86,16}/\partial T_{w,16,2}$ = 0.000	0.00 %
$T_{w,16,3}$ = 20.353±0.060	$\partial Nus_{R22,GunWin86,16}/\partial T_{w,16,3}$ = -6.710	20.91 %
$T_{w,16,4}$ = 14.736±0.060	$\partial Nus_{R22,GunWin86,16}/\partial T_{w,16,4}$ = 6.599	20.22 %
$Nus_{R22,GunWin87,16}$ = 209.635±1.377		
$\dot{m}_{w,16,1}$ = 0.06380±0.00006	$\partial Nus_{R22,GunWin87,16}/\partial \dot{m}_{w,16,1}$ = 0.00000	0.00 %
$\dot{m}_{w,16,2}$ = 0.07901±0.00008	$\partial Nus_{R22,GunWin87,16}/\partial \dot{m}_{w,16,2}$ = -995.44847	0.33 %
$\dot{m}_{w,16,3}$ = 0.07039±0.00007039	$\partial Nus_{R22,GunWin87,16}/\partial \dot{m}_{w,16,3}$ = -1581	0.65 %
$m_{R22,16}$ = 0.02482±0.00004964	$\partial Nus_{R22,GunWin87,16}/\partial m_{R22,16}$ = 14410	26.99 %
$P_{16,1}$ = 1092±1.092	$\partial Nus_{R22,GunWin87,16}/\partial P_{16,1}$ = 0	0.00 %
$P_{16,2}$ = 487.1±0.4871	$\partial Nus_{R22,GunWin87,16}/\partial P_{16,2}$ = 0	0.00 %
$P_{16,3}$ = 477.4±0.4774	$\partial Nus_{R22,GunWin87,16}/\partial P_{16,3}$ = -0.118	0.17 %
$P_{16,4}$ = 378.5±0.3785	$\partial Nus_{R22,GunWin87,16}/\partial P_{16,4}$ = -0.1293	0.13 %
$P_{16,5}$ = 357.3±0.3573	$\partial Nus_{R22,GunWin87,16}/\partial P_{16,5}$ = -0.03906	0.01 %
$T_{16,1}$ = 17.326±0.060	$\partial Nus_{R22,GunWin87,16}/\partial T_{16,1}$ = 0.000	0.00 %
$T_{16,2}$ = -0.626±0.060	$\partial Nus_{R22,GunWin87,16}/\partial T_{16,2}$ = 0.000	0.00 %
$T_{16,3}$ = -0.858±0.060	$\partial Nus_{R22,GunWin87,16}/\partial T_{16,3}$ = 0.206	0.01 %
$T_{16,4}$ = -7.862±0.060	$\partial Nus_{R22,GunWin87,16}/\partial T_{16,4}$ = 0.260	0.01 %
$T_{16,5}$ = 37.807±0.060	$\partial Nus_{R22,GunWin87,16}/\partial T_{16,5}$ = 2.005	0.76 %
$T_{w,16,1}$ = 20.556±0.060	$\partial Nus_{R22,GunWin87,16}/\partial T_{w,16,1}$ = 0.000	0.00 %
$T_{w,16,2}$ = 11.365±0.060	$\partial Nus_{R22,GunWin87,16}/\partial T_{w,16,2}$ = 0.000	0.00 %
$T_{w,16,3}$ = 20.353±0.060	$\partial Nus_{R22,GunWin87,16}/\partial T_{w,16,3}$ = -13.783	36.07 %
$T_{w,16,4}$ = 14.736±0.060	$\partial Nus_{R22,GunWin87,16}/\partial T_{w,16,4}$ = 13.553	34.88 %
$Nus_{R22,GunWinPhil,16}$ = 229.769±0.995		
$\dot{m}_{w,16,1}$ = 0.06380±0.00006	$\partial Nus_{R22,GunWinPhil,16}/\partial \dot{m}_{w,16,1}$ = 0.00000	0.00 %
$\dot{m}_{w,16,2}$ = 0.07901±0.00008	$\partial Nus_{R22,GunWinPhil,16}/\partial \dot{m}_{w,16,2}$ = -573.30592	0.21 %
$\dot{m}_{w,16,3}$ = 0.07039±0.00007039	$\partial Nus_{R22,GunWinPhil,16}/\partial \dot{m}_{w,16,3}$ = -2413	2.91 %
$m_{R22,16}$ = 0.02482±0.00004964	$\partial Nus_{R22,GunWinPhil,16}/\partial m_{R22,16}$ = 13844	47.70 %
$P_{16,1}$ = 1092±1.092	$\partial Nus_{R22,GunWinPhil,16}/\partial P_{16,1}$ = 0	0.00 %
$P_{16,2}$ = 487.1±0.4871	$\partial Nus_{R22,GunWinPhil,16}/\partial P_{16,2}$ = 0	0.00 %

$P_{16,3}$ = 477.4±0.4774	$\partial Nus_{R22,GunWinPhil,16}/\partial P_{16,3}$ = -0.01582	0.01 %
$P_{16,4}$ = 378.5±0.3785	$\partial Nus_{R22,GunWinPhil,16}/\partial P_{16,4}$ = -0.1085	0.17 %
$P_{16,5}$ = 357.3±0.3573	$\partial Nus_{R22,GunWinPhil,16}/\partial P_{16,5}$ = -0.0596	0.05 %
$T_{16,1}$ = 17.326±0.060	$\partial Nus_{R22,GunWinPhil,16}/\partial T_{16,1}$ = 0.000	0.00 %
$T_{16,2}$ = -0.626±0.060	$\partial Nus_{R22,GunWinPhil,16}/\partial T_{16,2}$ = 0.000	0.00 %
$T_{16,3}$ = -0.858±0.060	$\partial Nus_{R22,GunWinPhil,16}/\partial T_{16,3}$ = -0.987	0.35 %
$T_{16,4}$ = -7.862±0.060	$\partial Nus_{R22,GunWinPhil,16}/\partial T_{16,4}$ = -0.628	0.14 %
$T_{16,5}$ = 37.807±0.060	$\partial Nus_{R22,GunWinPhil,16}/\partial T_{16,5}$ = 3.059	3.40 %
$T_{w,16,1}$ = 20.556±0.060	$\partial Nus_{R22,GunWinPhil,16}/\partial T_{w,16,1}$ = 0.000	0.00 %
$T_{w,16,2}$ = 11.365±0.060	$\partial Nus_{R22,GunWinPhil,16}/\partial T_{w,16,2}$ = 0.000	0.00 %
$T_{w,16,3}$ = 20.353±0.060	$\partial Nus_{R22,GunWinPhil,16}/\partial T_{w,16,3}$ = -7.938	22.91 %
$T_{w,16,4}$ = 14.736±0.060	$\partial Nus_{R22,GunWinPhil,16}/\partial T_{w,16,4}$ = 7.806	22.15 %
$Nus_{R22,KTF,16}$ = 362.626±1.056		
$\dot{m}_{W,16,1}$ = 0.06380±0.00006	$\partial Nus_{R22,KTF,16}/\partial \dot{m}_{W,16,1}$ = 0.00000	0.00 %
$\dot{m}_{W,16,2}$ = 0.07901±0.00008	$\partial Nus_{R22,KTF,16}/\partial \dot{m}_{W,16,2}$ = 504.92410	0.14 %
$\dot{m}_{W,16,3}$ = 0.07039±0.00007039	$\partial Nus_{R22,KTF,16}/\partial \dot{m}_{W,16,3}$ = -2957	3.88 %
$m_{R22,16}$ = 0.02482±0.00004964	$\partial Nus_{R22,KTF,16}/\partial m_{R22,16}$ = 16519	60.25 %
$P_{16,1}$ = 1092±1.092	$\partial Nus_{R22,KTF,16}/\partial P_{16,1}$ = 0	0.00 %
$P_{16,2}$ = 487.1±0.4871	$\partial Nus_{R22,KTF,16}/\partial P_{16,2}$ = 0	0.00 %
$P_{16,3}$ = 477.4±0.4774	$\partial Nus_{R22,KTF,16}/\partial P_{16,3}$ = 0.0428	0.04 %
$P_{16,4}$ = 378.5±0.3785	$\partial Nus_{R22,KTF,16}/\partial P_{16,4}$ = 0.07927	0.08 %
$P_{16,5}$ = 357.3±0.3573	$\partial Nus_{R22,KTF,16}/\partial P_{16,5}$ = -0.07305	0.06 %
$T_{16,1}$ = 17.326±0.060	$\partial Nus_{R22,KTF,16}/\partial T_{16,1}$ = 0.000	0.00 %
$T_{16,2}$ = -0.626±0.060	$\partial Nus_{R22,KTF,16}/\partial T_{16,2}$ = 0.000	0.00 %
$T_{16,3}$ = -0.858±0.060	$\partial Nus_{R22,KTF,16}/\partial T_{16,3}$ = 0.000	0.00 %
$T_{16,4}$ = -7.862±0.060	$\partial Nus_{R22,KTF,16}/\partial T_{16,4}$ = 0.000	0.00 %
$T_{16,5}$ = 37.807±0.060	$\partial Nus_{R22,KTF,16}/\partial T_{16,5}$ = 3.750	4.54 %
$T_{w,16,1}$ = 20.556±0.060	$\partial Nus_{R22,KTF,16}/\partial T_{w,16,1}$ = 0.000	0.00 %
$T_{w,16,2}$ = 11.365±0.060	$\partial Nus_{R22,KTF,16}/\partial T_{w,16,2}$ = 0.000	0.00 %
$T_{w,16,3}$ = 20.353±0.060	$\partial Nus_{R22,KTF,16}/\partial T_{w,16,3}$ = 6.991	15.77 %
$T_{w,16,4}$ = 14.736±0.060	$\partial Nus_{R22,KTF,16}/\partial T_{w,16,4}$ = -6.875	15.25 %
$Nus_{R22,LuWin,16}$ = 331.318±0.856		
$\dot{m}_{W,16,1}$ = 0.06380±0.00006	$\partial Nus_{R22,LuiWin,16}/\partial \dot{m}_{W,16,1}$ = 0.00000	0.00 %
$\dot{m}_{W,16,2}$ = 0.07901±0.00008	$\partial Nus_{R22,LuiWin,16}/\partial \dot{m}_{W,16,2}$ = 337.52312	0.10 %
$\dot{m}_{W,16,3}$ = 0.07039±0.00007039	$\partial Nus_{R22,LuiWin,16}/\partial \dot{m}_{W,16,3}$ = -2354	3.75 %
$m_{R22,16}$ = 0.02482±0.00004964	$\partial Nus_{R22,LuiWin,16}/\partial m_{R22,16}$ = 14483	70.57 %
$P_{16,1}$ = 1092±1.092	$\partial Nus_{R22,LuiWin,16}/\partial P_{16,1}$ = 0	0.00 %
$P_{16,2}$ = 487.1±0.4871	$\partial Nus_{R22,LuiWin,16}/\partial P_{16,2}$ = 0	0.00 %
$P_{16,3}$ = 477.4±0.4774	$\partial Nus_{R22,LuiWin,16}/\partial P_{16,3}$ = 0.01352	0.01 %
$P_{16,4}$ = 378.5±0.3785	$\partial Nus_{R22,LuiWin,16}/\partial P_{16,4}$ = 0.04235	0.04 %
$P_{16,5}$ = 357.3±0.3573	$\partial Nus_{R22,LuiWin,16}/\partial P_{16,5}$ = -0.05814	0.06 %
$T_{16,1}$ = 17.326±0.060	$\partial Nus_{R22,LuiWin,16}/\partial T_{16,1}$ = 0.000	0.00 %
$T_{16,2}$ = -0.626±0.060	$\partial Nus_{R22,LuiWin,16}/\partial T_{16,2}$ = 0.000	0.00 %
$T_{16,3}$ = -0.858±0.060	$\partial Nus_{R22,LuiWin,16}/\partial T_{16,3}$ = -0.012	0.00 %
$T_{16,4}$ = -7.862±0.060	$\partial Nus_{R22,LuiWin,16}/\partial T_{16,4}$ = -0.009	0.00 %
$T_{16,5}$ = 37.807±0.060	$\partial Nus_{R22,LuiWin,16}/\partial T_{16,5}$ = 2.984	4.38 %
$T_{w,16,1}$ = 20.556±0.060	$\partial Nus_{R22,LuiWin,16}/\partial T_{w,16,1}$ = 0.000	0.00 %
$T_{w,16,2}$ = 11.365±0.060	$\partial Nus_{R22,LuiWin,16}/\partial T_{w,16,2}$ = 0.000	0.00 %
$T_{w,16,3}$ = 20.353±0.060	$\partial Nus_{R22,LuiWin,16}/\partial T_{w,16,3}$ = 4.673	10.73 %
$T_{w,16,4}$ = 14.736±0.060	$\partial Nus_{R22,LuiWin,16}/\partial T_{w,16,4}$ = -4.596	10.38 %
$Nus_{R22,Philip,16}$ = 111.149±1.100		
$\dot{m}_{W,16,1}$ = 0.06380±0.00006	$\partial Nus_{R22,Philip,16}/\partial \dot{m}_{W,16,1}$ = 0.00000	0.00 %
$\dot{m}_{W,16,2}$ = 0.07901±0.00008	$\partial Nus_{R22,Philip,16}/\partial \dot{m}_{W,16,2}$ = 710.06098	0.26 %
$\dot{m}_{W,16,3}$ = 0.07039±0.00007039	$\partial Nus_{R22,Philip,16}/\partial \dot{m}_{W,16,3}$ = -906.7	0.34 %
$m_{R22,16}$ = 0.02482±0.00004964	$\partial Nus_{R22,Philip,16}/\partial m_{R22,16}$ = 5064	5.22 %
$P_{16,1}$ = 1092±1.092	$\partial Nus_{R22,Philip,16}/\partial P_{16,1}$ = -5.075E-11	0.00 %
$P_{16,2}$ = 487.1±0.4871	$\partial Nus_{R22,Philip,16}/\partial P_{16,2}$ = -1.137E-10	0.00 %
$P_{16,3}$ = 477.4±0.4774	$\partial Nus_{R22,Philip,16}/\partial P_{16,3}$ = -0.03154	0.02 %
$P_{16,4}$ = 378.5±0.3785	$\partial Nus_{R22,Philip,16}/\partial P_{16,4}$ = -0.02036	0.00 %
$P_{16,5}$ = 357.3±0.3573	$\partial Nus_{R22,Philip,16}/\partial P_{16,5}$ = -0.0224	0.01 %
$T_{16,1}$ = 17.326±0.060	$\partial Nus_{R22,Philip,16}/\partial T_{16,1}$ = -0.000	0.00 %
$T_{16,2}$ = -0.626±0.060	$\partial Nus_{R22,Philip,16}/\partial T_{16,2}$ = 0.000	0.00 %
$T_{16,3}$ = -0.858±0.060	$\partial Nus_{R22,Philip,16}/\partial T_{16,3}$ = 3.647	3.96 %
$T_{16,4}$ = -7.862±0.060	$\partial Nus_{R22,Philip,16}/\partial T_{16,4}$ = 2.455	1.79 %
$T_{16,5}$ = 37.807±0.060	$\partial Nus_{R22,Philip,16}/\partial T_{16,5}$ = 1.150	0.39 %

$T_{w,16,1}$ = 20.556±0.060	$\partial Nus_{R22,Philip,16}/\partial T_{w,16,1}$ = -0.043	0.00 %
$T_{w,16,2}$ = 11.365±0.060	$\partial Nus_{R22,Philip,16}/\partial T_{w,16,2}$ = -0.045	0.00 %
$T_{w,16,3}$ = 20.353±0.060	$\partial Nus_{R22,Philip,16}/\partial T_{w,16,3}$ = 8.805	23.07 %
$T_{w,16,4}$ = 14.736±0.060	$\partial Nus_{R22,Philip,16}/\partial T_{w,16,4}$ = -14.774	64.94 %

$Nus_{R22,Pierre,16}$ = 407.525±1.954

$\dot{m}_{W,16,1}$ = 0.06380±0.00006	$\partial Nus_{R22,Pierre,16}/\partial \dot{m}_{W,16,1}$ = 0.00000	0.00 %
$\dot{m}_{W,16,2}$ = 0.07901±0.00008	$\partial Nus_{R22,Pierre,16}/\partial \dot{m}_{W,16,2}$ = -1147.78871	0.22 %
$\dot{m}_{W,16,3}$ = 0.07039±0.00007039	$\partial Nus_{R22,Pierre,16}/\partial \dot{m}_{W,16,3}$ = -3718	1.79 %
$m_{R22,16}$ = 0.02482±0.00004964	$\partial Nus_{R22,Pierre,16}/\partial m_{R22,16}$ = 27334	48.24 %
$P_{16,1}$ = 1092±1.092	$\partial Nus_{R22,Pierre,16}/\partial P_{16,1}$ = 0	0.00 %
$P_{16,2}$ = 487.1±0.4871	$\partial Nus_{R22,Pierre,16}/\partial P_{16,2}$ = 0	0.00 %
$P_{16,3}$ = 477.4±0.4774	$\partial Nus_{R22,Pierre,16}/\partial P_{16,3}$ = -0.1707	0.17 %
$P_{16,4}$ = 378.5±0.3785	$\partial Nus_{R22,Pierre,16}/\partial P_{16,4}$ = -0.1248	0.06 %
$P_{16,5}$ = 357.3±0.3573	$\partial Nus_{R22,Pierre,16}/\partial P_{16,5}$ = -0.09186	0.03 %
$T_{16,1}$ = 17.326±0.060	$\partial Nus_{R22,Pierre,16}/\partial T_{16,1}$ = 0.000	0.00 %
$T_{16,2}$ = -0.626±0.060	$\partial Nus_{R22,Pierre,16}/\partial T_{16,2}$ = 0.000	0.00 %
$T_{16,3}$ = -0.858±0.060	$\partial Nus_{R22,Pierre,16}/\partial T_{16,3}$ = 1.609	0.24 %
$T_{16,4}$ = -7.862±0.060	$\partial Nus_{R22,Pierre,16}/\partial T_{16,4}$ = 1.774	0.30 %
$T_{16,5}$ = 37.807±0.060	$\partial Nus_{R22,Pierre,16}/\partial T_{16,5}$ = 4.715	2.10 %
$T_{w,16,1}$ = 20.556±0.060	$\partial Nus_{R22,Pierre,16}/\partial T_{w,16,1}$ = 0.000	0.00 %
$T_{w,16,2}$ = 11.365±0.060	$\partial Nus_{R22,Pierre,16}/\partial T_{w,16,2}$ = 0.000	0.00 %
$T_{w,16,3}$ = 20.353±0.060	$\partial Nus_{R22,Pierre,16}/\partial T_{w,16,3}$ = -15.892	23.82 %
$T_{w,16,4}$ = 14.736±0.060	$\partial Nus_{R22,Pierre,16}/\partial T_{w,16,4}$ = 15.628	23.03 %

$Nus_{R22,Rous,16}$ = 110.093±1.070

$\dot{m}_{W,16,1}$ = 0.06380±0.00006	$\partial Nus_{R22,Rous,16}/\partial \dot{m}_{W,16,1}$ = 0.00000	0.00 %
$\dot{m}_{W,16,2}$ = 0.07901±0.00008	$\partial Nus_{R22,Rous,16}/\partial \dot{m}_{W,16,2}$ = 659.17827	0.24 %
$\dot{m}_{W,16,3}$ = 0.07039±0.00007039	$\partial Nus_{R22,Rous,16}/\partial \dot{m}_{W,16,3}$ = -898.1	0.35 %
$m_{R22,16}$ = 0.02482±0.00004964	$\partial Nus_{R22,Rous,16}/\partial m_{R22,16}$ = 5016	5.42 %
$P_{16,1}$ = 1092±1.092	$\partial Nus_{R22,Rous,16}/\partial P_{16,1}$ = 0	0.00 %
$P_{16,2}$ = 487.1±0.4871	$\partial Nus_{R22,Rous,16}/\partial P_{16,2}$ = 0	0.00 %
$P_{16,3}$ = 477.4±0.4774	$\partial Nus_{R22,Rous,16}/\partial P_{16,3}$ = -0.03124	0.02 %
$P_{16,4}$ = 378.5±0.3785	$\partial Nus_{R22,Rous,16}/\partial P_{16,4}$ = -0.02017	0.01 %
$P_{16,5}$ = 357.3±0.3573	$\partial Nus_{R22,Rous,16}/\partial P_{16,5}$ = -0.02219	0.01 %
$T_{16,1}$ = 17.326±0.060	$\partial Nus_{R22,Rous,16}/\partial T_{16,1}$ = 0.000	0.00 %
$T_{16,2}$ = -0.626±0.060	$\partial Nus_{R22,Rous,16}/\partial T_{16,2}$ = 0.000	0.00 %
$T_{16,3}$ = -0.858±0.060	$\partial Nus_{R22,Rous,16}/\partial T_{16,3}$ = 3.578	4.03 %
$T_{16,4}$ = -7.862±0.060	$\partial Nus_{R22,Rous,16}/\partial T_{16,4}$ = 2.409	1.83 %
$T_{16,5}$ = 37.807±0.060	$\partial Nus_{R22,Rous,16}/\partial T_{16,5}$ = 1.139	0.41 %
$T_{w,16,1}$ = 20.556±0.060	$\partial Nus_{R22,Rous,16}/\partial T_{w,16,1}$ = -0.115	0.00 %
$T_{w,16,2}$ = 11.365±0.060	$\partial Nus_{R22,Rous,16}/\partial T_{w,16,2}$ = -0.116	0.00 %
$T_{w,16,3}$ = 20.353±0.060	$\partial Nus_{R22,Rous,16}/\partial T_{w,16,3}$ = 8.540	22.95 %
$T_{w,16,4}$ = 14.736±0.060	$\partial Nus_{R22,Rous,16}/\partial T_{w,16,4}$ = -14.344	64.75 %

$Nus_{R22,RousAnn,16}$ = 541.752±0.444

$\dot{m}_{W,16,1}$ = 0.06380±0.00006	$\partial Nus_{R22,RousAnn,16}/\partial \dot{m}_{W,16,1}$ = 0.00000	0.00 %
$\dot{m}_{W,16,2}$ = 0.07901±0.00008	$\partial Nus_{R22,RousAnn,16}/\partial \dot{m}_{W,16,2}$ = 74.46676	0.02 %
$\dot{m}_{W,16,3}$ = 0.07039±0.00007039	$\partial Nus_{R22,RousAnn,16}/\partial \dot{m}_{W,16,3}$ = 2413	14.61 %
$m_{R22,16}$ = 0.02482±0.00004964	$\partial Nus_{R22,RousAnn,16}/\partial m_{R22,16}$ = 5791	41.87 %
$P_{16,1}$ = 1092±1.092	$\partial Nus_{R22,RousAnn,16}/\partial P_{16,1}$ = 0	0.00 %
$P_{16,2}$ = 487.1±0.4871	$\partial Nus_{R22,RousAnn,16}/\partial P_{16,2}$ = 0	0.00 %
$P_{16,3}$ = 477.4±0.4774	$\partial Nus_{R22,RousAnn,16}/\partial P_{16,3}$ = -0.3399	13.34 %
$P_{16,4}$ = 378.5±0.3785	$\partial Nus_{R22,RousAnn,16}/\partial P_{16,4}$ = 0.1241	1.12 %
$P_{16,5}$ = 357.3±0.3573	$\partial Nus_{R22,RousAnn,16}/\partial P_{16,5}$ = 0.05961	0.23 %
$T_{16,1}$ = 17.326±0.060	$\partial Nus_{R22,RousAnn,16}/\partial T_{16,1}$ = 0.000	0.00 %
$T_{16,2}$ = -0.626±0.060	$\partial Nus_{R22,RousAnn,16}/\partial T_{16,2}$ = 0.000	0.00 %
$T_{16,3}$ = -0.858±0.060	$\partial Nus_{R22,RousAnn,16}/\partial T_{16,3}$ = 2.055	7.70 %
$T_{16,4}$ = -7.862±0.060	$\partial Nus_{R22,RousAnn,16}/\partial T_{16,4}$ = 0.353	0.23 %
$T_{16,5}$ = 37.807±0.060	$\partial Nus_{R22,RousAnn,16}/\partial T_{16,5}$ = -3.060	17.07 %
$T_{w,16,1}$ = 20.556±0.060	$\partial Nus_{R22,RousAnn,16}/\partial T_{w,16,1}$ = 0.000	0.00 %
$T_{w,16,2}$ = 11.365±0.060	$\partial Nus_{R22,RousAnn,16}/\partial T_{w,16,2}$ = 0.000	0.00 %
$T_{w,16,3}$ = 20.353±0.060	$\partial Nus_{R22,RousAnn,16}/\partial T_{w,16,3}$ = 1.031	1.94 %
$T_{w,16,4}$ = 14.736±0.060	$\partial Nus_{R22,RousAnn,16}/\partial T_{w,16,4}$ = -1.014	1.87 %

R22 DATA SET 2

Unit Settings: [J]/[C]/[kPa]/[kg]/[degrees]

Variable±Uncertainty	Partial derivative	% of uncertainty
$Nus_{R22,Chen,61}$ = 267.621±0.934		
$\dot{m}_{W,61,1}$ = 0.07737±0.00008	$\partial Nus_{R22,Chen,61}/\partial \dot{m}_{W,61,1}$ = 0.00000	0.00 %
$\dot{m}_{W,61,2}$ = 0.10109±0.00010	$\partial Nus_{R22,Chen,61}/\partial \dot{m}_{W,61,2}$ = -268.31783	0.08 %
$\dot{m}_{W,61,3}$ = 0.08607±0.00008607	$\partial Nus_{R22,Chen,61}/\partial \dot{m}_{W,61,3}$ = -481.3	0.20 %
$m_{R22,61}$ = 0.03064±0.00006128	$\partial Nus_{R22,Chen,61}/\partial m_{R22,61}$ = 15180	99.12 %
$P_{61,1}$ = 1215±1.215	$\partial Nus_{R22,Chen,61}/\partial P_{61,1}$ = -9.354E-12	0.00 %
$P_{61,2}$ = 587.1±0.5871	$\partial Nus_{R22,Chen,61}/\partial P_{61,2}$ = -5.325E-11	0.00 %
$P_{61,3}$ = 578.8±0.5788	$\partial Nus_{R22,Chen,61}/\partial P_{61,3}$ = -0.07564	0.22 %
$P_{61,4}$ = 483.2±0.4832	$\partial Nus_{R22,Chen,61}/\partial P_{61,4}$ = -0.0737	0.15 %
$P_{61,5}$ = 460.4±0.4604	$\partial Nus_{R22,Chen,61}/\partial P_{61,5}$ = -0.01037	0.00 %
$T_{61,1}$ = 17.817±0.006	$\partial Nus_{R22,Chen,61}/\partial T_{61,1}$ = 0.000	0.00 %
$T_{61,2}$ = 5.145±0.006	$\partial Nus_{R22,Chen,61}/\partial T_{61,2}$ = 0.000	0.00 %
$T_{61,3}$ = 5.024±0.006	$\partial Nus_{R22,Chen,61}/\partial T_{61,3}$ = 0.949	0.00 %
$T_{61,4}$ = -0.915±0.006	$\partial Nus_{R22,Chen,61}/\partial T_{61,4}$ = 1.078	0.00 %
$T_{61,5}$ = 28.710±0.006	$\partial Nus_{R22,Chen,61}/\partial T_{61,5}$ = 0.479	0.00 %
$T_{w,61,1}$ = 19.697±0.006	$\partial Nus_{R22,Chen,61}/\partial T_{w,61,1}$ = 0.004	0.00 %
$T_{w,61,2}$ = 13.368±0.006	$\partial Nus_{R22,Chen,61}/\partial T_{w,61,2}$ = 0.006	0.00 %
$T_{w,61,3}$ = 19.462±0.006	$\partial Nus_{R22,Chen,61}/\partial T_{w,61,3}$ = -4.850	0.10 %
$T_{w,61,4}$ = 13.933±0.006	$\partial Nus_{R22,Chen,61}/\partial T_{w,61,4}$ = 5.602	0.13 %
$Nus_{R22,GunWin86,61}$ = 262.602±0.460		
$\dot{m}_{W,61,1}$ = 0.07737±0.00008	$\partial Nus_{R22,GunWin86,61}/\partial \dot{m}_{W,61,1}$ = 0.00000	0.00 %
$\dot{m}_{W,61,2}$ = 0.10109±0.00010	$\partial Nus_{R22,GunWin86,61}/\partial \dot{m}_{W,61,2}$ = 78.33136	0.03 %
$\dot{m}_{W,61,3}$ = 0.08607±0.00008607	$\partial Nus_{R22,GunWin86,61}/\partial \dot{m}_{W,61,3}$ = -1494	7.83 %
$m_{R22,61}$ = 0.03064±0.00006128	$\partial Nus_{R22,GunWin86,61}/\partial m_{R22,61}$ = 7174	91.42 %
$P_{61,1}$ = 1215±1.215	$\partial Nus_{R22,GunWin86,61}/\partial P_{61,1}$ = 0	0.00 %
$P_{61,2}$ = 587.1±0.5871	$\partial Nus_{R22,GunWin86,61}/\partial P_{61,2}$ = 0	0.00 %
$P_{61,3}$ = 578.8±0.5788	$\partial Nus_{R22,GunWin86,61}/\partial P_{61,3}$ = 0.03057	0.15 %
$P_{61,4}$ = 483.2±0.4832	$\partial Nus_{R22,GunWin86,61}/\partial P_{61,4}$ = 0.05678	0.36 %
$P_{61,5}$ = 460.4±0.4604	$\partial Nus_{R22,GunWin86,61}/\partial P_{61,5}$ = -0.03221	0.10 %
$T_{61,1}$ = 17.817±0.006	$\partial Nus_{R22,GunWin86,61}/\partial T_{61,1}$ = 0.000	0.00 %
$T_{61,2}$ = 5.145±0.006	$\partial Nus_{R22,GunWin86,61}/\partial T_{61,2}$ = 0.000	0.00 %
$T_{61,3}$ = 5.024±0.006	$\partial Nus_{R22,GunWin86,61}/\partial T_{61,3}$ = -0.355	0.00 %
$T_{61,4}$ = -0.915±0.006	$\partial Nus_{R22,GunWin86,61}/\partial T_{61,4}$ = -0.368	0.00 %
$T_{61,5}$ = 28.710±0.006	$\partial Nus_{R22,GunWin86,61}/\partial T_{61,5}$ = 1.488	0.04 %
$T_{w,61,1}$ = 19.697±0.006	$\partial Nus_{R22,GunWin86,61}/\partial T_{w,61,1}$ = 0.000	0.00 %
$T_{w,61,2}$ = 13.368±0.006	$\partial Nus_{R22,GunWin86,61}/\partial T_{w,61,2}$ = 0.000	0.00 %
$T_{w,61,3}$ = 19.462±0.006	$\partial Nus_{R22,GunWin86,61}/\partial T_{w,61,3}$ = 1.473	0.04 %
$T_{w,61,4}$ = 13.933±0.006	$\partial Nus_{R22,GunWin86,61}/\partial T_{w,61,4}$ = -1.428	0.03 %
$Nus_{R22,GunWin87,61}$ = 162.164±0.497		
$\dot{m}_{W,61,1}$ = 0.07737±0.00008	$\partial Nus_{R22,GunWin87,61}/\partial \dot{m}_{W,61,1}$ = 0.00000	0.00 %
$\dot{m}_{W,61,2}$ = 0.10109±0.00010	$\partial Nus_{R22,GunWin87,61}/\partial \dot{m}_{W,61,2}$ = -193.10437	0.15 %
$\dot{m}_{W,61,3}$ = 0.08607±0.00008607	$\partial Nus_{R22,GunWin87,61}/\partial \dot{m}_{W,61,3}$ = -1084	3.52 %
$m_{R22,61}$ = 0.03064±0.00006128	$\partial Nus_{R22,GunWin87,61}/\partial m_{R22,61}$ = 7917	95.22 %
$P_{61,1}$ = 1215±1.215	$\partial Nus_{R22,GunWin87,61}/\partial P_{61,1}$ = 0	0.00 %
$P_{61,2}$ = 587.1±0.5871	$\partial Nus_{R22,GunWin87,61}/\partial P_{61,2}$ = 0	0.00 %
$P_{61,3}$ = 578.8±0.5788	$\partial Nus_{R22,GunWin87,61}/\partial P_{61,3}$ = -0.03925	0.21 %
$P_{61,4}$ = 483.2±0.4832	$\partial Nus_{R22,GunWin87,61}/\partial P_{61,4}$ = -0.06954	0.46 %
$P_{61,5}$ = 460.4±0.4604	$\partial Nus_{R22,GunWin87,61}/\partial P_{61,5}$ = -0.02337	0.05 %
$T_{61,1}$ = 17.817±0.006	$\partial Nus_{R22,GunWin87,61}/\partial T_{61,1}$ = 0.000	0.00 %
$T_{61,2}$ = 5.145±0.006	$\partial Nus_{R22,GunWin87,61}/\partial T_{61,2}$ = 0.000	0.00 %
$T_{61,3}$ = 5.024±0.006	$\partial Nus_{R22,GunWin87,61}/\partial T_{61,3}$ = 0.158	0.00 %
$T_{61,4}$ = -0.915±0.006	$\partial Nus_{R22,GunWin87,61}/\partial T_{61,4}$ = 0.190	0.00 %
$T_{61,5}$ = 28.710±0.006	$\partial Nus_{R22,GunWin87,61}/\partial T_{61,5}$ = 1.080	0.02 %
$T_{w,61,1}$ = 19.697±0.006	$\partial Nus_{R22,GunWin87,61}/\partial T_{w,61,1}$ = 0.000	0.00 %
$T_{w,61,2}$ = 13.368±0.006	$\partial Nus_{R22,GunWin87,61}/\partial T_{w,61,2}$ = 0.000	0.00 %
$T_{w,61,3}$ = 19.462±0.006	$\partial Nus_{R22,GunWin87,61}/\partial T_{w,61,3}$ = -3.632	0.19 %
$T_{w,61,4}$ = 13.933±0.006	$\partial Nus_{R22,GunWin87,61}/\partial T_{w,61,4}$ = 3.521	0.18 %
$Nus_{R22,GunWinPhil,61}$ = 158.253±0.338		
$\dot{m}_{W,61,1}$ = 0.07737±0.00008	$\partial Nus_{R22,GunWinPhil,61}/\partial \dot{m}_{W,61,1}$ = 0.00000	0.00 %
$\dot{m}_{W,61,2}$ = 0.10109±0.00010	$\partial Nus_{R22,GunWinPhil,61}/\partial \dot{m}_{W,61,2}$ = 196.72284	0.35 %
$\dot{m}_{W,61,3}$ = 0.08607±0.00008607	$\partial Nus_{R22,GunWinPhil,61}/\partial \dot{m}_{W,61,3}$ = -1117	8.08 %
$m_{R22,61}$ = 0.03064±0.00006128	$\partial Nus_{R22,GunWinPhil,61}/\partial m_{R22,61}$ = 5234	89.93 %
$P_{61,1}$ = 1215±1.215	$\partial Nus_{R22,GunWinPhil,61}/\partial P_{61,1}$ = 0	0.00 %
$P_{61,2}$ = 587.1±0.5871	$\partial Nus_{R22,GunWinPhil,61}/\partial P_{61,2}$ = 0	0.00 %

$P_{61,3}$ = 578.8±0.5788	$\partial Nus_{R22,GunWinPhil,61}/\partial P_{61,3}$ = 0.02611	0.20 %
$P_{61,4}$ = 483.2±0.4832	$\partial Nus_{R22,GunWinPhil,61}/\partial P_{61,4}$ = -0.04692	0.45 %
$P_{61,5}$ = 460.4±0.4604	$\partial Nus_{R22,GunWinPhil,61}/\partial P_{61,5}$ = -0.02408	0.11 %
$T_{61,1}$ = 17.817±0.006	$\partial Nus_{R22,GunWinPhil,61}/\partial T_{61,1}$ = 0.000	0.00 %
$T_{61,2}$ = 5.145±0.006	$\partial Nus_{R22,GunWinPhil,61}/\partial T_{61,2}$ = 0.000	0.00 %
$T_{61,3}$ = 5.024±0.006	$\partial Nus_{R22,GunWinPhil,61}/\partial T_{61,3}$ = -0.488	0.01 %
$T_{61,4}$ = -0.915±0.006	$\partial Nus_{R22,GunWinPhil,61}/\partial T_{61,4}$ = -0.292	0.00 %
$T_{61,5}$ = 28.710±0.006	$\partial Nus_{R22,GunWinPhil,61}/\partial T_{61,5}$ = 1.112	0.04 %
$T_{w,61,1}$ = 19.697±0.006	$\partial Nus_{R22,GunWinPhil,61}/\partial T_{w,61,1}$ = 0.000	0.00 %
$T_{w,61,2}$ = 13.368±0.006	$\partial Nus_{R22,GunWinPhil,61}/\partial T_{w,61,2}$ = 0.000	0.00 %
$T_{w,61,3}$ = 19.462±0.006	$\partial Nus_{R22,GunWinPhil,61}/\partial T_{w,61,3}$ = 3.700	0.43 %
$T_{w,61,4}$ = 13.933±0.006	$\partial Nus_{R22,GunWinPhil,61}/\partial T_{w,61,4}$ = -3.587	0.40 %
$Nus_{R22,KTF,61}$ = 304.675±0.643		
$\dot{m}_{W,61,1}$ = 0.07737±0.00008	$\partial Nus_{R22,KTF,61}/\partial \dot{m}_{W,61,1}$ = 0.00000	0.00 %
$\dot{m}_{W,61,2}$ = 0.10109±0.00010	$\partial Nus_{R22,KTF,61}/\partial \dot{m}_{W,61,2}$ = 883.83766	1.93 %
$\dot{m}_{W,61,3}$ = 0.08607±0.00008607	$\partial Nus_{R22,KTF,61}/\partial \dot{m}_{W,61,3}$ = -2114	8.00 %
$m_{R22,61}$ = 0.03064±0.00006128	$\partial Nus_{R22,KTF,61}/\partial m_{R22,61}$ = 9651	84.56 %
$P_{61,1}$ = 1215±1.215	$\partial Nus_{R22,KTF,61}/\partial P_{61,1}$ = 0	0.00 %
$P_{61,2}$ = 587.1±0.5871	$\partial Nus_{R22,KTF,61}/\partial P_{61,2}$ = 0	0.00 %
$P_{61,3}$ = 578.8±0.5788	$\partial Nus_{R22,KTF,61}/\partial P_{61,3}$ = 0.0621	0.31 %
$P_{61,4}$ = 483.2±0.4832	$\partial Nus_{R22,KTF,61}/\partial P_{61,4}$ = 0.08283	0.39 %
$P_{61,5}$ = 460.4±0.4604	$\partial Nus_{R22,KTF,61}/\partial P_{61,5}$ = -0.04556	0.11 %
$T_{61,1}$ = 17.817±0.006	$\partial Nus_{R22,KTF,61}/\partial T_{61,1}$ = 0.000	0.00 %
$T_{61,2}$ = 5.145±0.006	$\partial Nus_{R22,KTF,61}/\partial T_{61,2}$ = 0.000	0.00 %
$T_{61,3}$ = 5.024±0.006	$\partial Nus_{R22,KTF,61}/\partial T_{61,3}$ = 0.000	0.00 %
$T_{61,4}$ = -0.915±0.006	$\partial Nus_{R22,KTF,61}/\partial T_{61,4}$ = 0.000	0.00 %
$T_{61,5}$ = 28.710±0.006	$\partial Nus_{R22,KTF,61}/\partial T_{61,5}$ = 2.105	0.04 %
$T_{w,61,1}$ = 19.697±0.006	$\partial Nus_{R22,KTF,61}/\partial T_{w,61,1}$ = 0.000	0.00 %
$T_{w,61,2}$ = 13.368±0.006	$\partial Nus_{R22,KTF,61}/\partial T_{w,61,2}$ = 0.000	0.00 %
$T_{w,61,3}$ = 19.462±0.006	$\partial Nus_{R22,KTF,61}/\partial T_{w,61,3}$ = 16.624	2.41 %
$T_{w,61,4}$ = 13.933±0.006	$\partial Nus_{R22,KTF,61}/\partial T_{w,61,4}$ = -16.115	2.26 %
$Nus_{R22,LuiWin,61}$ = 286.828±0.596		
$\dot{m}_{W,61,1}$ = 0.07737±0.00008	$\partial Nus_{R22,LuiWin,61}/\partial \dot{m}_{W,61,1}$ = 0.00000	0.00 %
$\dot{m}_{W,61,2}$ = 0.10109±0.00010	$\partial Nus_{R22,LuiWin,61}/\partial \dot{m}_{W,61,2}$ = 551.85629	0.88 %
$\dot{m}_{W,61,3}$ = 0.08607±0.00008607	$\partial Nus_{R22,LuiWin,61}/\partial \dot{m}_{W,61,3}$ = -1691	5.97 %
$m_{R22,61}$ = 0.03064±0.00006128	$\partial Nus_{R22,LuiWin,61}/\partial m_{R22,61}$ = 9260	90.77 %
$P_{61,1}$ = 1215±1.215	$\partial Nus_{R22,LuiWin,61}/\partial P_{61,1}$ = 0	0.00 %
$P_{61,2}$ = 587.1±0.5871	$\partial Nus_{R22,LuiWin,61}/\partial P_{61,2}$ = 0	0.00 %
$P_{61,3}$ = 578.8±0.5788	$\partial Nus_{R22,LuiWin,61}/\partial P_{61,3}$ = 0.02337	0.05 %
$P_{61,4}$ = 483.2±0.4832	$\partial Nus_{R22,LuiWin,61}/\partial P_{61,4}$ = 0.03985	0.10 %
$P_{61,5}$ = 460.4±0.4604	$\partial Nus_{R22,LuiWin,61}/\partial P_{61,5}$ = -0.03645	0.08 %
$T_{61,1}$ = 17.817±0.006	$\partial Nus_{R22,LuiWin,61}/\partial T_{61,1}$ = 0.000	0.00 %
$T_{61,2}$ = 5.145±0.006	$\partial Nus_{R22,LuiWin,61}/\partial T_{61,2}$ = 0.000	0.00 %
$T_{61,3}$ = 5.024±0.006	$\partial Nus_{R22,LuiWin,61}/\partial T_{61,3}$ = 0.004	0.00 %
$T_{61,4}$ = -0.915±0.006	$\partial Nus_{R22,LuiWin,61}/\partial T_{61,4}$ = 0.008	0.00 %
$T_{61,5}$ = 28.710±0.006	$\partial Nus_{R22,LuiWin,61}/\partial T_{61,5}$ = 1.684	0.03 %
$T_{w,61,1}$ = 19.697±0.006	$\partial Nus_{R22,LuiWin,61}/\partial T_{w,61,1}$ = 0.000	0.00 %
$T_{w,61,2}$ = 13.368±0.006	$\partial Nus_{R22,LuiWin,61}/\partial T_{w,61,2}$ = 0.000	0.00 %
$T_{w,61,3}$ = 19.462±0.006	$\partial Nus_{R22,LuiWin,61}/\partial T_{w,61,3}$ = 10.380	1.09 %
$T_{w,61,4}$ = 13.933±0.006	$\partial Nus_{R22,LuiWin,61}/\partial T_{w,61,4}$ = -10.062	1.03 %
$Nus_{R22,Philip,61}$ = 158.248±0.425		
$\dot{m}_{W,61,1}$ = 0.07737±0.00008	$\partial Nus_{R22,Philip,61}/\partial \dot{m}_{W,61,1}$ = 0.00000	0.00 %
$\dot{m}_{W,61,2}$ = 0.10109±0.00010	$\partial Nus_{R22,Philip,61}/\partial \dot{m}_{W,61,2}$ = 1161.54593	7.64 %
$\dot{m}_{W,61,3}$ = 0.08607±0.00008607	$\partial Nus_{R22,Philip,61}/\partial \dot{m}_{W,61,3}$ = -1099	4.95 %
$m_{R22,61}$ = 0.03064±0.00006128	$\partial Nus_{R22,Philip,61}/\partial m_{R22,61}$ = 5013	52.29 %
$P_{61,1}$ = 1215±1.215	$\partial Nus_{R22,Philip,61}/\partial P_{61,1}$ = 1.193E-10	0.00 %
$P_{61,2}$ = 587.1±0.5871	$\partial Nus_{R22,Philip,61}/\partial P_{61,2}$ = 9.126E-10	0.00 %
$P_{61,3}$ = 578.8±0.5788	$\partial Nus_{R22,Philip,61}/\partial P_{61,3}$ = -0.02218	0.09 %
$P_{61,4}$ = 483.2±0.4832	$\partial Nus_{R22,Philip,61}/\partial P_{61,4}$ = -0.01141	0.02 %
$P_{61,5}$ = 460.4±0.4604	$\partial Nus_{R22,Philip,61}/\partial P_{61,5}$ = -0.02368	0.07 %
$T_{61,1}$ = 17.817±0.006	$\partial Nus_{R22,Philip,61}/\partial T_{61,1}$ = 0.000	0.00 %
$T_{61,2}$ = 5.145±0.006	$\partial Nus_{R22,Philip,61}/\partial T_{61,2}$ = 0.000	0.00 %
$T_{61,3}$ = 5.024±0.006	$\partial Nus_{R22,Philip,61}/\partial T_{61,3}$ = 9.604	1.84 %
$T_{61,4}$ = -0.915±0.006	$\partial Nus_{R22,Philip,61}/\partial T_{61,4}$ = 5.525	0.61 %
$T_{61,5}$ = 28.710±0.006	$\partial Nus_{R22,Philip,61}/\partial T_{61,5}$ = 1.094	0.02 %

$T_{w,61,1}$ = 19.697±0.006	$\partial Nus_{R22,Philp,61}/\partial T_{w,61,1}$ = -0.063	0.00 %
$T_{w,61,2}$ = 13.368±0.006	$\partial Nus_{R22,Philp,61}/\partial T_{w,61,2}$ = -0.098	0.00 %
$T_{w,61,3}$ = 19.462±0.006	$\partial Nus_{R22,Philp,61}/\partial T_{w,61,3}$ = 20.359	8.27 %
$T_{w,61,4}$ = 13.933±0.006	$\partial Nus_{R22,Philp,61}/\partial T_{w,61,4}$ = -34.841	24.21 %

$Nus_{R22,Pierre,61}$ = 508.938±1.782

$\dot{m}_{w,61,1}$ = 0.07737±0.00008	$\partial Nus_{R22,Pierre,61}/\partial \dot{m}_{w,61,1}$ = 0.00000	0.00 %
$\dot{m}_{w,61,2}$ = 0.10109±0.00010	$\partial Nus_{R22,Pierre,61}/\partial \dot{m}_{w,61,2}$ = 183.52177	0.01 %
$\dot{m}_{w,61,3}$ = 0.08607±0.00008607	$\partial Nus_{R22,Pierre,61}/\partial \dot{m}_{w,61,3}$ = -4391	4.50 %
$m_{R22,61}$ = 0.03064±0.00006128	$\partial Nus_{R22,Pierre,61}/\partial m_{R22,61}$ = 28339	95.01 %
$P_{61,1}$ = 1215±1.215	$\partial Nus_{R22,Pierre,61}/\partial P_{61,1}$ = 0	0.00 %
$P_{61,2}$ = 587.1±0.5871	$\partial Nus_{R22,Pierre,61}/\partial P_{61,2}$ = 0	0.00 %
$P_{61,3}$ = 578.8±0.5788	$\partial Nus_{R22,Pierre,61}/\partial P_{61,3}$ = -0.1579	0.26 %
$P_{61,4}$ = 483.2±0.4832	$\partial Nus_{R22,Pierre,61}/\partial P_{61,4}$ = -0.1149	0.10 %
$P_{61,5}$ = 460.4±0.4604	$\partial Nus_{R22,Pierre,61}/\partial P_{61,5}$ = -0.09464	0.06 %
$T_{61,1}$ = 17.817±0.006	$\partial Nus_{R22,Pierre,61}/\partial T_{61,1}$ = 0.000	0.00 %
$T_{61,2}$ = 5.145±0.006	$\partial Nus_{R22,Pierre,61}/\partial T_{61,2}$ = 0.000	0.00 %
$T_{61,3}$ = 5.024±0.006	$\partial Nus_{R22,Pierre,61}/\partial T_{61,3}$ = 2.491	0.01 %
$T_{61,4}$ = -0.915±0.006	$\partial Nus_{R22,Pierre,61}/\partial T_{61,4}$ = 2.685	0.01 %
$T_{61,5}$ = 28.710±0.006	$\partial Nus_{R22,Pierre,61}/\partial T_{61,5}$ = 4.373	0.02 %
$T_{w,61,1}$ = 19.697±0.006	$\partial Nus_{R22,Pierre,61}/\partial T_{w,61,1}$ = 0.000	0.00 %
$T_{w,61,2}$ = 13.368±0.006	$\partial Nus_{R22,Pierre,61}/\partial T_{w,61,2}$ = 0.000	0.00 %
$T_{w,61,3}$ = 19.462±0.006	$\partial Nus_{R22,Pierre,61}/\partial T_{w,61,3}$ = 3.452	0.01 %
$T_{w,61,4}$ = 13.933±0.006	$\partial Nus_{R22,Pierre,61}/\partial T_{w,61,4}$ = -3.346	0.01 %

$Nus_{R22,Rous,61}$ = 153.312±0.403

$\dot{m}_{w,61,1}$ = 0.07737±0.00008	$\partial Nus_{R22,Rous,61}/\partial \dot{m}_{w,61,1}$ = 0.00000	0.00 %
$\dot{m}_{w,61,2}$ = 0.10109±0.00010	$\partial Nus_{R22,Rous,61}/\partial \dot{m}_{w,61,2}$ = 1028.90643	6.67 %
$\dot{m}_{w,61,3}$ = 0.08607±0.00008607	$\partial Nus_{R22,Rous,61}/\partial \dot{m}_{w,61,3}$ = -1065	5.18 %
$m_{R22,61}$ = 0.03064±0.00006128	$\partial Nus_{R22,Rous,61}/\partial m_{R22,61}$ = 4857	54.64 %
$P_{61,1}$ = 1215±1.215	$\partial Nus_{R22,Rous,61}/\partial P_{61,1}$ = 0	0.00 %
$P_{61,2}$ = 587.1±0.5871	$\partial Nus_{R22,Rous,61}/\partial P_{61,2}$ = 0	0.00 %
$P_{61,3}$ = 578.8±0.5788	$\partial Nus_{R22,Rous,61}/\partial P_{61,3}$ = -0.02149	0.10 %
$P_{61,4}$ = 483.2±0.4832	$\partial Nus_{R22,Rous,61}/\partial P_{61,4}$ = -0.01105	0.02 %
$P_{61,5}$ = 460.4±0.4604	$\partial Nus_{R22,Rous,61}/\partial P_{61,5}$ = -0.02294	0.07 %
$T_{61,1}$ = 17.817±0.006	$\partial Nus_{R22,Rous,61}/\partial T_{61,1}$ = 0.000	0.00 %
$T_{61,2}$ = 5.145±0.006	$\partial Nus_{R22,Rous,61}/\partial T_{61,2}$ = 0.000	0.00 %
$T_{61,3}$ = 5.024±0.006	$\partial Nus_{R22,Rous,61}/\partial T_{61,3}$ = 9.014	1.80 %
$T_{61,4}$ = -0.915±0.006	$\partial Nus_{R22,Rous,61}/\partial T_{61,4}$ = 5.185	0.60 %
$T_{61,5}$ = 28.710±0.006	$\partial Nus_{R22,Rous,61}/\partial T_{61,5}$ = 1.060	0.02 %
$T_{w,61,1}$ = 19.697±0.006	$\partial Nus_{R22,Rous,61}/\partial T_{w,61,1}$ = -0.241	0.00 %
$T_{w,61,2}$ = 13.368±0.006	$\partial Nus_{R22,Rous,61}/\partial T_{w,61,2}$ = -0.263	0.00 %
$T_{w,61,3}$ = 19.462±0.006	$\partial Nus_{R22,Rous,61}/\partial T_{w,61,3}$ = 18.775	7.83 %
$T_{w,61,4}$ = 13.933±0.006	$\partial Nus_{R22,Rous,61}/\partial T_{w,61,4}$ = -32.241	23.08 %

$Nus_{R22,RousAnn,61}$ = 657.737±0.981

$\dot{m}_{w,61,1}$ = 0.07737±0.00008	$\partial Nus_{R22,RousAnn,61}/\partial \dot{m}_{w,61,1}$ = 0.00000	0.00 %
$\dot{m}_{w,61,2}$ = 0.10109±0.00010	$\partial Nus_{R22,RousAnn,61}/\partial \dot{m}_{w,61,2}$ = -1082.20250	1.24 %
$\dot{m}_{w,61,3}$ = 0.08607±0.00008607	$\partial Nus_{R22,RousAnn,61}/\partial \dot{m}_{w,61,3}$ = -30.65	0.00 %
$m_{R22,61}$ = 0.03064±0.00006128	$\partial Nus_{R22,RousAnn,61}/\partial m_{R22,61}$ = 15465	93.24 %
$P_{61,1}$ = 1215±1.215	$\partial Nus_{R22,RousAnn,61}/\partial P_{61,1}$ = 0	0.00 %
$P_{61,2}$ = 587.1±0.5871	$\partial Nus_{R22,RousAnn,61}/\partial P_{61,2}$ = 0	0.00 %
$P_{61,3}$ = 578.8±0.5788	$\partial Nus_{R22,RousAnn,61}/\partial P_{61,3}$ = -0.264	2.42 %
$P_{61,4}$ = 483.2±0.4832	$\partial Nus_{R22,RousAnn,61}/\partial P_{61,4}$ = -0.05489	0.07 %
$P_{61,5}$ = 460.4±0.4604	$\partial Nus_{R22,RousAnn,61}/\partial P_{61,5}$ = -0.0006607	0.00 %
$T_{61,1}$ = 17.817±0.006	$\partial Nus_{R22,RousAnn,61}/\partial T_{61,1}$ = 0.000	0.00 %
$T_{61,2}$ = 5.145±0.006	$\partial Nus_{R22,RousAnn,61}/\partial T_{61,2}$ = 0.000	0.00 %
$T_{61,3}$ = 5.024±0.006	$\partial Nus_{R22,RousAnn,61}/\partial T_{61,3}$ = 1.680	0.01 %
$T_{61,4}$ = -0.915±0.006	$\partial Nus_{R22,RousAnn,61}/\partial T_{61,4}$ = 0.935	0.00 %
$T_{61,5}$ = 28.710±0.006	$\partial Nus_{R22,RousAnn,61}/\partial T_{61,5}$ = 0.031	0.00 %
$T_{w,61,1}$ = 19.697±0.006	$\partial Nus_{R22,RousAnn,61}/\partial T_{w,61,1}$ = 0.000	0.00 %
$T_{w,61,2}$ = 13.368±0.006	$\partial Nus_{R22,RousAnn,61}/\partial T_{w,61,2}$ = 0.000	0.00 %
$T_{w,61,3}$ = 19.462±0.006	$\partial Nus_{R22,RousAnn,61}/\partial T_{w,61,3}$ = -20.356	1.55 %
$T_{w,61,4}$ = 13.933±0.006	$\partial Nus_{R22,RousAnn,61}/\partial T_{w,61,4}$ = 19.732	1.46 %

R407C DATA SET 1

Unit Settings: [J]/[C]/[kPa]/[kg]/[degrees]

Variable±Uncertainty	Partial derivative	% of uncertainty
$Nus_{R407C,Chen,12}$ = 325.922±5.788		
$\dot{m}_{W,12,1}$ = 0.05058±0.00005058	$\partial Nus_{R407C,Chen,12}/\partial \dot{m}_{W,12,1}$ = 0	0.00 %
$\dot{m}_{W,12,2}$ = 0.06998±0.00007	$\partial Nus_{R407C,Chen,12}/\partial \dot{m}_{W,12,2}$ = -4888.28074	0.35 %
$\dot{m}_{W,12,3}$ = 0.09716±0.00009716	$\partial Nus_{R407C,Chen,12}/\partial \dot{m}_{W,12,3}$ = -3252	0.30 %
$m_{R407C,12}$ = 0.01961±0.00003922	$\partial Nus_{R407C,Chen,12}/\partial m_{R407C,12}$ = 38144	6.68 %
$P_{12,1}$ = 1218±1.218	$\partial Nus_{R407C,Chen,12}/\partial P_{12,1}$ = 0	0.00 %
$P_{12,2}$ = 484.4±0.4844	$\partial Nus_{R407C,Chen,12}/\partial P_{12,2}$ = 0	0.00 %
$P_{12,3}$ = 477.4±0.4774	$\partial Nus_{R407C,Chen,12}/\partial P_{12,3}$ = -0.3684	0.09 %
$P_{12,4}$ = 413.9±0.4139	$\partial Nus_{R407C,Chen,12}/\partial P_{12,4}$ = -0.3067	0.05 %
$P_{12,5}$ = 399.2±0.3992	$\partial Nus_{R407C,Chen,12}/\partial P_{12,5}$ = -0.1056	0.01 %
$T_{12,1}$ = 18.22±0.06	$\partial Nus_{R407C,Chen,12}/\partial T_{12,1}$ = 0	0.00 %
$T_{12,2}$ = -3.382±0.06	$\partial Nus_{R407C,Chen,12}/\partial T_{12,2}$ = 0	0.00 %
$T_{12,3}$ = -0.328±0.06	$\partial Nus_{R407C,Chen,12}/\partial T_{12,3}$ = -0.5385	0.00 %
$T_{12,4}$ = 2.586±0.06	$\partial Nus_{R407C,Chen,12}/\partial T_{12,4}$ = -0.5632	0.00 %
$T_{12,5}$ = 40.74±0.06	$\partial Nus_{R407C,Chen,12}/\partial T_{12,5}$ = 7.435	0.59 %
$T_{w,12,1}$ = 21.24±0.06	$\partial Nus_{R407C,Chen,12}/\partial T_{w,12,1}$ = 0.005516	0.00 %
$T_{w,12,2}$ = 11.77±0.06	$\partial Nus_{R407C,Chen,12}/\partial T_{w,12,2}$ = 0.005022	0.00 %
$T_{w,12,3}$ = 20.847±0.060	$\partial Nus_{R407C,Chen,12}/\partial T_{w,12,3}$ = -62.949	42.58 %
$T_{w,12,4}$ = 15.47±0.06	$\partial Nus_{R407C,Chen,12}/\partial T_{w,12,4}$ = 67.77	49.35 %
$Nus_{R407C,GunWin86,12}$ = 317.166±0.777		
$\dot{m}_{W,12,1}$ = 0.05058±0.00005058	$\partial Nus_{R407C,GunWin86,12}/\partial \dot{m}_{W,12,1}$ = 0	0.00 %
$\dot{m}_{W,12,2}$ = 0.06998±0.00007	$\partial Nus_{R407C,GunWin86,12}/\partial \dot{m}_{W,12,2}$ = -418.44215	0.14 %
$\dot{m}_{W,12,3}$ = 0.09716±0.00009716	$\partial Nus_{R407C,GunWin86,12}/\partial \dot{m}_{W,12,3}$ = -1347	2.83 %
$m_{R407C,12}$ = 0.01961±0.00003922	$\partial Nus_{R407C,GunWin86,12}/\partial m_{R407C,12}$ = 14587	54.20 %
$P_{12,1}$ = 1218±1.218	$\partial Nus_{R407C,GunWin86,12}/\partial P_{12,1}$ = 0	0.00 %
$P_{12,2}$ = 484.4±0.4844	$\partial Nus_{R407C,GunWin86,12}/\partial P_{12,2}$ = 0	0.00 %
$P_{12,3}$ = 477.4±0.4774	$\partial Nus_{R407C,GunWin86,12}/\partial P_{12,3}$ = -0.01145	0.00 %
$P_{12,4}$ = 413.9±0.4139	$\partial Nus_{R407C,GunWin86,12}/\partial P_{12,4}$ = 0.02277	0.01 %
$P_{12,5}$ = 399.2±0.3992	$\partial Nus_{R407C,GunWin86,12}/\partial P_{12,5}$ = -0.04372	0.05 %
$T_{12,1}$ = 18.22±0.06	$\partial Nus_{R407C,GunWin86,12}/\partial T_{12,1}$ = 0	0.00 %
$T_{12,2}$ = -3.382±0.06	$\partial Nus_{R407C,GunWin86,12}/\partial T_{12,2}$ = 0	0.00 %
$T_{12,3}$ = -0.328±0.06	$\partial Nus_{R407C,GunWin86,12}/\partial T_{12,3}$ = -0.4518	0.12 %
$T_{12,4}$ = 2.586±0.06	$\partial Nus_{R407C,GunWin86,12}/\partial T_{12,4}$ = -0.4443	0.12 %
$T_{12,5}$ = 40.74±0.06	$\partial Nus_{R407C,GunWin86,12}/\partial T_{12,5}$ = 3.079	5.65 %
$T_{w,12,1}$ = 21.24±0.06	$\partial Nus_{R407C,GunWin86,12}/\partial T_{w,12,1}$ = 0	0.00 %
$T_{w,12,2}$ = 11.77±0.06	$\partial Nus_{R407C,GunWin86,12}/\partial T_{w,12,2}$ = 0	0.00 %
$T_{w,12,3}$ = 20.847±0.060	$\partial Nus_{R407C,GunWin86,12}/\partial T_{w,12,3}$ = -5.428	17.56 %
$T_{w,12,4}$ = 15.47±0.06	$\partial Nus_{R407C,GunWin86,12}/\partial T_{w,12,4}$ = 5.691	19.30 %
$Nus_{R407C,GunWin87,12}$ = 191.824±1.333		
$\dot{m}_{W,12,1}$ = 0.05058±0.00005058	$\partial Nus_{R407C,GunWin87,12}/\partial \dot{m}_{W,12,1}$ = 0	0.00 %
$\dot{m}_{W,12,2}$ = 0.06998±0.00007	$\partial Nus_{R407C,GunWin87,12}/\partial \dot{m}_{W,12,2}$ = -1027.41299	0.29 %
$\dot{m}_{W,12,3}$ = 0.09716±0.00009716	$\partial Nus_{R407C,GunWin87,12}/\partial \dot{m}_{W,12,3}$ = -927	0.46 %
$m_{R407C,12}$ = 0.01961±0.00003922	$\partial Nus_{R407C,GunWin87,12}/\partial m_{R407C,12}$ = 16085	22.40 %
$P_{12,1}$ = 1218±1.218	$\partial Nus_{R407C,GunWin87,12}/\partial P_{12,1}$ = 0	0.00 %
$P_{12,2}$ = 484.4±0.4844	$\partial Nus_{R407C,GunWin87,12}/\partial P_{12,2}$ = 0	0.00 %
$P_{12,3}$ = 477.4±0.4774	$\partial Nus_{R407C,GunWin87,12}/\partial P_{12,3}$ = -0.1208	0.19 %
$P_{12,4}$ = 413.9±0.4139	$\partial Nus_{R407C,GunWin87,12}/\partial P_{12,4}$ = -0.1311	0.17 %
$P_{12,5}$ = 399.2±0.3992	$\partial Nus_{R407C,GunWin87,12}/\partial P_{12,5}$ = -0.03009	0.01 %
$T_{12,1}$ = 18.22±0.06	$\partial Nus_{R407C,GunWin87,12}/\partial T_{12,1}$ = 0	0.00 %
$T_{12,2}$ = -3.382±0.06	$\partial Nus_{R407C,GunWin87,12}/\partial T_{12,2}$ = 0	0.00 %
$T_{12,3}$ = -0.328±0.06	$\partial Nus_{R407C,GunWin87,12}/\partial T_{12,3}$ = 0.3402	0.02 %
$T_{12,4}$ = 2.586±0.06	$\partial Nus_{R407C,GunWin87,12}/\partial T_{12,4}$ = 0.3106	0.02 %
$T_{12,5}$ = 40.74±0.06	$\partial Nus_{R407C,GunWin87,12}/\partial T_{12,5}$ = 2.119	0.91 %
$T_{w,12,1}$ = 21.24±0.06	$\partial Nus_{R407C,GunWin87,12}/\partial T_{w,12,1}$ = 0	0.00 %
$T_{w,12,2}$ = 11.77±0.06	$\partial Nus_{R407C,GunWin87,12}/\partial T_{w,12,2}$ = 0	0.00 %
$T_{w,12,3}$ = 20.847±0.060	$\partial Nus_{R407C,GunWin87,12}/\partial T_{w,12,3}$ = -13.328	35.99 %
$T_{w,12,4}$ = 15.47±0.06	$\partial Nus_{R407C,GunWin87,12}/\partial T_{w,12,4}$ = 13.97	39.55 %
$Nus_{R407C,GunWinPhil,12}$ = 189.599±0.922		
$\dot{m}_{W,12,1}$ = 0.05058±0.00005058	$\partial Nus_{R407C,GunWinPhil,12}/\partial \dot{m}_{W,12,1}$ = 0	0.00 %
$\dot{m}_{W,12,2}$ = 0.06998±0.00007	$\partial Nus_{R407C,GunWinPhil,12}/\partial \dot{m}_{W,12,2}$ = -599.03957	0.21 %
$\dot{m}_{W,12,3}$ = 0.09716±0.00009716	$\partial Nus_{R407C,GunWinPhil,12}/\partial \dot{m}_{W,12,3}$ = -1410	2.21 %
$m_{R407C,12}$ = 0.01961±0.00003922	$\partial Nus_{R407C,GunWinPhil,12}/\partial m_{R407C,12}$ = 14655	38.86 %
$P_{12,1}$ = 1218±1.218	$\partial Nus_{R407C,GunWinPhil,12}/\partial P_{12,1}$ = 0	0.00 %
$P_{12,2}$ = 484.4±0.4844	$\partial Nus_{R407C,GunWinPhil,12}/\partial P_{12,2}$ = 0	0.00 %

$P_{12,3}$ = 477.4±0.4774	$\partial Nus_{R407C,GunWinPhil,12}/\partial P_{12,3}$ = -0.02629	0.02 %
$P_{12,4}$ = 413.9±0.4139	$\partial Nus_{R407C,GunWinPhil,12}/\partial P_{12,4}$ = -0.1209	0.29 %
$P_{12,5}$ = 399.2±0.3992	$\partial Nus_{R407C,GunWinPhil,12}/\partial P_{12,5}$ = -0.04578	0.04 %
$T_{12,1}$ = 18.22±0.06	$\partial Nus_{R407C,GunWinPhil,12}/\partial T_{12,1}$ = 0	0.00 %
$T_{12,2}$ = -3.382±0.06	$\partial Nus_{R407C,GunWinPhil,12}/\partial T_{12,2}$ = 0	0.00 %
$T_{12,3}$ = -0.328±0.06	$\partial Nus_{R407C,GunWinPhil,12}/\partial T_{12,3}$ = -0.547	0.13 %
$T_{12,4}$ = 2.586±0.06	$\partial Nus_{R407C,GunWinPhil,12}/\partial T_{12,4}$ = -0.6029	0.15 %
$T_{12,5}$ = 40.74±0.06	$\partial Nus_{R407C,GunWinPhil,12}/\partial T_{12,5}$ = 3.224	4.40 %
$T_{w,12,1}$ = 21.24±0.06	$\partial Nus_{R407C,GunWinPhil,12}/\partial T_{w,12,1}$ = 0	0.00 %
$T_{w,12,2}$ = 11.77±0.06	$\partial Nus_{R407C,GunWinPhil,12}/\partial T_{w,12,2}$ = 0	0.00 %
$T_{w,12,3}$ = 20.847±0.060	$\partial Nus_{R407C,GunWinPhil,12}/\partial T_{w,12,3}$ = -7.771	25.57 %
$T_{w,12,4}$ = 15.47±0.06	$\partial Nus_{R407C,GunWinPhil,12}/\partial T_{w,12,4}$ = 8.147	28.11 %
$Nus_{R407C,KTF,12}$ = 297.426±0.703		
$\dot{m}_{w,12,1}$ = 0.05058±0.00005058	$\partial Nus_{R407C,KTF,12}/\partial \dot{m}_{w,12,1}$ = 0	0.00 %
$\dot{m}_{w,12,2}$ = 0.06998±0.00007	$\partial Nus_{R407C,KTF,12}/\partial \dot{m}_{w,12,2}$ = 73.59624	0.01 %
$\dot{m}_{w,12,3}$ = 0.09716±0.00009716	$\partial Nus_{R407C,KTF,12}/\partial \dot{m}_{w,12,3}$ = -1596	4.86 %
$m_{R407C,12}$ = 0.01961±0.00003922	$\partial Nus_{R407C,KTF,12}/\partial m_{R407C,12}$ = 16421	83.93 %
$P_{12,1}$ = 1218±1.218	$\partial Nus_{R407C,KTF,12}/\partial P_{12,1}$ = 0	0.00 %
$P_{12,2}$ = 484.4±0.4844	$\partial Nus_{R407C,KTF,12}/\partial P_{12,2}$ = 0	0.00 %
$P_{12,3}$ = 477.4±0.4774	$\partial Nus_{R407C,KTF,12}/\partial P_{12,3}$ = -0.01602	0.01 %
$P_{12,4}$ = 413.9±0.4139	$\partial Nus_{R407C,KTF,12}/\partial P_{12,4}$ = 0.01733	0.01 %
$P_{12,5}$ = 399.2±0.3992	$\partial Nus_{R407C,KTF,12}/\partial P_{12,5}$ = -0.0518	0.09 %
$T_{12,1}$ = 18.22±0.06	$\partial Nus_{R407C,KTF,12}/\partial T_{12,1}$ = 0	0.00 %
$T_{12,2}$ = -3.382±0.06	$\partial Nus_{R407C,KTF,12}/\partial T_{12,2}$ = 0	0.00 %
$T_{12,3}$ = -0.328±0.06	$\partial Nus_{R407C,KTF,12}/\partial T_{12,3}$ = 0.0001449	0.00 %
$T_{12,4}$ = 2.586±0.06	$\partial Nus_{R407C,KTF,12}/\partial T_{12,4}$ = 0.0001279	0.00 %
$T_{12,5}$ = 40.74±0.06	$\partial Nus_{R407C,KTF,12}/\partial T_{12,5}$ = 3.648	9.70 %
$T_{w,12,1}$ = 21.24±0.06	$\partial Nus_{R407C,KTF,12}/\partial T_{w,12,1}$ = 0	0.00 %
$T_{w,12,2}$ = 11.77±0.06	$\partial Nus_{R407C,KTF,12}/\partial T_{w,12,2}$ = 0	0.00 %
$T_{w,12,3}$ = 20.847±0.060	$\partial Nus_{R407C,KTF,12}/\partial T_{w,12,3}$ = 0.955	0.66 %
$T_{w,12,4}$ = 15.47±0.06	$\partial Nus_{R407C,KTF,12}/\partial T_{w,12,4}$ = -1.001	0.73 %
$Nus_{R407C,LuiWin,12}$ = 316.833±0.834		
$\dot{m}_{w,12,1}$ = 0.05058±0.00005058	$\partial Nus_{R407C,LuiWin,12}/\partial \dot{m}_{w,12,1}$ = 0	0.00 %
$\dot{m}_{w,12,2}$ = 0.06998±0.00007	$\partial Nus_{R407C,LuiWin,12}/\partial \dot{m}_{w,12,2}$ = 401.59416	0.11 %
$\dot{m}_{w,12,3}$ = 0.09716±0.00009716	$\partial Nus_{R407C,LuiWin,12}/\partial \dot{m}_{w,12,3}$ = -1488	3.01 %
$m_{R407C,12}$ = 0.01961±0.00003922	$\partial Nus_{R407C,LuiWin,12}/\partial m_{R407C,12}$ = 16647	61.31 %
$P_{12,1}$ = 1218±1.218	$\partial Nus_{R407C,LuiWin,12}/\partial P_{12,1}$ = 0	0.00 %
$P_{12,2}$ = 484.4±0.4844	$\partial Nus_{R407C,LuiWin,12}/\partial P_{12,2}$ = 0	0.00 %
$P_{12,3}$ = 477.4±0.4774	$\partial Nus_{R407C,LuiWin,12}/\partial P_{12,3}$ = -0.00843	0.00 %
$P_{12,4}$ = 413.9±0.4139	$\partial Nus_{R407C,LuiWin,12}/\partial P_{12,4}$ = 0.02291	0.01 %
$P_{12,5}$ = 399.2±0.3992	$\partial Nus_{R407C,LuiWin,12}/\partial P_{12,5}$ = -0.04831	0.05 %
$T_{12,1}$ = 18.22±0.06	$\partial Nus_{R407C,LuiWin,12}/\partial T_{12,1}$ = 0	0.00 %
$T_{12,2}$ = -3.382±0.06	$\partial Nus_{R407C,LuiWin,12}/\partial T_{12,2}$ = 0	0.00 %
$T_{12,3}$ = -0.328±0.06	$\partial Nus_{R407C,LuiWin,12}/\partial T_{12,3}$ = -0.004459	0.00 %
$T_{12,4}$ = 2.586±0.06	$\partial Nus_{R407C,LuiWin,12}/\partial T_{12,4}$ = -0.007471	0.00 %
$T_{12,5}$ = 40.74±0.06	$\partial Nus_{R407C,LuiWin,12}/\partial T_{12,5}$ = 3.402	5.99 %
$T_{w,12,1}$ = 21.24±0.06	$\partial Nus_{R407C,LuiWin,12}/\partial T_{w,12,1}$ = 0	0.00 %
$T_{w,12,2}$ = 11.77±0.06	$\partial Nus_{R407C,LuiWin,12}/\partial T_{w,12,2}$ = 0	0.00 %
$T_{w,12,3}$ = 20.847±0.060	$\partial Nus_{R407C,LuiWin,12}/\partial T_{w,12,3}$ = 5.210	14.05 %
$T_{w,12,4}$ = 15.47±0.06	$\partial Nus_{R407C,LuiWin,12}/\partial T_{w,12,4}$ = -5.462	15.45 %
$Nus_{R407C,Philip,12}$ = 123.509±1.345		
$\dot{m}_{w,12,1}$ = 0.05058±0.00005058	$\partial Nus_{R407C,Philip,12}/\partial \dot{m}_{w,12,1}$ = 0.000001868	0.00 %
$\dot{m}_{w,12,2}$ = 0.06998±0.00007	$\partial Nus_{R407C,Philip,12}/\partial \dot{m}_{w,12,2}$ = 898.47782	0.22 %
$\dot{m}_{w,12,3}$ = 0.09716±0.00009716	$\partial Nus_{R407C,Philip,12}/\partial \dot{m}_{w,12,3}$ = -663	0.23 %
$m_{R407C,12}$ = 0.01961±0.00003922	$\partial Nus_{R407C,Philip,12}/\partial m_{R407C,12}$ = 6820	3.95 %
$P_{12,1}$ = 1218±1.218	$\partial Nus_{R407C,Philip,12}/\partial P_{12,1}$ = 0	0.00 %
$P_{12,2}$ = 484.4±0.4844	$\partial Nus_{R407C,Philip,12}/\partial P_{12,2}$ = 0	0.00 %
$P_{12,3}$ = 477.4±0.4774	$\partial Nus_{R407C,Philip,12}/\partial P_{12,3}$ = -0.04617	0.03 %
$P_{12,4}$ = 413.9±0.4139	$\partial Nus_{R407C,Philip,12}/\partial P_{12,4}$ = -0.03217	0.01 %
$P_{12,5}$ = 399.2±0.3992	$\partial Nus_{R407C,Philip,12}/\partial P_{12,5}$ = -0.02152	0.00 %
$T_{12,1}$ = 18.22±0.06	$\partial Nus_{R407C,Philip,12}/\partial T_{12,1}$ = 0	0.00 %
$T_{12,2}$ = -3.382±0.06	$\partial Nus_{R407C,Philip,12}/\partial T_{12,2}$ = 0	0.00 %
$T_{12,3}$ = -0.328±0.06	$\partial Nus_{R407C,Philip,12}/\partial T_{12,3}$ = 4.407	3.86 %
$T_{12,4}$ = 2.586±0.06	$\partial Nus_{R407C,Philip,12}/\partial T_{12,4}$ = 4.001	3.18 %
$T_{12,5}$ = 40.74±0.06	$\partial Nus_{R407C,Philip,12}/\partial T_{12,5}$ = 1.516	0.46 %

$T_{w,12,1}$ = 21.24±0.06	$\partial Nus_{R407C,Philip,12}/\partial T_{w,12,1}$ = -0.02689	0.00 %
$T_{w,12,2}$ = 11.77±0.06	$\partial Nus_{R407C,Philip,12}/\partial T_{w,12,2}$ = -0.02448	0.00 %
$T_{w,12,3}$ = 20.847±0.060	$\partial Nus_{R407C,Philip,12}/\partial T_{w,12,3}$ = 9.589	18.29 %
$T_{w,12,4}$ = 15.47±0.06	$\partial Nus_{R407C,Philip,12}/\partial T_{w,12,4}$ = -18.73	69.76 %

$Nus_{R407C,Pierre,12}$ = 410.474±2.579

$\dot{m}_{w,12,1}$ = 0.05058±0.00005058	$\partial Nus_{R407C,Pierre,12}/\partial \dot{m}_{w,12,1}$ = 0	0.00 %
$\dot{m}_{w,12,2}$ = 0.06998±0.00007	$\partial Nus_{R407C,Pierre,12}/\partial \dot{m}_{w,12,2}$ = -1827.99947	0.25 %
$\dot{m}_{w,12,3}$ = 0.09716±0.00009716	$\partial Nus_{R407C,Pierre,12}/\partial \dot{m}_{w,12,3}$ = -2793	1.11 %
$m_{R407C,12}$ = 0.01961±0.00003922	$\partial Nus_{R407C,Pierre,12}/\partial m_{R407C,12}$ = 37108	31.84 %
$P_{12,1}$ = 1218±1.218	$\partial Nus_{R407C,Pierre,12}/\partial P_{12,1}$ = 0	0.00 %
$P_{12,2}$ = 484.4±0.4844	$\partial Nus_{R407C,Pierre,12}/\partial P_{12,2}$ = 0	0.00 %
$P_{12,3}$ = 477.4±0.4774	$\partial Nus_{R407C,Pierre,12}/\partial P_{12,3}$ = -0.2246	0.17 %
$P_{12,4}$ = 413.9±0.4139	$\partial Nus_{R407C,Pierre,12}/\partial P_{12,4}$ = -0.1656	0.07 %
$P_{12,5}$ = 399.2±0.3992	$\partial Nus_{R407C,Pierre,12}/\partial P_{12,5}$ = -0.09067	0.02 %
$T_{12,1}$ = 18.22±0.06	$\partial Nus_{R407C,Pierre,12}/\partial T_{12,1}$ = 0	0.00 %
$T_{12,2}$ = -3.382±0.06	$\partial Nus_{R407C,Pierre,12}/\partial T_{12,2}$ = 0	0.00 %
$T_{12,3}$ = -0.328±0.06	$\partial Nus_{R407C,Pierre,12}/\partial T_{12,3}$ = 2.133	0.25 %
$T_{12,4}$ = 2.586±0.06	$\partial Nus_{R407C,Pierre,12}/\partial T_{12,4}$ = 2.043	0.23 %
$T_{12,5}$ = 40.74±0.06	$\partial Nus_{R407C,Pierre,12}/\partial T_{12,5}$ = 6.386	2.21 %
$T_{w,12,1}$ = 21.24±0.06	$\partial Nus_{R407C,Pierre,12}/\partial T_{w,12,1}$ = 0	0.00 %
$T_{w,12,2}$ = 11.77±0.06	$\partial Nus_{R407C,Pierre,12}/\partial T_{w,12,2}$ = 0	0.00 %
$T_{w,12,3}$ = 20.847±0.060	$\partial Nus_{R407C,Pierre,12}/\partial T_{w,12,3}$ = -23.714	30.43 %
$T_{w,12,4}$ = 15.47±0.06	$\partial Nus_{R407C,Pierre,12}/\partial T_{w,12,4}$ = 24.86	33.44 %

$Nus_{R407C,Rous,12}$ = 122.554±1.314

$\dot{m}_{w,12,1}$ = 0.05058±0.00005058	$\partial Nus_{R407C,Rous,12}/\partial \dot{m}_{w,12,1}$ = -8.429E-08	0.00 %
$\dot{m}_{w,12,2}$ = 0.06998±0.00007	$\partial Nus_{R407C,Rous,12}/\partial \dot{m}_{w,12,2}$ = 829.15307	0.19 %
$\dot{m}_{w,12,3}$ = 0.09716±0.00009716	$\partial Nus_{R407C,Rous,12}/\partial \dot{m}_{w,12,3}$ = -657.8	0.24 %
$m_{R407C,12}$ = 0.01961±0.00003922	$\partial Nus_{R407C,Rous,12}/\partial m_{R407C,12}$ = 6768	4.08 %
$P_{12,1}$ = 1218±1.218	$\partial Nus_{R407C,Rous,12}/\partial P_{12,1}$ = 0	0.00 %
$P_{12,2}$ = 484.4±0.4844	$\partial Nus_{R407C,Rous,12}/\partial P_{12,2}$ = 0	0.00 %
$P_{12,3}$ = 477.4±0.4774	$\partial Nus_{R407C,Rous,12}/\partial P_{12,3}$ = -0.04581	0.03 %
$P_{12,4}$ = 413.9±0.4139	$\partial Nus_{R407C,Rous,12}/\partial P_{12,4}$ = -0.03192	0.01 %
$P_{12,5}$ = 399.2±0.3992	$\partial Nus_{R407C,Rous,12}/\partial P_{12,5}$ = -0.02136	0.00 %
$T_{12,1}$ = 18.22±0.06	$\partial Nus_{R407C,Rous,12}/\partial T_{12,1}$ = 0	0.00 %
$T_{12,2}$ = -3.382±0.06	$\partial Nus_{R407C,Rous,12}/\partial T_{12,2}$ = 0	0.00 %
$T_{12,3}$ = -0.328±0.06	$\partial Nus_{R407C,Rous,12}/\partial T_{12,3}$ = 4.339	3.93 %
$T_{12,4}$ = 2.586±0.06	$\partial Nus_{R407C,Rous,12}/\partial T_{12,4}$ = 3.939	3.24 %
$T_{12,5}$ = 40.74±0.06	$\partial Nus_{R407C,Rous,12}/\partial T_{12,5}$ = 1.504	0.47 %
$T_{w,12,1}$ = 21.24±0.06	$\partial Nus_{R407C,Rous,12}/\partial T_{w,12,1}$ = -0.1307	0.00 %
$T_{w,12,2}$ = 11.77±0.06	$\partial Nus_{R407C,Rous,12}/\partial T_{w,12,2}$ = -0.129	0.00 %
$T_{w,12,3}$ = 20.847±0.060	$\partial Nus_{R407C,Rous,12}/\partial T_{w,12,3}$ = 9.348	18.22 %
$T_{w,12,4}$ = 15.47±0.06	$\partial Nus_{R407C,Rous,12}/\partial T_{w,12,4}$ = -18.27	69.59 %

$Nus_{R407C,RousAnn,12}$ = 123.066±0.366

$\dot{m}_{w,12,1}$ = 0.05058±0.00005058	$\partial Nus_{R407C,RousAnn,12}/\partial \dot{m}_{w,12,1}$ = 0	0.00 %
$\dot{m}_{w,12,2}$ = 0.06998±0.00007	$\partial Nus_{R407C,RousAnn,12}/\partial \dot{m}_{w,12,2}$ = 237.01513	0.21 %
$\dot{m}_{w,12,3}$ = 0.09716±0.00009716	$\partial Nus_{R407C,RousAnn,12}/\partial \dot{m}_{w,12,3}$ = -583.6	2.40 %
$m_{R407C,12}$ = 0.01961±0.00003922	$\partial Nus_{R407C,RousAnn,12}/\partial m_{R407C,12}$ = 5623	36.32 %
$P_{12,1}$ = 1218±1.218	$\partial Nus_{R407C,RousAnn,12}/\partial P_{12,1}$ = 0	0.00 %
$P_{12,2}$ = 484.4±0.4844	$\partial Nus_{R407C,RousAnn,12}/\partial P_{12,2}$ = 0	0.00 %
$P_{12,3}$ = 477.4±0.4774	$\partial Nus_{R407C,RousAnn,12}/\partial P_{12,3}$ = -0.07757	1.02 %
$P_{12,4}$ = 413.9±0.4139	$\partial Nus_{R407C,RousAnn,12}/\partial P_{12,4}$ = -0.06614	0.56 %
$P_{12,5}$ = 399.2±0.3992	$\partial Nus_{R407C,RousAnn,12}/\partial P_{12,5}$ = -0.01895	0.04 %
$T_{12,1}$ = 18.22±0.06	$\partial Nus_{R407C,RousAnn,12}/\partial T_{12,1}$ = 0	0.00 %
$T_{12,2}$ = -3.382±0.06	$\partial Nus_{R407C,RousAnn,12}/\partial T_{12,2}$ = 0	0.00 %
$T_{12,3}$ = -0.328±0.06	$\partial Nus_{R407C,RousAnn,12}/\partial T_{12,3}$ = 0.7035	1.33 %
$T_{12,4}$ = 2.586±0.06	$\partial Nus_{R407C,RousAnn,12}/\partial T_{12,4}$ = -0.00258	0.00 %
$T_{12,5}$ = 40.74±0.06	$\partial Nus_{R407C,RousAnn,12}/\partial T_{12,5}$ = 1.334	4.78 %
$T_{w,12,1}$ = 21.24±0.06	$\partial Nus_{R407C,RousAnn,12}/\partial T_{w,12,1}$ = 0	0.00 %
$T_{w,12,2}$ = 11.77±0.06	$\partial Nus_{R407C,RousAnn,12}/\partial T_{w,12,2}$ = 0	0.00 %
$T_{w,12,3}$ = 20.847±0.060	$\partial Nus_{R407C,RousAnn,12}/\partial T_{w,12,3}$ = 3.075	25.41 %
$T_{w,12,4}$ = 15.47±0.06	$\partial Nus_{R407C,RousAnn,12}/\partial T_{w,12,4}$ = -3.223	27.93 %

R407C DATA SET 2

Unit Settings: [J]/[C]/[kPa]/[kg]/[degrees]

Variable±Uncertainty	Partial derivative	% of uncertainty
$Nus_{R407C,Chen,65}$ = 344.936±2.158		
$\dot{m}_{W,65,1}$ = 0.08452±0.00008452	$\partial Nus_{R407C,Chen,65}/\partial \dot{m}_{W,65,1}$ = 0	0.00 %
$\dot{m}_{W,65,2}$ = 0.09981±0.00010	$\partial Nus_{R407C,Chen,65}/\partial \dot{m}_{W,65,2}$ = -1031.35300	0.23 %
$\dot{m}_{W,65,3}$ = 0.09633±0.00009633	$\partial Nus_{R407C,Chen,65}/\partial \dot{m}_{W,65,3}$ = -1262	0.32 %
$m_{R407C,65}$ = 0.03001±0.00006002	$\partial Nus_{R407C,Chen,65}/\partial m_{R407C,65}$ = 19236	28.62 %
$P_{65,1}$ = 1360±1.36	$\partial Nus_{R407C,Chen,65}/\partial P_{65,1}$ = 0	0.00 %
$P_{65,2}$ = 584.1±0.5841	$\partial Nus_{R407C,Chen,65}/\partial P_{65,2}$ = 0	0.00 %
$P_{65,3}$ = 572.1±0.5721	$\partial Nus_{R407C,Chen,65}/\partial P_{65,3}$ = -0.1908	0.26 %
$P_{65,4}$ = 450.6±0.4506	$\partial Nus_{R407C,Chen,65}/\partial P_{65,4}$ = -0.1832	0.15 %
$P_{65,5}$ = 424±0.424	$\partial Nus_{R407C,Chen,65}/\partial P_{65,5}$ = -0.03614	0.01 %
$T_{65,1}$ = 17.89±0.06	$\partial Nus_{R407C,Chen,65}/\partial T_{65,1}$ = 0	0.00 %
$T_{65,2}$ = 2.136±0.06	$\partial Nus_{R407C,Chen,65}/\partial T_{65,2}$ = 0	0.00 %
$T_{65,3}$ = 5.065±0.06	$\partial Nus_{R407C,Chen,65}/\partial T_{65,3}$ = 0.7315	0.04 %
$T_{65,4}$ = 0.017±0.06	$\partial Nus_{R407C,Chen,65}/\partial T_{65,4}$ = 0.8695	0.06 %
$T_{65,5}$ = 38.86±0.06	$\partial Nus_{R407C,Chen,65}/\partial T_{65,5}$ = 2.497	0.48 %
$T_{w,65,1}$ = 23.94±0.06	$\partial Nus_{R407C,Chen,65}/\partial T_{w,65,1}$ = 0.005457	0.00 %
$T_{w,65,2}$ = 14.97±0.06	$\partial Nus_{R407C,Chen,65}/\partial T_{w,65,2}$ = 0.01147	0.00 %
$T_{w,65,3}$ = 23.813±0.060	$\partial Nus_{R407C,Chen,65}/\partial T_{w,65,3}$ = -20.239	31.66 %
$T_{w,65,4}$ = 18.77±0.06	$\partial Nus_{R407C,Chen,65}/\partial T_{w,65,4}$ = 22.23	38.19 %
$Nus_{R407C,GunWin86,65}$ = 348.090±0.692		
$\dot{m}_{W,65,1}$ = 0.08452±0.00008452	$\partial Nus_{R407C,GunWin86,65}/\partial \dot{m}_{W,65,1}$ = 0	0.00 %
$\dot{m}_{W,65,2}$ = 0.09981±0.00010	$\partial Nus_{R407C,GunWin86,65}/\partial \dot{m}_{W,65,2}$ = -141.10242	0.04 %
$\dot{m}_{W,65,3}$ = 0.09633±0.00009633	$\partial Nus_{R407C,GunWin86,65}/\partial \dot{m}_{W,65,3}$ = -1564	4.73 %
$m_{R407C,65}$ = 0.03001±0.00006002	$\partial Nus_{R407C,GunWin86,65}/\partial m_{R407C,65}$ = 10022	75.46 %
$P_{65,1}$ = 1360±1.36	$\partial Nus_{R407C,GunWin86,65}/\partial P_{65,1}$ = 0	0.00 %
$P_{65,2}$ = 584.1±0.5841	$\partial Nus_{R407C,GunWin86,65}/\partial P_{65,2}$ = 0	0.00 %
$P_{65,3}$ = 572.1±0.5721	$\partial Nus_{R407C,GunWin86,65}/\partial P_{65,3}$ = -0.008985	0.01 %
$P_{65,4}$ = 450.6±0.4506	$\partial Nus_{R407C,GunWin86,65}/\partial P_{65,4}$ = 0.01471	0.01 %
$P_{65,5}$ = 424±0.424	$\partial Nus_{R407C,GunWin86,65}/\partial P_{65,5}$ = -0.04477	0.08 %
$T_{65,1}$ = 17.89±0.06	$\partial Nus_{R407C,GunWin86,65}/\partial T_{65,1}$ = 0	0.00 %
$T_{65,2}$ = 2.136±0.06	$\partial Nus_{R407C,GunWin86,65}/\partial T_{65,2}$ = 0	0.00 %
$T_{65,3}$ = 5.065±0.06	$\partial Nus_{R407C,GunWin86,65}/\partial T_{65,3}$ = -0.4746	0.17 %
$T_{65,4}$ = 0.017±0.06	$\partial Nus_{R407C,GunWin86,65}/\partial T_{65,4}$ = -0.4866	0.18 %
$T_{65,5}$ = 38.86±0.06	$\partial Nus_{R407C,GunWin86,65}/\partial T_{65,5}$ = 3.094	7.19 %
$T_{w,65,1}$ = 23.94±0.06	$\partial Nus_{R407C,GunWin86,65}/\partial T_{w,65,1}$ = 0	0.00 %
$T_{w,65,2}$ = 14.97±0.06	$\partial Nus_{R407C,GunWin86,65}/\partial T_{w,65,2}$ = 0	0.00 %
$T_{w,65,3}$ = 23.813±0.060	$\partial Nus_{R407C,GunWin86,65}/\partial T_{w,65,3}$ = -2.821	5.97 %
$T_{w,65,4}$ = 18.77±0.06	$\partial Nus_{R407C,GunWin86,65}/\partial T_{w,65,4}$ = 2.865	6.16 %
$Nus_{R407C,GunWin87,65}$ = 239.543±1.385		
$\dot{m}_{W,65,1}$ = 0.08452±0.00008452	$\partial Nus_{R407C,GunWin87,65}/\partial \dot{m}_{W,65,1}$ = 0	0.00 %
$\dot{m}_{W,65,2}$ = 0.09981±0.00010	$\partial Nus_{R407C,GunWin87,65}/\partial \dot{m}_{W,65,2}$ = -665.71742	0.23 %
$\dot{m}_{W,65,3}$ = 0.09633±0.00009633	$\partial Nus_{R407C,GunWin87,65}/\partial \dot{m}_{W,65,3}$ = -1243	0.75 %
$m_{R407C,65}$ = 0.03001±0.00006002	$\partial Nus_{R407C,GunWin87,65}/\partial m_{R407C,65}$ = 12589	29.78 %
$P_{65,1}$ = 1360±1.36	$\partial Nus_{R407C,GunWin87,65}/\partial P_{65,1}$ = 0	0.00 %
$P_{65,2}$ = 584.1±0.5841	$\partial Nus_{R407C,GunWin87,65}/\partial P_{65,2}$ = 0	0.00 %
$P_{65,3}$ = 572.1±0.5721	$\partial Nus_{R407C,GunWin87,65}/\partial P_{65,3}$ = -0.1198	0.25 %
$P_{65,4}$ = 450.6±0.4506	$\partial Nus_{R407C,GunWin87,65}/\partial P_{65,4}$ = -0.146	0.23 %
$P_{65,5}$ = 424±0.424	$\partial Nus_{R407C,GunWin87,65}/\partial P_{65,5}$ = -0.03557	0.01 %
$T_{65,1}$ = 17.89±0.06	$\partial Nus_{R407C,GunWin87,65}/\partial T_{65,1}$ = 0	0.00 %
$T_{65,2}$ = 2.136±0.06	$\partial Nus_{R407C,GunWin87,65}/\partial T_{65,2}$ = 0	0.00 %
$T_{65,3}$ = 5.065±0.06	$\partial Nus_{R407C,GunWin87,65}/\partial T_{65,3}$ = 0.3725	0.03 %
$T_{65,4}$ = 0.017±0.06	$\partial Nus_{R407C,GunWin87,65}/\partial T_{65,4}$ = 0.435	0.04 %
$T_{65,5}$ = 38.86±0.06	$\partial Nus_{R407C,GunWin87,65}/\partial T_{65,5}$ = 2.458	1.13 %
$T_{w,65,1}$ = 23.94±0.06	$\partial Nus_{R407C,GunWin87,65}/\partial T_{w,65,1}$ = 0	0.00 %
$T_{w,65,2}$ = 14.97±0.06	$\partial Nus_{R407C,GunWin87,65}/\partial T_{w,65,2}$ = 0	0.00 %
$T_{w,65,3}$ = 23.813±0.060	$\partial Nus_{R407C,GunWin87,65}/\partial T_{w,65,3}$ = -13.310	33.26 %
$T_{w,65,4}$ = 18.77±0.06	$\partial Nus_{R407C,GunWin87,65}/\partial T_{w,65,4}$ = 13.52	34.30 %
$Nus_{R407C,GunWinPhil,65}$ = 206.268±0.731		
$\dot{m}_{W,65,1}$ = 0.08452±0.00008452	$\partial Nus_{R407C,GunWinPhil,65}/\partial \dot{m}_{W,65,1}$ = 0	0.00 %
$\dot{m}_{W,65,2}$ = 0.09981±0.00010	$\partial Nus_{R407C,GunWinPhil,65}/\partial \dot{m}_{W,65,2}$ = -224.76161	0.09 %
$\dot{m}_{W,65,3}$ = 0.09633±0.00009633	$\partial Nus_{R407C,GunWinPhil,65}/\partial \dot{m}_{W,65,3}$ = -1548	4.16 %
$m_{R407C,65}$ = 0.03001±0.00006002	$\partial Nus_{R407C,GunWinPhil,65}/\partial m_{R407C,65}$ = 9476	60.60 %
$P_{65,1}$ = 1360±1.36	$\partial Nus_{R407C,GunWinPhil,65}/\partial P_{65,1}$ = 0	0.00 %
$P_{65,2}$ = 584.1±0.5841	$\partial Nus_{R407C,GunWinPhil,65}/\partial P_{65,2}$ = 0	0.00 %

$P_{65,3}$ = 572.1±0.5721	$\partial Nus_{R407C,GunWinPhil,65}/\partial P_{65,3}$ = -0.01088	0.01 %
$P_{65,4}$ = 450.6±0.4506	$\partial Nus_{R407C,GunWinPhil,65}/\partial P_{65,4}$ = -0.1177	0.53 %
$P_{65,5}$ = 424±0.424	$\partial Nus_{R407C,GunWinPhil,65}/\partial P_{65,5}$ = -0.04431	0.07 %
$T_{65,1}$ = 17.89±0.06	$\partial Nus_{R407C,GunWinPhil,65}/\partial T_{65,1}$ = 0	0.00 %
$T_{65,2}$ = 2.136±0.06	$\partial Nus_{R407C,GunWinPhil,65}/\partial T_{65,2}$ = 0	0.00 %
$T_{65,3}$ = 5.065±0.06	$\partial Nus_{R407C,GunWinPhil,65}/\partial T_{65,3}$ = -0.766	0.40 %
$T_{65,4}$ = 0.017±0.06	$\partial Nus_{R407C,GunWinPhil,65}/\partial T_{65,4}$ = -0.497	0.17 %
$T_{65,5}$ = 38.86±0.06	$\partial Nus_{R407C,GunWinPhil,65}/\partial T_{65,5}$ = 3.062	6.32 %
$T_{w,65,1}$ = 23.94±0.06	$\partial Nus_{R407C,GunWinPhil,65}/\partial T_{w,65,1}$ = 0	0.00 %
$T_{w,65,2}$ = 14.97±0.06	$\partial Nus_{R407C,GunWinPhil,65}/\partial T_{w,65,2}$ = 0	0.00 %
$T_{w,65,3}$ = 23.813±0.060	$\partial Nus_{R407C,GunWinPhil,65}/\partial T_{w,65,3}$ = -4.494	13.62 %
$T_{w,65,4}$ = 18.77±0.06	$\partial Nus_{R407C,GunWinPhil,65}/\partial T_{w,65,4}$ = 4.563	14.04 %

$Nus_{R407C,KTF,65}$ = 340.165±0.979

$\dot{m}_{W,65,1}$ = 0.08452±0.00008452	$\partial Nus_{R407C,KTF,65}/\partial \dot{m}_{W,65,1}$ = 0	0.00 %
$\dot{m}_{W,65,2}$ = 0.09981±0.00010	$\partial Nus_{R407C,KTF,65}/\partial \dot{m}_{W,65,2}$ = 370.63841	0.14 %
$\dot{m}_{W,65,3}$ = 0.09633±0.00009633	$\partial Nus_{R407C,KTF,65}/\partial \dot{m}_{W,65,3}$ = -1940	3.64 %
$m_{R407C,65}$ = 0.03001±0.00006002	$\partial Nus_{R407C,KTF,65}/\partial m_{R407C,65}$ = 11391	48.74 %
$P_{65,1}$ = 1360±1.36	$\partial Nus_{R407C,KTF,65}/\partial P_{65,1}$ = 0	0.00 %
$P_{65,2}$ = 584.1±0.5841	$\partial Nus_{R407C,KTF,65}/\partial P_{65,2}$ = 0	0.00 %
$P_{65,3}$ = 572.1±0.5721	$\partial Nus_{R407C,KTF,65}/\partial P_{65,3}$ = -0.005902	0.00 %
$P_{65,4}$ = 450.6±0.4506	$\partial Nus_{R407C,KTF,65}/\partial P_{65,4}$ = 0.01669	0.01 %
$P_{65,5}$ = 424±0.424	$\partial Nus_{R407C,KTF,65}/\partial P_{65,5}$ = -0.05554	0.06 %
$T_{65,1}$ = 17.89±0.06	$\partial Nus_{R407C,KTF,65}/\partial T_{65,1}$ = 0	0.00 %
$T_{65,2}$ = 2.136±0.06	$\partial Nus_{R407C,KTF,65}/\partial T_{65,2}$ = 0	0.00 %
$T_{65,3}$ = 5.065±0.06	$\partial Nus_{R407C,KTF,65}/\partial T_{65,3}$ = 0.0002302	0.00 %
$T_{65,4}$ = 0.017±0.06	$\partial Nus_{R407C,KTF,65}/\partial T_{65,4}$ = 0.0002847	0.00 %
$T_{65,5}$ = 38.86±0.06	$\partial Nus_{R407C,KTF,65}/\partial T_{65,5}$ = 3.839	5.53 %
$T_{w,65,1}$ = 23.94±0.06	$\partial Nus_{R407C,KTF,65}/\partial T_{w,65,1}$ = 0	0.00 %
$T_{w,65,2}$ = 14.97±0.06	$\partial Nus_{R407C,KTF,65}/\partial T_{w,65,2}$ = 0	0.00 %
$T_{w,65,3}$ = 23.813±0.060	$\partial Nus_{R407C,KTF,65}/\partial T_{w,65,3}$ = 7.410	20.61 %
$T_{w,65,4}$ = 18.77±0.06	$\partial Nus_{R407C,KTF,65}/\partial T_{w,65,4}$ = -7.525	21.26 %

$Nus_{R407C,LuiWin,65}$ = 379.916±1.371

$\dot{m}_{W,65,1}$ = 0.08452±0.00008452	$\partial Nus_{R407C,LuiWin,65}/\partial \dot{m}_{W,65,1}$ = 0	0.00 %
$\dot{m}_{W,65,2}$ = 0.09981±0.00010	$\partial Nus_{R407C,LuiWin,65}/\partial \dot{m}_{W,65,2}$ = 659.85887	0.23 %
$\dot{m}_{W,65,3}$ = 0.09633±0.00009633	$\partial Nus_{R407C,LuiWin,65}/\partial \dot{m}_{W,65,3}$ = -1817	1.63 %
$m_{R407C,65}$ = 0.03001±0.00006002	$\partial Nus_{R407C,LuiWin,65}/\partial m_{R407C,65}$ = 12084	27.97 %
$P_{65,1}$ = 1360±1.36	$\partial Nus_{R407C,LuiWin,65}/\partial P_{65,1}$ = 0	0.00 %
$P_{65,2}$ = 584.1±0.5841	$\partial Nus_{R407C,LuiWin,65}/\partial P_{65,2}$ = 0	0.00 %
$P_{65,3}$ = 572.1±0.5721	$\partial Nus_{R407C,LuiWin,65}/\partial P_{65,3}$ = 0.001243	0.00 %
$P_{65,4}$ = 450.6±0.4506	$\partial Nus_{R407C,LuiWin,65}/\partial P_{65,4}$ = 0.02292	0.01 %
$P_{65,5}$ = 424±0.424	$\partial Nus_{R407C,LuiWin,65}/\partial P_{65,5}$ = -0.05202	0.03 %
$T_{65,1}$ = 17.89±0.06	$\partial Nus_{R407C,LuiWin,65}/\partial T_{65,1}$ = 0	0.00 %
$T_{65,2}$ = 2.136±0.06	$\partial Nus_{R407C,LuiWin,65}/\partial T_{65,2}$ = 0	0.00 %
$T_{65,3}$ = 5.065±0.06	$\partial Nus_{R407C,LuiWin,65}/\partial T_{65,3}$ = -0.0008935	0.00 %
$T_{65,4}$ = 0.017±0.06	$\partial Nus_{R407C,LuiWin,65}/\partial T_{65,4}$ = 0.007351	0.00 %
$T_{65,5}$ = 38.86±0.06	$\partial Nus_{R407C,LuiWin,65}/\partial T_{65,5}$ = 3.595	2.47 %
$T_{w,65,1}$ = 23.94±0.06	$\partial Nus_{R407C,LuiWin,65}/\partial T_{w,65,1}$ = 0	0.00 %
$T_{w,65,2}$ = 14.97±0.06	$\partial Nus_{R407C,LuiWin,65}/\partial T_{w,65,2}$ = 0	0.00 %
$T_{w,65,3}$ = 23.813±0.060	$\partial Nus_{R407C,LuiWin,65}/\partial T_{w,65,3}$ = 13.192	33.31 %
$T_{w,65,4}$ = 18.77±0.06	$\partial Nus_{R407C,LuiWin,65}/\partial T_{w,65,4}$ = -13.4	34.36 %

$Nus_{R407C,Philip,65}$ = 143.224±1.913

$\dot{m}_{W,65,1}$ = 0.08452±0.00008452	$\partial Nus_{R407C,Philip,65}/\partial \dot{m}_{W,65,1}$ = 0.000002556	0.00 %
$\dot{m}_{W,65,2}$ = 0.09981±0.00010	$\partial Nus_{R407C,Philip,65}/\partial \dot{m}_{W,65,2}$ = 883.86000	0.21 %
$\dot{m}_{W,65,3}$ = 0.09633±0.00009633	$\partial Nus_{R407C,Philip,65}/\partial \dot{m}_{W,65,3}$ = -817.6	0.17 %
$m_{R407C,65}$ = 0.03001±0.00006002	$\partial Nus_{R407C,Philip,65}/\partial m_{R407C,65}$ = 4798	2.27 %
$P_{65,1}$ = 1360±1.36	$\partial Nus_{R407C,Philip,65}/\partial P_{65,1}$ = 0	0.00 %
$P_{65,2}$ = 584.1±0.5841	$\partial Nus_{R407C,Philip,65}/\partial P_{65,2}$ = 0	0.00 %
$P_{65,3}$ = 572.1±0.5721	$\partial Nus_{R407C,Philip,65}/\partial P_{65,3}$ = -0.04198	0.02 %
$P_{65,4}$ = 450.6±0.4506	$\partial Nus_{R407C,Philip,65}/\partial P_{65,4}$ = -0.03215	0.01 %
$P_{65,5}$ = 424±0.424	$\partial Nus_{R407C,Philip,65}/\partial P_{65,5}$ = -0.02341	0.00 %
$T_{65,1}$ = 17.89±0.06	$\partial Nus_{R407C,Philip,65}/\partial T_{65,1}$ = 0	0.00 %
$T_{65,2}$ = 2.136±0.06	$\partial Nus_{R407C,Philip,65}/\partial T_{65,2}$ = 0	0.00 %
$T_{65,3}$ = 5.065±0.06	$\partial Nus_{R407C,Philip,65}/\partial T_{65,3}$ = 5.491	2.97 %
$T_{65,4}$ = 0.017±0.06	$\partial Nus_{R407C,Philip,65}/\partial T_{65,4}$ = 3.799	1.42 %
$T_{65,5}$ = 38.86±0.06	$\partial Nus_{R407C,Philip,65}/\partial T_{65,5}$ = 1.618	0.26 %

$T_{w,65,1}$ = 23.94±0.06	$\partial Nus_{R407C,Philip,65}/\partial T_{w,65,1}$ = -0.02997	0.00 %
$T_{w,65,2}$ = 14.97±0.06	$\partial Nus_{R407C,Philip,65}/\partial T_{w,65,2}$ = -0.06301	0.00 %
$T_{w,65,3}$ = 23.813±0.060	$\partial Nus_{R407C,Philip,65}/\partial T_{w,65,3}$ = 16.312	26.19 %
$T_{w,65,4}$ = 18.77±0.06	$\partial Nus_{R407C,Philip,65}/\partial T_{w,65,4}$ = -25.99	66.49 %

$Nus_{R407C,Pierre,65}$ = 502.307±2.236

$\dot{m}_{w,65,1}$ = 0.08452±0.00008452	$\partial Nus_{R407C,Pierre,65}/\partial \dot{m}_{w,65,1}$ = 0	0.00 %
$\dot{m}_{w,65,2}$ = 0.09981±0.00010	$\partial Nus_{R407C,Pierre,65}/\partial \dot{m}_{w,65,2}$ = -810.55540	0.13 %
$\dot{m}_{w,65,3}$ = 0.09633±0.00009633	$\partial Nus_{R407C,Pierre,65}/\partial \dot{m}_{w,65,3}$ = -3533	2.32 %
$m_{R407C,65}$ = 0.03001±0.00006002	$\partial Nus_{R407C,Pierre,65}/\partial m_{R407C,65}$ = 27428	54.21 %
$P_{65,1}$ = 1360±1.36	$\partial Nus_{R407C,Pierre,65}/\partial P_{65,1}$ = 0	0.00 %
$P_{65,2}$ = 584.1±0.5841	$\partial Nus_{R407C,Pierre,65}/\partial P_{65,2}$ = 0	0.00 %
$P_{65,3}$ = 572.1±0.5721	$\partial Nus_{R407C,Pierre,65}/\partial P_{65,3}$ = -0.2197	0.32 %
$P_{65,4}$ = 450.6±0.4506	$\partial Nus_{R407C,Pierre,65}/\partial P_{65,4}$ = -0.1772	0.13 %
$P_{65,5}$ = 424±0.424	$\partial Nus_{R407C,Pierre,65}/\partial P_{65,5}$ = -0.1011	0.04 %
$T_{65,1}$ = 17.89±0.06	$\partial Nus_{R407C,Pierre,65}/\partial T_{65,1}$ = 0	0.00 %
$T_{65,2}$ = 2.136±0.06	$\partial Nus_{R407C,Pierre,65}/\partial T_{65,2}$ = 0	0.00 %
$T_{65,3}$ = 5.065±0.06	$\partial Nus_{R407C,Pierre,65}/\partial T_{65,3}$ = 2.451	0.43 %
$T_{65,4}$ = 0.017±0.06	$\partial Nus_{R407C,Pierre,65}/\partial T_{65,4}$ = 2.643	0.50 %
$T_{65,5}$ = 38.86±0.06	$\partial Nus_{R407C,Pierre,65}/\partial T_{65,5}$ = 6.991	3.52 %
$T_{w,65,1}$ = 23.94±0.06	$\partial Nus_{R407C,Pierre,65}/\partial T_{w,65,1}$ = 0	0.00 %
$T_{w,65,2}$ = 14.97±0.06	$\partial Nus_{R407C,Pierre,65}/\partial T_{w,65,2}$ = 0	0.00 %
$T_{w,65,3}$ = 23.813±0.060	$\partial Nus_{R407C,Pierre,65}/\partial T_{w,65,3}$ = -16.205	18.91 %
$T_{w,65,4}$ = 18.77±0.06	$\partial Nus_{R407C,Pierre,65}/\partial T_{w,65,4}$ = 16.46	19.50 %

$Nus_{R407C,Rous,65}$ = 140.165±1.807

$\dot{m}_{w,65,1}$ = 0.08452±0.00008452	$\partial Nus_{R407C,Rous,65}/\partial \dot{m}_{w,65,1}$ = 3.363E-08	0.00 %
$\dot{m}_{w,65,2}$ = 0.09981±0.00010	$\partial Nus_{R407C,Rous,65}/\partial \dot{m}_{w,65,2}$ = 809.67051	0.20 %
$\dot{m}_{w,65,3}$ = 0.09633±0.00009633	$\partial Nus_{R407C,Rous,65}/\partial \dot{m}_{w,65,3}$ = -800.1	0.18 %
$m_{R407C,65}$ = 0.03001±0.00006002	$\partial Nus_{R407C,Rous,65}/\partial m_{R407C,65}$ = 4695	2.43 %
$P_{65,1}$ = 1360±1.36	$\partial Nus_{R407C,Rous,65}/\partial P_{65,1}$ = 0	0.00 %
$P_{65,2}$ = 584.1±0.5841	$\partial Nus_{R407C,Rous,65}/\partial P_{65,2}$ = 0	0.00 %
$P_{65,3}$ = 572.1±0.5721	$\partial Nus_{R407C,Rous,65}/\partial P_{65,3}$ = -0.04108	0.02 %
$P_{65,4}$ = 450.6±0.4506	$\partial Nus_{R407C,Rous,65}/\partial P_{65,4}$ = -0.03147	0.01 %
$P_{65,5}$ = 424±0.424	$\partial Nus_{R407C,Rous,65}/\partial P_{65,5}$ = -0.02291	0.00 %
$T_{65,1}$ = 17.89±0.06	$\partial Nus_{R407C,Rous,65}/\partial T_{65,1}$ = 0	0.00 %
$T_{65,2}$ = 2.136±0.06	$\partial Nus_{R407C,Rous,65}/\partial T_{65,2}$ = 0	0.00 %
$T_{65,3}$ = 5.065±0.06	$\partial Nus_{R407C,Rous,65}/\partial T_{65,3}$ = 5.259	3.05 %
$T_{65,4}$ = 0.017±0.06	$\partial Nus_{R407C,Rous,65}/\partial T_{65,4}$ = 3.638	1.46 %
$T_{65,5}$ = 38.86±0.06	$\partial Nus_{R407C,Rous,65}/\partial T_{65,5}$ = 1.583	0.28 %
$T_{w,65,1}$ = 23.94±0.06	$\partial Nus_{R407C,Rous,65}/\partial T_{w,65,1}$ = -0.128	0.00 %
$T_{w,65,2}$ = 14.97±0.06	$\partial Nus_{R407C,Rous,65}/\partial T_{w,65,2}$ = -0.1481	0.00 %
$T_{w,65,3}$ = 23.813±0.060	$\partial Nus_{R407C,Rous,65}/\partial T_{w,65,3}$ = 15.351	25.98 %
$T_{w,65,4}$ = 18.77±0.06	$\partial Nus_{R407C,Rous,65}/\partial T_{w,65,4}$ = -24.54	66.40 %

$Nus_{R407C,RousAnn,65}$ = 161.170±0.210

$\dot{m}_{w,65,1}$ = 0.08452±0.00008452	$\partial Nus_{R407C,RousAnn,65}/\partial \dot{m}_{w,65,1}$ = 0	0.00 %
$\dot{m}_{w,65,2}$ = 0.09981±0.00010	$\partial Nus_{R407C,RousAnn,65}/\partial \dot{m}_{w,65,2}$ = 97.13983	0.21 %
$\dot{m}_{w,65,3}$ = 0.09633±0.00009633	$\partial Nus_{R407C,RousAnn,65}/\partial \dot{m}_{w,65,3}$ = 670.2	9.45 %
$m_{R407C,65}$ = 0.03001±0.00006002	$\partial Nus_{R407C,RousAnn,65}/\partial m_{R407C,65}$ = 628.2	3.22 %
$P_{65,1}$ = 1360±1.36	$\partial Nus_{R407C,RousAnn,65}/\partial P_{65,1}$ = 0	0.00 %
$P_{65,2}$ = 584.1±0.5841	$\partial Nus_{R407C,RousAnn,65}/\partial P_{65,2}$ = 0	0.00 %
$P_{65,3}$ = 572.1±0.5721	$\partial Nus_{R407C,RousAnn,65}/\partial P_{65,3}$ = -0.07703	4.40 %
$P_{65,4}$ = 450.6±0.4506	$\partial Nus_{R407C,RousAnn,65}/\partial P_{65,4}$ = 0.04136	0.79 %
$P_{65,5}$ = 424±0.424	$\partial Nus_{R407C,RousAnn,65}/\partial P_{65,5}$ = 0.01919	0.15 %
$T_{65,1}$ = 17.89±0.06	$\partial Nus_{R407C,RousAnn,65}/\partial T_{65,1}$ = 0	0.00 %
$T_{65,2}$ = 2.136±0.06	$\partial Nus_{R407C,RousAnn,65}/\partial T_{65,2}$ = 0	0.00 %
$T_{65,3}$ = 5.065±0.06	$\partial Nus_{R407C,RousAnn,65}/\partial T_{65,3}$ = 0.7595	4.71 %
$T_{65,4}$ = 0.017±0.06	$\partial Nus_{R407C,RousAnn,65}/\partial T_{65,4}$ = 0.1647	0.22 %
$T_{65,5}$ = 38.86±0.06	$\partial Nus_{R407C,RousAnn,65}/\partial T_{65,5}$ = -1.326	14.34 %
$T_{w,65,1}$ = 23.94±0.06	$\partial Nus_{R407C,RousAnn,65}/\partial T_{w,65,1}$ = 0	0.00 %
$T_{w,65,2}$ = 14.97±0.06	$\partial Nus_{R407C,RousAnn,65}/\partial T_{w,65,2}$ = 0	0.00 %
$T_{w,65,3}$ = 23.813±0.060	$\partial Nus_{R407C,RousAnn,65}/\partial T_{w,65,3}$ = 1.942	30.77 %
$T_{w,65,4}$ = 18.77±0.06	$\partial Nus_{R407C,RousAnn,65}/\partial T_{w,65,4}$ = -1.972	31.74 %